Ecological aspects of plants inhabiting Mediterranean cliffs

Challenges and prospects of life in vertical environments

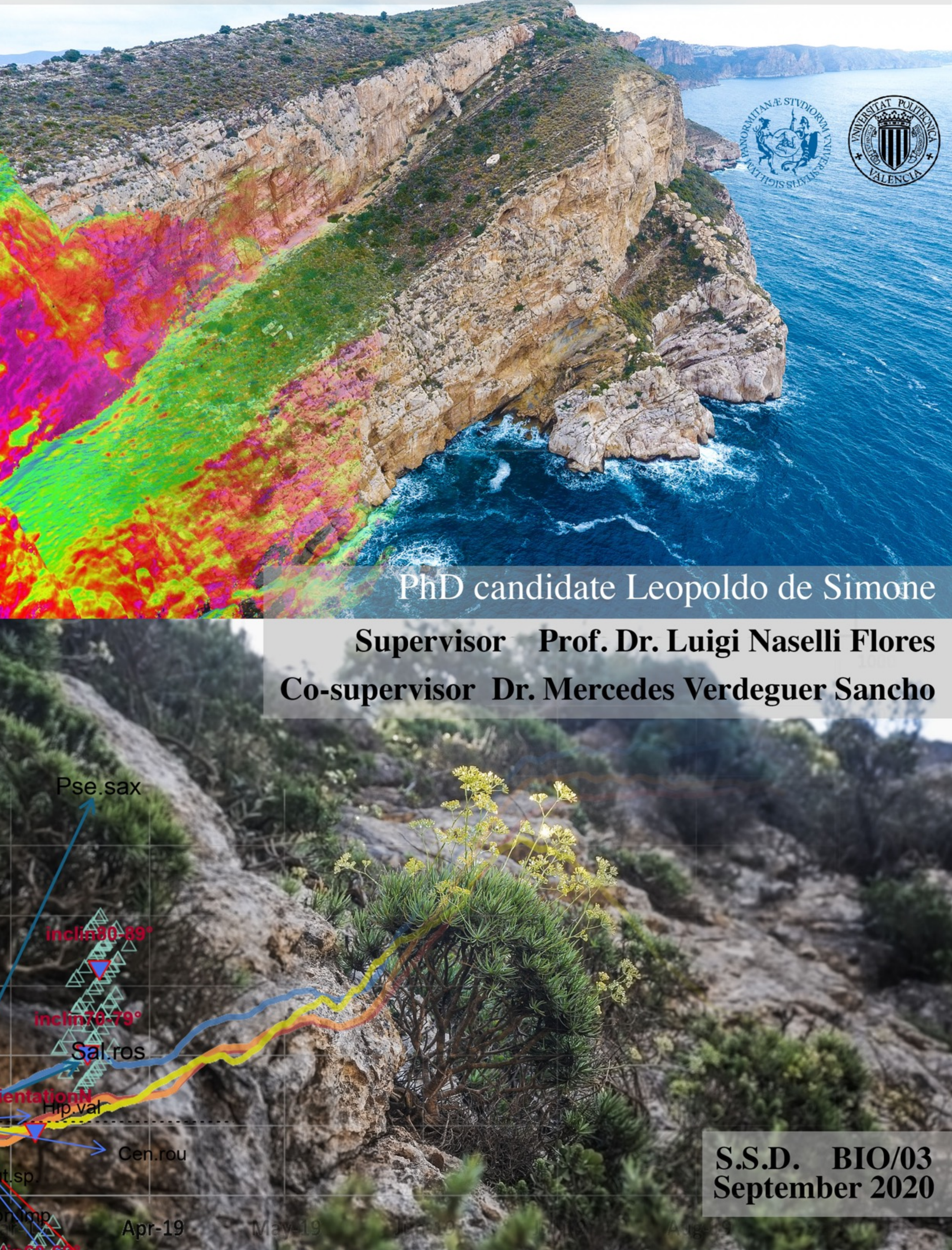

PhD candidate Leopoldo de Simone

Supervisor Prof. Dr. Luigi Naselli Flores

Co-supervisor Dr. Mercedes Verdeguer Sancho

S.S.D. BIO/03
September 2020

Biodiversità Mediterranea – Internazionale
Scienze Agrarie, Alimentari e Forestali
BIO/03

Ecological aspects of plants inhabiting Mediterranean cliffs
Challenges and prospects of life in vertical environments

PhD CANDIDATE

LEOPOLDO DE SIMONE

PhD COORDINATOR

PROF.
MARIA ANTONIETTA GERMANA'

SUPERVISOR

PROF.
LUIGI NASELLI-FLORES

CO-SUPERVISOR

PROF.
MERCEDES MARÍA VERDEGUER SANCHO

S.S.D BIO/03
September 2020

Contents

Summary

This thesis investigated opportunities, challenges and limitations for plant ecological research in the context of Mediterranean cliffs. In particular, chasmophytic species, whose natural habitats are very steep, limestone mountain slopes in the proximity of the sea, in the Central and Western part of the Mediterranean area are considered as study objects. Studies were carried out in the coastal mountain belts of both North-western Sicily and Dianic coasts in the Valencian Community (Spain).

The first chapter, entitled "The complexity of environmental factors: cliff microclimate", investigates the variability of cliff microclimate in three different areas in Sicily and Spain, analysing the environmental conditions created by the cliff at very fine scale. Six independent and comparable datasets including the main meteorological variables were compiled in a total period of 18 months. The resulting spectra of environmental conditions are compared pairwise along two key environmental gradients: North/South cliff orientation and proximity to the sea. Intraspecific leaf traits are used in order to investigate variations in the functional response of plants living on opposite orientations. The resulting variation is then correlated with the influence of microclimatic conditions created by slope and functional aspects of the aforementioned plant traits.

The second chapter, entitled "Compositional data and analyses of areas and plant communities in the coastal cliffs of the Valencian Community (Spain)", presents an ordination of the study sites and of the plant species inhabiting the cliff zones of the mountain belt along the coasts of the Dianic region in Eastern Spain. The study revealed significant correlations between the vegetation units and the sites with reference to the broad North/South geographical orientation. However, it was poorly informative in respect to reveal the major differences observed in the structure of the plant assemblage related to the micro-topographic variations recorded in the dataset.

In the third chapter, entitled "UAV (drone) surveys for the study of plant-microtopography relationships and for the conservation of rare species", a proposed survey methodology for investigating inaccessible vertical environments is described. Challenges and opportunities of plant ecological research in these typically inaccessible areas were also

analysed. A first set of data is comprised of partial and total visual census of two narrow endemic cliff species in the Spanish and Italian study areas. Through the use of aerial close-range photogrammetry and 3D modelling, it was possible to study the effects of micro-topography on niche segregation, both at community and species level. Ordination methods were used to correlate selected endemic species and entire plant assemblages to environmental factors such as local and global aspect, slope and distance from cliff edges.

The fourth chapter, entitled "Distribution, ecology, conservation status and phylogeography of *Pseudoscabiosa limonifolia*, a paleo-endemic chasmophytic species from Sicily (Italy)", is addressed to analyse in details the phylogeographic structure of a cliff narrow endemic species, *Pseudoscabiosa limonifolia* (VAHL) DEVESA (Caprifoliaceae, subfamily Dipsacaceae), also taking in consideration its closest sister taxa. Furthermore, its total distribution was determined by field surveys, characterizing its habitat, and assessing its conservation status as Vulnerable according to IUCN red list guidelines.

Castellano

Esta tesis investiga las oportunidades, desafíos y limitaciones para la investigación en el campo de la ecología vegetal, en el contexto de los acantilados mediterráneos. En concreto, las especies casmofiticas, cuyos hábitats naturales se caracterizan por su acusada pendiente. Las laderas de las montañas de piedra caliza en la proximidad del mar, en la parte central y occidental del área mediterránea se consideran objetos de estudio. Los estudios se llevaron a cabo en los cinturones costeros de montaña de las costas del noroeste de Sicilia y la costa diánica en la Comunidad Valenciana.

El primer capítulo, titulado "The complexity of environmental factors: cliff microclimate", investiga la variabilidad del microclima del acantilado en tres áreas diferentes en Sicilia y España, analizando las condiciones ambientales creadas por el acantilado en una escala muy estrecha. Se recopilaron seis conjuntos de datos independientes y comparables que recogen las principales variables meteorológicas a lo largo de un período total de 18 meses. La gama resultante de condiciones ambientales se compara por pares a lo largo de dos gradientes ambientales principales: la orientación del acantilado Norte/Sur y la proximidad al mar. Además, los rasgos foliares intraespecíficos se utilizan para estudiar la variación en la respuesta funcional de las plantas que viven en las orientaciónes opuestas en una misma área de investigación. La variación resultante se correlaciona con la influencia de las condiciones microclimáticas creadas por la pendiente y el aspecto en los rasgos de la planta antes mencionados.

El segundo capítulo, titulado “Compositional data and analyses of areas and plant communities in the coastal cliffs of the Valencian Community (Spain)”, presenta una ordenación de los sitios de estudio y de las especies vegetales que habitan en las zonas de acantilados del cinturón montañoso a lo largo de las costas de la región diánica en el este de España. El estudio reveló correlaciones significativas entre las unidades de vegetación y los sitios con referencia a la amplia orientación geográfica Norte/Sur. Sin embargo, fue poco informativo con respecto a revelar las principales diferencias observadas en la estructura del conjunto de plantas relacionadas con laa variaciones microtopográficas registradas en el conjunto de datos.

En el tercer capítulo, titulado “UAV (drone) surveys for the study of plant-microtopography relationships and for the conservation of rare species”, se describe la metodología propuesta para investigar entornos verticales poco accesibles. También se analizaron los desafíos y las oportunidades de la investigación ecológica vegetal en estas áreas tipicamente inaccesibles. Un primer conjunto de datos comprende un censo visual parcial y total de dos especies endémicas de acantilados estrechos en las áreas de estudio españolas e italianas. Mediante el uso de la fotogrametría aérea de corto alcance y el modelado 3D, fue posible estudiar los efectos de la micro topografía en la segregación de nichos, tanto a nivel de comunidad como de especie. Se utilizaron métodos de ordenación para correlacionar las especies endémicas seleccionadas y conjuntos de plantas con factores ambientales como el aspecto local y global, la pendiente y la distancia desde los bordes de los acantilados.

En el cuarto capítulo, titulado “Distribution, ecology, conservation status and phylogeography of *Pseudoscabiosa limonifolia*, a paleo-endemic chasmophytic species from Sicily (Italy)”, se analiza en detalle la estructura filogeográfica de una especie endémica de acantilados, *Pseudoscabiosa limonifolia* (Caprifoliaceae, subfamilia Dipsacaceae), también considerando las relaciones filogeográficas con sus taxones más próximos. Además, su distribución total se determinó mediante observaciones de campo, caracterizando su hábitat y evaluando su estado de conservación como Vulnerable de acuerdo con las directrices de la lista roja de la UICN.

Valencià

Aquesta tesi va investigar les oportunitats, reptes i limitacions per a la investigació en el camp de l'ecologia vegetal, en el context dels penya-segats mediterranis. En concret, les espècies casmofitiques, amb hàbitats naturals que es caracteritzen pel seu acusat pendent. Les vessants de les muntanyes de pedra calcària en la proximitat del mar, a la part central i occidental de l'àrea mediterrània són considerats objectes d'estudi. Els estudis es portaren a terme als cinturons costers de muntanya de les costes del nord de Sicília i la costa diànica a la Comunitat Valenciana.

El primer capítol, titulat "The complexity of environmental factors: cliff microclimate", investiga la variabilitat del microclima del penya-segat en tres àrees diferents de Sicília i Espanya, analitzant les condicions ambientals creades pel penya-segat a una escala molt estreta. Es recopilen sis conjunts de dades independents i comparables que reconeixen les principals variables meteorològiques a llarg termini durant un període total de 18 mesos. Les dades resultants de les condicions ambientals es comparen per parells al llarg de dos gradients ambientals principals: l'orientació del penya-segat Nord/Sud i la proximitat a la mar. A més, els trests foliars intraespecífics s'utilitzen per estudiar la variació en la resposta funcional de les plantes que habiten orientacions oposades dins d'un àrea d' investigació. La variació resultant es correlaciona amb la influència de les condicions microclimàtiques creades pel vessant i els aspectos funcionals dels trets vegetals esmentats.

El segon capítol, titulat "Compositional data and analyses of areas and plant communities in the coastal cliffs of the Valencian Community (Spain)", presenta una ordenació dels llocs d'estudi i de les espècies de plantes que habiten a les zones de penya-segats del cinturó de muntanya al llarg de les costes de la regió diànica de España. L'estudi va a revelar correlacions significatives entre les unitats de vegetació i els llocs amb referència a l'amplias orientació geogràfica Nord/Sud. No obstant això, va ser poc informatiu per poder revelar les diferències observades en l'estructura del conjunt de plantes relacionades amb les variacions microtopogràfiques registrades al conjunt de dades

Al tercer capítol, titulat "UAV (drone) surveys for the study of plant-microtopography relationships and for the conservation of rare species", es descriu la metodologia proposada per a investigar entorns verticals poc accessibles. També es van analitzar els reptes i les oportunitats de la investigació ecològica vegetal en aquestes àrees normalment inaccesibles. Un primer conjunt de dades inclou el cens visual parcial i el total de dues espècies endèmiques de penya-segats a les àrees d'estudi espanyoles i italianes. Mitjançant la fotogrametria aèrea a curt abast i el modelat 3D, va ser possible estudiar els efectes de la microtopografia en la segregació de nínxols, tant a nivell comunitari com d'espècies. Es van utilitzar mètodes d'ordenació per a correlacionar les espècies endèmiques seleccionades i conjunts vegetals sencers amb factors ambientals com ara l'aspecte local i global, el pendent i la distància de les vores dels penya-segats.

En el quart capítol, titulat "Distribution, ecology, conservation status and phylogeography of *Pseudoscabiosa limonifolia*, a paleo-endemic chasmophytic species from Sicily (Italy)", que s'analitza en detall l'estructura filogeográfica d'una espècie endèmica de penya-segats, *Pseudoscabiosa limonifolia* (Caprifoliaceae, subfamilia Dipsacaceae), considerant tambè les relacions filogeogràfiques amb els seus taxons més propers. A més, la seva distribució total es va determinar mitjançant observacions de camp, caracteritzant el seu hàbitat i avaluant el seu estat de conservació com a Vulnerable, d'acord amb les directrius de la llista roja de la UICN.

General introduction

This research analyses different aspects of plant-environment interactions in multiple independent coastal cliff zones in the Thermomediterranean bioclimatic belt of the Central-western Mediterranean region. Selected study areas share an equivalent sea proximity between 0 and 2000 m (see chap. 1 for a more detailed microclimate comparison) and a dolomitic limestone geology, with altitude ranging between 100 and 800 m a.s.l. Replications of the research design and dataset collection were carried out in Southwest Italy and East Spain to have a broader relevance, overcoming the problem due to effects linked to regionality and isolation. Given the need to characterise environmental drivers of species assemblages at local level, more than one non-continuous cliff system was included in the study.

The research questions addressed in this thesis involve different models of species and plant assemblages growing on Mediterranean cliffs, in the framework of analysis of plant diversity and their genetic connections at population and community level. Overall, the approach to study plant ecology on cliffs adopted in this thesis analysed the primary theme via different research questions, all sharing the need to acquire data at a narrow ecological scale. Such choice was driven by the nature of the extreme, but largely understudied, environmental complexity of these hardly accessible environments.

"The very limited distribution of many saxatile [chasmophytic] species and communities is a feature that must strike any botanist who has travelled in the Mediterranean."

P.H. Davis (1951)

When using the term 'cliffs', or 'vertical cliffs', geomorphologists refer to rock walls with high and very steep slopes. These zones differ considerably from the surrounding habitats (see Larson et al., 2000 for a review) both for their physical factors (such as local temperature, water retention, air humidity, solar radiation, wind speed and soil availability) and for the distinct flora living there. Generally, plants growing among rocks are defined saxicolous, but those living on cliffs in association with vertical angles of slopes, in narrow holes and crevices, are termed chasmophytes (Davis, 1951, European Red List of Habitats, 2016). A third ecological category is represented by comophytes, which are species generally found on small pokets of soils deposited on ledges and crevices (Font Quer, 1953; Schimper & Faber, 1935).

The Mediterranean Basin is known for its complex geological and paleoclimatic history (Combourieu-Nebout et al., 2015; Fauquette et al., 1999, 2007; Rosembaum et al., 2002; Suc, 1984). Moreover, the region is characterised by an impressive diversity of habitats (Medail & Quezel, 1997). This paleogeographic and topographic complexity is manifested in a high richness of regional and/or local endemic species (Blondel & Aronson 1999; Kruckeberg & Rabinowitz 1985), which account for almost 60% of the total endemism (Thompson, 2005).

In the Mediterranean context, limestone and dolomitic cliffs are frequently encountered with a discontinuous and disjunct distribution (for a map, see: European Red List of Habitats, 2016). For this reason, according to the definition of a chasmophytic species, it can be said that the ecological niche of strict chasmophytes is not different from that of edaphic taxa. They are in fact distributed on sparse, distant "ecological islands" (*sensu* Stebbins, 1980) separated by "oceans" of unsuitable (non-vertical) environments. In general, geographic confinement and spatial and ecological isolation are known to be primary drivers of speciation in the Mediterranean region (Buira et al., 2020; Molina-Venegas et al. 2013; Rundel et al. 2016). At the same time, the topographic heterogeneity created by cliffs and areas with high slope generate a complex mosaic of microclimatic conditions (Bennie et al., 2008; Fawcett et al., 2019; Finkel et al., 2001; Garcia et al., 2020; Ospedal et al., 2015; Scherrer & Körner, 2010, 2011; Suggitt et al., 2011). These areas then favour the persistence of conditions which can be very different from the regional average climate, supporting the existence (or persistence) of species adapted to the peculiar, local microclimate. As a consequence of the particular microclimate, cliffs might be included in the category of "microrefugia" (Dobrowski, 2011).

As microrefugia, cliffs and rocky habitats are thought to favour the persistence of some palaeoendemics, that have survived only in these remote places (Brullo et al., 2013; Egli et al., 1990; Panitsa & Kontopanou; 2017; Strid & Tan 1997), and of species outside their main distribution areas (Egli, 1989; Hedderson & Blockeel, 2013; Snogerup, 1971). The definition of cliffs as microrefugia is supported by a higher frequency of relict lineages

(Fernández-Mazuecos et al., 2014; Mejías et al., 2018; Silva Hernández de Santaolalla et al., 2015) and/or disjunct populations (the so called schizoendemic species, Contandriopoulos, 1962; Favarger & Contandriopoulos, 1961) than that recorded in the surrounding territories (Abeli et al., 2018; Harrison & Noss, 2017; Molina-Venegas et al., 2017; Morelli et al., 2016).

Being caused by isolation, persistence or speciation, the amount of rare or narrow endemic taxa among chasmophytes in comparison with species inhabiting other habitats is, at least, fascinating. It hints at how these stressful habitats act as an environmental driver of selection of a certain amount of species. Moreover the ecological, exaptative and evolutionary processes that bring a certain species to a life on cliffs is recursive and convergent among genera and families. For example, it has been estimated that evolutionary shifts to rocky habitat took place over at least five independent times along the genealogic history of the genus *Sonchus* (Mejias et al., 2018). For the same reason, recurrent endemic taxa within the same genus or family are found on different geographic locations (e.g. *Lomelosia cretica* and *L. variifolia*; the genera *Asperula*, *Centaurea, Seseli, Campanula, Hieracium, Saxifraga, Silene* and *Teucrium*; the family Fumariaceae).

Chasmophytes have a lower ability to compete for resources than widespread species (Lavergne et al. 2004; Médail & Verlaque, 1997; Thompson et al., 2005) and show lower growth rates (Davis, 1951). Davis (1951) for example described Mediterranean cliff communities not only as sheltered areas with regard to unfavourable climatic change, but also with regard to competition with hillside communities, and to grazing.

In general, there is a wide acceptance among botanists and ecologists about the positive correlation between slope and plant endemism, especially (but not only) in the Mediterranean region. In the work of Lavergne et al. (2004), authors compared widespread and endemic congeneric species, finding the latter to occur in habitats with significantly steeper slopes and higher percentage of bedrock and rock cover. The pattern of correlation between endemic or narrow distributed species and high values of slopes stands out in any work involving cliff areas. The relationships between endemism and cliffs/high slopes appear both at large (Appalachian mountains: White & Miller, 1988; Finland: Heikkinen, 1998; Sardinia: Fois et al., 2017; Greece: Panitsa & Kontopanou, 2017; Spain: Buira et al., 2020) and at local scale (Palestine/Sinai Mediterranean areas: Davis, 1951; Greece and the Balkans: Polunin, 1980; Strid & Papanicolaou, 1985; Corsica: Gamisans, 1999; Sardinia: Bacchetta et al., 2007; Balearic islands: Alomar et al., 1997). For example, it has been calculated that 53.8 % of species inhabiting cliffs in Greece are national endemics, whereas 75.3 % of chasmophytes are range restricted (Panitsa & Kontopanou, 2017). In Sardinia 50.4 % of species encountered on cliffs resulted in regional endemics (Bacchetta et al., 2007).

Certainly, the inaccessibility of these environments preserved chasmophytes from agricultural uses and other anthropic modifications (Lavergne et al., 2005). Probably the most important historic advantage of plant assemblages on cliffs is the minor or absent impact of the widespread grazing provoked by local farming activities. During field observations carried out both in Spain and Sicily, goats and sheep, which are run free by farmers, strongly influence the structure of plant communities at landscape level. Their influence on cliff species community composition and structure is evident in almost any location where they get to reach, especially the "land bridges" i.e. the upper ridge and base of a cliff. By contrast, cliffs with slope angles higher than 70-80° were hardly or inaccessible to vertebrate herbivores. Accordingly, the present study made it possible to record the differences in plant community composition and structure which most likely depended, among other factors, on grazing impact.

Another external factor of disturbance in the Mediterranean is fire (Keeley et al., 2012). Thanks to their inaccessibility, scarce organic matter and low fuel load, fires have a reduced effect on cliff assemblages, especially at a distance from the cliff boundaries. For all these reasons, the topographic protection provided by the cliff produces a number of ecological opportunities for the flora.

Finally, cliffs acted as refugia with respect to this particular set of ecological conditions. There, topo-climatic and mechanical factors have protected paleoendemic species and promoted speciation.

General features of the studied sites

The first study area is located in the Easternmost part of the Valencian Community, Spain. It follows the cliff systems of coastal reliefs of the area between the towns of Denia and Altea (Alicante). The investigated chasmophytic plant assemblages belong to the Montgò massif, Cabo de San Antonio coastal cliffs, Moraira, Cap d'Or, Ifac and Toix massifs. All these areas have a complex topography pertaining to the Baetic system. The Baetic mountain belt starts in Andalusia and the Portuguese Algarve, heading toward SW-NE until reaching the North-easternmost peninsula of the Alicante province to then re-emerge in the Pitiusa islands of the Balearic archipelago (Ibiza and Formentera). Study areas in Spain pertains to the internal Prebetic portion of the Baetic mountain belt, (Fig. I). The geological composition of these mountains is mainly Meso-Cenozoic compact dolomitic limestones. During the Miocene the Baetic belt system connected North Africa and South Andalusia with the Valencian Community and the Balearic Islands (Baetic-Rifan orogenic belt; geologic map in Sanz de Galdeano & Ruiz Cruz, 2016).

This land bridge, together with its complex terrain had a substantial biogeographic importance for this area of the Mediterranean. It led to the formation and fragmentation of many areals and thus to, favouring speciation of many chasmophytic vicariant species in the Balearic Islands, SE Spain, Morocco, Algerian Kabilia (Aguilella et al., 2010; Laguna, 1998, 2007).

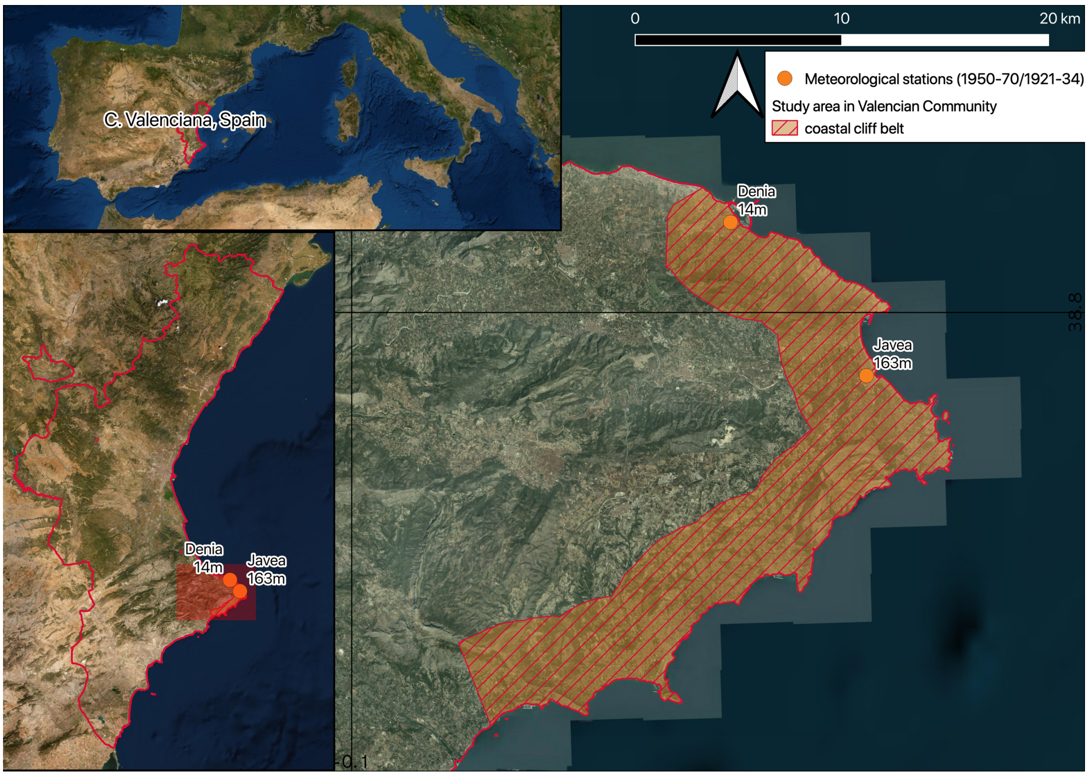

Fig I. Boundaries of the study area in Spain.

The second research area is located in the North-western sector of Sicily (Italy) (Fig. II). These mountains ridges compose the coastal cliff belt of North-west Sicily, that coincide with tectonic highs and were set on Mesozoic carbonate rocks (Di Maggio et al., 2017). They are coastal carbonate massifs sharing common geomorphologic, geologic and phytogeographic characteristics. In fact, Capo Gallo, Monte Cofano, Monte Pecoraro, Monte Palmeto, Monte Pellegrino and the area denominated "Mountains of Palermo" represent the outcrops of a carbonate platform denominated Panormide (for a map, see Catalano et al., 2013).

These areas are particularly rich in endemic species, whose chasmophytes are a considerable component (Cusimano et al., 2017; Raimondo et al., 2001).

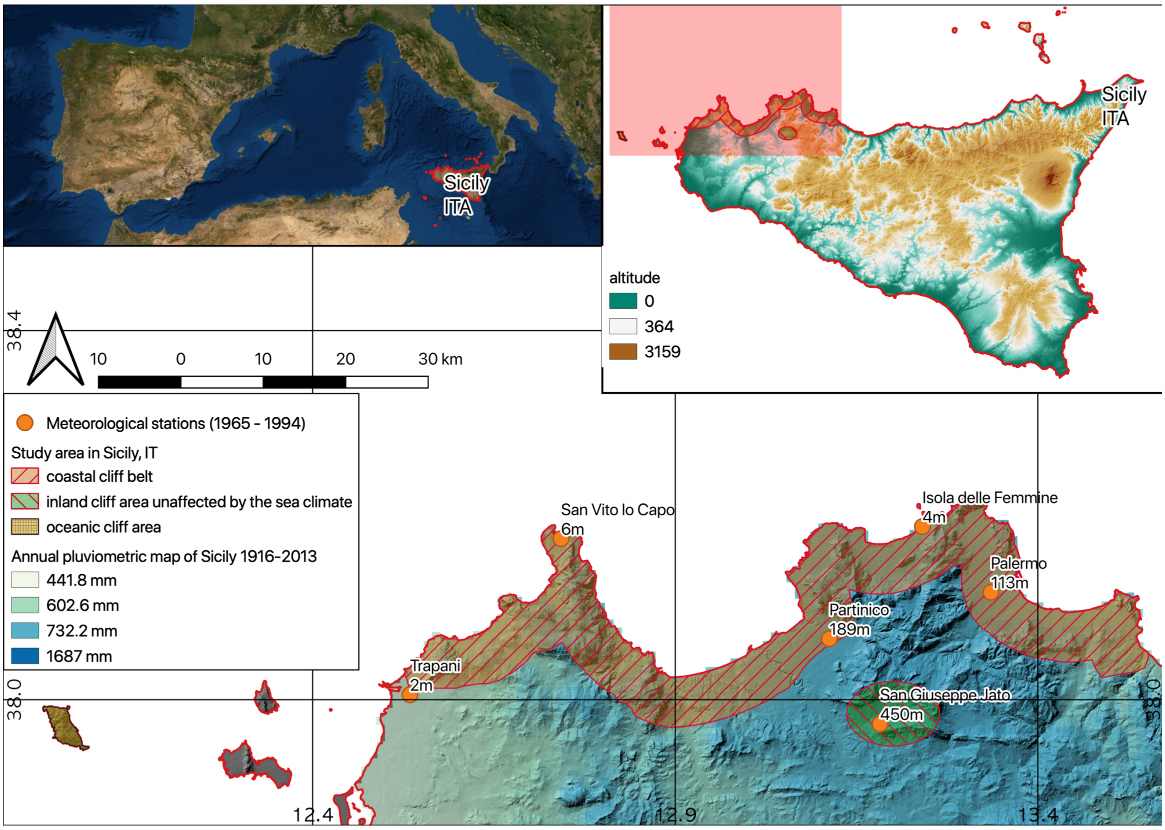

Fig II. Boundaries of the study area in Italy.

Both study areas share a complex phytogeographic history (see also Guarino & Pasta, 2018). In a broader geologic context, they are both pelagic and pericontinental facies of the southern termination of the Alpine fold-and-thrust belt in the Western Mediterranean (for a map, see: Escosa et al., 2018; Vera, 2004).

Chapter overview and problems addressed

The first chapter investigates the variability of cliff microclimate in both study areas of Sicily and Spain. Three different areas were selected for the installation of six weather stations. Scope of the research was to analyse the environmental conditions created by the cliff at very fine scale. All datasets were comparable and included the main meteorological variables (temperature, relative humidity and incoming solar radiation) in a total period of 18 months. The resulting spectra of environmental conditions were compared pairwise along two key environmental gradients: North/South cliff orientation and proximity to the sea.

Intraspecific leaf traits were used in order to investigate variation in the functional response of plants living on opposite orientations. The resulting variation was then correlated with the influence of microclimatic conditions created by slope and functional aspects of the aforementioned plant traits.

The second chapter presents an ordination of the study sites of the mountain belt along the coasts of the Dianic region in Eastern Spain. The ordination took in account a set of local geomorphological environmental conditions, all visually estimated. It followed a cluster analysis of sites according to their floristic composition, individuating the main units which composed the encountered plant assemblages inhabiting the cliff. The study aims were to find significant correlations between the vegetation units and the sites with reference to the regional geographical orientation, the local orientation of the plots, its inclination and distance from the boundaries of the cliff surface. The goals of the study were: 1) to test the effectiveness of classic relevé-type sampling retrieved from field transects along vertical areas; 2) to investigate the relationship between species compositional data and microtopographic variables retrieved from a visual, distance observation; and 3) to produce a numerical classification of the studied sites in order to link floristic composition and species abundances to regional variation in cliff assemblages.

In the third chapter a proposed survey methodology for investigating hardly accessible vertical environments is described. Challenges and opportunities of plant ecological research in these typically inaccessible areas were also analysed. Through the use of aerial close-range photogrammetry and 3D modelling, the goals of this study were: 1) to study the effects of micro-topography on niche segregation, both at community and species level; 2) to correlate selected endemic species and entire plant assemblages' to environmental factors through ordination methods; 3) to assess a) whether the number of individuals in the extant continental populations of an endemic species has maintained constant value through time; b) the niche preferences of 2 co-occurring endemic strictly chasmophytic species; c)the niche preferences of a widespread chasmophytic species and of its endemic counterpart.

The fourth chapter is addressed at analysing in details the phylogeographic structure of a cliff narrow endemic species, *Pseudoscabiosa limonifolia* (VAHL) DEVESA (Dipsacaceae s.s.), also taking in consideration its closest sister taxa. Furthermore, its total distribution was determined by field surveys, characterizing its habitat, and assessing its conservation status as Vulnerable according to IUCN red list guidelines. In detail, the goals of the investigation were: 1) to assess the genetic variability among all the extant populations of *P. limonifolia* through comparing the degree of cpDNA variation; 2) to compare this variability to that of its 2 closely related species; 3) to evaluate its colonisation patterns in Sicily, also considering its diaspore anemochorous dispersal syndrome. Furthermore, a new IUCN conservation assessment for *P. limonifolia* has been produced. Through fine scale mapping, it was also 1) estimated the actual species distribution; 2) characterized the narrow ecological requirements of this paleoendemic obligated chasmophyte; and 3) identified the threats that could endanger its survival.

Bibliography

Abeli, T., Vamosi, J.C., Orsenigo, S. (2018). The importance of marginal population hotspots of cold-adapted species for research on climate change and conservation
Species Divers., 45, pp. 977-985, 10.1111/jbi.13196

Aguilella, A., Fos, S. & Laguna, E. (2010). Catálogo Valenciano de Especies de Flora Amenazadas. Colección Biodiversidad, 18. Conselleria de Medi Ambient, Aigua, Urbanisme i Habitatge, Generalitat Valenciana. Valencia.

Alomar, G., Mus, M., Rosselló, J.A. (1997). Flora endèmica de les Balears. Consell Insular de Mallorca, Palma.

Bacchetta, G., Casti, M., Mossa, L. (2007). New ecological and distributive data regarding rupicolous flora in Sardinia. Journal de Botanique de la Société Botanique de France, 38: 73-83.

Bennie, J., Huntley, B., Wiltshire, A., Hill, M.O., Baxter, R. (2008). Slope, aspect and climate: spatially explicit and implicit models of topographic microclimate in chalk grass-land. Ecol. Model. 216 (1), 47–59.

Blondel, J. & Aronson, J. (1999). Biology and Wildlife of the Mediterranean Region. Oxford University Press.

Brullo, C., Brullo, S., Downie, S., Danderson, C., Giusso del Galdo, G. (2013). *Siculosciadium*, A New Monotypic Genus of Apiaceae from Sicily. Annals of the Missouri Botanical Garden. 99. 1-18. 10.3417/2011009.

Buira, A., Cabezas, F. & Aedo, C. (2020). Disentangling ecological traits related to plant endemism, rarity and conservation status in the Iberian Peninsula. Biodivers Conserv 29, 1937–1958. https://doi.org/10.1007/s10531-020-01957-z

Catalano, R., Valenti, V., Accaino, F., Sulli, A., Tinivella, U., Gasparo Morticelli, M., Zanolla, C. & Giustiniani, M. (2013. Sicily's fold/thrust belt and slab roll-back: the SI.RI.PRO. seismic crustal transect. Journal of the Geological Society, London, 170 (3),451-464. doi: 10.1144/0016-76492012-099

Combourieu-Nebout, N., Bertini, A., Russo-Ermolli, E., Peyron, O., Klotz, S., Montade, V., Fauquette, S., Allen, J., Fusco, F., Goring, S., Huntley, B., Joannin, S., Lebreton, V., Magri, D., Martinetto, E., Orain, R., Sadori, L. (2015). Climate changes in the central Mediterranean and Italian vegetation dynamics since the Pliocene. Review of Palaeobotany and Palynology. 218. 10.1016/j.revpalbo.2015.03.001.

Contandriopoulos, J. (1962). Essai de classification des endémiques corses. – Rev. Cytol. Biol. Vég. 25(3-4): 449-459.

Cusimano, D., Guarino, R., & Ilardi, V. (2017). Discovery of a second locality for the narrow endemic Anthemis ismelia (Asteraceae) in NW Sicily. Flora Mediterranea, 27(27), 151-158.

Davis, P. (1951). Cliff Vegetation in the Eastern Mediterranean. Journal of Ecology, 39(1), 63-93.

Di Maggio, C., Madonia, G., Vattano, M., Agnesi, V., & Monteleone, S. (2017). Geomorphological evolution of western Sicily, Italy. Geologica Carpathica, 68, 80 - 93.

Dobrowski, S.Z. (2011). A climatic basis for microrefugia: the influence of terrain on climate Glob. Chang. Biol., 17, pp. 1022-1035, 10.1111/j.1365-2486.2010.02263.x

Egli, B.R. (1989). Ecology of dolines in the mountains of Crete (Greece). Bielefelder Ökol Beitr 4:59–63

Egli, B.R., Gerstberger, P., Greuter, W., Risse, H. (1990). Horstrissea dolinicola, a new genus and species of umbels (Umbelliferae, Apiaceae) from Kriti (Greece). Willdenowia 19:389–399

Escosa, F.O., Ferrer, 0., Roca, E. (2018). Geology of the Eastern Prebetic Zone at the Jumilla region (SE Iberia), Journal of Maps, 14:2, 77-86, DOI: 10.1080/17445647.2018.1433562

European Red List Of Habitats (2016). ISBN 978-92-79-61588-7 https://ec.europa.eu/environment/nature/knowledge/pdf/terrestrial_EU_red_list_report.pdf

Fauquette, S., Suc, J.-P., Guiot, J., Diniz, F., Feddi, N., Zheng, Z., Bessais, E., Drivaliari, A. (1999). Climate and biomes in the west Mediterranean area during the Pliocene. Palaeogeogr. Palaeoclimatol. Palaeoecol. 152, 15–36.

Fauquette, S., Suc, J.-P., Jiménez-Moreno, G., Favre, E., Jost, A., Micheels, A., Bachiri-Taoufiq, N., Bertini, A., Clet-Pellerin, M., Diniz, F., Farjanel, G., Feddi, N., Zheng, Z. (2007). Latitudinal climatic gradients in Western European and Mediterranean regions from the Mid-Miocene (~15 Ma) to the Mid-Pliocene (~3.6 Ma) as quantified from pollen data. In: Williams, M., Haywood, A.M., Gregory, F.J., Schmidt, D.N. (Eds.), Deep-time perspectives on climate change: marrying the signal from computer models and biological proxies. The Micropalaeontological Society Special Publications. The Geological Society, London, pp. 481–502.

Favarger, C., Contrandriopoulos, J. (1961). Essai sur l'endémisme. Bulletin de la Société botanique Suisse, 71: 383-408.

Fawcett, S., Sistla, S., Dacosta Calheiros, M., Kahraman, A., Reznicek, A.A., Rosenberg, R., Wettberg von, E.J.B. (2019). Tracking microhabitat temperature variation with iButton data loggers. Appl. Plant Sci., 7 (2019), Article e01237, 10.1002/aps3.1237

Fernández-Mazuecos, M., Jiménez-Mejías, P., Rotllan-Puig, X., Vargas, P. (2014). Narrow endemics to Mediterranean islands: Moderate genetic diversity but narrow climatic niche of the ancient, critically endangered Naufraga (Apiaceae). Perspectives in Plant Ecology Evolution and Systematics. 16. 190-202. 10.1016/j.ppees.2014.05.003.

Finkel, M., Fragman, O., Nevo, E. (2001). Biodiversity and interslope divergence of vascular plants caused by sharp microclimatic differences at “Evolution Canyon II”, Lower Nahal Keziv, Upper Galilee, Israel. Isr. J. Plant Sci. 49 (4), 285–295.

Fois, M, Fenu, G, Cañadas, EM, Bacchetta, G (2017). Disentangling the influence of environmental and anthropogenic factors on the distribution of endemic vascular plants in Sardinia. PLoS ONE 12(8): e0182539. https://doi.org/ 10.1371/journal.pone.0182539

Font Quer, P. (1953). Diccionario de Botanica, 1, 2. Editorial Labor, Barcelona 1244 p.

Gamisans, J. (1999). La végétation de la Corse. Aix-en-Provence, Edisud, 391 p.

García, M.B., Domingo, D., Pizarro, M., Font, X., Gómez, D., Ehrlén, J. (2020). Rocky habitats as microclimatic refuges for biodiversity. A close-up thermal approach. Environmental and Experimental Botany, Volume 170

Harrison, S., Noss, R. (2017). Endemism hotspots are linked to stable climatic refugia Ann. Bot., 119, pp. 207-214, 10.1093/aob/mcw248

Hedderson, T.A., Blockeel, T.L. (2013). Oncophorus dendrophilus, a new moss species from Cyprus and Crete. J Bryol 28:357–359

Heikkinen, R.K. (1998). Can richness patterns of rarities be predicted from mesoscale atlas data? A case study of vascular plants in the Kevo Reserve. Biological Conservation, 83, 133–143.

Keeley, J.E., Bond, W.J., Bradstock, R.A., Pausas, J.G., Rundel, P.W. (2012), Fire in Mediterranean Ecosystems: ecology, evolution and management, Cambridge University Press, 515 p.

Kruckeberg, A.R., Rabinowitz, D. (1985). Biological aspects of endemism in higher plants. Annu Rev Ecol Syst 16:447–479. https://doi.org/10.1146/annurev.es.16.110185.002311

Laguna, E. (coord.) (1998). Flora endémica, rara o amenazada de la Comunidad Valenciana. Conselleria de Medi Ambient, Generalitat Valenciana. Valencia.

Laguna, E. (2007). Un viatge pel món de les plantes. La Flora endèmica a les terres valencianes. Mètode, 52: 97-105.

Larson, D.W., Matthes, U., & Kelly, P.E. (2000). Cliff Ecology: Pattern and Process in Cliff Ecosystems.

Lavergne, S., Thompson, J.D., Garnier, E. and Debussche, M. (2004). The biology and ecology of narrow endemic and widespread plants: a comparative study of trait variation in 20 congeneric pairs. Oikos, 107: 505-518. doi:10.1111/j.0030-1299.2004.13423.x

Lavergne, S., Thuiller, W., Molina, J. et al. (2005). Environmental and human factors influencing rare plant local occurrence, extinction and persistence: a 115 year study in the Mediterranean region. Journal of Biogeography, 32, 799–811.

Médail, F. & Quézel, P. (1997). Hot-Spots Analysis for conservation of Plant Biodiversity in the Mediterranean Basin. Annals of the Missouri Botanical Garden, 84, 112-127. http://dx.doi.org/10.2307/2399957

Médail, F. & Verlaque, R. (1997). Ecological characteristics and rarity of endemic plants from Southeast France and Corsica: implications for biodiversity conservation. Biol. Conserv., 80: 269-281.

Mejías, J.A., Chambouleyron, M., Kim, S. et al. (2018). Phylogenetic and morphological analysis of a new cliff-dwelling species reveals a remnant ancestral diversity and evolutionary parallelism in Sonchus (Asteraceae). Plant Syst Evol 304, 1023–1040. https://doi.org/10.1007/s00606-018-1523-2

Molina-Venegas, R., Aparicio, A., Pina, F.J., Valdés, B., Arroyo, J. (2013). Disentangling environmental correlates of vascular plant biodiversity in a Mediterranean hotspot. Ecol Evol 3:3879–3894. https://doi.org/10.1002/ ece3.762

Morelli, T.L., Daly, C., Dobrowski, S.Z., PLoS, D.D. (2016). Managing climate change refugia for climate adaptation. PLoS One 10.1371/journal.pone.0159909.t001

Ospedal, Ø.H., Scott Armbruster, W. & Graae, B.J. (2015). Linking small-scale topography with microclimate, plant species diversity and intra-specific trait variation in an alpine landscape, Plant Ecology & Diversity, 8:3, 305-315, DOI: 10.1080/17550874.2014.987330

Panitsa, M., & Kontopanou, A. (2017). Diversity of chasmophytes in the vascular flora of Greece : floristic analysis and phytogeographical patterns.

Polunin O. (1980). Flowers of Greece and the Balkans: a Field guide. Oxford University Press, Oxford.

Raimondo, F.M., Mazzola, P., Schicchi, R. (2001). Rapporti fitogeografico fra i promontori carbonatici della costa tirrenica della Sicilia. - Biogeographia 22: 65-77

Rosenbaum, G., Lister, G.S. & Duboz, C. (2002). Reconstruction of the tectonic evolution of the western Mediterranean since the Oligocene. Journal of the Virtual Explorer 8 107-130. https://doi.org/10.3809/jvirtex.2002.00053

Rundel, P.W., Arroyo, M.T.K., Cowling, R.M., Keeley, J.E., Lamont, B.B., Vargas, P. (2016) Mediterranean biomes: evolution of their vegetation, floras, and climate. Annu Rev Ecol Evol Syst 47:383–407. https://doi. org/10.1146/annurev-ecolsys-121415-032330

Sanz de Galdeano, C. & Ruiz Cruz, M.D. (2016). Late Palaeozoic to Triassic formations unconformably deposited over the Ronda peridotites (Betic Cordilleras): Evidence for their

Variscan time of crustal emplacement. Estudios Geológicos 72(1): e043. http://dx.doi.org/10.3989/egeol.42046.368.

Scherrer, D., Körner, C. (2010). Infra-red thermometry of alpine landscapes challenges climatic warming projections. Glob Change Biol 16:2602–2613

Scherrer, D., Körner, C. (2011). Topographically controlled thermal-habitat differentiation buffers alpine plant diversity against climate warming. Species Divers., 38 (2011), pp. 406-416, 10.1111/j.1365-2699.2010.02407.x

Schimper, A.F.W. & Faber, F.C. (1935). Pflanzengeographie auf physiologischer Grundlage, 1,2. Verlag von Gustab Fischer, Jena.

Silva Hernández de Santaolalla, J., Lim, S., Kim, S., Mejías, J. (2015). Phylogeography of cliff-dwelling relicts with a highly narrow and disjunct distribution in the Western Mediterranean. American journal of botany. 102. 10.3732/ajb.1500152.

Snogerup, S. (1971). Evolutionary and plant geographical aspects of chasmophytic communities. In: Davis PH, Harper PC & Hedge IC (eds.), Plant life of south-west Asia, pp. 157-170, Botanical Society of Edinburgh, Edinburgh.

Stebbins, G.L. (1980). Rarity of plant species: a synthetic viewpoint. Rhodora.; 82:77–86.

Strid,A. & Papanicolaou, K. (1985). The Greek mountains. In Gómez-Campo, C.(ed.): Plant conservation in the Mediterranean area, pp. 89-111.

Strid, A. & Tan, K. (eds.). (1997). Flora Hellenica 1. University of Copenhagen, Koeltz Scientific Books, Koenigstein.

Suc, J.P. (1984). Origin and evolution of the Mediterranean vegetation and climate in Europe. Nature. 307. 429-432. 10.1038/307429a0.

Suggitt, A.J., Gillingham, P.K., Hill, J.K., Huntley, B., Kunin, W.E., Roy, D.B. and Thomas, C.D. (2011). Habitat microclimates drive fine-scale variation in extreme temperatures. Oikos, 120: 1-8. doi:10.1111/j.1600-0706.2010.18270.x

Thompson, J.D. (2005). Plant evolution in the Mediterranean. Oxford University Press, Oxford

Thompson, J.D., Lavergne, S., Affre, L., Gaudeul, M., Debussche, M. (2005). Ecological differentiation of Mediterranean endemic plants. Taxon 54:967–976. https://doi.org/10.2307/25065481

Vera, J. A. (2004). Geología de España. Madrid: SGE-IGME.

White, P.S. & Miller, R.I. (1988). Topographic models of vascular plant richness in the southern Appalachian high peaks. Journal of Ecology,76, 192–199.

Chapter 1: The complexity of environmental factors: cliff microclimate

Introduction

The Mediterranean Basin is considered as a world hotspot of plant biodiversity (Myers et al., 2000). About 60% of the autochthonous species of this region are also endemic (Greuter, 1991; Quezel, 1985, 1995). Geographically, endemism rates in the Mediterranean are particularly relevant in certain areas, as for example on islands (Balearic Islands, Sicily, Crete, Sardinia) and on mountains (Alps, Sierra Nevada, Apennines) (*cfr*. Greuter, 1991; Médail & Quézel, 1997). While the overall floristic diversity is primarily attributed to the regional complex geological and climatic history (Thompson, 2005 and citations therein), terrain heterogeneity and especially limestone cliffs acted as ecological and microclimatic refugia, harbouring a great portion of rare and endemic species (Buira et al., 2020; Fois et al., 2017; Lavergne et al., 2004; Polunin, 1980; Snogerup, 1971; Thompson, 2005).

As in any other discrete habitats, the extant distribution of species able to colonise cliffs in the Mediterranean (but also on other locations) is affected by both climatic and non-climatic factors. Some generalist widespread Mediterranean species (e.g. *Erica multiflora, Salvia rosmarinus, Stipa offneri, Osyris alba*, etc) are less affected by the cliff specific microclimatic conditions. By contrast, chasmophytes (e.g. *Iberis semperflorens, Pseudoscabiosa limonifolia, Bupleurum dianthifolium, Silene sessionis, Hirtellina fruticosa*, etc.) are obligate cliff specialists, being adapted solely to a life on vertical and subvertical terrains (and often to specific orientations) and its microclimatic conditions. In this context, examining the microclimate created by cliffs is a fundamental key to understanding the ecology of chasmophytic species and to interpret species demographic, distribution and eco-physiological responses.

In recent years, a microclimate-based focus in ecological studies has been adopted in order to quantify the effects of anthropogenic climate change, whose ecological consequences on many species is becoming increasingly evident (e.g. Bellard et al., 2012; Lenoir & Svenning, 2015; Pauli et al., 2012; Pecl et al., 2017; Settele et al., 2014; Thackeray et al., 2016). Fine scale microclimatic conditions are found to be particularly variable in areas with high topographic roughness and rocky habitats (Bennie et al., 2008; Fawcett et al., 2019; Finkel et al., 2001; Garcia et al., 2020; Ospedal et al., 2014; Scherrer & Körner, 2010, 2011; Suggitt et al., 2011). In these areas, which include cliffs, topographic heterogeneity controls the amount of incoming solar radiation (see Larson et al., 2000 and citations therein). In turn, a decoupled irradiance influences different thermal profiles and soil moisture levels. Neglecting the effects of microclimate could then result in overlooking climatically suitable zones for a certain species, under both current and future conditions (Gillingham et al., 2012; Trivedi et al., 2008). This could in turn lead to failing to detect the allocation of potential microrefugia for certain narrow endemic species. In fact, within the coarse grid-size employed by climate models (typically 16 km^2), temperature may vary by as much as 33°C (Hijmans et al., 2005). By contrast, fine-scale field measurements are more appropriate when studying community compositional and structural changes related to local conditions. For example, it was found that fine scale measurements of annual temperatures within a similar elevation band in mountain areas, may vary more than 2 °C (Ackerly et al., 2010; Graae et al., 2012; Scherrer and Körner 2011). On mountain cliffs, other authors studied the close relationship between a narrow endemic taxon and its microtopographic-induced thermal habitat. The studied species lived exclusively under the shade of rock boulders and small cliffs, which were observed to have a synchronic temperature difference up to 13 °C compared to adjacent zones exposed to sun (Garcia et al., 2020).

In general, plant species experience climate at a fine scale and their suitable microclimatic conditions can significantly deviate from the macroclimate of the area where they grow (Bramer et al., 2018) (Fig. 1.1).

Fig. 1.1. Topographically controlled microclimates. The verticality of cliffs and their orientation influence airflow, inducing a differential condensation on North-oriented slopes. Monte Cofano, Italy. 12/2019

Measuring fine-scale climate variability often contrasts with the use of coarse-scale averages from meteorological stations. The distance between meteorological stations on the territory can be as much as 10,000-fold the body size of the species being studied (Potter et al., 2013). This in turn results in the limited utility of such data for the characterisation of species microclimatic niches (*cf.* Easterling et al., 2000; Parmesan et al., 2000). Moreover, criteria for the installation of meteorological stations are specifically designed to reduce local influences to the minimum (Bramer et al., 2018; WMO, 2018). According to Bramer et al. (2018) and Slavich et al. (2014), the use of such type of data in order to assess ecological processes that have a strong microclimate influence [as in the case of cliff areas] decreases the predictive accuracy of species' responses to climate change.

Differences in soil moisture, temperature and microclimate are correlated to both slope and aspect in the Qinghai-Tibetan plateau (Xue et al., 2018). Such differences can be mainly ascribed to the amount of received solar radiation (Bennie et al., 2018; Granger & Schulze; 1977). Cliffs, which represent areas with the highest level of slope, experience therefore the greatest variation in the exposure to sunny or shaded conditions according to their orientation. Moreover, it is known that spatial variation in the inclination gradient and orientation is a fundamental determinant of vegetation pattern, species distribution and ecosystem processes (Bennie et al., 2008; Scherrer & Körner, 2010, 2011).

In this study a combination of on-site meteorological data were used to examine: (1) how temperature (recorded in the open air, under the shade of vegetation, and directly on the ground), air relative humidity, and solar irradiance shape plant assemblages composition, structure and intraspecific trait variation on cliffs; the effect of different temperatures recorded in each sampling place was also considered; (2) how much North-South exposure and/or distance from the sea can influence the cliff microclimate in the Thermomediterranean and Mesomediterranean bioclimatic belts.

Materials and methods

Study design and site selection

Study areas were chosen to compare microclimate aspects related to the topographic discontinuity of a vertical cliff. Therefore, data obtained were by design in opposition to the recommendations about site selection of the World Meteorological Organisation (WMO, 2018: paragraph 1.3.3.1(a)). The study was carried out during one year in three locations, two in Sicily (Italy) and one in the Valencian Community (Spain) (Fig. 1.2). The study design was aimed at creating six independent, comparable datasets of abiotic variables known to influence plant fitness and species assemblages: temperature, relative humidity and solar irradiance.

Air temperature in the proximity of an object is affected by the nature and colour of the object's surface. In order to get comparable data, area selection was based on the lithology of the cliff surfaces. All areas were therefore chosen according to their lithological nature: compact white dolomitic limestone.

Country	Location	Meteorological station label	Sea influence	Altitude (Ellipsoid)	Coord 1	Coord 2	Starting - ending
Italy	Monte Cofano (COF)	COFN	Coastal	150.33	12.6677	38.1109	08/18 – 09/19
		COFS	Coastal	293.72	12.6707	38.1028	08/18 – 06/19
	Jato (JAT)	JATN	Inland	592.94	13.2088	37.9711	08/18 – 08/19
		JATS	Inland	599.34	13.2101	38.0025	08/18 – 08/19
Spain	Cabo de San Antonio (CSA)	CSAN	Coastal	140.41	0.1948	38.8041	03/18 – 04/19
		CSAS	Coastal	131.15	0.1956	38.8012	03/18 – 04/19

Table 1.1. Coordinates, label and location of the six installed meteorological stations. Coordinates and altitudes refer to the WGS84 ellipsoid (EPSG 4326). Sea influence refer to the proximity of the area to the coastline.

A total of six meteorological stations were installed (Table 1.1). A set of methodological constrains were applied both at regional and local scale for the standardization of measurements. For each study area a total of two meteorological stations were installed on opposite orientations. Following the World Meteorological Organization (WMO) guidelines on the characteristics and standard of meteorological measurements (WMO, 2018), the exposed vertical cliffs were located far from tree vegetation and from the influences caused by any adjacent micro-topographic discontinuity. In particular, the term micro-topography or local aspect refers to a set of narrow changes in the orientation of a cliff wall. These changes can naturally occur on any cliff area and at different extent. In the present context, the effect of exclusive North or South orientation on cliff microclimate was considered in the experimental design at both regional (distance among the different cliffs) and local (different micro-orientation of the same cliff) scale.

Accordingly, opposite cliffs of the local topographic unit were selected (Fig 1.2). At local level, sites were selected as suitable for the study when a square surface of 50x50 m, with a slope of 85-90° was present on the cliff.

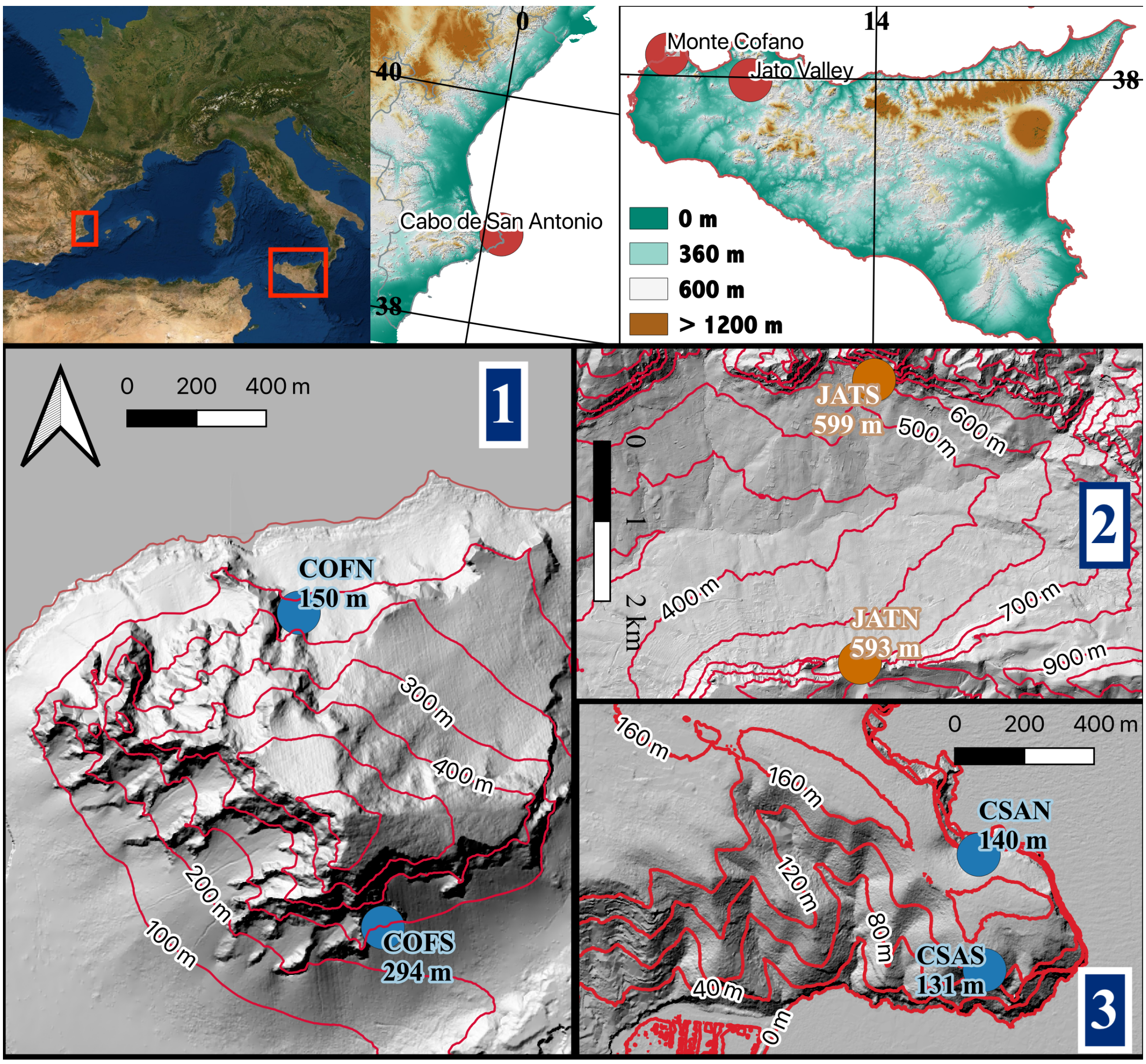

Fig. 1.2. The 3 areas selected for the placement of meteorological stations and their altitudes. 1: Monte Cofano (Italy). 2: Jato Valley (Italy). 3: Cabo de San Antonio (Spain). Blue labels indicate a coastal area. Brown labels indicate an inland area.

Two main environmental gradients were considered: orientation and influence from the sea. Local and regional geomorphological characteristics did not permit a standard altitude of installation for all meteorological stations. For this reason, the altitudinal gradient resulted entwined with some of the pairwise analyses and could not be avoided.

The Italian study area is situated in the Mediterranean biogeographic region, Western Mediterranean Subregion, Italo-Tyrrhenian province (Rivas-Martínez et al., 2004), Eusicilian sector, Western subsector, Drepano-Panormitan district (Brullo et al., 1995).

The Spanish study area is situated in the Mediterranean biogeographic region, Western Mediterranean Subregion, Balearic-Catalonian-Provençal province, Valencian-Catalonian sector (Rivas-Martínez et al. 2004)

Area 1. Monte Cofano coastal cliffs, Italy

Monte Cofano (38.10 °N; 12.66 °E), labelled COF (Table 1.1), is a coastal isolated mountain (659 m a.s.l.) on the North-West limits of Tyrrhenian Sicilian coast (Fig 1.2).

Due to its proximity to the sea and its extended limestone cliff systems hosting two of the model species used in this thesis (see Chapters 3 and 4) this area was selected to host meteorological stations. Two stations were installed at the base of a cliff in a Thermomediterranean bioclimatic belt (Bazan et al., 2015; Gianguzzi et al., 2005)

The first meteorological station, labelled COFN (COFano North), was installed on the North-oriented side of Monte Cofano at an elevation of 150.33 m (Table 1.1; Fig. 1.2, 1.3 A). The North-oriented cliff system where it was installed had a plain distance from the sea of 250 m and a total altitudinal range of 250 m. The continuity of the cliff wall is interrupted by several heterogeneous zones which form a steep slope rather than a continuous cliff face. Therefore, the meteorological station was installed on a locally continuous North-facing surface of 85-90° slope with a vertical extension of 35 m.

The second station of Monte Cofano, labelled COFS (COFano South), was installed on the South-facing cliff system of the area. It was located in exact opposition to COFN (Table 1.1.; Fig. 1.2, 1.3 B).

The height of the South-facing cliffs ranged between 200 and 400 m a.s.l. Overall, the vertical portion of the South-oriented cliff system was at a higher altitude than the North sector. The lowest cliff site suitable for the installation in accordance with the research design was at an altitude of 293.7 m. The plain geographic distance between COFS and COFN was 939 m.

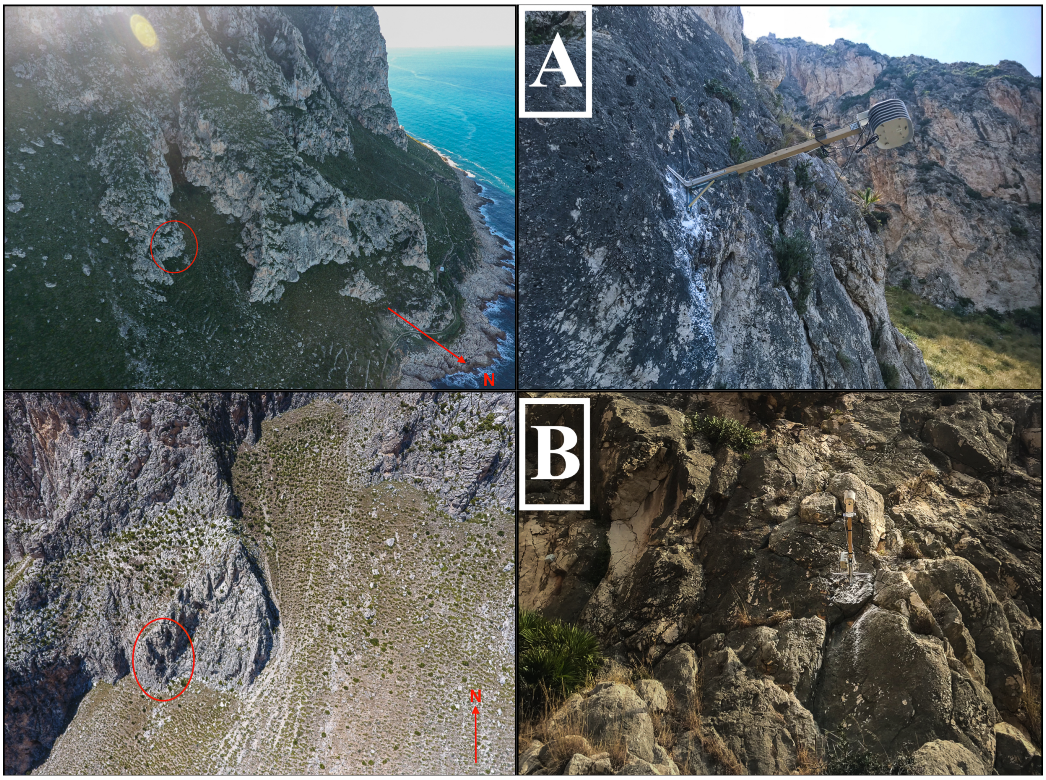

Fig. 1.3 The installation site of Monte Cofano. A: COFN. B: COFS

Area 2. Jato valley inland cliffs, Italy

The area denominated Jato is a valley situated in the northern sector of Western Sicily (37.99 °N; 13.21 °E) (Fig. 1.2). The Jato valley, labelled JAT, is delimited by 2 parallel systems of large structural mountains. These mountains ridges coincide with tectonic highs and were set on Mesozoic carbonate rocks (Di Maggio et al., 2017). Geomorphologically, they are anticline-type mountains, which were divided by a triangle zone-type river valley (Di Maggio et al., 2017). Both mountain ridges and intermediate valley followed a W-E direction, exposing the inner mountain cliffs to a N/S opposite orientation.

The meteorological stations installed at Jato were positioned on the opposite cliffs that closed the valley (Table 1.1; Fig. 1.2, 1.4). The North-oriented meteorological station of Jato valley (labelled JATN, JATo North) was installed on the Southern mountain ridge of the valley, on the mountain named Jato (Fig 1.4 A). By contrast, the South-oriented meteorological station (labelled JATS, JATo South) was positioned on the Northern mountain ridge, which is named Pizzo Mirabella (Fig 1.4 B). Both stations were positioned at the base of the corresponding cliff system. They both had a comparable altitude of ≅ 600 m in the Mesomediterranean bioclimatic belt (Bazan et al., 2015). The plain geographic distance between JATS and JATN was 3489 m.

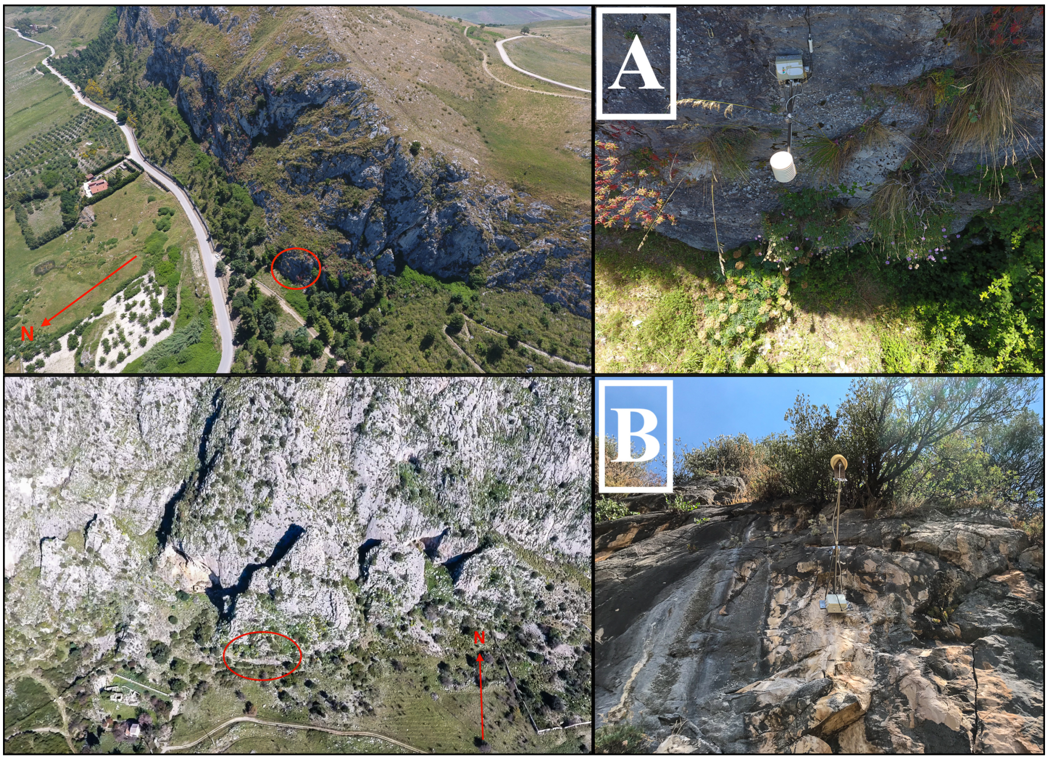

Fig. 1.4. The installation site of Jato Valley. A: JATN. B: JATS

Area 3. Cabo de San Antonio maritime cliffs, Spain

The area of Cabo de San Antonio, labelled CSA, is a small coastal cape in the Eastern Spanish province of Alicante, Spain (38.8 °N; 0.19 °E). Similar to Sicily, this coastal cape is located in an endemism-rich area (Medail & Quezel, 1997). In fact, Cabo de San Antonio represents the easternmost corner of the Prebetic mountain belt. The peninsula extends along a W-E axis. Coastal cliffs that characterise this area have an opposite North-South orientation and are located in a Thermomediterranean bioclimatic belt (Rivas-Martínez et al. 2004).

The two research zones were labelled CSAN (Cabo de San Antonio North) and CSAS (Cabo de San Antonio South) according to their opposite North-South orientation (Fig. 1.2; Table 1.1). The plain geographic distance between CSAN and CSAS was 333 m. CSAN (Fig. 1.5 A) had an altitude of 140.3 m, meanwhile CSAS (Fig 1.5 B) was 131.1 m. Both stations were installed at the ridge-end of the coastal cliff due to the impossibility to access to the site from the bottom.

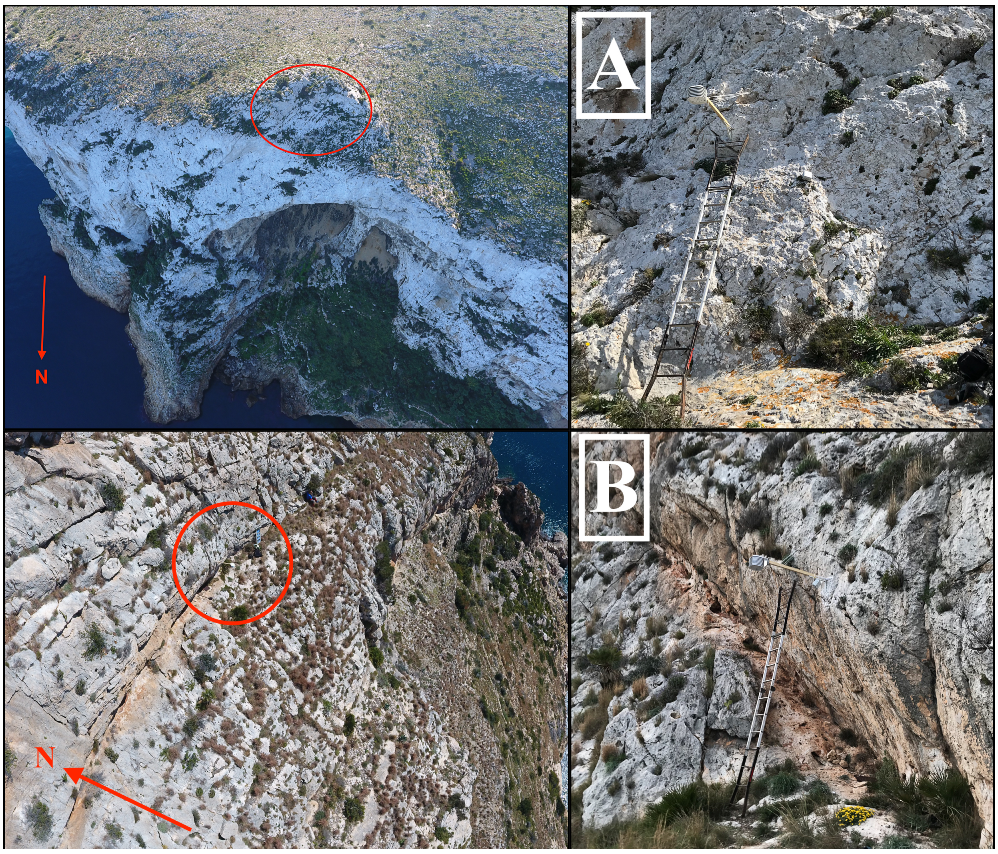

Fig. 1.5. The installation site of Cabo de San Antonio. A: CSAN. B: CSAS

Field measurements

The overall recorded microclimatic variables were (see also table 1.2 for more sensor details):

a) Solar irradiance (or solar radiation) in the range of 300-700 νm. This variable was recorded at a perpendicular distance of 1 m from the cliff surface. The unit used for its measurement was μmol $m^{-2}s^{-1}$ to the second decimal position. The sensors were positioned horizontally with respect to the ground.

b) Open air temperature (also denominated air temperature). This variable was measured at a perpendicular distance of 120 cm from the cliff surface. Air temperature values were measured in °C. Sensors were accurate to the third decimal position.

c) Air temperature under canopy. The sensor was positioned under the cover of a small shrub. The position was proximal to the cliff surface, but not touching the rock or the soil. The temperature sensor was positioned under the perpetual shade created by the small canopy. Air temperature under canopy values were measured in °C. Sensors (probes) were accurate to the first decimal position. The plants selected for the installation did not exceed a diameter of 50 cm. Used species for this purpose were: *Convolvulus cneorum* (COFS); (*Pseudoscabiosa limonifolia* + *Hieracium cophanense*) (COFN); *Stipa offneri* (CSAS); *Sanguisorba ancistroides* (CSAN) (see Appendix 1, Fig. S1.7).

d) Soil temperature. A small fracture in the vertical cliff was used to position the temperature sensor. The selected fracture was filled with soil and the sensor was positioned within the first 2 cm of soil in the fracture. Soil temperature values were measured in °C. Sensors (probes) were accurate to the first decimal position.

e) Air relative humidity (also denominated RH). The unit used for measuring relative humidity values was a %. Sensors were accurate to the first decimal position. This variable was measured at a perpendicular distance of 120 cm from the cliff surface.

Meteorological stations were installed on a 1 m long metallic or wooden beam (see Appendix 1, Fig. S1.5, S1.6). Each meteorological station was placed on the cliff wall at approx. 6 meters of height from the ground level. This distance permitted to lower the horizontal ground influence on the sensors (WMO, 2018). The beam was places perpendicularly to the cliff surface and parallel to the ground. Its purpose was to distance the sensors from the cliff surface. At the distal end of the beam, a solar radiation shield (model RS1, Onset Computer Corporation), which contained the sensors of air temperature and relative humidity, was installed. The summed length of the mechanical support and solar radiation shield placed the sensors 120 cm away from the cliff surface Sensors of solar radiation were as well positioned at the distal end of the beam. Conversely, their distance from the cliff surface corresponded to the length of the beam (100 cm). This field setup allowed the recording of air temperature and relative humidity measurements while minimising the thermal influence exerted by the cliff surface.

Temperature sensors used to measure soil and air temperature under canopy were inserted in selected zones of the cliff surface. All sensors were positioned within a 3 m radius from the meteorological station.

All variables were recorded at hourly intervals. Data download was manually retrieved, and field maintenance was planned with a frequency that allowed data download, battery replacement, and cleaning of the solar radiation sensors (usually one time per month).

The sampling period for each station is given in Table 1.1. The italian and the spanish datasets were not synchronic: the spanish measurements started in March 2018 and ended in April 2019; the Italian measurements started in August 2018 and ended in August/September 2019.

Due to technical constraints, a different setup of sensors and data loggers was used for each zone (Table 1.2). The area CSA (Spain) was not equipped with solar radiation sensors. The area JAT (Italy) did not measure air temperature under canopy.

Zone	Data loggers	Air temperature	Air temperature under canopy	Soil temperature	Relative humidity	Solar radiation
COFN	Spectrum technologies Watchdog mini series 1650	Spectrum technologies Watchdog mini series 1650	Spectrum technologies external probe	Spectrum technologies external probe	Spectrum technologies Watchdog mini series 1650	Spectrum technologies PAR sensor (450 – 700 vm) + UV sensor (300 -450 vm)
COFS	Onset HOBO Micro Station H21 002/ Spectrum technologies Watchdog model 400	Onset Temperature/ Relative Humidity Smart Sensor	Spectrum technologies external probe	Spectrum technologies external probe	Onset Temperature /Relative Humidity Smart Sensor	Onset solar pyranometer (300 – 1100 vm)
JATN	Onset HOBO Micro Station H21 002	Onset Temperature/ Relative Humidity Smart Sensor	x	Onset Temperature sensor	Onset Temperature /Relative Humidity Smart Sensor	Onset solar pyranometer (300 – 1100 vm)
JATS	Onset HOBO Micro Station H21 002	Onset Temperature/ Relative Humidity Smart Sensor	x	Onset Temperature sensor	Onset Temperature /Relative Humidity Smart Sensor	Onset solar pyranometer (300 – 1100 vm)
CSAN	Onset HOBO Pro v2 / Spectrum technologies Watchdog model 400	Onset HOBO Pro v2	Spectrum technologies external probe	Spectrum technologies external probe	Onset HOBO Pro v2	x
CSAS	Onset HOBO Pro v2/ Spectrum technologies Watchdog model 400	Onset HOBO Pro v2	Spectrum technologies external probe	Spectrum technologies external probe	Onset HOBO Pro v2	x

Table 1.2. Instrumental setup used for each zone.

In order to study the effect of microclimate on species distribution and density a plot-based sampling was performed on vegetation. Plot sampling was visually retrieved in April and May 2019 following the classic relevé method. Plant identification followed Pignatti (1982) for Italy and Castroviejo (1986) for Spain. The unit of sampling was a 3 x 3 m square and the cover was estimated using the original Braun-Blanquet scale (r, +, 1, 2, 3, 4, 5). Ten to 14 plots were taken in each zone. Plots were positioned not far from the meteorological stations and inside the boundary of the cliff surface. Microtopographic heterogeneity of the cliff surface was taken in consideration for plot size and placement. In order to cover all the possible rupicolous microhabitats plots covered a broad range of inclination classes and positions on the cliff. The 9 m^2 dimension was selected after previous trials as an intermediate working solution considering the high terrain heterogeneity and low plant density on cliffs (see also chapt. 2 and 3). A smaller grain size was found to excessively reduce the number of specimens encountered within the plot space. Conversely, a larger plot dimension jeopardized the importance of the slope threshold value of $\cong$ 50-60° for sampling a homogeneous cliff assemblage. In fact, larger plot dimensions produced a higher probability of sampling heterogeneous assemblages and ecotonal zones. Such difference in the biotic component is caused by the presence on cliffs of multiple environments, mainly produced by the relationship between slope angle and soil retention.

The coastal areas of COF (Italy) and CSA (Spain) were used to study the effect of coastal cliff microclimate on Intraspecific Trait Variability (ITV). In recent years, a growing evidence has accumulated on the ecological and evolutionary role of ITV in plant communities (Albert, 2015). Variability of functional traits at the specific level is particularly important at a local scale (*cfr.* Albert et al., 2011; see also: Siefert et al., 2015) and/or under strong environmental gradients (Carlucci et al., 2015). For the purpose of measuring ITV, seven plant species from COF and three from CSA were selected. Species were chosen for being abundant on plots in the North and South-oriented zones of each area. The selected species in COF were: *Asperula rupestris*, *Centaurea panormitana*, *Convolvulus cneorum*, *Helichrysum pendulum*, *Glandora rosmarinifolia*, *Lomelosia cretica*, *Seseli bocconei*. The 3 species selected in CSA were: *Sedum sediforme* subsp. *dianium*, *Centaurea rouyi*, *Sonchus tenerrimus* subsp. *dianae*.

Between April (CSA) and June (COF) 2019 two leaf traits (Specific Leaf Area or SLA; Leaf Dry Matter Content or LDMC) were measured. For each zone, ramets of each selected species were cut from 3 to 7 individuals. The sampling followed a 400 m long transect in a radius of 200 metres from the corresponding meteorological station. From each individual, 3 to 20 adult leaves were collected. The protocol for the storage and processing of plant material followed Pérez-Harguindeguy et al. (2013). Each ramet was stored in a plastic box between moist paper, immediately after collection. Plastic boxes were put during the field collection inside a refrigerator in order to avoid desiccation. Samples were afterward stored overnight in a cooling chamber (4°C) under dark conditions.

Leaves including the petiole were processed in the successive 24 hours from collection. First, fresh leaves were dried from excessive moist and weighted to measure the water-saturated fresh weight (Wilson et al., 1999). Subsequently, a photograph of the flattened leaves was taken using a DSLR camera. The leaf surface was then calculated from photos by using the image analysis software ImageJ (Rueden et al., 2017). Afterwards, samples were dried at 70°C for 72 h and dry weight was measured using an Acculab digital scale (accuracy 1 mg). SLA was expressed in cm^2/g, and LDMC was expressed in mg/g.

Statistical analysis

All meteorological variables except solar radiation were analysed by considering both their daily and hourly variability. A daily variation in any variable except solar radiation is defined as the 24 hours mean from 00.00 h to 23.00 h. For solar radiation this is meaningless, and daily mean was considered as the average diurnal variability. For this purpose, each dataset was partitioned in its diurnal and nocturnal composition, and only the diurnal portion of solar radiation was daily averaged. For this purpose, the sunrise/sunset hours for the closest city to the installed meteorological station were used.

The pyranometers installed in COFS, JATN and JATS measured the total solar radiation in W/m^2 in the range of 300 – 1100 νm. By contrast, the PAR and UV sensors installed in COFN recorded light intensity in the 300 – 700 νm range using Photon Flux Density (PFD) units (μmol m^{-2} s^{-1}). In order to compare the incoming solar radiation values among all zones, an *a-posteriori* conversion was performed. The 300-700 νm fraction of the daily averaged solar radiation was extracted from COFS, JATN and JATS. Subsequently, the obtained fraction was multiplied by a constant value of 2.5961 in order to convert it to μmol $m^{-2}s^{-1}$ (modified from McCree, 1981).

Maximum and minimum daily temperatures for each zone and each class of temperature measurement were extracted from hourly records. The difference between the daily maximum and minimum temperatures values (daily temperature range) was then calculated.

Maximum and minimum open air temperatures for each month were represented using barplots. Similarly, a barplot was used to represent the monthly average of the daily air temperature range (Fig. 1.9)

Meteorological data were plotted and compared in order to examine the dynamical characteristics of their temporal trends. Daily temperatures, temperature ranges and solar radiation were visualised using a moving average in order to smooth out short-term fluctuations. The monthly trend of variability along the measured period was computed using daily averages over sequential sets of 31 observations moving through time. Moreover, the moving average was centred (15 days before and 15 days after each day).

A boxplot visualisation was used to summarize relative humidity data. Hourly measures for each zone were grouped with respect to each month. Each boxplot showed the monthly median, upper and lower quartiles and extreme values. A trend line was drawn using the monthly median values in order to show seasonal trends.

Air temperature data for each zone were used to produce 6 bioclimatic predictors (Hijmans, 2004; Nix, 1986). The Bioclimatic predictors were used to condense the encountered seasonal trends with a single value. The calculated predictors were: Annual Mean Diurnal Range (BIO 02, measured in °C); Isothermality (BIO 03, °C); Temperature Seasonality (BIO 04, °C); Max Temperature of Warmest Month (BIO 05, °C); Min Temperature of Coldest Month (BIO 06, °C); and Annual Temperature Range (BIO 07, °C). These predictors were computed according to O'Donnell & Ignizio (2012).

Comparisons among different meteorological measurements followed three spatially hierarchical levels:

1. Within a zone. The subjects were temperatures taken at an incremental distance from the cliff surface within the same zone. The scope was to visualize the thermal influence of a cliff surface with respect to the received irradiance. For each zone monthly trends of soil temperature (maximum proximity), air temperature under canopy (proximal) and open air temperature (120 cm distant) were plotted together with the received solar radiation (Fig. 1.7).

2. Between two opposite oriented zones within the same area. The scope was to visualize the influence of opposite orientations on microclimate.
    2.1. The subjects were daily air and soil temperature ranges. For each area these variables were plotted together (Fig. 1.8)
    2.2. The subjects were air temperature, air temperature under canopy, soil temperature and solar radiation. A difference between the hourly records of the South-oriented zone and the corresponding North-oriented zone was calculated. For each listed variable, the monthly trend of variability of such difference was plotted according to the corresponding area (Fig. 1.10).
    2.3. The subject was relative humidity. Hourly records of relative humidity were grouped in boxplots with respect to each month. Boxplots were pairwise visualised according to opposite zones of the same area (Fig. 1.11). Moreover, a North-South difference within an area between corresponding hourly values was calculated. The scope was to visualise within a 24 h span any potential repeating pattern of difference in relative humidity. For each area, a scatterplot of the hourly differences of relative humidity among zones was produced (Fig. 1.12). Values were grouped with respect to their month and hour within the day.
3. Between two zones with a same orientation but with different distances from the sea. The scope was to visualize the influence of sea proximity on relative humidity. Only the Italian areas of JAT and COF were compared due to their synchronic records and geographic unity. Hourly records of relative humidity were grouped in boxplots with respect to the month of record. Boxplots of two different areas were pairwise visualised according to their equal North or South orientation (Fig. 1.11d,e).

All calculations and data visualisation of the meteorological variables were performed using the software Microsoft Excel and Tableau (www.tableau.com).

The Italian fraction of species and meteorological data was used for the analysis of the species distributional properties with respect to microclimate. The choice to analyse only the Italian data took in consideration the presence of 4 synchronic meteorological datasets.

A redundancy analysis (RDA), a form of constrained multivariate analysis, was used to interpret the explanatory effect of microclimate on species abundances. Prior to the analysis, species cover was transformed in a 1-9 scale following van der Maarel (1979). The species cover matrix was Hellinger transformed prior to the ordination analysis. Explanatory variables used for the canonical ordination were the 6 calculated bioclimatic predictors.

The resulting ordination was visualised as a correlation triplot. Following the suggestions of Oksanen (2019), sites were plotted using their weighted sums of species (wa scores). A scaling 1 was used for visualising the correlation triplot (Legendre & Legendre, 2012). In order to produce a clear and exhaustive visualisation of response variables in the triplot space, species are plotted in 2 groups the same multivariate space. The first group represents species with a goodness of fit ≥ 0.3. The second group is formed by those species with a goodness of fit between 0.1 and 0.29 [package vegan, function "goodness"]. The 2 groups are plotted using a different colour and multiplying factor in order to obtain a clear visualisation. To obtain this result it was used the function "ordiArrowMul", which finds the correct multiplier for the coordinates of the head of the vector such that they occupy fill proportion of the plot region (Oksanen, 2019).

Furthermore, both the adjusted and unadjusted R2 values were extrapolated (Peres-neto et al., 2006). ANOVA like permutation tests were performed to test the global significance of the RDA analysis and the significance of each of its axes. A significance test for each term (constraining variable) in the presence of all the other variables in the model was also performed [permutation by = 'margin'] (Legendre et al., 2011).

The ordination was implemented in R 3.6.1 (R Core Team 2019) using the R studio interface (RStudio Team, 2018) and the package "vegan".

The mean of SLA and LDMC values for each species in each zone was calculated. Intraspecific leaf-trait variability as mean and median values was compared among opposite zones. A parametric and a non-parametric statistical test were used: Mann-Whitney U and Student. The parametric Student test was produced only when the distribution of data resulted normal with a $P < 0.05$ or if the sample comprised > 20 measurements.

Results

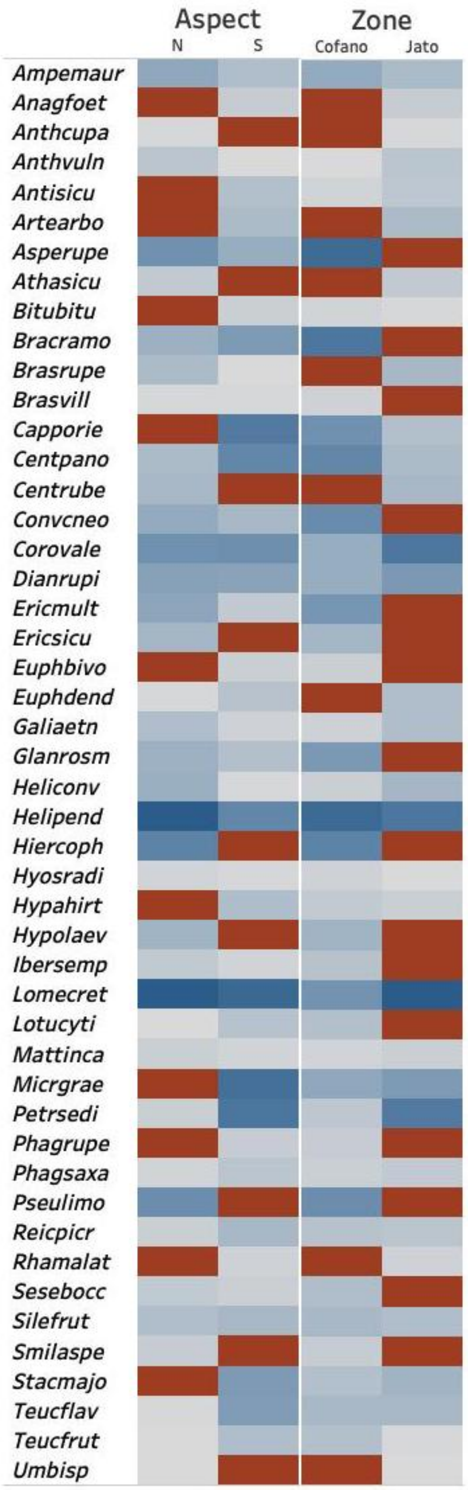

Fig. 1.6. Community compositions of Jato and Cofano. Red are absences; blue gradient represents species relative abundances. For an acronym list see Table 1.3 (next page).

In total, 48 species were recorded on the cliffs of the two Sicilian sites, Cofano and Jato (Table 1.3). The two plant communities differed both in their floristic composition and abundances (Fig 1.6). Jato showed a lower species diversity, with 66.67 % (32) of the total recorded species. By contrast, 81,25 % (39) of the entire species pool was found on Cofano.

When considering orientation, 9 species were recorded exclusively on the North cliffs (18.75 %), meanwhile 11 species (22.92 %) were found exclusively on the South-oriented cliffs. A total of 27 species (56.25 %) were found on both North and South oriented cliffs.

A total of 15 species (31.25 %) were endemic of South Italy. Endemic species were found mostly in the coastal areas of Cofano (13 endemic species). By contrast, 6 endemic species were encountered in the inland cliffs of Jato. Interestingly, 9 of the 13 endemic species of Cofano were also recorded only in this area. Moreover, the narrow endemic cliff exclusive species *Erica sicula, Hieracium cophanense* and *Pseudoscabiosa limonifolia* were recorded only on the North-oriented zone of Cofano. Generally, a higher amount of endemic species was found on North-oriented cliffs (14) then on South-oriented zones (11).

Overall, only a fraction (17) of the recorded species had a preferential rupicolous ecology (primary habitat on vertical zones). The sampling strategy adopted for this study included in the plot space a heterogeneous range of cliff environments with respect to inclination and position on the cliff wall. As a result of the cliff boundaries inclusion, some of the encountered species were both preferentially rupicolous and pertaining to the Mediterranean dry grasslands (e.g. *Ampelodesmos mauritanicus* and *Bituminaria bituminosa)*.

The majority of preferential rupicolous species were found both on North and South aspects (13). The residual rupicolous species (*Hieracium cophanense*, *Athamanta sicula*, *P. limonifolia* and *E. sicula*) were recorded only on North-oriented cliffs. Moreover, the majority of these species (9; 52.94 %) were encountered exclusively on the coastal cliffs of Cofano. By contrast, only 2 preferential rupicolous species were exclusively encountered on Jato inland cliffs.

Ampelodesmos mauritanicus (POIR.) T. DURAND & SCHINZ	Ampemaur	*Helichrysum pendulum* (C. PRESL) C. PRESL*	Helipend
Anagyris foetida L.	Anagfoet	*helictotrichon convolutum* (C. PRESL) HENRARD	Heliconv
Anthemis cupaniana TOD. EX NYMAN *	Anthcupa	*Hieracium cophanense* LOJAC.**	Hiercoph
Anthyllis vulneraria subsp. *maura* (BECK) MAIRE	Anthvuln	*Hyoseris radiata* L.	Hyosradi
Antirrhinum siculum MILL.	Antisicu	*Hyparrhenia hirta* (L.) STAPF	Hypahirt
Artemisia arborescens L.	Artearbo	*Hypochaeris laevigata* (L.) CES., PASS. & GIBELLI	Hypolaev
Asperula rupestris TINEO*	Asperupe	*Iberis semperflorens* L.*	Ibersemp
Athamanta sicula L.*	Athasicu	*Lomelosia cretica* (L.) GREUTER & BURDET*	Lomecret
Bituminaria bituminosa (L.) C.H. STIRT.	Bitubitu	*Lotus cytisoides* L.	Lotucyti
Brachypodium ramosum (PERS.) P. BEAUV.	Bracramo	*Matthiola incana* subsp. *rupestris* (RAF.) NYMAN*	Mattinca
Brassica rupestris RAF. subsp. *rupestris**	Brasvill	*Micromeria graeca* (L.) BENTH. EX RCHB.	Micrgrae
Brassica villosa subsp. *drepanensis* (CARUEL) RAIMONDO & MAZZOLA*	Brasrupe	*Petrosedum sediforme* (JACQ.) GRULICH	Petrsedi
Capparis orientalis VEILL.	Capporie	*Phagnalon rupestre* (L.) DC.	Phagrupe
Centaurea panormitana LOJAC.*	Centpano	*Phagnalon saxatile* (L.) CASS.	Phagsaxa
Centranthus ruber (L.) DC.	Centrube	*Pseudoscabiosa limonifolia* (VAHL) DEVESA**	Pseulimo
Convolvulus cneorum L.*	Convcneo	*Reichardia picroides* (L.) ROTH	Reicpicr
Coronilla valentina L.*	Corovale	*Rhamnus alaternus* L.	Rhamalat
Dianthus rupicola BIV. subsp. *rupicola**	Dianrupi	*Seseli bocconei* GUSS.*	Sesebocc
Erica multiflora L.	Ericmult	*Silene fruticosa* L.*	Silefrut
Erica sicula GUSS.*	Ericsicu	*Smilax aspera* L.	Smilaspe
Euphorbia bivonae STEUD.	Euphbivo	*Stachys major* (L.) BARTOLUCCI & PERUZZI	Stacmajo
Euphorbia dendroides L.	Euphdend	*Teucrium flavum* L.	Teucflav
Galium pallidum C. PRESL	Galiaetn	*Teucrium fruticans* L.	Teucfrut
Glandora rosmarinifolia (TEN.) D.C. THOMAS*	Glanrosm	*Umbilicus sp* DC.	Umbisp

Table 1.3. Species encountered in the Italian study areas and their abbreviations. Species marked with * are preferential rupicolous species. ** = narrow endemic chasmophytes.

A

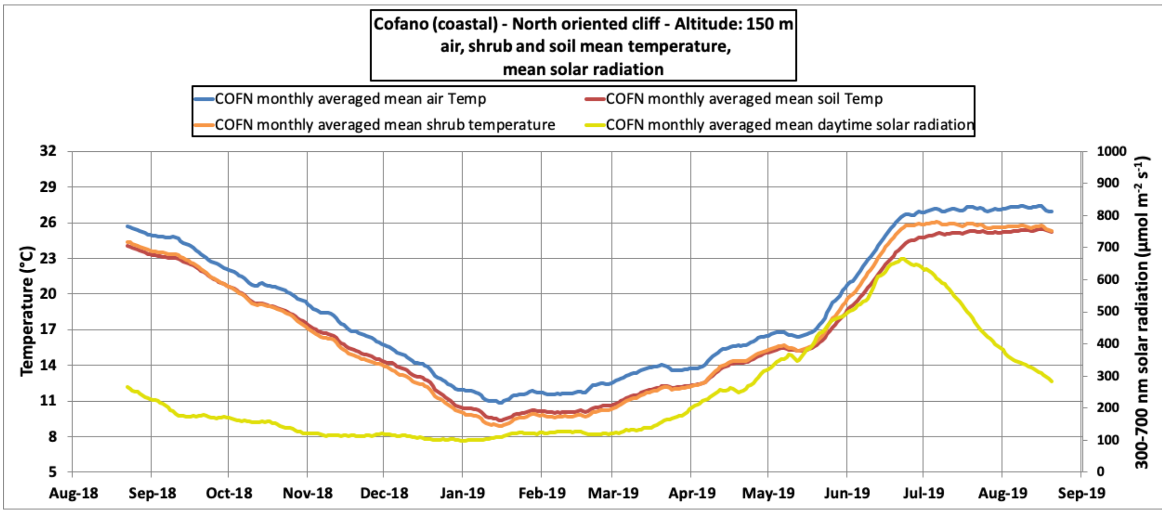

B

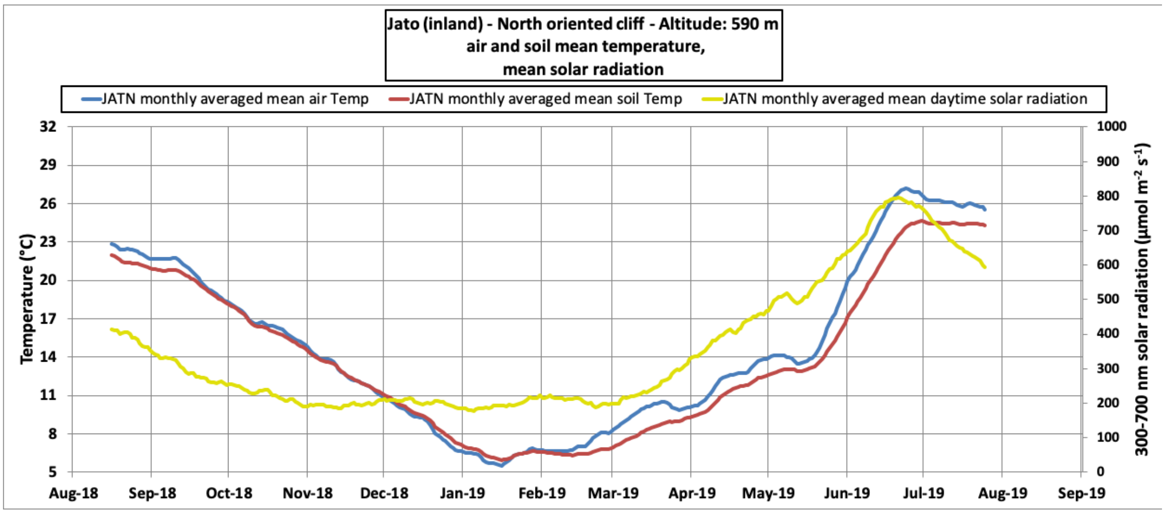

C

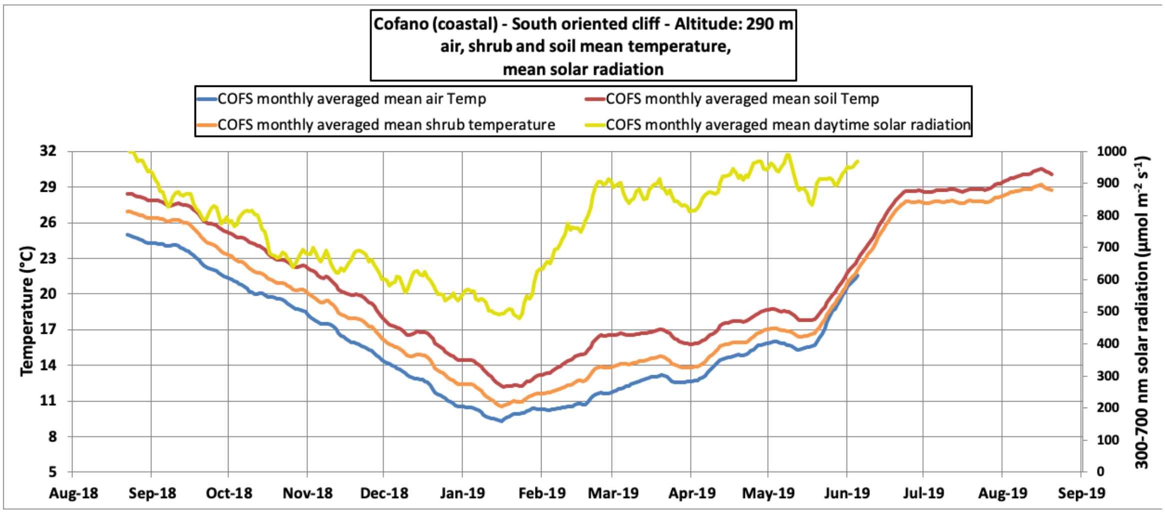

Fig. 1.7. Continue

D

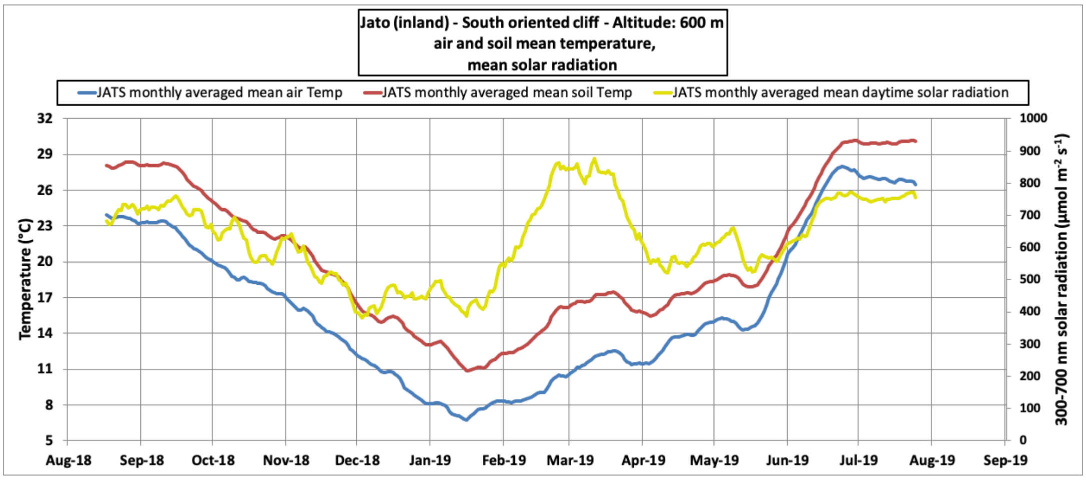

E

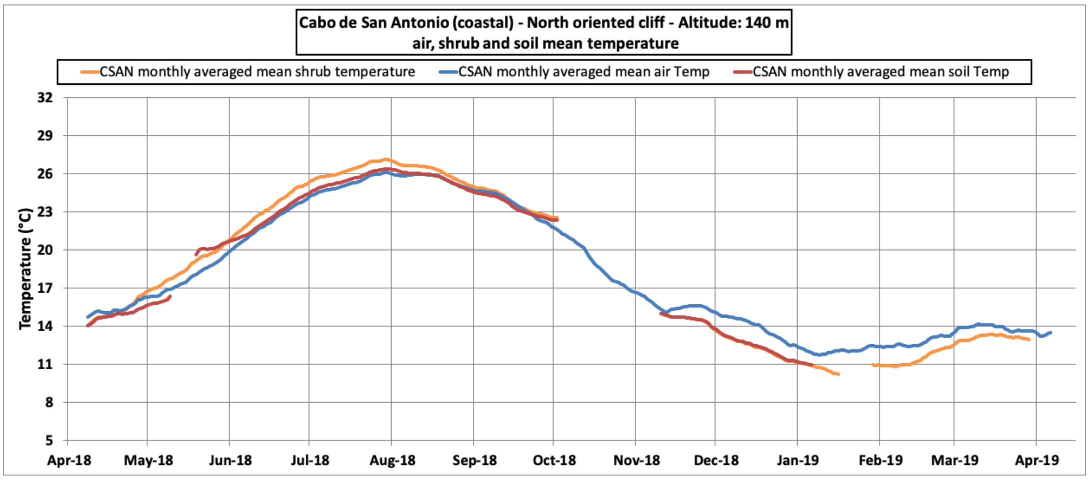

F

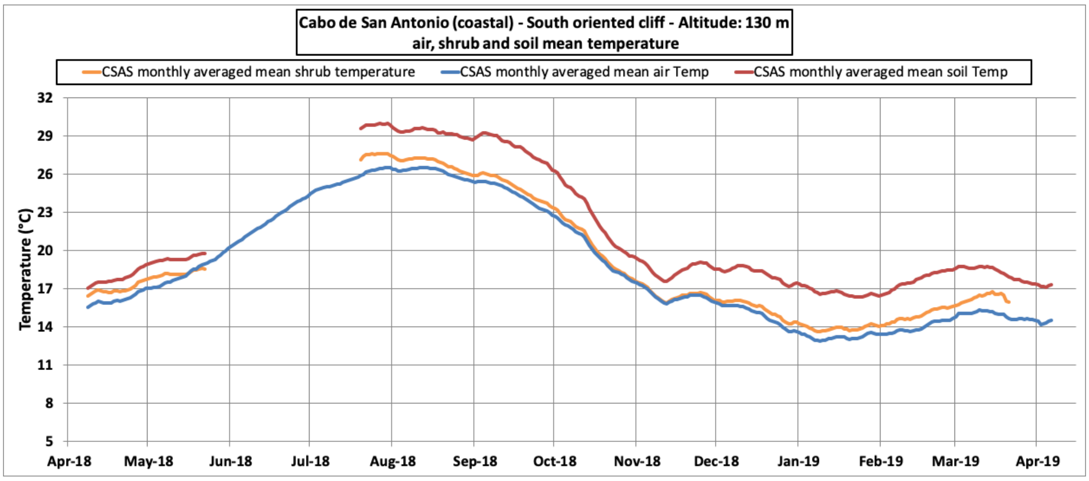

Fig. 1.7. The simultaneous annual trend of solar radiation (yellow), air (blue), vegetation shaded (orange) and soil (red) temperatures for a North or South oriented cliff. Each graph refers to a zone within a research area. Each trend line represents a centred moving average of daily values of order 31 days. Each unit of the X axis represents the first day of the corresponding month. The average value of trend lines for a month can be read between two units of the X axis.

Fig. 1.7 shows the temperature and solar radiation fluctuations recorded in the study sites. In the areas of Jato (Fig. 1.7b and 1.7d) and Cofano (Fig. 1.7a and 1.7c) the solar irradiance sensors exposed a pattern of superposition between the trends of incoming solar radiation and temperature along the year.

The annual trends of incoming solar radiation were very similar when considering the same geographic orientation. A figure displaying simultaneously all recorded values of solar radiations (Fig. S1.1) and air temperatures for a same orientation (North: Fig. S1.2; South: Fig. S1.3) is provided as an appendix. COFN was the most shaded area, whereas COFS the most exposed. Both the South-oriented cliffs of COFS and JATS experienced a saw-tooth profiled reduction in solar irradiance. This decrease started in September and reached the minimum values in December and January. The trend showed a steep increase in February and peaked in March. The irradiance in COFS was constant for the rest of the spring and in summer. In this period JATS experienced a relevant localised weakening of solar radiation (Fig. 1.7d, April and May 2019). This local behaviour could be attributed to the annual stochasticity of weather conditions. Another possible explanation is the shading profile of the monitoring site with respect to the surrounding topographic units.

By contrast, the North-oriented cliffs of COFN and JATN received a very limited amount of solar radiation for almost all the monitored period. A few peaks for both zones were recorded at the end of June.

By comparing the recorded synchronous temperatures of soil, air under canopy and open air, it can be seen a general trend of increment correlated with the cliff proximity. South-oriented cliffs displayed the strongest pattern of such behaviour. For COFS (Fig. 1.7c) and JATS (Fig. 1.7d) the temperature difference between air and soil synchronically peaked with irradiance. In fact, in February and March solar radiation average values increased up to ≅ 850 μmol $m^{-2}s^{-1}$ for JATS and up to ≅ 900 μmol $m^{-2}s^{-1}$ for COFS. In this period the temperature difference between air-shrub, shrub-soil and air-soil was maximal: COFS, respectively ≅ 3 °C; 2 °C; 5 °C; JATS, air-soil ≅ 6 °C).

Conversely, in the North-oriented cliffs weak differences in temperature values were recorded between air and soil. Moreover, in these zones the temperature trends of soil and air under canopy were very similar. In COFN and JATN the air-soil difference reached its maximum in the summer months, when the trend of solar radiations reached values of ≅ 660 μmol $m^{-2}s^{-1}$ and ≊ 800 μmol $m^{-2}s^{-1}$, respectively. For these areas the maximal air-shrub, shrub-soil, air-soil differences were: COFN, respectively ≊ 1 °C; 1 °C; 2 °C; JATN, air-soil ≊ 3 °C.

A

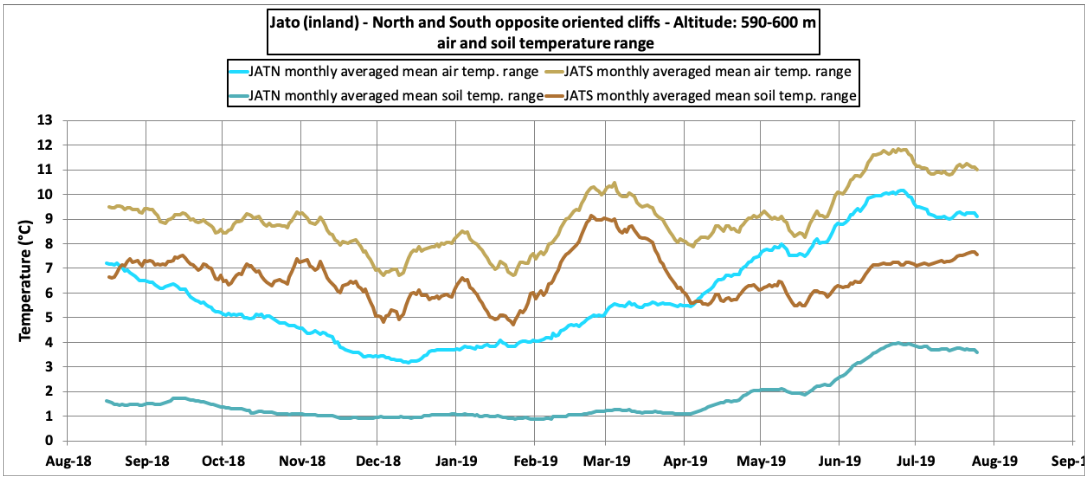

B

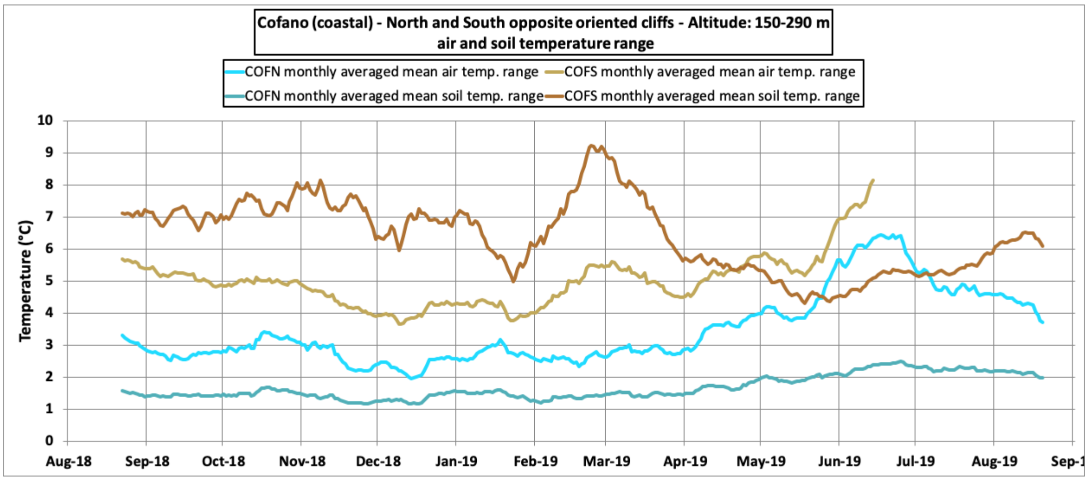

C

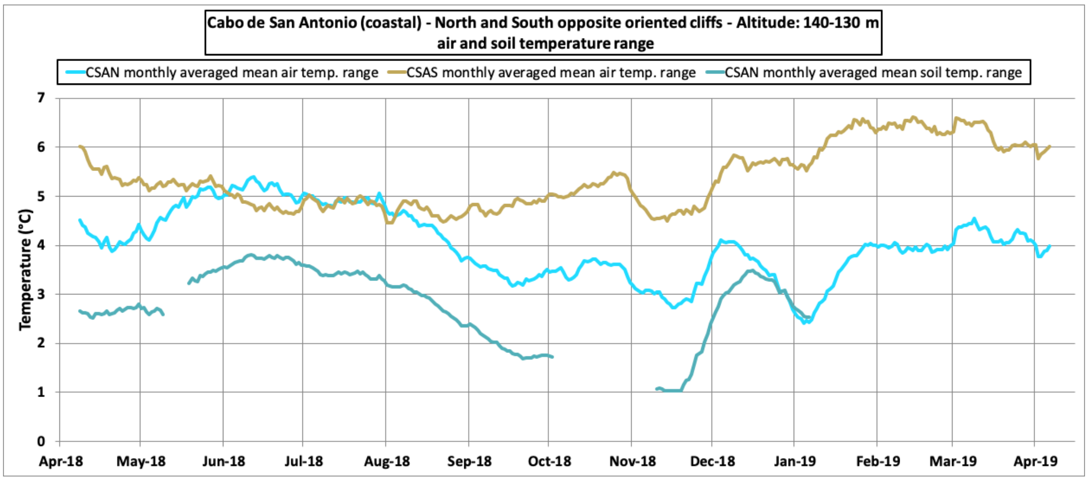

Fig. 1.8 shows the monthly averaged daily air (pale brown and light blue) and soil (dark brown and brilliant blue) temperature ranges for a same area. Graphs refer to the areas of Jato, Cofano and Cabo de San Antonio. Each trend line represents a centred moving average of daily values of order 31 days. Each unit of the X axis represents the first day of the corresponding month. The average value of trend lines for a single month can be read between two units of the X axis.

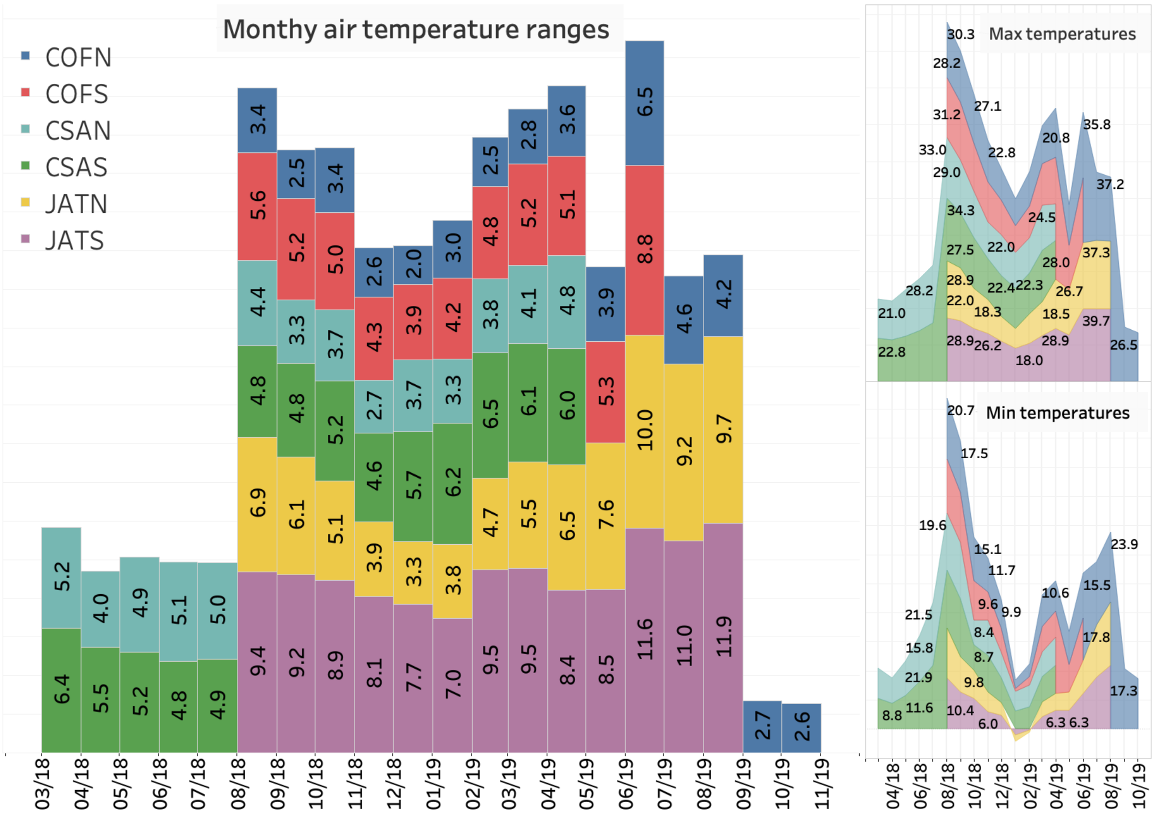

Fig. 1.9. Left: monthly air temperature ranges. Displayed values are the monthly averaged values of the daily temperature ranges. Right: extreme values of temperatures: temperature maximum (up-right) and minimum (down right) values for the studied areas. Values refer to the daily minimum and maximum for each recorded month.

The annual trend of daily temperature ranges can be seen in Fig. 1.8. It can be noted that the temperature ranges of COF (Fig. 1.8b) and JAT (Fig. 1.8a) showed a similar profile of the solar radiation trends seen in Fig. 1.7a-d. For North-oriented areas, soil temperature ranges were always less extended than the respective air ranges. This behaviour was also observed in the inland South-oriented area of Jato. By contrast, soil temperature ranges in the south oriented coastal zones of COFS and CSAS exceed for most of the year the corresponding air ranges.

The minimum variability of daily temperature ranges was observed in the North-oriented cliffs. Soil daily temperature ranges varied in JATN from ≅ 1°C (main value) to up to ≅ 4 °C, meanwhile COFN values were stable around ≅ 1.5 °C for almost all year. The most variable soil temperature ranges for a North-oriented cliff were recorded in CSAN, with a daily difference of up to ≅ 3.8 °C.

Fig. 1.9 (left) provides an overall visualisation of the monthly averaged daily air temperature fluctuations. It can be seen that fluctuations in air temperature were reduced in the North-oriented cliffs. Another aspect to be underlined was that inland cliffs of JAT exhibited the largest ranges. The South-oriented zone of JAT for instance showed the overall highest variability, with a minimum of 7 ± 2.9 °C in January (peak of Winter) to up to 11.9 ± 2.2 °C in August (peak of Summer). The North-oriented cliffs of this zone were less variable, with a minimum of 3.3 ± 0.9 °C in December to a maximum of 9.7 ± 2.1 °C in August and 10°C in June. On the other hand, it is also easy to see that ranges were less severe in coastal areas. North oriented cliffs of the Spanish zone CSA exhibited a variation in ranges between 2.7 ± 1.2 °C in November and 5.2 ± 1.7 °C in March. The amplitude of daily temperature fluctuations was even less extended for the North-oriented coastal cliffs of the Italian area of Cofano. There, the range variation was almost constant for the entire year, with a minimum value of 2 ± 0.9 °C in December and a maximum of 6.5 ± 2.7 °C in June. The ranges of variation in Southern coastal cliffs were proportionally larger. COFS exhibited a minimum variation of 3.9 ± 1.2 °C in December and a maximum of 8.8 ± 3.1 °C in June. Finally, the South oriented cliffs of CSA showed a similar behaviour of COFS, with an overall range between 4.6 ± 1.7 °C and 6.5 ± 1.6 °C.

The fluctuations of air temperatures along the year are resumed by the diurnal range of air temperatures index (BIO 02). Values of this year-based index were in accordance to what previously stated for daily temperature ranges: South-facing vertical cliffs suffered higher fluctuations respect to Northern areas, and temperature ranges grew with the sea distance. BIO 02 index was ≊ 20°C for JATS and ≊ 14°C for CSAS and COFS. Conversely, the North-facing cliffs marked lesser annual temperature ranges, from ≊ 16°C (JATN) to ≊ 12 °C (COFN and CSAN).

The values of BIO 02 condensed the air temperature annual trends of each areas expressed in Fig.1.7. In general, it is notable the similarity of COF and CSA which had a comparable altitude, latitude (38.1° and 38.8° N, respectively) and distance from the sea. BIO 02 values and the amplitude of the sinusoidal trends in Fig. 1.7a,c,e,f showed a limited annual temperature fluctuation. On the other hand, JAT was positioned more inland and less prone of sea mitigation. BIO 02 values and Fig. 1.7b,d showed that the sinusoidal curves of annual air temperatures were more pronounced. In fact, this zone exhibited higher annual temperature fluctuations respect to the coastal areas.

Both trends of yearly and daily air temperature fluctuations are confirmed by observing the BIO 05 (annual maximum recorded air temperature) and BIO 06 (annual minimum recorded air temperature) values. They were more extreme for the inland area of JAT (max ≊

36 °C, min ≅ -2 °C N; max ≅ 40 °C, min ≅ -2 °C S) compared to the coastal cliffs of COF (max ≅ 36 °C, min ≅ 3 °C N; max ≅ 35 °C, min ≅ 1 °C S) and CSA (max ≅ 33 °C, min ≅ 7 °C N; max ≅ 34 °C, min ≅ 6 °C S). From the barplots in Fig. 1.9 (right) it is possible to observe the values of temperature extremes for each month. Finally, it has to be underlined that only the inland area of JAT was subject to negative temperatures.

Fig. 1.10 provide information about the differences of a same variable between opposite cliffs of a geographic area. Fig. 1.10a and 1.10b showed together temperature and solar radiation trends of difference in the areas of JAT and COF. As for in the previous graphs (Fig. 1.7a-d), also differentials among zones formed a pattern of superposition between solar radiation and temperature.

It can be seen that air temperatures among opposite orientations expressed the least variability in confront to other variables. By contrast, temperatures of soil and air under vegetation were the most different among opposite zones. Furthermore, in any area the air temperature differences were overall considerably steady.

The monthly averaged air temperatures on the South cliffs of JAT were between ≅ 0.7 °C and 2.4 °C higher than the corresponding North-oriented zone (Fig. 1.10a). CSA instead showed a lesser difference: ≅ 0.1 °C to 1.3 °C (Fig. 1.10c). Contrarily to other areas, air temperatures in Cofano were overall colder on the South-oriented zone (a difference of ≅ -1.5 °C to 0 °C) (Fig. 1.10b).

It was also found that differences among South/North-oriented zones were increasing in proportion to the proximity of the measure to the cliff surface A similar behaviour was previously observed for the soil-shrub-air temperature trends in a single orientation (graphs 1.1-1.6). Soil temperatures between JATS and JATN displayed a maximum difference of up to ≅ +9.4 °C in the early spring. The same variable in that period was less pronounced in COF (≅ +5.9°C). The trend of difference in air temperatures under canopy (Fig. 1.10b,c) appeared intermediated between those of air and soil. It can be also observed that such difference displayed a similar trend with the shape of the soil temperature differential. Contrarily to soil differences, the trend lines of air temperatures under canopy were overall ≅ 2 °C to 3 °less pronounced.

A

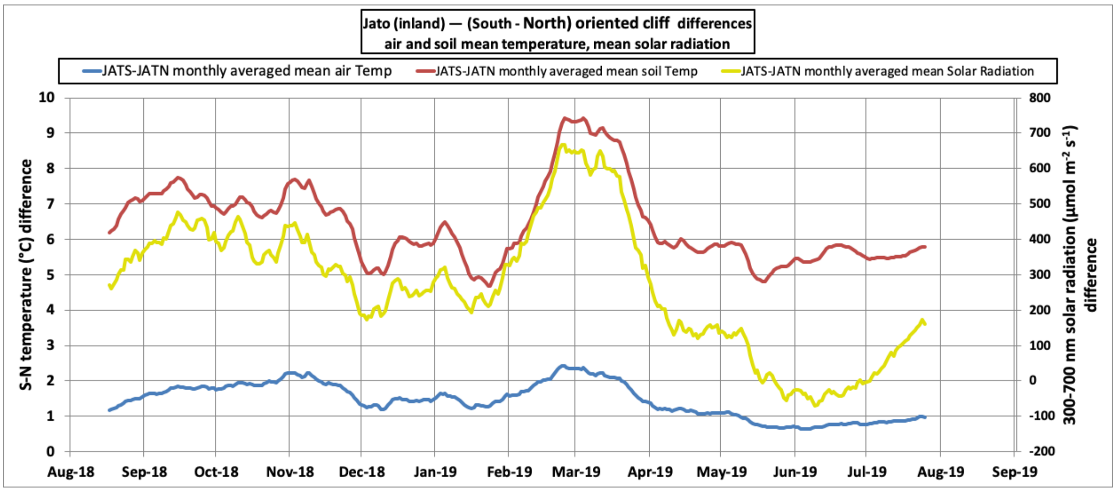

B

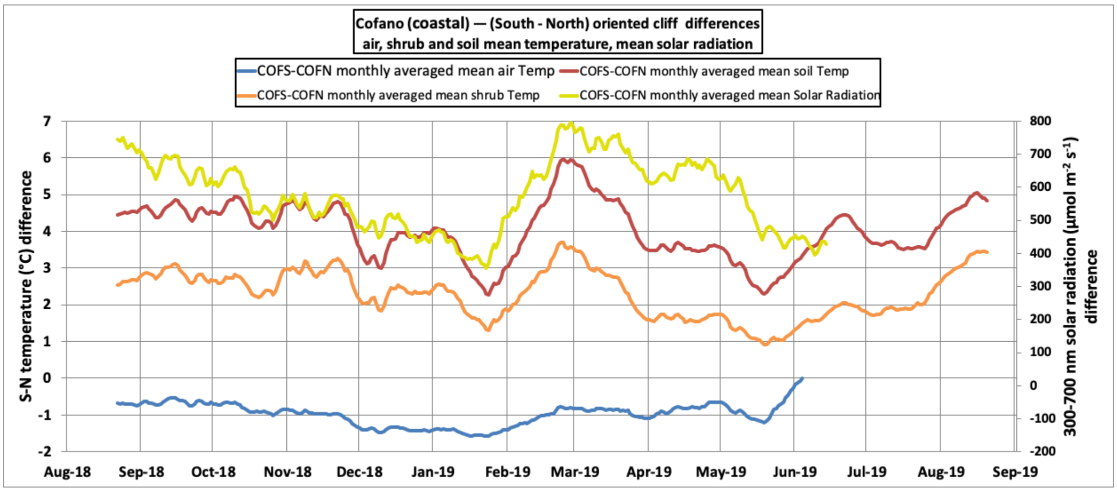

C

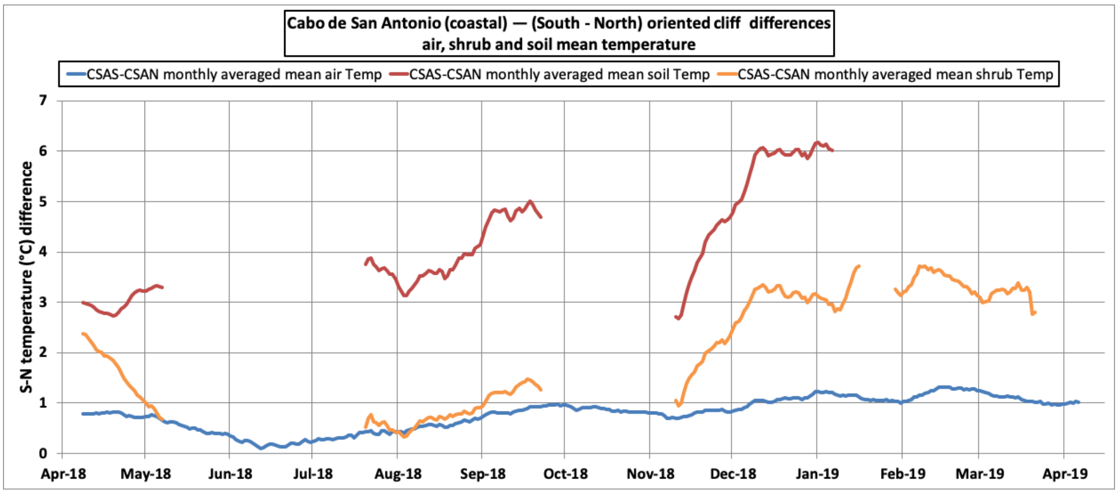

Fig. 1.10. Trend of the differences between a South and a North exposed cliff in a same area. The calculated differences refer to the 31 days moving average daily means among zones. Illustrated variables are: solar radiation Δ (yellow), air temperature Δ (blue), vegetation shaded temperature Δ (orange) and soil temperature Δ (red).

The maximum values of differentiation coincide with the averaged uppermost difference in solar irradiance for the area (≅ 670 and 800 μmol $m^{-2}s^{-1}$ for JAT and COF, respectively). Also, following the local trend of solar radiations, the soil temperature differences in JAT were stable between ≅ +7 and ≅ +8 °C in autumn and ≅ +5/+6° in Winter, late Spring and Summer. In COF the differences were stable between ≅ +4 and ≅ +5 °C in Autumn, for most of the Winter and in Summer, meanwhile were less severe in January and late Spring. Although soil and vegetation shaded T data for CSA were fragmentary, the same trend could be visible with values to up to ≅ +6 °C of soil temperature differences.

Boxplots in Fig. 1.11 show the monthly distribution of relative humidity among different areas. The coastal cliffs of COF and CSA (Fig. 1.11 a,c) received an overall high and continuous amount of relative humidity along all year. Moreover, the North-oriented cliffs of these zones exhibited a similar pattern of RH distribution, with a constant increase in Summer and Autumn. However, this behaviour was more emphasized in CSAN. RH values in the North-oriented cliffs of Cofano were particularly constant along the year (medians of ≅ 60 % to ≅ 70 %). By contrast, the South-oriented zones of this area were in general more humid (medians of ≅ 70 % to ≅ 75 %) but differed substantially in the summer months. During this period, COFN maintained its constant humidity values, whereas COFS dropped substantially to a median of ≅ 55% in June. (Fig. 1.11a). Conversely, the opposite oriented areas of CSA (Fig. 1.11 c) were overall more humid than the corresponding areas in COF. Moreover, there was no substantial humidity drop in the South cliffs. In fact, CSAN and CSAS had a similar annual trend of relative humidity, with a median of ≅ 65 % to ≅ 70% between the late Autumn and Winter and ≅ 70 % to ≅ 82% in the rest of the year. The South oriented areas here were always ≅ 3 % to ≅ 8% less humid than the North ones. The differential in humidity among areas was especially marked in winter months.

The inland areas of JAT were characterised by a bimodal distribution of relative humidity along the year (Fig. 1.11 b). Winter months were especially humid in this area, with median values between October and January of ≅ 80 % to ≅ 85 % for JATN and ≅ 71 % to ≅ 80 % for JATS. Conversely, Spring exhibited an increasing drop in air humidity, with a median value of ≅ 70 % for JATN and ≅ 62 % to ≅ 68 % for JATS. The trend of reduction in air humidity continued during summer months. June and July were in fact characterised by an additional and considerable drop. Median values for these months were ≅ 44 % to ≅ 47 % in North oriented areas and ≅ 41 % to ≅ 45 % in South-oriented ones.

Fig. 1.11d,e confronted the monthly distribution of RH in a same orientation with respect to a gradient of proximity to the sea. Despite the fact that winter months were more humid in JATN (a median of RH between ≊ 10 to 25 points higher in January and February), the coastal cliffs of COFN received a constant relative humidity throughout all year. This behaviour differentiated the two areas especially in the summer months, where the RH values of JATN dropped to almost 20 points less than COFN.

Another difference between South and North oriented cliffs consisted in the RH fluctuations along 24 hours. Fig. 1.12 highlighted that for every month and any area there was a daily drop in RH values in the South-oriented zones. These orientations suffered a decrease in RH between 11 a.m. and 18 p.m. The hour within a day with the lowest relative humidity was generally 14 p.m. By contrast, North-oriented cliffs maintained a comparable median amount of RH throughout all day.

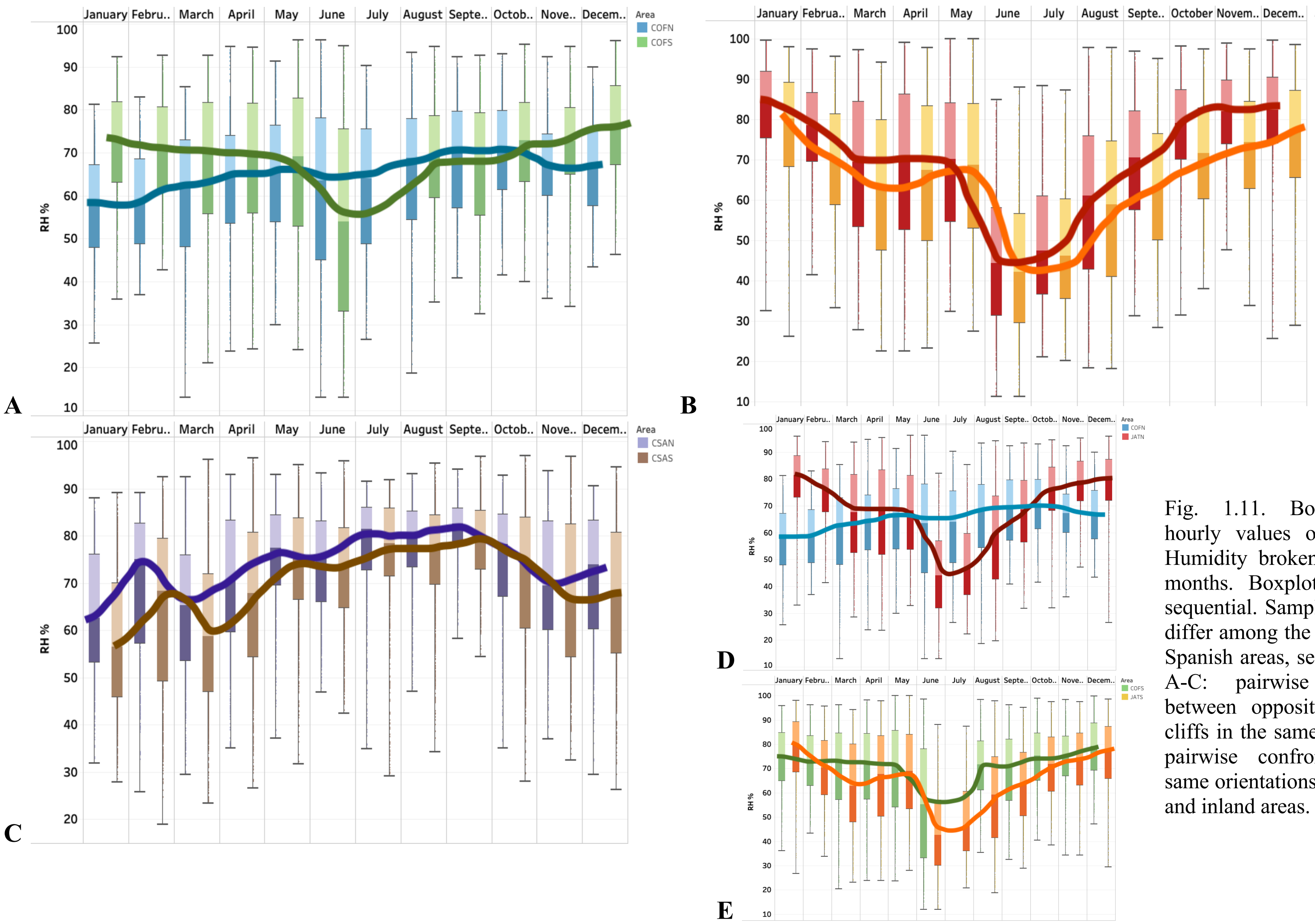

Fig. 1.11. Boxplots of hourly values of Relative Humidity broken down by months. Boxplots are not sequential. Sampling period differ among the Italian and Spanish areas, see methods. A-C: pairwise confront between opposite oriented cliffs in the same area. D-E pairwise confront among same orientations on coastal and inland areas.

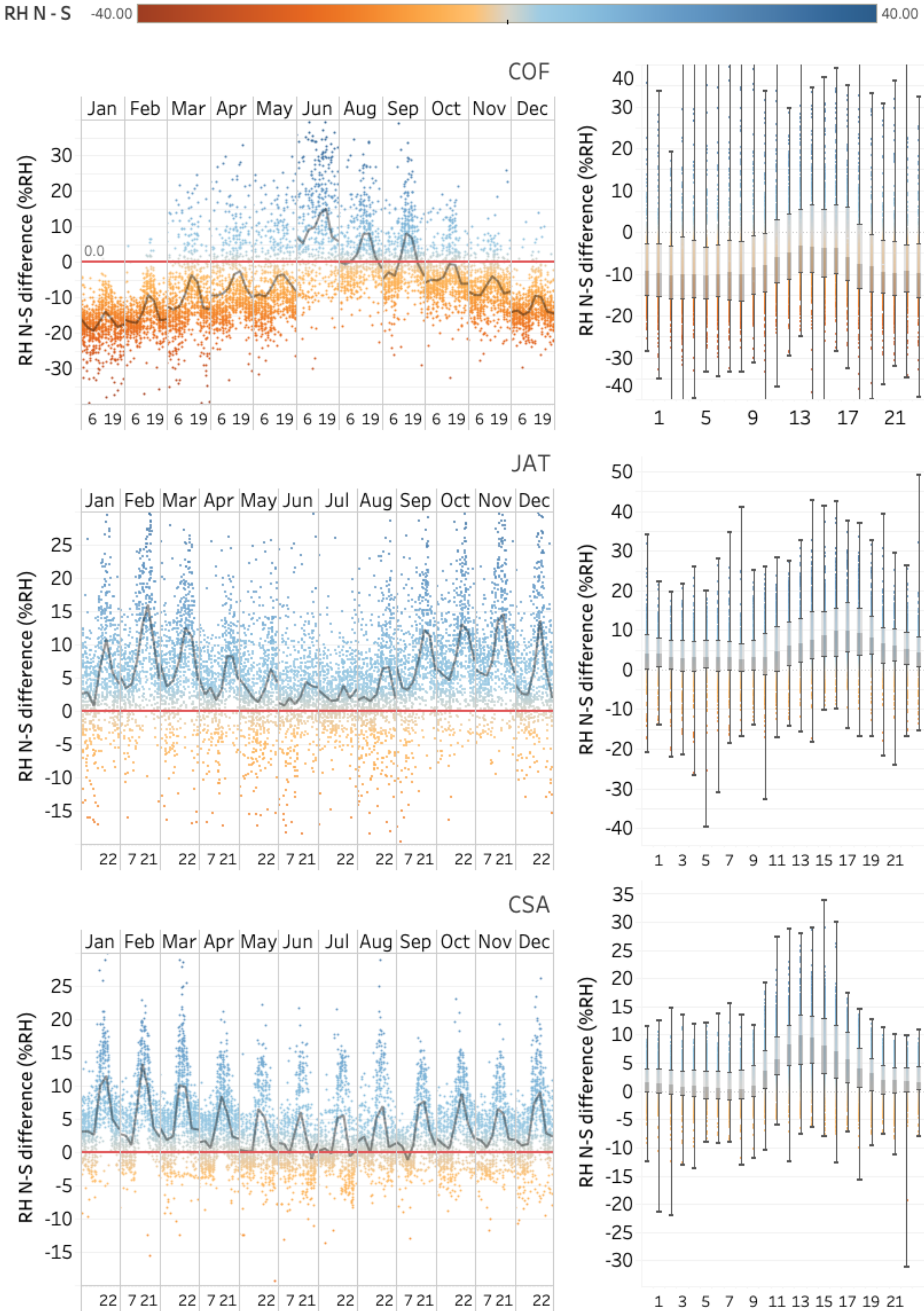

Fig. 1.12. Pairwise differences in hourly values of relative humidity among opposite oriented zones within an area. Differences refer to the subtraction of each RH hourly value in a South-oriented zone from the value in the corresponding North-oriented zone. Left: scatterplots show the 24 h distribution of RH differences broken down by months. Right: boxplots distribute in the 24 h the encountered differences of hourly RH values among zones within an area. Sampling periods differed among the Italian and Spanish areas, see methods.

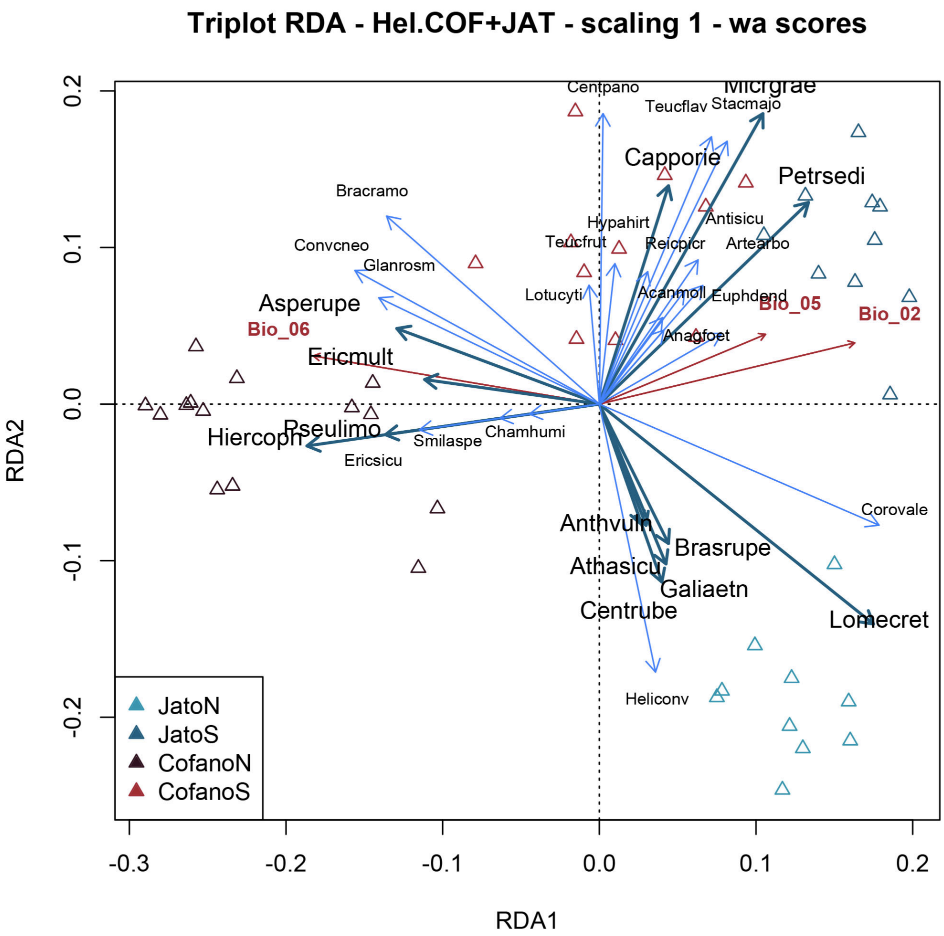

Fig 1.13. RDA of species abundances in Cofano and Jato, constrained by BIO 02, BIO 05 and BIO 06 indexes. Species names are given in Table 1.3. Two groups of response variables are plotted in the same multivariate space. Group 1: dark blue arrows represents species with a goodness of fit ≥ 0.3; group 2: pale blue arrows are species with a goodness of fit between 0.1 and 0.29. Group 1 is plotted using a multiplying factor of 0.442 over its species scores; group 2 uses a multiplying factor of 0.762. Sites are grouped according to zone. Grouping colours are indicated in the legend.

The redundancy analysis (RDA) explained a total variance of 0.7. The constrained fraction of the total variance was 34.7% (R^2 = 0.3468). The adjusted R^2 was 0.299. The constraints BIO 03, BIO 04 and BIO 07 resulted collinear and were aliased by the analysis. Thus, the canonical ordination axes were 3, with 41 unconstrained axes for the residuals. The cumulative proportion of variance explained by the first two axes was 0.29 of the total variance and 83.73 % of the constrained variance. The first axis held 0.54 and the second 0.29 of the constrained variance. The permutation tests of the RDA analysis were significant for both the overall ordination and all three canonical axes ($P < 0.001$). A significance test for each term revealed that all constraints were highly significant ($P < 0.001$). BIO 02 expressed most of the tested variance (0.11), meanwhile BIO 06 and BIO 05 expressed respectively 0.07 and 0.06 of the variance.

The non-colinear constraints resulted positioned on different sectors of the ordination triplot (Fig. 1.13). It can be seen that BIO 06 was the main contributor of RDA1 negative semi-axis and (BIO 05 + BIO 02) group of RDA1 positive semi-axis. Moreover, the growing directions of these 2 groups were close to opposite. For this reason, their influence on sites and species can be interpreted as co-occurring with an inverse intensity. Thus, species and sites encountered on the second and third sectors displayed a positive correlation with warmer minimum temperatures (BIO 06). At the same time, these variables experienced a negative correlation with maximum annual temperatures (BIO 05) and temperature fluctuations (BIO 02). The opposite is true for species and sites in the first and fourth sectors.

By observing the colour of the sites, it can be said that North-oriented zones were well segregated among them and with respect to their pertaining areas. Sites of COFN were aggregated and positioned between the second and third sectors, whereas sites of JATN were positioned on the fourth sector. By contrast, South-oriented sites were scarcely separated among JATS and COFS areas, indicating a similar behaviour with respect to constraints.

	BIO 02	BIO 05	BIO 06
Anthvuln	82,4	91,7	120,6
Asperupe	146,0	136,8	10,9
Athasicu	84,1	93,4	118,9
Brasrupe	77,1	86,4	125,9
Capporie	58,9	49,7	98,0
Centrube	84,1	93,4	118,9
Ericmult	158,5	149,2	1,6
Galiaetn	80,9	90,1	122,2
Hiercoph	174,7	165,4	17,7
Lomecret	52,2	61,5	150,8
Micrgrae	47,1	37,9	109,8
Petrsedi	30,5	21,2	126,5
Pseulimo	174,7	165,4	17,7

Table 1.4. RDA analysis: angles among main response variables and constraints. Blue to white to red colour gradient indicates a positive to neutral to negative correlation, respectively.

It is possible to recognise 3 different assemblages of species. The first assemblage is scattered along the negative RDA1 semi-axis on the left part of the triplot. It held species like *Asperula rupestris*, *Erica multiflora*, *Hieracium cophanense* and *Pseudoscabiosa limonifolia*. These species were positively correlated with a growing BIO 06 and proportionally correlated negatively with BIO 02 and BIO 05. The corresponding acute angles formed with BIO 06 were respectively 10.9°, 1.56° and 17.71° (Table 1.4). Moreover, these species were preferentially (some exclusively) correlated with COFN.

The second assemblage of species was found connected with JATN sites, on the lower-right corner of the graph. Main species pertaining to this group were *Lomelosia cretica*, *Athamanta sicula*, *Brassica rupestris* and *Centranthus ruber* It was calculated that the angles of correlation among the species of group 2 and all constraints were between widely acute to obtuse (Table 1.4), indicating a scarce preferentiality toward a specific set of bioclimatic variables. Among the group, *L. cretica* was the unique species that resulted slightly positively correlated with BIO 02 and BIO 05. The third and final assemblage was preferentially found on South-oriented cliffs, both on COFS and JATS. Main species of this group were *Capparis orientalis*, *Petrosedum sediforme* and *Micromeria graeca* subsp. *graeca*. All species of this group exhibited a certain degree of positive correlation with growing maximum temperatures and higher temperature fluctuations (see Table 1.4).

A total of 477 and 120 leaves were analysed from the areas of Cofano and Cabo de San Antonio, respectively. The data were concordant for all species and both areas: with a North-oriented cliff, individuals had higher SLA and lower LDMC (Fig. 1.14 A-B). Statistical tests were always significant except for the Mann-Whitney U applied to SLA of *Sonchus tenerrimus* subsp. *dianae* (Table 1.5).

	SLA		**LDMC**	
COF	**Student t**	**Mann-Whitn U**	**Student t**	**Mann-Whitn U**
Asperula rupestris		0*	12.779***	0***
Centaurea panormitana		2*	9.949***	1***
Convolvulus cneorum		0*	17.581***	0***
Glandora rosmarinifolia	3.081*	0**	15.308***	0***
Helichrisum pendulum		4*	8.249***	114***
Lomelosia cretica		0*	5.769***	86***
Seseli bocconei		0*	12.533***	1***
Overall	6.507***	172***	14.688***	9104***
CSA				
Sonchus tenerrimus subsp. *dianae*		0'	7.079***	5***
Centaurea rouyi		0**	12.678***	1***
Sedum sediforme subsp. *dianium*		0*	36.308***	0***
Overall	4.583***	25***	5.837***	773***

Table 1.5. Results of the Mann Whitney U and Student tests on SLA and LDMC traits.
*** p < 0.001; ** p < 0.01; * p < 0.05; ‘ p > 0.05

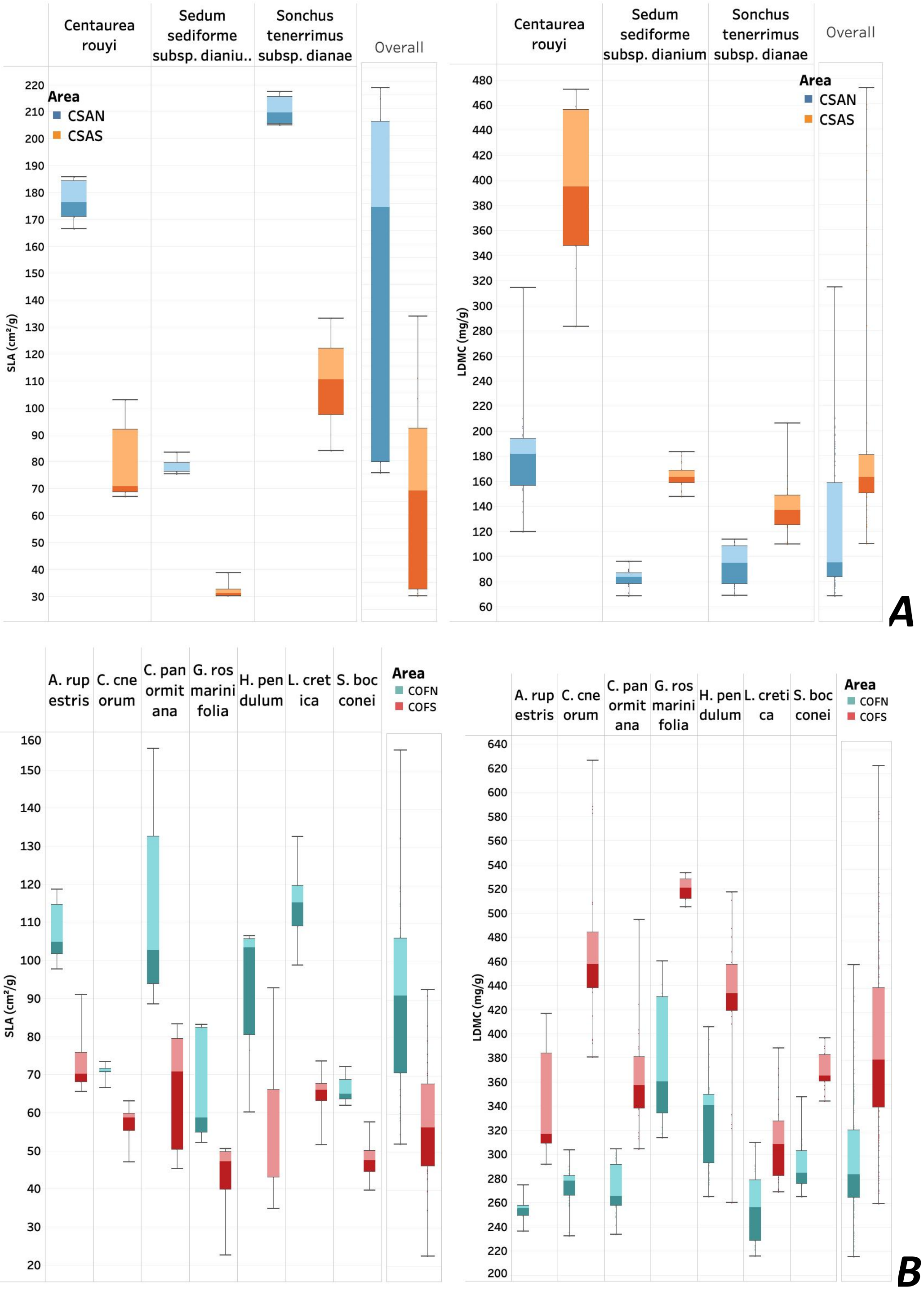

Fig. 1.14. Pairwise boxplots of intra-specific trait variability for each species of A = Cabo de San Antonio and B = Cofano. Intraspecific variation for each species in the North-oriented zones is expressed by a blue (Fig 1.14 A) and turquoise (Fig 1.14 B) colour. Values of the South oriented areas are plotted in orange (Fig. 1.14 A) and red (Fig. 1.14 B). Intraspecific variation of specific leaf area (SLA; cm^2/g) are plotted in the left panels. Right panels show the intraspecific variation of the leaf dry matter content (LDMC; mg/g). Overall and for each species, differences of median and mean values among zones within an area resulted significant (Table 1.5). The only non-significant difference was encountered for the SLA trait of *Sonchus tenerrimus* subsp. *dianae* (Fig 1.14 A, left panel)

Discussion

The recorded profiles of temperatures through a progressive distance from the cliff surface were especially divergent in South-oriented areas. Such thermal effect related to surface proximity showed how air, air under canopy and soil temperatures on cliffs resulted positively influenced by southern orientations. This result agrees with the idea that air temperatures (and their measurements through standard criteria for the installation of a meteorological station) would not constitute a good proxy of temperatures experienced by plants (Körner and Hiltbrunner, 2018). Moreover, as Nogués-Bravo et al. (2007) suggested, most of the climate models (global or regional) are not able to account for the complex, topography-driven patterns of temperature and other regional climate features.

Throughout my data, one or another cliff orientation produced similar patterns of microhabitat complexity. The resulting trends of temperatures, solar radiation and relative humidity constitute the topography-driven repeating patterns of cliff microclimates. My data contributed to understand the importance of terrain complexity in cliffs. In fact, microclimatic conditions caused by terrain complexity were previously linked to the reduction of species range and extinction risks due to climatic change (Maclean et al., 2015; Meineri & Hylander, 2017; Niskanen et al., 2017; Slavich et al., 2014; Suggitt et al., 2015, 2018). My compositional dataset and the microclimatic characterization suggest that cliffs do not represent at all a homogeneous environment from a conservation standpoint. It is then necessary to take in consideration the microclimatic heterogeneity of cliffs for the prediction of the effect of ongoing climatic change on the landscape. My results confirm the necessity of such microclimatic-based approach on cliff areas in order to precisely allocate topoclimatic microrefugia (Patsiou et al., 2014).

As expected, a difference in incoming solar irradiance among North-South zones determined a proportional trend of differences in temperatures. For the North oriented zones, the overall trend of solar irradiance was always lower than the corresponding South-oriented zones. In addition to a low and constant amount of solar radiation for most of the year, their trend profile experienced a peak of irradiance in June-July. This suggests a potential correlation with the summer sun elevation and the total insolation received by the cliff (see appendix 1, Fig S1.9 - S1.11). In fact, the total solar energy received by a unit of area per one day is defined as the integration of total insolation over the daylight hours (Liou, 2002). During summer months daylight hours are higher because of the prologed trajectory of the sun in the sky (Appendix 1, Fig S1.9). Moreover, as suggested by the graphs in appendix 1, such larger trajectory is determinant in order to understand when the North-oriented cliffs are directly exposed to the sunlight. From the hourly measured solar radiaton data (appendix 1, Cofano: Fig. S1.10; Jato: Fig. S1.11) it is clear that JAT and COF receive a direct irradiance only in summer during the early morning and preferentially between 14:00 and 19:00.

However, the amount of received solar radiation was as well at least partially influenced by a southern orientation. In fact, both trends in COFS and JATS did not show a complete sinusoidal behaviour, hinting for a topographic influence.

By measuring the North-South differences in solar radiation income, I also showed that, as a consequence, North-oriented cliffs buffer extreme temperatures. Between 0 and 500 m a.s.l. in the Mediterranean context, maximum rather than minimum temperatures and high levels of solar radiation represent a limiting factor for species distribution. They are in fact a direct proxy of high evapotranspiration levels. According to my observations on floristic data in Sicily, such factors do not limit the distribution of the majority of rupicolous species, which can be found on both North and South orientations within an area. By contrast, they exclude narrow endemic species from South-oriented zones. In fact, chasmophytes with a topo-geographic limited distribution such as *Pseudoscabiosa limonifolia*, *Erica sicula* and *Hieracium cophanense* were located only in the North side of Monte Cofano. Based on the microclimatic characterization of North-oriented zones, I then propose that the topographic buffering effect on temperatures and solar radiations is causally related with the refugial role of these areas. In addition, my results confirmed that coastal cliffs rather than inland areas were even more seasonally stabilised by the sea proximity. My considerations are in line with the known link between climatic stability and endemism rates at coarse scale, which is normally mediated by rugged topography (Harrison & Noos, 2017). Therefore, my results support the hypothesis that North-oriented cliffs on coastal areas in the Mediterranean might have protected rare chasmophytes from past climatic changes, promoting the accumulation [if not induced speciation] of singular flora (Davis, 1951; Garcia et al., 2020).

The climatic stability of the North-oriented coastal cliffs of COFN (Italy) and CSAN (Spain) was particularly evident in the pattern of diurnal temperature fluctuations and relative humidity. The diurnal range of temperatures for example was observed to oscillate between 2 and 6.5 °C. Relative humidity was high and constant, both on a daily basis and year-round. This last factor differentiated these zones from a visible summer drop in moisture observed on the inland and South-oriented zones.

As revealed by other authors, the recognition of intraspecific trait variability is particularly important in studies at a local scale (Siefert et al., 2015). In this regard, my results on the intraspecific trait diversity demonstrate that there was a remarkable environmental gradient among opposite orientations. Specific Leaf Area (SLA) is the ratio between the leaf surface (LA) and its dry weight (DW). In literature, species characteristic of shaded understorey usually develop lower Leaf Mass per Area values (LMA = 1/SLA) than species under sunny conditions (for a review see Westoby et al., 2002; Bongers & Popma, 1990; Hladik & Miquel, 1990; King, 1994; Lusk & Contreras, 1999; Suehiro & Kameyama, 1992; Valladares et al., 2000; Xu et al., 1990). Within species, also individuals growing in shade show lower LMA (Miyaji et al., 1997; Reich et al., 2002; Steinke, 1988). The measured microclimatic difference between the North and South zones of Cofano and Cabo de San Antonio was characterised by a great differential amount of solar radiations and a higher annual levels of air humidity. The species shift from low-radiation conditions of shaded cliffs corresponded then to a decrease in the leaf area and a consequent reduction of SLA. Moreover, Leuschner (2002) showed that plants grown at high humidity levels had larger leaves and leaf epidermal cells, and a lower stomatal frequency than plants grown with low humidity treatments. However, mature plants in the wild may respond differently in cliff environments with rapidly changing diurnal RH. The high and persistent levels of humidity encountered in COFN and CSAN then potentially contributed to a stimulation of leaf expansion.

Leaf Dry Matter Content is the ratio between leaf dry weight (DW) and fresh weight (FW). The univocal pattern of decrease in LDMC on North-oriented coastal zones could be explained by the amount of water available in the soil. Unfortunately, this hypothesis cannot be demonstrated directly by my dataset, because soil moisture levels were not measured. However, geographic proximity of meteorological stations within an area (a plain distance of ≅ 400-1000 m for CSA and COF, respectively) could suggest that precipitations were similar. The differential amount of solar radiations received by the zones could then be used as a proxy of soil aridity. According to this interpretation, South zones are characterised by a less availability of water and thus a reduced fresh weight and higher LDMC.

In conclusion, the observed microclimate of North-oriented coastal cliffs was predominantly hyperoceanic, with year-round moisture, small thermoperiods and warm, stable temperatures (*cfr.* Larcher, 2003). According to the most recent paleoclimatic reconstructions (Combourieu-Nebout et al., 2015; Fauquette and Bertini, 2003; Fauquette et al., 1999, 2007), similar conditions were predominant in the South Mediterranean during the Early Pliocene.

Conclusions

This work highlighted the value of cliff areas in shaping the microclimatic differences between different orientations and distance from the sea. The microclimate stability produced by a North-oriented cliff, especially in the coastal areas, resulted being of fundamental importance for the survival of narrow endemic chasmophytes. These island-like patches of vertical zones resulted being drastically different from their South oriented counterparts, constituting long-term "safe" places for relictual species. Altogether, my results demonstrate that the microclimatic conditions on cliffs with different orientations create fine-scale habitats that are inhabited by species with different thermal preferences. Among them, narrow endemics may be limited to North-oriented surfaces. Such behaviour is connected to their paleogeographic history, linked to Plio-Pleistocenic subtropical conditions.

Bibliography

Ackerly, D.D., Loarie, S.R., Cornwell, W.K., Weiss, S.B., Hamilton, H., Branciforte, R. and Kraft, N.J.B. (2010). The geography of climate change: implications for conservation biogeography. Diversity and Distributions, 16: 476-487. doi:10.1111/j.1472-4642.2010.00654.x

Albert, C.H. (2015). Intraspecific trait variability matters. J Veg Sci, 26: 7-8. doi:10.1111/jvs.12240

Albert, C.H., Grassein, F., Schurr, F.M., Vieilledent, G. & Violle, C. (2011). When and how should intraspecific variability be considered in traitbased plant ecology? Perspectives in Plant Ecology, Evolution and Systematics 13: 217–225.

Bazan, G., Marino, P., Guarino, R., Domina, G., Schicchi, R. (2015). Bioclimatology and Vegetation Series in Sicily: A Geostatistical Approach. Annales Botanici Fennici, 52(1–2), 1-18

Bellard, C., Bertelsmeier, C., Leadley, P., Thuiller, W. and Courchamp, F. (2012). Impacts of climate change on the future of biodiversity. Ecology Letters, 15: 365–377. doi: 10.1111/j.1461-0248.2011.01736.x

Bennie, J., Huntley, B., Wiltshire, A., Hill, M.O., Baxter, R. (2008). Slope, aspect and climate: spatially explicit and implicit models of topographic microclimate in chalk grass-land. Ecol. Model. 216 (1), 47–59.

Bongers, F, Popma, J. (1990). Leaf characteristics of the tropical rain forest flora of Los Tuxtlas, Mexico. Bot. Gaz. 151:354–65

Bramer, I, Anderson, B.J., Bennie, J., Bladon, A.J., De Frenne, P., Hemming, D., Hill, R.A., Kearney, M.R., Körner, C, Korstjens, A.H., Lenoir, J., Maclean, I.M.D., Marsh, C.D., Morecroft, M.D., Ohlemüller R., Slater, H.D., Suggitt, A.J., Zellweger, F. & Gillingham, P.K. (2018). Advances in monitoring and modelling climate at ecologically relevant scales. In D. A. Bohan, A. J. Dumbrell, G. Woodward, & M. Jackson (Eds.). Advances in ecological research: Vol. 58. Next generation biomonitoring: part 1 (pp. 101-161).

Brullo, S. & Minissale, P. & Spampinato, G. (1995). Considerazioni fitogeografiche sulla flora della Sicilia. Ecologia Mediterranea. 21. 99-117.

Buira, A., Cabezas, F. & Aedo, C. (2020). Disentangling ecological traits related to plant endemism, rarity and conservation status in the Iberian Peninsula. Biodivers Conserv 29, 1937–1958. https://doi.org/10.1007/s10531-020-01957-z

Carlucci, M., Debastiani, V., Pillar, V. & Duarte, L. (2014). Between- and within-species trait variability and the assembly of sapling communities in forest patches. Journal of Vegetation Science 26: DOI: 10.1111/jvs.12223.

Castroviejo, S. (coord. gen.) (1986-2012). Flora iberica 1-8, 10-15, 17-18, 21. Real Jardín Botánico, CSIC, Madrid.

Combourieu-Nebout, N., Bertini, A., Russo-Ermolli, E., Peyron, O., Klotz, S., Montade, V., Fauquette, S., Allen, J., Fusco, F., Goring, S., Huntley, B., Joannin, S., Lebreton, V., Magri, D., Martinetto, E., Orain, R., Sadori, L. (2015). Climate changes in the central Mediterranean and Italian vegetation dynamics since the Pliocene. Review of Palaeobotany and Palynology. 218. 10.1016/j.revpalbo.2015.03.001.

Davis, P. (1951). Cliff Vegetation in the Eastern Mediterranean. Journal of Ecology, 39(1), 63-93.

Di Maggio, C., Madonia, G., Vattano, M., Agnesi, V., & Monteleone, S. (2017). Geomorphological evolution of western Sicily, Italy. Geologica Carpathica, 68, 80 - 93.

Easterling, D.R., Meehl, G.A., Parmesan, C., Changnon, S.A., Karl, T.R., Mearns, L.O. (2000). Climate extremes: observations, modeling, and impacts. Science 289 (5487), 2068–2074.

Fauquette, S., Bertini, A. (2003). Quantification of northern Italy Pliocene climate from pollen data: evidences for a very peculiar climate pattern. Boreas 32, 361–369.

Fauquette, S., Suc, J.-P., Guiot, J., Diniz, F., Feddi, N., Zheng, Z., Bessais, E., Drivaliari, A. (1999). Climate and biomes in the west Mediterranean area during the Pliocene. Palaeogeogr. Palaeoclimatol. Palaeoecol. 152, 15–36.

Fauquette, S., Suc, J.-P., Jiménez-Moreno, G., Favre, E., Jost, A., Micheels, A., Bachiri-Taoufiq, N., Bertini, A., Clet-Pellerin, M., Diniz, F., Farjanel, G., Feddi, N., Zheng, Z. (2007). Latitudinal climatic gradients in Western European and Mediterranean regions from the Mid-Miocene (~15 Ma) to the Mid-Pliocene (~3.6 Ma) as quantified from pollen data. In: Williams, M., Haywood, A.M., Gregory, F.J., Schmidt, D.N. (Eds.), Deep-time perspectives on climate change: marrying the signal from computer models and biological proxies. The Micropalaeontological Society Special Publications. The Geological Society, London, pp. 481–502.

Fawcett, S., Sistla, S., Dacosta Calheiros, M., Kahraman, A., Reznicek, A.A., Rosenberg, R., Wettberg von, E.J.B. (2019). Tracking microhabitat temperature variation with iButton data loggers. Appl. Plant Sci., 7 (2019), Article e01237, 10.1002/aps3.1237

Finkel, M., Fragman, O., Nevo, E. (2001). Biodiversity and interslope divergence of vascular plants caused by sharp microclimatic differences at "Evolution Canyon II", Lower Nahal Keziv, Upper Galilee, Israel. Isr. J. Plant Sci. 49 (4), 285–295.

Fois, M, Fenu, G, Cañadas, EM, Bacchetta, G (2017). Disentangling the influence of environmental and anthropogenic factors on the distribution of endemic vascular plants in Sardinia. PLoS ONE 12(8): e0182539. https://doi.org/ 10.1371/journal.pone.0182539

García, M.B., Domingo, D., Pizarro, M., Font, X., Gómez, D., Ehrlén, J. (2020). Rocky habitats as microclimatic refuges for biodiversity. A close-up thermal approach. Environmental and Experimental Botany, Volume 170

Gianguzzi, L., La Mantia, A., Ottonello, D., Romano, S. (2005). La flora vascolare della Riserva naturale di Monte Cofano (Sicilia occidentale). Naturalista Sicil. 29 (3-4): 107-152.

Gillingham, P.K., Huntley, B., Kunin, W.E., Thomas, C.D. (2012). The effect of spatial resolution on projected responses to climate warming. Divers. Distrib. 18 (10), 990–1000.

Graae, B.J., De Frenne, P., Kolb, A., Brunet, J., Chabrerie, O., Verheyen, K., Pepin, N., Heinken, T., Zobel, M., Shevtsova, A., Nijs, I. and Milbau, A. (2012). On the use of weather data in ecological studies along altitudinal and latitudinal gradients. Oikos, 121: 3-19. doi:10.1111/j.1600-0706.2011.19694.x

Granger, J.E., Schulze, R.E. (1977). Incoming solar radiation patterns and vegetation response: Examples from the natal drakensberg. Plant Ecol 35, 47–54. https://doi.org/10.1007/BF02097134

Greuter, W. (1991). Botanical diversity, endemism, rarity and extinction in the Mediterranean Area: An analysis based on the published volumes of Med-Checklist. Botanika Chronika, 10: 63-79.

Hijmans, R.J. (2004). Arc Macro Language (AML®) version 2.1 for calculating 19 bioclimatic predictors: Berkeley, Calif, Museum of Vertebrate Zoology, University of California at Berkeley. Available at http://www.worldclim.org/bioclim.

Hladik, A., Miquel, S. (1990). Seedling types and plant establishment in an African rain forest. In Reproductive Ecology of Tropical Plants, ed. KS Bawa, M Hadley, pp. 261–82. Paris/Carnforth, UK: UNESCO/Parthenon

Harrison, S., Noss, R. (2017). Endemism hotspots are linked to stable climatic refugia Ann. Bot., 119, pp. 207-214, 10.1093/aob/mcw248

Hijmans, R.J., Cameron, S.E., Parra, J.L., Jones, P.G. & Jarvis, A. (2005). Very high resolution interpolated climate surfaces for global land areas. International Journal of Climatology 25: 1965–1978.

King, D.A. (1994). Influence of light level on the growth and morphology of saplings in a Panamanian forest. Am. J. Bot. 81:948–57

Körner, C., Hiltbrunner, E. (2018). The 90 ways to describe plant temperature Perspect. Plant Ecol. Evol. Syst., 30, pp. 16-21, 10.1016/j.ppees.2017.04.004

Larcher, W. (2003). Physiological Plant Ecology. Ecophysiology and Stress Physiology of Functional Groups. ISBN 978-3-540-43516-7 Springer-Verlag Berlin Heidelberg

Larson, D.W., Matthes, U., & Kelly, P.E. (2000). Cliff Ecology: Pattern and Process in Cliff Ecosystems.

Lavergne, S., Thompson, J.D., Garnier, E. and Debussche, M. (2004). The biology and ecology of narrow endemic and widespread plants: a comparative study of trait variation in 20 congeneric pairs. Oikos, 107: 505-518. doi:10.1111/j.0030-1299.2004.13423.x

Legendre, P. & Legendre, L. (2012). Numerical ecology, 3rd English edition. Elsevier Science BV, Amsterdam. xvi + 990 pp.

Legendre, P., Oksanen, J. & ter Braak, C.J.F. (2011). Testing the significance of canonical axes in redundancy analysis. Methods in Ecology and Evolution 2, 269–277.

Lenoir, J., Svenning, J.C. (2015). Climate-related range shifts—a global multidimensional synthesis and new research directions. Ecography 38 (1), 15–28.

Leuschner, C. (2002). Air humidity as an ecological factor for woodland herbs: leaf water status, nutrient uptake, leaf anatomy, and productivity of eight species grown at low or high vpd levels. Flora - Morphology, Distribution, Functional Ecology of Plants, Volume 197, Issue 4, Pages 262-274,

Liou, K.N. (editor) (2002). International Geophysics, Academic Press. Volume 84, Chapter 2 – Solar Radiation at the top of the atmosphere. ISBN 9780124514515, https://doi.org/10.1016/S0074-6142(02)80017-1.

Lusk, C.H., Contreras, O. (1999). Foliage area and crown nitrogen turnover in temperate rain forest juvenile trees of differing shade tolerance. J. Ecol. 87:973–83

Maclean, I.M.D., Hopkins, J.J., Bennie, J., Lawson, C.R., Wilson, R.J. (2015). Microclimates buffer the responses of plant communities to climate change. Global Ecol Biogeography, 24, pp. 1340-1350, 10.1111/geb.12359

McCree, K.J. (1981). Photosynthetically Active Radiation. In: Lange O.L., Nobel P.S., Osmond C.B., Ziegler H. (eds) Physiological Plant Ecology I. Encyclopaedia of Plant Physiology (New Series), vol 12 / A. Springer, Berlin, Heidelberg

Médail, F. & Quézel, P. (1997). Hot-Spots Analysis for conservation of Plant Biodiversity in the Mediterranean Basin. Annals of the Missouri Botanical Garden, 84, 112-127. http://dx.doi.org/10.2307/2399957

Meineri, E., Hylander, K. Fine-grain, large-domain climate models based on climate station and comprehensive topographic information improve microrefugia detection. Ecography, 40 (2017), pp. 1003-1013, 10.1111/ecog.02494

Miyaji, K.I., Dasilva, W.S., Alvim, P.D. (1997). Longevity of leaves of a tropical tree, Theobroma cacao, grown under shading, in relation to position within the canopy and time of emergence. New Phytol. 135:445–54

Myers, N., Mittermeier, R.A., Mittermeier, C.G., Da Fonseca, G.A.B., Kent, J. (2000). Biodiversity hotspots for conservation priorities. Nature, 403: 853-858.

Nix, H.A. (1986). A biogeographic analysis of Australian elapid snakes. In Longmore, R., ed., Atlas of elapid snakes of Australia: Canberra, Australian Flora and Fauna Series 7, Australian Government Publishing Service, p. 4–15.

Niskanen, A.K.J., Heikkinen, R.K., Mod, H.K., Väre, H., Luoto, M. (2017). Improving forecasts of arctic-alpine refugia persistence with landscape-scale variables. Geogr. Ann. Ser. A Phys. Geogr., 99 (2017), pp. 2-14, 10.1080/04353676.2016.1256746

Nogue´ s-Bravo, D., Arau´ jo, M.B., Errea, M.P. & Martı´nez-Rica, J.P. (2007). Exposure of global mountain systems to climate warming during the 21st Century. Global Environmental Change–Human and Policy Dimensions, 17, 420–428.

O'Donnell, M.S., & Ignizio, D.A. (2012). Bioclimatic predictors for supporting ecological applications in the conterminous United States: U.S. Geological Survey Data Series 691, 10 p.

Oksanen, J.A. (2019). Design decisions and implementation details in vegan.

Ospedal, Ø.H., Scott Armbruster, W. & Graae, B.J. (2015). Linking small-scale topography with microclimate, plant species diversity and intra-specific trait variation in an alpine landscape, Plant Ecology & Diversity, 8:3, 305-315, DOI: 10.1080/17550874.2014.987330

Peres-Neto, P., Legendre, P., Dray, S. & Borcard, D. (2006). Variation partitioning of species data matrices: estimation and comparison of fractions. Ecology 87, 2614–2625.

Pérez-Harguindeguy, N., Díaz, S., Garnier, E., Lavorel, S., Poorter, H., Jaureguiberry, P., Bret-Harte, M. S., Cornwell, W. K., Craine, J. M., Gurvich, D. E., Urcelay, C., Veneklaas, E. J., Reich, P. B., Poorter, L., Wright, I. J., Ray, P., Enrico, L., Pausas, J. G., de Vos, A. C., Buchmann, N., Funes, G., Quétier, F., Hodgson, J. G., Thompson, K., Morgan, H. D., ter Steege, H., van der Heijden, M. G. A., Sack, L., Blonder, B., Poschlod, P., Vaieretti, M. V., Conti, G., Staver, A. C., Aquino, S., Cornelissen, J. H. C.. (2013). New handbook for standardised measurement of plant functional traits worldwide. CSIRO. Retrieved from the University of Minnesota Digital Conservancy, http://hdl.handle.net/11299/177647.

Pignatti, S. (1982). Flora d'Italia. Edagricole, Bologna.

Quézel, P. (1985). Definition of the Mediterranean region and the origin of its flora. In C. Gomez-Campo, ed. Plant conservation in the Mediterranean area. Geobotany 7, p. 9-24. Dordrecht, the Netherlands, W. Junk.

Parmesan, C., Root, T.L., Willig, M.R. (2000). Impacts of extreme weather and climate on terrestrial biota. Bull. Am. Meteorol. Soc. 81 (3), 443–450.

Patsiou, T.S., Conti, E., Zimmermann, N.E., Theodoridis, S., Randin, C.F. (2014). Topo-climatic microrefugia explain the persistence of a rare endemic plant in the Alps during the last 21 millennia. Glob. Chang. Biol., 20, pp. 2286-2300, 10.1111/gcb.12515

Pauli, H., Gottfried, M., Dullinger, S., Abdaladze, O., Akhalkatsi, M., Alonso, J.L.B., Coldea, G., Dick, J., Erschbamer, B., Calzado, R.F., Ghosn, D. (2012). Recent plant diversity changes on Europe's mountain summits. Science 336 (6079), 353–355.

Pecl, G.T., Arau´jo, M.B., Bell, J.D., Blanchard, J., Bonebrake, T.C., Chen, I.C., Clark, T.D., Colwell, R.K., Danielsen, F., Evenga˚rd, B., Falconi, L. (2017). Biodiversity redistribution under climate change: impacts on ecosystems and human well-being. Science 355 (6332), p. eaai9214.

Polunin O. (1980). Flowers of Greece and the Balkans: a Field guide. Oxford University Press, Oxford.

Potter, K.A., Arthur Woods, H., Pincebourde, S. (2013). Microclimatic challenges in global change biology. Glob. Chang. Biol. 19 (10), 2932–2939.

Quezel, P. (1995). La flore du bassin méditerranéen: origine, mise en place, endémisme. Ecologia mediterranea, 20: 19-39.

R Core Team (2019). R: A language and environment for statistical computing. R Foundation for Statistical Computing, Vienna, Austria. URL http://www.R-project.org/.

R Studio Team (2018). RStudio: Integrated Development for R. RStudio, Inc., Boston, MA URL http://www.rstudio.com/

Reich, P., Uhl, C., Walters, M., Laura Prugh, & Ellsworth, D. (2004). Leaf Demography and Phenology in Amazonian Rain Forest: A Census of 40 000 Leaves of 23 Tree Species. Ecological Monographs, 74(1), 3-23.

Rivas-Martínez, S., Penas, A., Díaz, T. (2004). Biogeographic Map of Europe.

Rueden, C.T., Schindelin,J. & Hiner, M.C. et al. (2017). "ImageJ2: ImageJ for the next generation of scientific image data", BMC Bioinformatics 18:529, PMID 29187165, doi:10.1186/s12859-017-1934-z

Scherrer, D., Körner, C. (2010). Infra-red thermometry of alpine landscapes challenges climatic warming projections. Glob Change Biol 16:2602–2613

Scherrer, D., Körner, C. (2011). Topographically controlled thermal-habitat differentiation buffers alpine plant diversity against climate warming. Species Divers., 38 (2011), pp. 406-416, 10.1111/j.1365-2699.2010.02407.x

Settele, J., Scholes, R., Betts, R.A., Bunn, S., Leadley, P., Nepstad, D., Overpeck, J.T., Taboada, M.A., Fischlin, A., Moreno, J.M., Root, T. (2014). Terrestrial and inland water systems. In: Field, C.B., Barros, V.R. (Eds.), Climate Change 2014 Impacts, Adaptation and Vulnerability: Part A: Global and Sectoral Aspects. Cambridge University Press.

Siefert, A, Violle, C, Chalmandrier, L, et al. (2015). A global meta-analysis of the relative extent of intraspecific trait variation in plant communities. Ecol Lett18:1406–19.

Slavich, E., Warton, D.I., Ashcroft, M.B., Gollan, J.R., Ramp, D. (2014). Topoclimate versus macroclimate: how does climate mapping methodology affect species distribution models and climate change projections? Divers. Distrib. 20 (8), 952–963.

Snogerup, S. (1971). Evolutionary and plant geographical aspects of chasmophytic communities. In: Davis PH, Harper PC & Hedge IC (eds.), Plant life of south-west Asia, pp. 157-170, Botanical Society of Edinburgh, Edinburgh.

Steinke, T.D. (1988). Vegetative and floral phenology of three mangroves in Mgeni Estuary. S. Afr. J. Bot 54:97–102

Suehiro, K., Kameyama, K. (1992). Leaf age composition of evergreen broadleaved trees. Jpn. J. Ecol. 42:137–47

Suggitt, A.J., Gillingham, P.K., Hill, J.K., Huntley, B., Kunin, W.E., Roy, D.B. and Thomas, C.D. (2011). Habitat microclimates drive fine-scale variation in extreme temperatures. Oikos, 120: 1-8. doi:10.1111/j.1600-0706.2010.18270.x

Suggitt, A.J., Wilson, R.J., August, T.A., Fox, R., Isaac, N.J., Macgregor, N.A., Morecroft, M.D., Maclean, I.M.D. (2015). Microclimate affects landscape level persistence in the British Lepidoptera. J. Insect Conserv. 19 (2), 237–253.

Suggitt, A.J., Wilson, R.J., Isaac, N.J.B., Beale, C.M., Auffret, A.G., August, T., Bennie, J.J., Crick, H.Q.P., Duffield, S., Fox, R., Hopkins, J.J., Macgregor, N.A., Morecroft, M.D., Walker, K.J., Maclean, I.M.D. (2018). Extinction risk from climate change is reduced by microclimatic buffering. Nat. Clim. Chang., 8, pp. 713-717, 10.1038/s41558-018-0231-9

Thackeray, S.J., Henrys, P.A., Hemming, D., Bell, J.R., Botham, M.S., Burthe, S., Helaouet, P., Johns, D.G., Jones, I.D., Leech, D.I., Mackay, E.B. (2016). Phenological sensitivity to climate across taxa and trophic levels. Nature 535 (7611), 241–245.

Thompson, J.D. (2005). Plant evolution in the Mediterranean. Oxford University Press, Oxford

Trivedi, M.R., Berry, P.M., Morecroft, M.D., Dawson, T.P. (2008). Spatial scale affects bioclimate model projections of climate change impacts on mountain plants. Glob. Chang. Biol. 14 (5), 1089–1103.

Valladares, F, Wright, S.J., Lasso, E., Kitajima, K., Pearcy, R.W. (2000). Plastic phenotypic response to light of 16 congeneric shrubs from a Panamanian rainforest. Ecology 81:1925–36

van der Maarel, E. (1979). Transformation of cover-abundance values in phytosociology and its effects on community similarity. Vegetatio 39, 97–114. https://doi.org/10.1007/BF00052021

Westoby, M., Falster,D.S., Moles,A.T., Vesk, P.A., & Wright, I.J. (2002). Plant Ecological Strategies: Some Leading Dimensions of Variation Between Species. Annual Review of Ecology and Systematics 2002 33:1, 125-159

Wilson, P.J., Thompson, K., Hodgson, J.G. (1999). Specific leaf area and leaf dry matter content as alternative predictors of plant strategies. New Phytologist143:155–62.

World Meteorological Organization (WMO) (2018). Guide to Instruments and Methods of Observation

Xu, G., Ninomiya, I., Ogino, K. (1990). The change of leaf longevity and morphology of several tree species grown under different light conditions. Bull. Ehime Univ. For. 28:35–44

Xue, R., Yang, Q., Miao, F., Wang, X., & Shen, Y. (2018). Slope aspect influences plant biomass, soil properties and microbial composition in alpine meadow on the Qinghai-Tibetan plateau. Journal of soil science and plant nutrition, 18(1), 1-12. https://dx.doi.org/10.4067/S0718-95162018005000101

Chapter 2: Compositional data and cluster analysis of zones and plant communities in the coastal cliffs of Valencian Community (Spain).

Introduction

Cliff environments are difficult to study because of their inaccessibility. In fact, these areas are generally defined by geomorphologists as zones with very steep slopes (Minelli et al., 2006). Cliffs are also characterized by a high environmental heterogeneity. The vertical "integrity" of a single cliff surface is always fragmented by a continuous variation in its inclination. Pockets of soil accumulate in small ledges within the cliff area, creating a patched landscape of vertical and subvertical zones, divided often by small non-vertical screes and rocky areas. Moreover, the orientation of a cliff surface may vary continuously or abruptly along even a plain distance of 50 m (Fig. 2.1).

Fig. 2.1. Heterogeneity of cliffs areas. It is possible to appreciate a continuous change in the local orientation of the cliff system. Each vertical plane that constitutes a cliff surface is interposed by a small or large portion of non-vertical areas.

02/2018 Marettimo, Italy

Plant species are not evenly distributed on cliffs. The various microenvironments within a cliff, in fact, segregate different plant communities and influence the assembly rules (Davis, 1951). On the basis of inclination, Davis (1951) divided plant assemblages on cliffs according to 6 classes of environments: pavement (small or no inclination), sloping rock (25° to 75° zones), vertical rock (76° to 90° zones), overhanging rock (more than 90°), step-crevice (a landscape created by step-like blocks of rock alternated by large crevices), and ledge. From the ecological point of view, this subdivision is associated to a species classification into chasmophytes, chomophytes and chasmo-comophytes (Davis, 1951; Font Quer, 1953; Schimper & Faber, 1935). While chomophytes can easily be found on zones with soil deposits (small inclinations), chasmophytes are almost always found on vertical zones. Lavergne et al. (2003) affirmed that in cliffs and subvertical habitats the small number of micro-areas favourable for installation limit the establishment and growth of many species (chomophytes and non-rupicolous flora). Moreover, cliffs (and thus a vertical slope gradient) in the Mediterranean constitute an important reservoir of endemic and rare species (Spain: Buira et al., 2020; Greece: Panitsa & Kontopanou, 2017; Sardinia: Bacchetta et al., 2007).

Despite the ecological importance of discriminating cliff microhabitats, flaws and difficulties arise from a practical standpoint (Davis, 1951; Escudero, 1996; Heywood, 1953; Meier & Braun-Blanquet, 1934; Rivas-Martinez, 1960). Problems are related to accessibility and were mostly connected to the difficulty in characterizing the physical environment in a visual sampling (Bartlett et al., 1990; John & Dale, 1990). In addition, the classic phytosociological method used by several authors to study cliff vegetation was focused on the characterization of the regional diversity of cliff assemblages and not on identifying the local micro-habitats patches (Escudero, 1996).

The aims of this study were: 1) to test the effectiveness of classic relevé-type sampling retrieved from field transects along vertical areas; 2) to investigate the relationship between species compositional data and microtopographic variables retrieved from a visual, distance observation; and 3) to produce a numerical classification of the studied sites in order to link floristic composition and species abundances to regional variation in cliff assemblages.

Materials and methods

Site	Coordinates (WGS84)	Min-max elevation of plots (m)	N
Montgò	38°48'28" N 0° 7'9" E	285-432	10
Cabo de San Antonio	38°48'9" N 0°11'40" E	121-150	21
Cap d'Or	38°41'16" N 0° 9'11" E	112-151	10
Toix	38°37'56" N 0° 1'6" E	181-288	28
Monduber	39° 0'13" N 0°15'31" W	635	1
Chulilla	39°40'6" N 0°53'37" W	305	1

Table 2.1. Sites characteristics including latitude, longitude, number of plots (N) and min-max altitude of samples. Altitudes are ellipsoidal (WGS 84 EPSG 4326).

Between February 2017 and April 2019, plant cover-abundance was measured using the original Braun-Blanquet scale (r, +, 1, 2, 3, 4, 5) in 71 5 x 5 m (25 m^2) plots arrayed across 6 areas of the Valencian Community, Spain (Table 2.1). The main surveyed areas (4) fall within the coastal cliff belt of Eastern Spanish province of Alicante, represented in Fig I. Two additional plots were retrieved from 2 areas in the inland cliffs of the Valencian Community region (sites: Monduber and Chulilla). All plots except Monduber were sampled inside the Thermomediterranean bioclimatic belt. Conversely, the area of Monduber has a Mesomediterranean bioclimate (Rivas-Martínez et al. 2004).

The isolated mountains in the coastal belt of Alicante have been selected to have a similar geomorphological and phytogeographic history (Aguilella et al., 2010). These areas are in fact part of the Prebetic mountain belt, which once connected the continental Spain to Balearic Islands (Baetic-Rifan orogenic belt; geologic map in Sanz de Galdeano & Ruiz Cruz, 2016).

Each area except Monduber, Cap d'Or and Chulilla was selected to be a topographic isolated unit characterised by a strong North/South gradient of regional orientation. Within each of these areas, the number of samples were subdivided among these sectors of regional orientation. The area of Cap d'Or is a peninsula with an NNE-SSW orientation. The sea cliffs in this area are homogeneously located on the East sector. The mountain of Monduber was not accessible from the North sector, thus the plot was located in the South sector. The area of Chulilla is a fluvial canyon without a specific set of regional orientations. All locations were undisturbed by grazing and fire at the moment of sampling. The number and position of plots on the cliff surface of each area were proportional to the heterogeneity of the zone. Plants were identified according to Castroviejo (1986). Generally, the sampling scheme followed a linear transect along the direction of the cliff area, with the subject in direct contact to the cliff surface. Each plot position was recorded with a GPS device (WGS 84 ellipsoid) and its ellipsoidal altitude noted. Plots were distanced a minimum of 4 m along the transect in order to avoid duplicates in terms of plant assemblage. Moreover, they were visually positioned (often with the help of a 10 x 50 binocular) on the cliff wall with a subject-to-plot distance that never exceeded 8 m in the vertical component. Following the characteristics of each zone, plots were placed locally in various slope orientations and inclinations. Such scheme approximated the representation of the continuum of soil abundance and moisture availability in the cliff (Whittaker 1960; Whittaker & Niering 1964). Furthermore, the surveyed surface within each plot was microtopographically homogeneous (e.g. same local orientation, same or similar inclination within the plot). Before any numerical analysis, plant cover was *a-posteriori* transformed in the (1-9) logarithmic scale following van der Maarel (1979). For every relevé were recorded the following environmental variables:

1. *Regional orientation* (also denominated global orientation). The direction toward which the plot is faced. The word "regional" or "global" refers to the sector of the topographic unit (e.g North sector of a mountain). Regional orientation was retrieved *a-posteriori* by the plot location within the topographic unit. It is a single qualitative descriptor of 4 classes: N, E, S, W.
2. *Local orientation*. At fine scale, the direction toward which the plot is faced. Local orientation was estimated on field using a magnetic compass. It was classified as a single qualitative descriptor of 16 classes: N, NNE, NE, E, ESE, SE, SSE, S, SSW, SW, WSW, W, WNW, NW, NNW. This classification, however, resulted too discrete for the number of samples and/or variation encountered. An *a-posteriori* reclassification followed. The final qualitative descriptor for local orientation had 4 classes: N, E, S, W.
3. *Inclination* (also denominated slope). The categorization of cliff according to inclination followed the conceptual classification described by Davis (1951). The cliff was divided in 3 qualitative classes of inclination: low to intermediate

inclination (corresponding to a 30° - 60° span), intermediate to high (60° - 90°) and overhanging (> 90°).

4. *Fracturation*. This variable considered the number of cracks, fractures, holes etc in the cliff surface. Fracturation was calculated as a qualitative descriptor with 3 classes: low, medium, high. It is considered as a proxy of the colonisable habitats within a cliff due to the possibility of seed establishment. Plant existence on cliffs is limited to the areas where fracturation is not zero. A zone without fracturation equals to a solid fraction of bare rock due to the impossibility of seed establishment in the first place.
5. *Position*. The position of the plot within the visual portion of the cliff. Position was a qualitative variable with 2 classes: "cliff" and "cliff base". The classes indicate whether the plot was positioned in close proximity to the boundary between a cliff and the surrounding environment (cliff base) or far from it (cliff). Any plot positioned within a distance from the base of 0 to 4 m (the approximated double height of the surveyor) was categorised as "cliff base". Conversely, plots with a distance from the base of 4 to 8 m was labelled as "cliff".

In order to present a structured view of site compositional data, a cluster partitioning was performed. Among many potential similarity functions (Legendre & Legendre, 2012), the Species x Sites transformed matrix was used to compute a Chord Distance similarity matrix of sites. A Ward's minimum variance clustering hierarchical method was subjectively chosen for clustering sites. To interpret and compare the dendrogram of the resulting site clustering, 2 to 10 cluster groups were subjectively selected by a visual examination. The analysis of the degree of membership of each site into its cluster group was performed using the average silhouette widths method (Rousseeuw, 1987; Boccard et al., 2018). The final number of cluster groups was 6. This number of groups presented the least misclassified objects. The original species x sites data Table was reordered according to the resulting clustering and cluster grouping. The spatial distribution of sites, together with their cluster group information is presented in appendix 2 (Fig. S2.1-S2.3).

The matrix of Sites x Cluster groups was subsequently visually interpreted by means of environmental variables. In order to achieve it, qualitative variables and the corresponding cluster group density were listed in tables.

A form of constrained canonical ordination (RDA) was then performed in order to visualise as a correlation triplot the constrained distribution of variance among species and sites. For this purpose, the sites x species matrix was previously Hellinger-transformed. Sites were plotted using their fitted site scores (lc scores, linear combinations of explanatory variables). A scaling 1 was used for visualising the correlation triplot (Legendre & Legendre, 2012). Both the adjusted and unadjusted R^2 values were extrapolated from the analysis (Peres-Neto et al., 2006). ANOVA like permutation tests were performed to test the global significance of the canonical analysis. The same test was used for the significance of each of its axes and term (constraining variable) in the presence of all the other variables in the model [permutation by = ‘margin’] (Legendre et al., 2011).

Cluster analysis was implemented in R 3.6.1 (R Core Team 2019) using the R studio interface (RStudio Team, 2018) and the package “stats”. Silhoutte widths method used instead the package “cluster”. The display of site-by-species abundance heatmap in connection with the clustering results was produced using the package “vegan”. The RDA ordination and its graphic representation were implemented using the package “vegan”.

Results

A total of 57 species were recorded during the survey (Table 2.2). The selected Ward clustering method produced six well-delimited groups and no outliers (Fig. 2.2). The cluster with the least number of sites was cluster 1 (3). It followed cluster 4 (9), cluster 3 (12), cluster 2 and 6 (15) and cluster 5 (17). The average silhouette width for the entire dataset was 0.13. Cluster 5 and 6 were the least coherent, having respectively 3 and 4 misclassified sites. Conversely, cluster 1, 2 and 4 were the most coherent. Cluster 3 had just one slightly misclassified site.

Analysing each group separately according to its main species, cluster 1 was the least variable. Few species were encountered in its plots (11). The dominant species were *Sanguisorba ancistroides* and *Sarcocapnos enneaphylla*. Twenty-seven species were encountered in cluster 2. In this group the dominant species were *Teucrium buxifolium* (very frequent and most abundant species), *Stipa offneri*, *Erica multiflora, Pseudoscabiosa saxatilis* and *Viola arborescens*. A comparable number of species to cluster 2 were encountered in cluster 3 (26 species). This group is hierarchically proximal to cluster 1 and 2 and shared with the last the dominant species *E. multiflora* and *P. saxatilis*. However, the dominant species here was *P. saxatilis*. In addition, *Rhamnus oleoides* subsp. *rivasgodayana* and *Salvia rosmarinus* were often encountered within its plots. Cluster 4, 5 and 6 were hierarchically associated and well distanced from the first 3 clusters. Plots categorized as pertaining to cluster 4 were the basal group respect to the cluster group (4 + 5 + 6) family. A total of 21 species were encountered in cluster 4. Among them the most abundant was *Hyparrhenia hirta*, followed by *Lavandula dentata*, *Centaurea rouyi* and *S. offneri*. As for cluster 4, 21 species were encountered in cluster 5. Here, *S. offneri* was as well very frequent, but not as abundant. The dominant species were *R. oleoides* subsp. *rivasgodayana*, *Hippocrepis valentina*, *S. rosmarinus* and *Satureja obovata* subsp. *valentina*. Finally, cluster 6 was characterised by the highest number of species (32). This group was characterised by the frequent and intense presence of *S. rosmarinus* in each plot. Other abundant species encountered in the group were *Rhamnus lycioides* subsp. *lycioides*, *S. obovata* subsp. *valentina*, *Stipa tenacissima*, *Pistacia lentiscus*, *E. multiflora* and *P. saxatilis*.

Table 2.2. Species and their abbreviations

Species	**label**	**Species**	**label**	**species**	**label**
Antirrhinum controversum PAU	Anti cont	*Ficus carica* L.	Ficu cari	*Rhamnus alaternus* L.	Rham alat
Asperula paui subsp. *dianensis* (FONT QUER) ROMO	Aspe paui	*Fumana ericoides* (CAV.) GANDOG.	Fuma eric	*Rhamnus oleoides* subsp. *rivasgodayana* RIVAS MART. & J.M. PIZARRO	Rham oleo
Ballota hirsuta BENTH.	Ball hirs	*Helichrysum pendulum (C. PRESL) C. PRESL*	Heli pend	*Rhamnus lycioides* L. subsp. *lycioides*	Rham lyci
Biscutella rosularis BOISS. & REUT.	Bisc rosu	*Hippocrepis valentina* BOISS.	Hipp vale	*Salvia rosmarinus* SCHLEID.	Salv rosm
Brachypodium retusum PERS. & P.BEAUV.	Brac rupe	*Hyparrhenia hirta* (L.) STAPF.	Hypa hirt	*Sanguisorba ancistroides* (DESF.) CES.	Sang anci
Brassica repanda (WILLD.) DC. subsp. *blancoana* (BOISS.) HEYWOOD	Bras repa	*Lavandula dentata* L.	Lava dent	*Sarcocapnos enneaphylla* (L.) DC.	Sarc enne

Bupleurum fruticescens LOEFL. EX L. subsp. *fruticescens*	Bupl frut	*Lavatera maritima* GOUAN	Lava mari	*Satureja obovata* Lag. subsp. *valentina* (G. LÓPEZ) M.B. CRESPO	Satu obov
Carduncellus dianius WEBB	Card dian	*Lonicera implexa* AITON.	Loni impl	*Sedum album* L.	Sedu albu
Centaurea rouyi COINCY	Cent rouy	*Micromeria inodora* (DESF.) BENTH.	Micr inod	*Silene hifacensis* ROUY EX WILLK.	Sile hifa
Centranthus ruber (L.) DC.	Cent rube	*Osyris lanceolata* HOCHST. & STEUD. EX A. DC.	Osyr lanc	*Sonchus tenerrimus* subsp. *dianae* (LACAITA) R.DE P.MALAGARRIGA HERAS	Sonc tene
Chaenorhinum origanifolium (L.) KOSTEL. subsp. *crassifolium* (CAV.) RIVAS GODAY	Chae orig	*Pallenis maritima* (L.) GREUTER	Pall mari	*Succowia balearica* (L.) MEDIK.	Succ bale
Chamaerops humilis L.	Cham humi	*Petrosedum sediforme* (JACQ.) GRULICH)	Petr sedi	*Stipa offneri* BREISTR.	Stip offn
Convolvulus althaeoides L.	Conv alth	*Phagnalon rupestre* (L.) DC.	Phag rupe	*Stipa tenacissima* L.	Stip tena
Coronilla juncea L.	Coro junc	*Phagnalon saxatile* (L.) CASS.	Phag saxa	*Teucrium buxifolium* SCHREB.	Teuc buxi
Dianthus broteri BOISS. & REUT. subsp. *valentinus* (WILLK.) RIVAS MART.	Dian brot	*Phillyrea latifolia* L.	Phil lati	*Teucrium pseudochamaepitys* L.	Teuc flav
Elaeoselinum asclepium (L.) BERTOL.	Elae ascl	*Pistacia lentiscus*, L.	Pist lent	*Teucrium flavum* L. subsp. *flavum*	Teuc pseu
Ephedra fragilis DESF.	Ephe frag	*Polygala rupestris* POURR.	Poly rupe	*Teucrium ronnigeri* SENNEN	Teuc ronn
Erica multiflora L.	Eric mult	*Pseudoscabiosa saxatilis* (CAV.) DEVESA	Pseu saxa	*Ulex parviflorus* subsp. *parviflorus* POURR.	Ulex parv
Erica terminalis. SALISB.	Eric term	*Quercus coccifera* L.	Quer cocc	*Viola arborescens* L.	Viol arbo

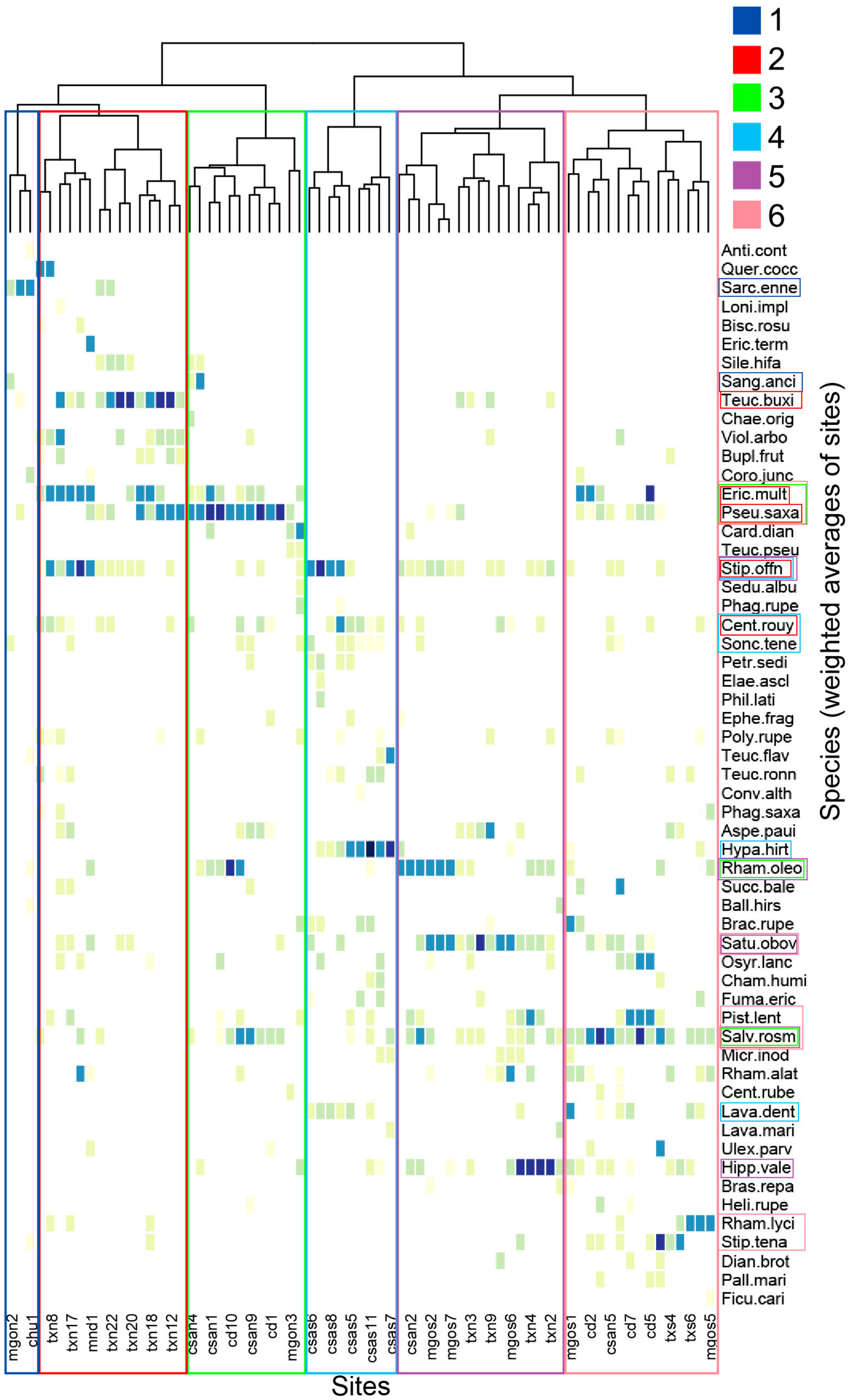

Fig 2.2. Heat map of the doubly ordered community Table. Up, the resulting dendrogram of Ward site clustering. Right and down are species and site names, respectively. Color scheme goes from pink to green to blue and is proportional to the species abundances. Cluster groups colors and labels are shown in the legend up right.

Global orientation	Local orientation	Cluster 1	2	3	4	5	6
E	E			3		2	4
	N			3			3
	S					1	
	Total			6		3	7
N	E	1	3			1	1
	N	1	11	4			1
	W			2			
	Total	2	14	6		1	2
S	S		1		8	8	6
	W				1	3	
	Total		1		9	11	6
W	N					2	
	W	1					
	Total	1				2	

Position	Slope	Cluster 1	2	3	4	5	6
cliff	30-60º		2	1	1		2
	61-90º		9	11	4	8	8
	Overhanging	3					
cliff_base	30-60º		3		4	7	4
	61-90º		1			2	1

A

Zone	Cluster 1	2	3	4	5	6
C. San Antonio			5	9	5	2
Cap D'Or			4			6
Chulilla	1					
Monduber		1				
Montgò	1		2		5	2
Toix	1	14	1		7	5

B

Table 2.3. Environmental variables categorised according to count of cluster groups. Data and colour gradient refer to plot counts for each variable and cluster group. Left: Distribution of clusters among local and global orientation categories. Right: A) data distributed among different categories of position and slope; B) sampling areas.

Table 2.3 (left) shows that cluster 5 was the unique ubiquitous group with respect to global orientation. By contrast, cluster 1 and 3 resulted absent from South-oriented areas, meanwhile cluster 4 was exclusively found on such orientation. Cluster 2 and 3 were more abundant on North-oriented areas, both globally and locally. Beside this case, no significant patterns of local orientation can be ascribed to any cluster group.

With respect to position (Table 2.3 A), cluster 1 and 3 were encountered exclusively on cliff. Similarly, cluster 2 was preferentially encountered on cliff rather than on cliff base. No other significant patterns arise from position. By contrast, it is evident from Table 2.3 B that slope plays an important role in discriminating clusters. With this regard, cluster 1 is exclusive of the overhanging areas. Moreover, cluster 2 and 3 are preferentially found on vertical (60° - 90°) rather than gentle (30° 60°) angles of slope. Other clusters are similarly distributed among slope categories.

All clusters except cluster 4 are distributed among 2 or more zones in the studied region. Cluster 4 was exclusively encountered in the cliffs of Cabo de San Antonio. A similar exclusivity is shown by cluster 2, which was preferentially encountered in the area of Toix.

The constrained fraction of the total variance in the RDA analysis (Fig. 2.3) was 29.4 % (R^2 = 0.29388). The adjusted R^2 was 0.1622. The analysis resulted in 11 canonical axes and 56 unconstrained axes for the residuals. The cumulative proportion of variance explained by the first two axes was 0.16 of the total variance or 54.45 % of the constrained variance. The first axis held 0.10 and the second 0.06 of the total variance. The proportion of variance explained by the first and the second residual structures (PC1 and PC2) were proximal to the first constrained axis and were higher than the second (0.078 and 0.077, respectively). It was then likely the existence of a residual structure in the response data.

The permutation tests for the whole RDA analysis and the first two constrained axes was significant for $P < 0.001$. Also, RDA3 was significant but with $P < 0.01$ meanwhile other axes resulted to be not significant. Regional orientation was highly significative ($P < 0.001$) and explained the majority of the tested constrained variance (41 %, 0.065). Slope was significative for $P < 0.01$, explaining 19 % (0.03) of the variance. Finally, the plot position on cliff explained 8.9 % of variance (0.014, $P < 0.05$). Local orientation and fracturation were found to be not significant.

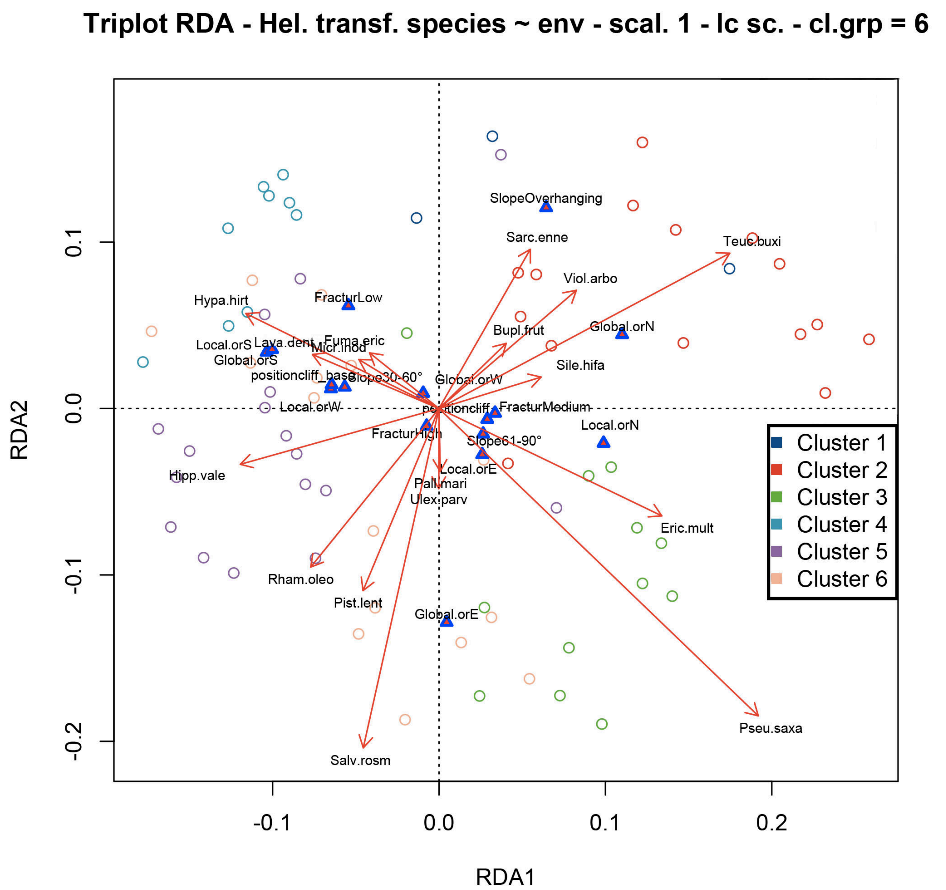

Fig. 2.3. RDA of species abundances constrained by fine scale microtopographic features of the cliff. Red arrows represent response variables (species) with a goodness of fit ≥ 0.1 Species are plotted using a multiplying factor of 0.079 over their species scores. Constraints are all categorical. Their centroids are represented by red and blue triangles.

Species assemblages were configured in 4 main groups and resulted scattered along the 4 quadrants of the ordination space. The first group of species is located on the first quadrant, being positively associated with both a positive RDA1 and RDA2. This group was characterised by strictly chasmophytic species as *Sarcocapnos enneaphylla*, *Viola arborescens*, *Bupleurum fruticosum*, *Silene hifacensis* and *Teucrium buxifolium*. Among these species, *S. enneaphylla* resulted strongly characterised by a positive relationship with overhanging zones. The second group of species is located on the fourth quadrant. This group was formed by only 2 species visible in the ordination (*Erica multiflora* and *Pseudoscabiosa saxatilis*) and was as well associated to a positive RDA1. As the first group, these species were positively associated with high inclinations (slope 61° - 90° centroid). The other 2 groups were located in the second and third quadrants, respectively. The third group of species was characterised by *Fumana ericoides, Micromeria inodora, Lavandula dentata* and *Hyparrhenia hirta*. The last assemblage did not appear as uniform as the third group and was formed by *Hippocrepis valentina, Rhamnus oleoides, Pistacia lentiscus, Salvia rosmarinus, Asteriscus maritimus* and *Ulex parviflorus*. The third group was positively associated with low levels of inclination (centroid 30° - 60°). By contrast, the fourth group was heterogeneous in this regard: species like *H. valentina* and *R. oleoides* were more associated to low levels of slope then others. The central subgroup of *R. oleoides, P. lentiscus* and *S. Rosmarinus* were more ubiquitous. The rest of the species in the group were more associated to high slopes but contributed less to the ordination (short arrows).

The first axis of variation was characterised by a main influence of the position of the centroids associated to regional orientation. The positive RDA1 semi-axis and species group 1 and 2 were positively associated with a North orientation. The negative portion of RDA1 together with group 3 and 4 were instead associated positively to a South orientation. An East orientation was almost neutral for the variation expressed by RDA1, but strongly associated to species group 3. West orientations contributed the least to the analysis, probably due to the scarcity of plots with this regional orientation. Site clusters were at least partially segregated. Clusters 1, 2 and 3 were positioned along a positive variation of RDA1, and thus associated positively to a Northern orientation. By contrast, cluster 4 and 5 followed an opposite behaviour, being associated to a negative variation of RDA1 and thus to a Southern orientation. At least cluster 1, 2 and 4 resulted coherent within their association to slope, whereas cluster 5 and 6 did not have a common pattern of association to this constraint.

Discussion

As can be seen from the analyses, the numerical classification separated the 6 site clusters in 2 major groups. Cluster 1, 2 and 3 were clearly defined by chasmophytes and species well adapted to colonise cliffs (mainly on North-oriented areas). According to the interpretation given to site ordination, cluster 4 and 5 were the most coherent, and corresponded to South oriented assemblages. Site cluster 6 resulted the most heterogeneous both regarding its floristic composition and environmental conditions. Cluster 6 is hierarchically connected to cluster 4 and 5, and similarly to those the main orientation where it was observed was on South and East, but not on North.

From a phytosociological standpoint, all groups were represented by at least a certain level of admixture of different associations and alliances. Cluster 1 was characterised by a strong association with overhang and defined by the diagnostic species *Sarcocapnos enneaphylla*. With few doubts it corresponds to the alliance *Sarcocapnion enneaphyllae* FERNÁNDEZ CASAS 1972.

With the exception of few sites, clusters 2 and 3 can be allocated in the *Teucrion buxifolii* RIVAS GODAY 1956 alliance and specifically in the association *Hippocrepido-Scabiosetum saxatilis* RIVAS GODAY EX O. BOLÒS, 1957. This alliance represents the characteristic Thermo-mesomediterranean chasmophytic vegetation of limestone cliffs in Western Mediterranean (Mucina et al., 2016). Both clusters are characterised by the frequent and most abundant diagnostic species *Pseudoscabiosa saxatilis*, with a continuous presence of the accompanying species *Erica multiflora*. Cluster 2 was encountered almost completely in one unique location, Toix, whereas cluster 3 was ubiquitous. Moreover Custer 3 could be distinguished by the absence of the diagnostic species *Teucrium buxifolium* and the presence of *Salvia rosmarinus* and *Rhamnus oleoides* subsp. r*ivasgodayana*. Cluster 4 is characterised by a consistent presence of gramineous species (*Stipa offneri* and *Hyparrhenia hirta*) and can be categorised as *Hyparrhenion hirtae* BR.-BL., P. SILVA & ROZEIRA *1956*, which is a typical alliance of dry grasslands in the Western Mediterranean (Díez-Garretas & Asensi, 1999; Rivas Martínez. & Loidi, 1999). Conversely to cluster 4, which was localised to the South-oriented areas of Cabo de San Antonio, cluster 5 was encountered on different locations. Cluster 5 is as well formed by a xerophilous association which was prevalent in South and east-oriented cliffs: *Rhamno borgiae-Teucrietum rivasii* MATEO & FIGUEROLA 1987 CORR. M.B. CRESPO 1993 (Mateo & Figuerola, 1987).

An important annotation should be made for *Hippocrepis valentina*, the most abundant species in the subgroup formed by the sites on the right of the cluster 5. This species is historically associated with the *Teucrion buxifolii* (see the plots investigated by Rivas Goday, 1954, but also Bolos, 1957), but also with the vegetation encountered at the base of cliffs localised on the Montgò mountain, the *Teucrio-Hippocrepidetum valentinae* O. BOLÒS 1956. These plots, most likely, pertain to this association by considering their environmental characteristics (mainly cliff base, 30-60° inclination).

Cluster 6 is composed by two main subgroups of plots according to the frequency and abundancy of *P. saxatilis*, *H. valentina, P. lentiscus, R. lycioides, S. obovata* and *S. tenacissima*. The dominant species of this entire cluster is *Salvia rosmarinus.* The left subgroup is formed by the first 9 plots in the cluster, which are characterised by the presence of a characteristic species of the *Teucrion buxifolii* alliance, *P. saxatilis*. Unfortunately, the complete clustering hierarchy of the analysis would make an alternative cutting level not desirable for the entire analysis, affecting not only cluster 6 but all the cluster groups. Based on the coherence of the other clusters, this possibility would in fact be counterproductive. As cluster 5, the last 6 plots on the right of cluster 6 are mainly dominated by species of the surrounding matorral, mixed with *H. valentina*. Hence, this subgroup can be categorised as *Teucrio-Hippocrepidetum valentinae*. Conversely, the other plots of cluster 6 are characterised by taxa typically encountered on the *Teucrion buxifolii* alliance as *E. multiflora* and *P. saxatilis* mixed in a background of the alliance *Rosmarinion officinalis* MOLINIER 1934. According to extensive observations of the ecological characteristics of *Hippocrepis valentina*, its simultaneous presence together with *P. saxatilis* is not at all typical of the *Hippocrepido-Scabiosetum saxatilis* as Rivas Goday (1954) and following authors suggest. In fact, *H. valentina* is only sporadically associated with vertical inclinations as also shown in Fig. 2.3. The joint presence of these 2 species should be noted as an ecotonal, intermediate state among the *Hippocrepido-Scabiosetum saxatilis* RIVAS GODAY EX O. BOLÒS, 1957 and the *Teucrio-Hippocrepidetum valentinae* O. BOLÒS 1956. In alternative, in the proximity of the coastal cliffs in this part of Spain it is also possible to find *H. valentina* in the *Rosmarinion officinalis* as a companion species.

Conclusions

With the except of cluster 6, the statistical ordination paired with the cluster analysis gave an acceptable discrete subdivision of plant communities according to their species composition and regional diversity. However, the close proximity of centroids in the canonical analysis suggested that the qualitative constraints were overlaid. My conclusions are that the analysis suffered two biases: a) the qualitative nature and number of categories of constraints was not adequate to describe the assemblage variation at local level; and b) the number and allocation of samples was too limited by the visible portion (8 m in vertical component) of the cliff surface.

Bibliography

Aguilella, A., Fos, S. & Laguna, E. (2010). Catálogo Valenciano de Especies de Flora Amenazadas. Colección Biodiversidad, 18. Conselleria de Medi Ambient, Aigua, Urbanisme i Habitatge, Generalitat Valenciana. Valencia.

Bacchetta, G., Casti, M., Mossa, L. (2007). New ecological and distributive data regarding rupicolous flora in Sardinia. Journal de Botanique de la Société Botanique de France, 38: 73-83.

Bartlett, R.M., Matthes. Sears, U. & Larson, D.W. (1990). Organization of the Niagara Escarpment cliff community. II. Characterization of the physical environment. Canadian Journal of Botany 68: 1931-1941.

Boccard, D., Gillert, F. & Legendre, P. (2018). Numerical Ecology with R. Springer, New York.

Bolòs O. de. (1957). De vegetatione valentina I. Collect Bot. 5 (2): 527-599.

Buira, A., Cabezas, F. & Aedo, C. (2020). Disentangling ecological traits related to plant endemism, rarity and conservation status in the Iberian Peninsula. Biodivers Conserv 29, 1937–1958. https://doi.org/10.1007/s10531-020-01957-z

Castroviejo, S. (coord. gen.) (1986-2012). Flora iberica 1-8, 10-15, 17-18, 21. Real Jardín Botánico, CSIC, Madrid.

Davis, P. (1951). Cliff Vegetation in the Eastern Mediterranean. Journal of Ecology, 39(1), 63-93.

Díez-Garretas, B., Asensi, A. (1999). Syntaxonomic analysis of theAndropogon-rich grasslands (Hyparrhenietalia hirtae) in the western Mediterranean region. Folia Geobot 34, 307. https://doi.org/10.1007/BF02912817

Escudero, A. (1996). Community patterns on exposed cliffs in a Mediterranean calcareous mountain. Vegetatio 125, 99–110 https://doi.org/10.1007/BF00045208

Font Quer, P. (1953). Diccionario de Botanica, 1, 2. Editorial Labor, Barcelona 1244 p.

Heywood, V.H. (1953). El concepto de asociaciòn en las comunidades rupicolas. Annales Instituto Botanico Cavanilles 11(2): 463-481.

John, E.A. & Dale, M.R.T. (1990). Environmental correlates of species distributions in a saxicolous lichen community. Journal of Vegetation Science 1: 385-392.

Lavergne, S., Garnier, E. & Debussche, M. (2003). Do rock endemic and widespread plant species differ under the Leaf-Height-Seed plant ecology strategy scheme? Ecology Letters 6: 398–404.

Legendre, P. & Legendre, L. (2012). Numerical ecology, 3rd English edition. Elsevier Science BV, Amsterdam. xvi + 990 pp.

Legendre, P., Oksanen, J. & ter Braak, C.J.F. (2011). Testing the significance of canonical axes in redundancy analysis. Methods in Ecology and Evolution 2, 269–277.

Mateo, G. & Figuerola, R. (1987). Sobre la vegetación del orden Asplenietalia petrarchae en las montañas valencianas. Lazaroa 7: 319-326.

Meier, H. & Braun-Blanquet, J. (1934). Prodrome des groupements vegetaux. 2. (Classe des Asplenietales rupestres-Groupements rupicoles). Marie-Lavit. Montpellier.

Minelli, A., Stoch, F. (2006). Quaderni habitat: Ghiaioni e rupi di montagna – una vita da pionieri tra le rocce. Ministero dell'Ambiente e della Tutela del Territorio Museo Friulano di Storia Naturale, Comune di Udine.

Mucina, L., Bültmann, H., Dierßen, K., Theurillat, J.-P., Raus, T., Čarni, A., Šumberová, K., Willner, W., Dengler, J., García, R.G., Chytrý, M., Hájek, M., Di Pietro, R., Iakushenko, D., Pallas, J., Daniëls, F.J., Bergmeier, E., Santos Guerra, A., Ermakov, N., Valachovič, M., Schaminée, J.H., Lysenko, T., Didukh, Y.P., Pignatti, S., Rodwell, J.S., Capelo, J., Weber, H.E., Solomeshch, A., Dimopoulos, P., Aguiar, C., Hennekens, S.M. and Tichý, L. (2016). Vegetation of Europe: hierarchical floristic classification system of vascular plant, bryophyte, lichen, and algal communities. Appl Veg Sci, 19: 3-264. doi:10.1111/avsc.12257

Panitsa, M., & Kontopanou, A. (2017). Diversity of chasmophytes in the vascular flora of Greece : floristic analysis and phytogeographical patterns.

Peres-Neto, P., Legendre, P., Dray, S. & Borcard, D. (2006). Variation partitioning of species data matrices: estimation and comparison of fractions. Ecology 87, 2614–2625.

R Core Team (2019). R: A language and environment for statistical computing. R Foundation for Statistical Computing, Vienna, Austria. URL http://www.R-project.org/.

R Studio Team (2018). RStudio: Integrated Development for R. RStudio, Inc., Boston, MA URL http://www.rstudio.com/

Rivas-Martinez, S. (1960). Roca, clima y comunidades rupicolas. Sinopsis de las alianzas hispanas de Asplenietea rupestris. Anales Real Academia de Farmacia 26: 153-168.

Rivas Martínez, S. & Loidi, J. (1999). Biogeography of the Iberian Peninsule. Pp. 49-67. In: Rivas-Martínez, S., Loidi, J., Costa, M., Díaz, T. E. & Penas, A. (eds.), Iter Ibericum A. D. MiM, Itinera Geobotanica 13: 49-67.

Rivas Goday, S. (1954). Algunas asociaciones de la Sierra de Callosa de Segura (prov. de Murcia) y consideraciones acerca de la Potentilletalia mediterránea. Anales Inst. Bot. Cavanilles 12(1): 469–500. Madrid.

Rivas-Martínez, S., Penas, A., Díaz, T. (2004). Biogeographic Map of Europe

Rousseeuw, P.J. (1987). Silhouettes: A graphical aid to the interpretation and validation of cluster analysis. J. Comput. Appl. Math., 20, 53–65.

Sanz de Galdeano, C. & Ruiz Cruz, M.D. (2016). Late Palaeozoic to Triassic formations unconformably deposited over the Ronda peridotites (Betic Cordilleras): Evidence for their Variscan time of crustal emplacement. Estudios Geológicos 72(1): e043. http://dx.doi.org/10.3989/egeol.42046.368.

Schimper, A.F.W. & Faber, F.C. (1935). Pflanzengeographie auf physiologischer Grundlage, 1,2. Verlag von Gustab Fischer, Jena.

van der Maarel, E. (1979). Transformation of cover-abundance values in phytosociology and its effects on community similarity. Vegetatio 39, 97–114. https://doi.org/10.1007/BF00052021

Whittaker, R.H. (1960). Vegetation of the Siskiyou Mountains, Oregon and California. Ecological Monographs 30: 279–338.

Whittaker, R.H. & Niering, W.A. (1964). Vegetation of the Santa Catalina Mountains, Arizona. I. Ecological classification and distribution of species. Journal of the Arizona Academy of Science 3: 9–34.

Chapter 3: UAV (drone) surveys for the study of plant–microtopography relationships and conservation of rare species.

Introduction

Observing the distribution and abundance of plants and their environmental drivers is a key aspect of plant ecology. In this regard, the possibility to gather large amount of environmental and species compositional data on cliffs is limited by their scarce accessibility (Davis, 1951). The use of traditional methods as for example transect or quadrats is limited to the accessible portion of the cliff surface and the time required (see chapt. 2).

Microclimate (see chapt 1) and fine scale changes in the landscape are nowadays a major topic in many fields of plant ecology (Bennie et al., 2018; Bramer et al., 2018; Garcia et al., 2020; Papadopouloua & Knowles, 2016) In recent years, utilization of micro–Unmanned Aerial Vehicles (micro-UAVs, unmanned aerial vehicles) for ecological research increased proportionally to the levels of image details they can provide (Baena et al., 2017) and their cost. In plant ecology, they were mainly used to produce orthomosaics of the landscape at fine-medium scale.

Other works were focused on the analysis of detailed vegetation location properties through the use of 3D models (Niederheiser et al., 2018).

The complexity of environmental conditions encountered on cliffs (see chapt 1 and 2), paired with the technical difficulties related to their accessibility (Fig. 3.1) have made ecological research (Davis, 1951; Kuntz & Larson, 2005) and conservation management (Goñi et al., 2006; Misfud, 2013) challenging in these zones.

The goal of this chapter is to describe a new developed methodology for obtaining vegetation relevés on Mediterranean cliffs based on drone aerial photogrammetry and 3D models. It will be showed the pros and cons of analysing vegetation composition and its location properties by using a 3D modelling approach. A number of factors to consider for planning aerial drone surveys will be addressed. The resulting plot-based datasets were used to study causal relationships between chasmophytes and their environment at fine scale.

Fields of interest include plant ecology, conservation and population ecology on inaccessible areas, with the intent to study and understand plant-environment relations on Mediterranean cliffs.

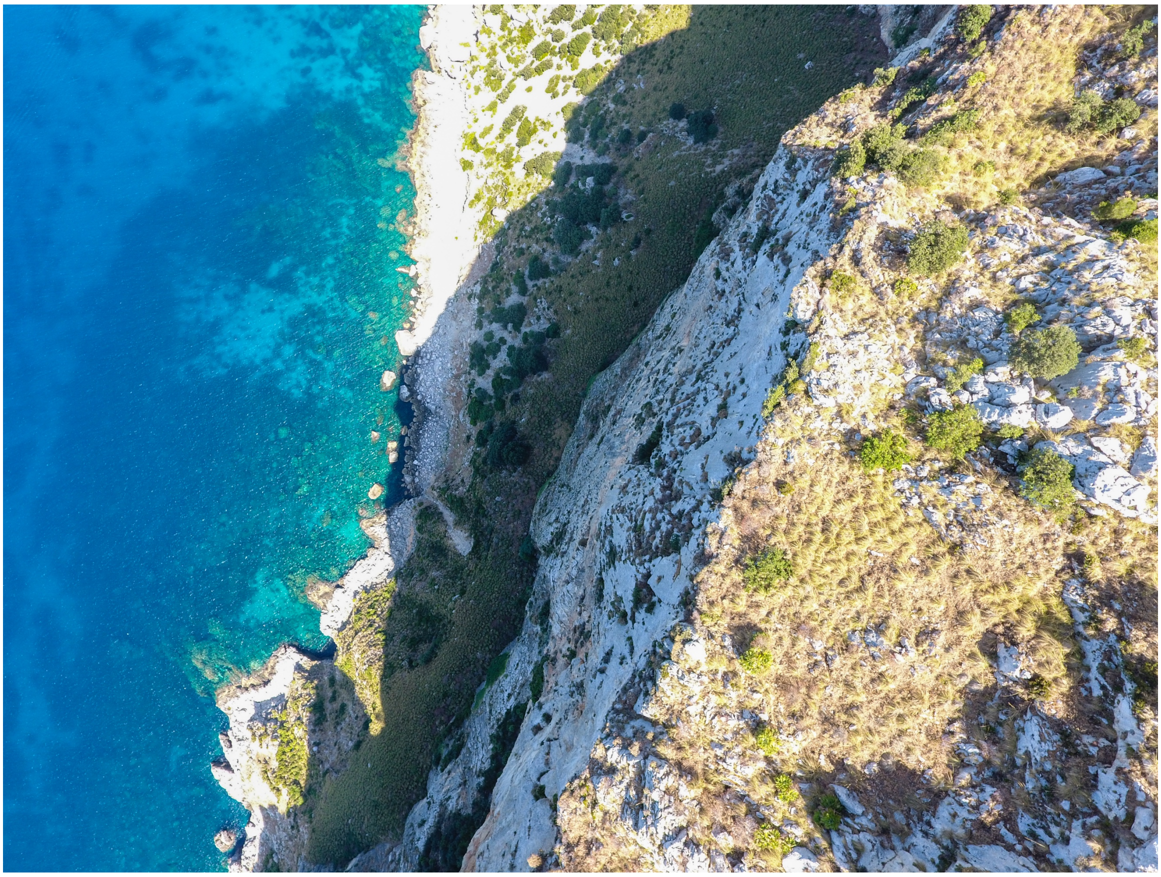

Fig. 3.1. Nadir view of a cliff measuring 240 m in height. A close inspection to the plant assemblages in such cases is reduced to the accessible portions: upper ledge and base.

Methods

General considerations

In recent years Structure-from-Motion Multi-View-Stereo (SfM-MVS) became a common approach in many fields, such as ecology and geosciences, to obtain digital high-resolution topographic information from still images (see Forsmoo et al., 2019 and literature therein). In brief, SfM-MVS requires a significant number of partially overlapping photographs of a subject taken from different angles. The algorithm returns a digital 3D model of the subject in the form of a dense cloud of points in a digital space.

Due to the vertical nature of cliffs, these environments are inaccessible without proper climbing devices and experience, not mentioning security issues, climbing feasibility and costs. The methodology proposed and discussed here applies the aerial photogrammetric techniques on an inaccessible vertical surface by using Unmanned Aerial Vehicles (UAVs), commonly known as drones. A drone equipped with an optical camera is then a lightweight, relatively inexpensive tool to collect close range, high resolution and georeferenced photos of hardly-to-reach areas. These photos are then used to obtain via SfM-MVS a georeferenced 3D point cloud of the cliff and its plant assemblages.

As discussed below, each 3D model collects a high amount of biological, topographic and geomorphological information. The creation of the 3D model allows to store the exact location of each pixel of any aligned photo. If the 3D model is georeferenced (as it is the case here), then the pixel will have a known geographical position as well.

Therefore, by identifying and tagging an object (e.g. a plant specimen, a plot, a fracture) in the aligned photos, it will be possible to know the absolute and local coordinates of its exact location on the cliff surface in the 3D digital model.

Assuming a proficient botanical knowledge of the local flora, the first layer of information gathered from a single drone flight allows the quantification, identification and position of the target specimen occurring in the cliff plant assemblage from the remotely collected dataset. Additionally, a second layer of information consists in the physical characterization of the cliff surface at a relevant spatial scale. These two combined datasets provide the necessary data matrix for a quantitative, highly accurate ecological characterization of cliff assemblages or target species.

Equipment

All aerial surveys were carried out with a DJI Phantom 4 (drone from now on) along vertical transects parallel to the cliff. The drone has a built-in gimbal mounting a 12 MP camera triggered by a remote radio controller (operative distance ranging from 0 to 150 m). The remote control is also connected to a screen that allows the operator to check the camera position and to trigger the image-capturing during the flight. The drone used for the data acquisition was equipped with 4 new 5350 mAh LiPo 4S batteries.

The Phantom 4 model is a light (total weight 1800 g), easy to operate, quadcopter. The device is very stable in flight thanks to its internal GPS tracking system which allows to precisely operate it at a close distance from the cliff surface. In fact, the internal GPS allows to maintain the position of the drone at a specific location and altitude and it geolocates each taken photograph. The importance of storing GPS coordinates, although not strictly necessary to create a 3D model, allows to get flight metadata in each image and to maintain the geographic properties of the surveyed area (i.e. geographic orientation of the model and the z direction).

Scope of each survey and related scale

Study area	Zone	Research target	Photos used for model building	GSD (cm/ pixel)	Mean cliff-to-photo distance ± s.d. [m]	Surface analysed (DSM) [m^2]	N. batt.	Dense cloud points
Cabo de San Antonio North cliffs	Alicante (Spain)	Scenario 1. Plant assemblages	219	0.099	2.3 ± 0.75	608.2	3	17.102.000
Cabo de San Antonio South cliffs			248	0.048	1.11 ± 0.74	239.4	2	9.153.000
Cap D'Or Pessebret partial			874	0.191	4.44 ± 1.34	2974.4	6	25.017.000
Cap D'Or Cueva de Les Cendres		Scenario 1, 2. Plant assemblages/conservation	756	0.087	2.02 ± 1.25	686.7	3	44.784.000
Cap D'Or Pessebret Complete		Scenario 2. Plant conservation	874	0.191	4.44 ± 1.34	4955	6	39.273.000
Morro de Toix			164	0.06	1,4	295	2	22.631.000
Monte Cofano South cliffs	Trapani (Italy)	Scenario 2. Target species	472	0.323	7.52 ± 3.55	14782.4	2	58.739.000
Monte Cofano West cliffs			587	0.278	6.47 ± 1.78	11455.7	2	39.564.000
Monte Cofano North cliffs			910	0.325	7.58 ± 3.41	25461.9	4	43.833.000
Monte Cofano East cliffs			325	0.229	5.34 ± 2.09	6599.6	3	47.381.000
Monte Gallo North cliffs	Palermo (Italy)		652	0.188	4.39 ± 2.52	6118.3	3	46.680.000

Table 3.1. Specifications of the produced 3D models. Used photos refer to the number of aerial photographs that were used by the program to build the 3D model. GSD = Ground Sampling Distance. The value is referred to the mean camera-to-cliff distance and the Phantom 4 lens specifics. Mean cliff-to-photo distance = the averaged distance of all the photos used to build the 3D model and the surface of the cliff. Surface analysed refers to the created 3D model in its integrity, including vegetation (equals to a Digital Surface Model, DSM). N. batt = number of batteries used for the creation of the 3D model.

Two classes of scenarios were taken into account in order to demonstrate the research possibilities allowed by a 3D methodology applied on cliffs. The scenario 1 research type aimed at identifying all the individuals forming a cliff plant assemblage, whereas the scenario 2 focussed only on one or several specific taxa. Both scenarios shared the simultaneous collection of environmental data of the cliff surface. The environmental data collected from the 3D model were of quantitative nature and refer to the geomorphology and topographic characteristics of the cliff surface.

Table 3.1 shows the characteristics and purposes of the 3D models analysed in this chapter, resumed in Fig. 3.2. Independently from the research focus and number of investigated species, all these 3D models were aimed at assessing the relationship between species and cliff conditions, with a special focus on causalities at fine ecological scale.

Scenario 1. Identifying all plant specimens living on the research area. Quantitative compositional data are extracted both from the whole study area included in the 3D model and from each of the sampling units contained in the study area. The number of flight missions per analysed surface is increased by the longer flight time required for this kind of survey; the final research area is relatively small, and it is affected by maximum number of aerial photos computable by a computer hardware to build the 3D model. **The main field of application of this scenario is the integration of quantitative compositional and environmental data in order to perform a fine scale analysis of niche segregation and ecological preferences for the single species forming the cliff plant assemblage.**

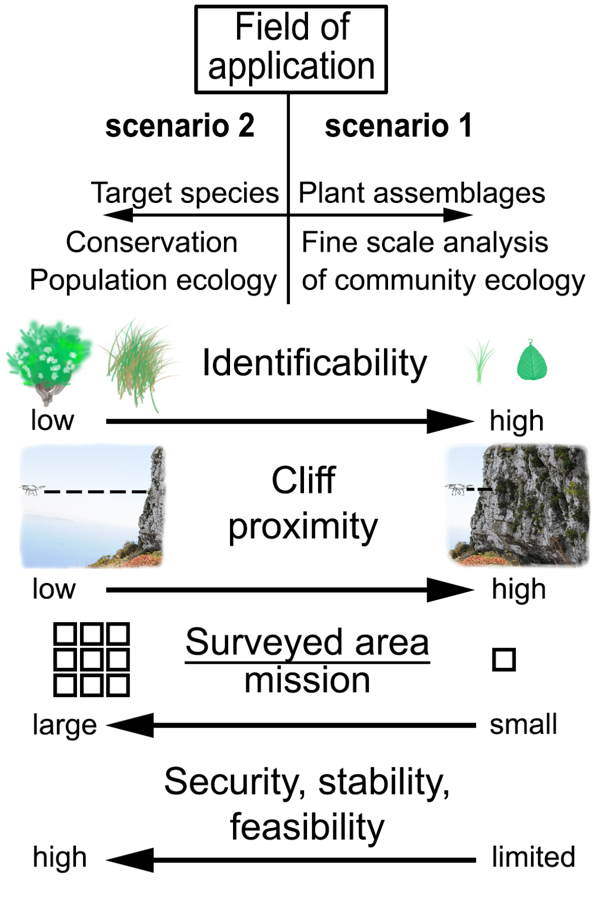

Fig. 3.2. Schematic subdivision of the proposed methodology and fields of application in plant ecology.

Scenario 2. Easy to identify target species. The investigated taxa need to have a minimum dimension and a set of morphological and/or phenological characteristics that can allow their photographic identification 5-10 m away from the cliff. Investigated areas are considerably larger than those in the scenario 1 research. **This method is especially suitable to study selected taxa at population level.** This approach was used in the present work to assess:

1. whether the number of individuals in the extant continental populations of an endemic species has maintained constant value through time;

2. the niche preferences of 2 co-occurring endemic strictly chasmophytic species;

3. the niche preferences of a widespread chasmophytic species and of its endemic counterpart.

The main difference between scenario 1 and 2 relies on the scale of plant identification from aerial images. Actually, the ability to discriminate among plant species depends strictly on 3 entwined factors: dimension of the plant, camera distance from the cliff and camera sensor specifics (i.e. resolution). In remote sensing the relationships among the three factors is expressed by the Ground Sample Distance (GSD), the distance in a photo between pixel centres measured on the ground. In Table 3.1 it is shown the mean GSD and camera distance used to carry out each case study described in this chapter. With the used instruments, a photographic plant ID in scenario 1 research types required close range photos taken from 25cm to up to 2 m from the cliff. A scenario 2 based on the studied species dimension, required a distance from the cliff of 3-6 m. The selected species in this study for a scenario 2 survey were 4 small shrubs of 20-80 cm in diameter: *Pseudoscabiosa limonifolia* (VAHL) DEVESA, *Erica sicula* GUSS., *Lomelosia cretica* (L.) GREUTER & BURDET and *Silene hifacensis* ROUY EX WILLK (Fig. 3.3).

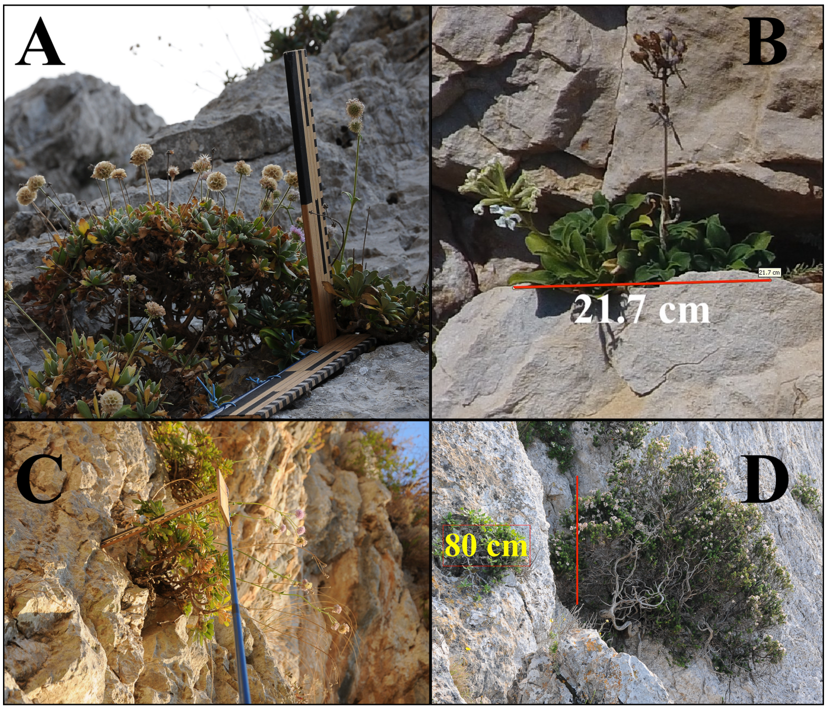

Fig. 3.3. Species used as models for scenario 2 research types. A: left *L. cretica*, right *P. limonifolia*. The wooden scale bar unit is 1 cm; entire length of scale bare = 40 cm. Monte Pecoraro (Italy), 07/2017. B: *S. hifacensis* from an aerial survey. Cap D'Or (Spain), 04/2019. C: *P. limonifolia*. Monte Monaco (Italy), 07/2017. D: an old individual of *E. sicula* at Monte Cofano (Italy), 07/2018.

Sampling strategy and field conditions prior to data collection

Since topographical constraints are hardly detectable on a map, an inspection of the investigation site and the establishment of an accurate flight planning is of primary importance, before starting data acquisition. In fact, it is crucial to plan the battery/surveyed surface ratio prior to the fieldwork. Flight time per battery and the number of batteries a researcher brings in the field can be the limiting factor of any survey.

Studying cliff experimental areas needs to take into account some logistic problems and extreme working conditions. The investigation sites were located at several walking hours of distance from the nearest infrastructure, often on hardly accessible trails. Just considering these scenarios, the number of batteries carried by the operator determines the actual daily extension of the survey. In fact, repeatedly moving back and forward from a field site to an infrastructure with electricity or a car in order to recharge batteries during a working day is highly unfeasible. Also, a portable solar charger or power bank needs to be excluded at the moment due to high costs, weight or long charging time per battery. Finally, a lightweight drone is not only suitable, but often it is the only solution for a single-operator survey in these remote and difficult to access areas.

Phantom 4 drone batteries have a weight of 500 g each, and, if brand new, a capacity of 5350 mHa. Fully charged, each battery permits a flight time of 18 to 25 min depending on the flight dynamics. For this study, a total of 4 batteries were used. Table 3.1 shows the number of batteries used for surveying each experimental area in this chapter. Although it is difficult to quantify exactly how much surface can be surveyed with a battery due to the influence of a large number of factors, as a rule of thumbs it can be said that a battery is suitable to survey 200-250 m^2 in a scenario 1 and 5500-6500 m^2 in a scenario 2 research type.

Finally, to compile an accurate working plan, the prior inspection of the area to be studied will allow a more precise evaluation of the time needed to complete the field assessment.

With regard to the operator position during the aerial photo acquisition, two main factors have to be taken in consideration. First, it is logistically mandatory (and in several countries regulated by law) to maintain a continuous line of sight between the operator and the drone during all the flight. Second, the inaccessibility and natural dangerousness of the areas close to a vertical cliff pose important obstacles. Actually, due to the perils of walking along the cliff edges it is warmly suggested, when feasible, to avoid this approach due to security reasons. Mission planning and field approach to the study areas should prioritise the base of a cliff instead. Only when it is not possible to work from the cliff base, the observation spot at the cliff edge must be chosen prioritising security.

Especially when working at the cliff edge (but it is always a good principle), it is a good practise to avoid moving during the flight mission. When changing the original position is strictly necessary (e.g. for better radio reception and/or to keep visual contact with the drone), firstly move the drone at a reasonable distance from the cliff face to avoid accidental collisions, then switch to auto flight mode and abandon the commands to have the hands free and move in security. The drone will continue hovering in its static position thanks to its GPS locking.

Weather conditions are another issue to be considered. Excluding rain for obvious reasons, winds and light conditions are the most important factors. Optimal conditions are clouded sky with diffuse and homogeneous light. In general, defined shadows and high contrasts should be avoided. The experience suggests that when shadow is lesser, the better will be the final result in terms of 3D texture and photo alignment.

Winds are the most critical factor in flight security. Due to the proximity of a cliff wall, wind speed has to be minimal during the aerial survey. This factor is particularly important for the scenario 1 research due to the drone critical proximity to the cliff. Additionally, microclimatic wind conditions constitute a subtle risk. In fact, at the vicinity of the cliff upper edge and borders generally blows a constant breeze that can destabilize the flight.

Field measurements and flight plan

Two to four ground control points (GCPs) were positioned on the cliff wall prior to the flight (Fig. 3.4). GCPs are 20x20 cm targets located on accessible sectors of the cliff with an open visibility. The position of the targets on the cliff allowed to capture them in several aerial photos. A Bosch laser distance meter (Bosch GLM 50. Range 50 m ±1.5 mm) was used to measure the distance between GCPs centres. These field measurements were used to optimize the camera positions and orientation data during the creation of the 3D model, obtaining a higher geometrical precision.

All flights were manually piloted in parallel to the cliff surface. Flight plan was set following the directives of the software Photoscan/Metashape (Agisoft PhotoScan User

Manual). The whole cliff surface can be categorised as a vertical façade interrupted by steep slopes. The capturing scenario in such cases considers height as the most important spatial component. Photographs suitable for such 3D model reconstructions were acquired using multiple planes of flight orthogonal to the surveyed cliff.

Fig. 3.4. Positioning of GCPs on the vertical surface

The drone integrated camera sensor was tilted 30° to 40° downward respect to the cliff surface in order to maximise the forward photo overlap and ground coverage (that in this case is vertical). After several trial surveys, the best results were obtained by flying the drone along multiple horizontal trajectories at incremental (or decremental) heights and constant distance from the cliff. Each horizontal flight plane maximised side photo overlap and allowed the operator to place accurately the drone in the photogrammetric grid. Conversely, vertical trajectories often misplaced the drone position respect to the surveyed area, resulting in a low side photo overlap.

The slight but constant GPS positioning error of the drone antenna is enhanced by the proximity of cliff. In fact, such types of environments partially shield the GPS field of reception. The closer to the cliff, the higher will be the shielding effect, resulting in a major pitch of the drone.

This "uncertainty principle" of the drone position poses a problem for the 3D reconstruction of a scenario 1 survey because of the production of blind zones (areas visible from less than 2 photographs). In fact, with an increasing proximity to the cliff, the camera field of view decreases accordingly. The resulting final 3D model could suffer the presence of holes or artefacts. In the best scenario, the operator has to adjust the flight trajectory and increase the number of passages over the same areas to cover missing spots. This results in longer flight missions (which could impair battery duration) or in an excessive photo acquisitions (which can prolong the processing time).

The problem was solved by capturing 2 photo sets at different distances from the cliff. The first set had the least camera-to-cliff distance suitable for plant recognition in a scenario 1 survey (25 cm to 2 m). The second photo set was captured using the same flight settings, but at an incremented distance (6 to 10 m). The second set was used by the SfM software as a patch for any eventual hole resulted from the first set.

During acquisition, camera exposition settings were set to auto and ISO values to 100. All photos were automatically georeferenced by the drone internal GPS system using the WGS84 ellipsoid. Coordinates were afterward converted in the local UTM cartographic system prior to the beginning of elaborations.

Data processing

After the aerial survey, data extraction and analysis were carried out following 4 different stages: 1) 3D model creation and surface calculations; 2) marking and identification of individual plants; 3) extraction of environmental parameters for the entire surface; 4) digital plot placement and dataset export.

Construction of the 3D model and plant identification

All photo datasets were processed in Agisoft Photoscan/Metashape (Agisoft LLC, St. Petersburg, Russia) to create a georeferenced dense cloud and a 3D model mesh (examples in Fig. 3.5, 3.6, 3.12). The general workflow suggested in the software user manual was followed. A first photo alignment was performed using "high" as accuracy settings. The resulting sparse cloud was cleaned by homologous points, external areas and artefacts. Subsequently, the targets positioned on cliff were manually marked in each photo and their real distance was added to the software. Such measurements resulted in an alignment optimisation. The final (last) steps were the building of a dense cloud and a mesh (3D model). Both these last steps were elaborated using "medium" quality settings. After the creation of the model, overall surface, height and length of the cliff area were calculated.

An important detail consists in the final relative accuracy of the model. The local accuracy (i.e. the reciprocal metric distance among elements within the 3D model) does not depend on the GPS accuracy. Local accuracy will be given by the quality of alignment, pre-measured GCPs distances and levels of photo overlap. Conversely, absolute accuracy represents the precision of the geodetic location of the model. Without an accurate set of GPS measurements on the field, the model will not reach a geographic sub-metric level of accuracy.

For this reason, altitude measurements given in this work were not deducted from 3D models. A Digital Surface Model (DSM 2 x 2 m) of the local area was used for this purpose. Altitude values refer to the base or the crest of the surveyed cliff (specified in each case) and are calculated on the local WGS84 UTM ellipsoid.

Once the dense cloud model was created, the whole photo dataset with the least camera-to-cliff distance was manually scrutinised in order to add plant markers (Fig. 3.7). Each plant specimen (regardless of its identification) was marked in its centroid with a progressive digital marker. Plant species were identified according to Castroviejo (1986) for Spain and Pignatti (1982) for Italy. It was not necessary to manually add a marker for the same plant in every photo. In fact, once added in one photo, the software automatically detects the pixel pinned by the marker. The marker will then appear in all corresponding areas of the aligned photoset and in the 3D space. For each plant marker the corresponding specimen was tagged with its specific name. The methodology proposed here uses a parsimonious approach on species identification: if the identification was doubtful, an "unknown" or a double specific name was added (e.g. *Rhamnus alaternus/Phillyrea latifolia*). Moreover, photo identification relied on plant vegetative aspect and/or blooming stage A series of preliminary tests on the validity of species identification was assessed, resulting in 100% accuracy in the number of positioned markers and species identification.

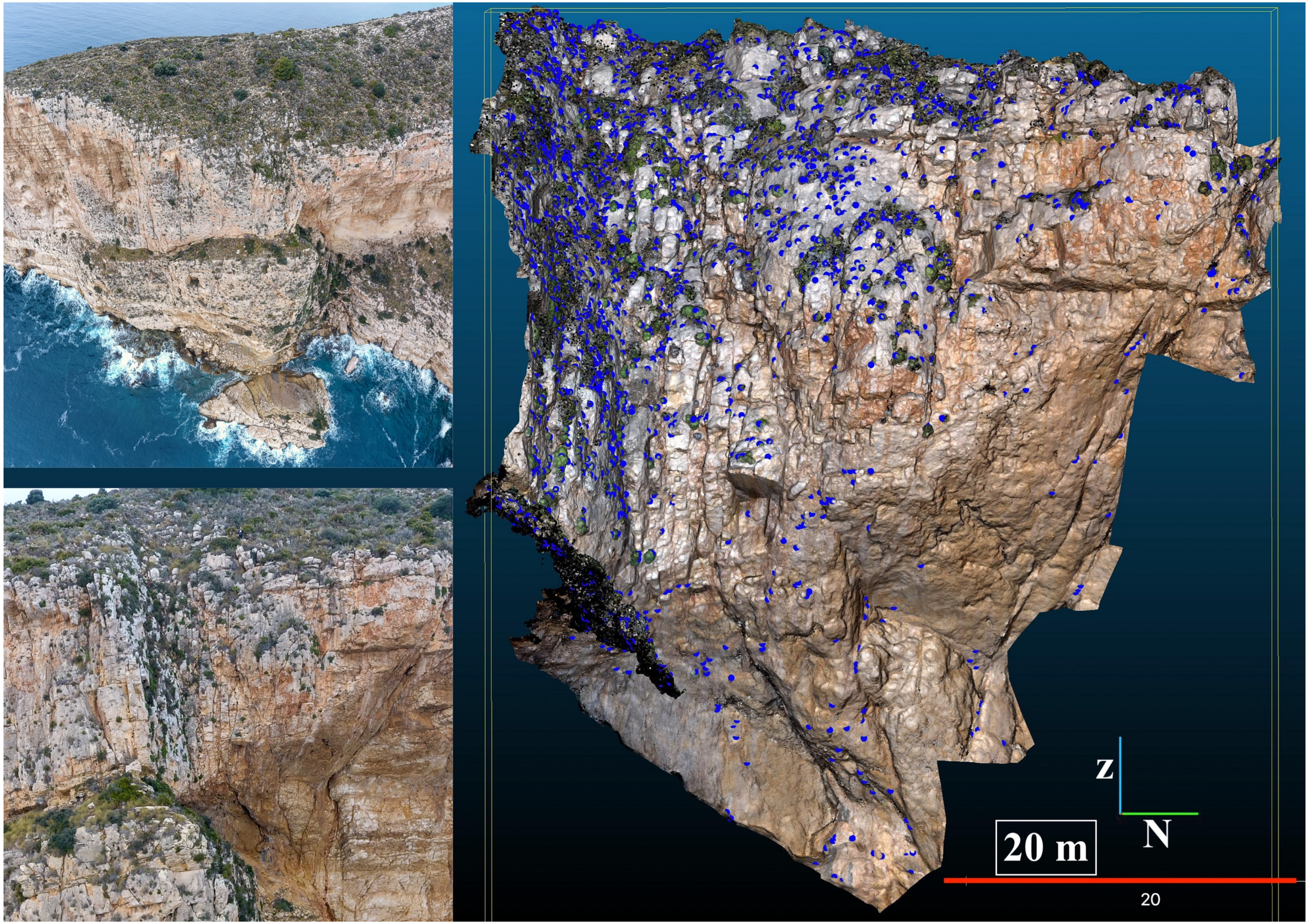

Fig. 3.5. An example of the final dense point cloud. Left: sea cliffs of Cap D'Or Pessebret (Spain). Cliffs were inaccessible without ropes. Right: dense point cloud in central perspective view. Each blue dot represents a marker (plant specimen). Z refers to the vertical positive direction. N is North. See case study 1 for more information. This dense cloud is represented by the position and RGB values of 25.017.000 points.

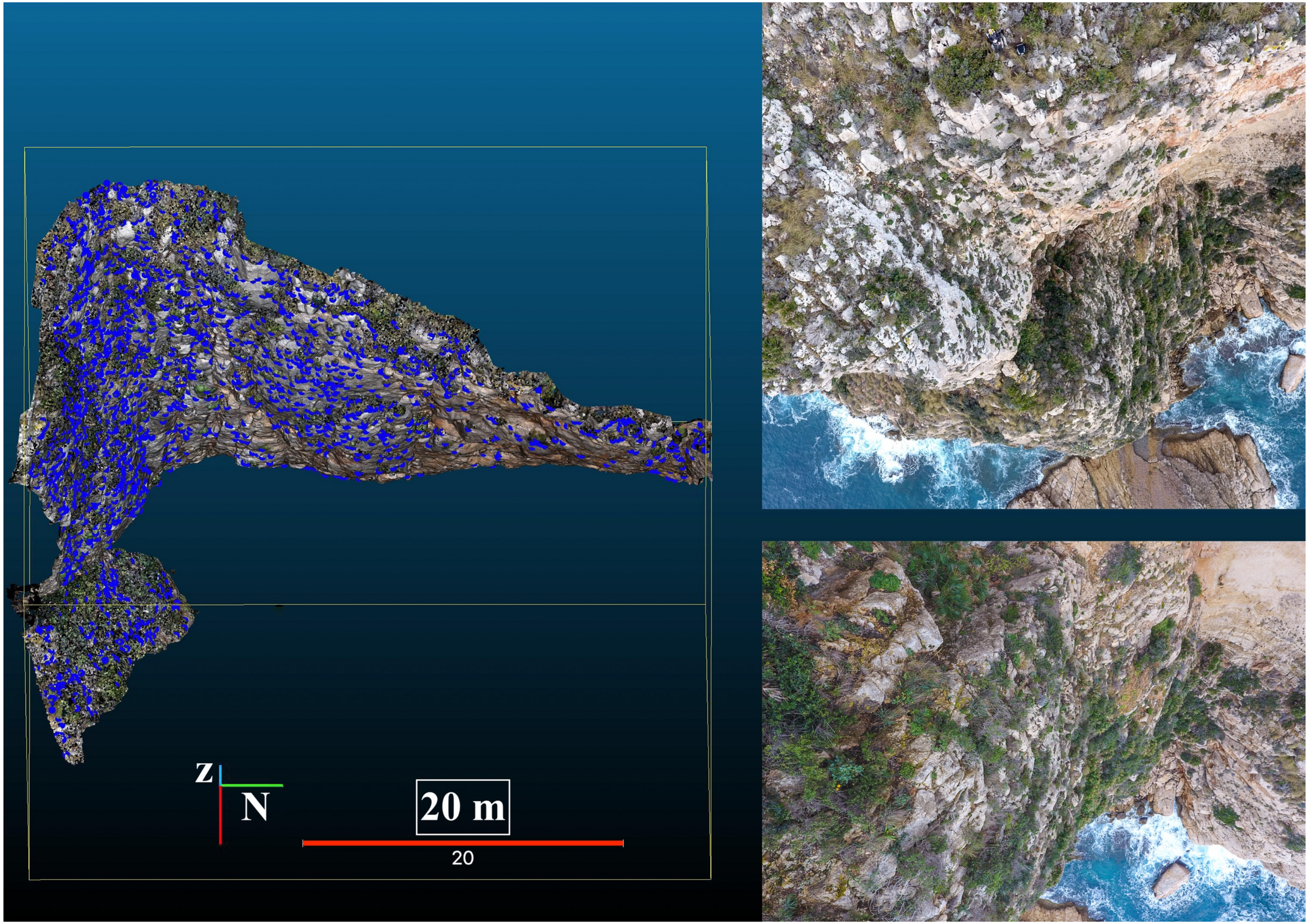

Fig. 3.6. The same area of Cap D'Or. A quasi-nadir (angle close to the vertical) view of the same dense cloud in Fig. 3.5.

Extensive continuous carpets of single small species (e.g. gramineous taxa) were rare on cliffs but abundant on ledges and ridges/bases. Since it was impossible to count each ramet separately, the number of used markers to tag individuals was considered proportional to the patch extent.

The dense cloud and the list of markers, with the information of their geographic position, species, life form and family identities were exported and uploaded to the Software CloudCompare (version 2.10; [GPL software]. (2019). Retrieved from http://www.cloudcompare.org/).

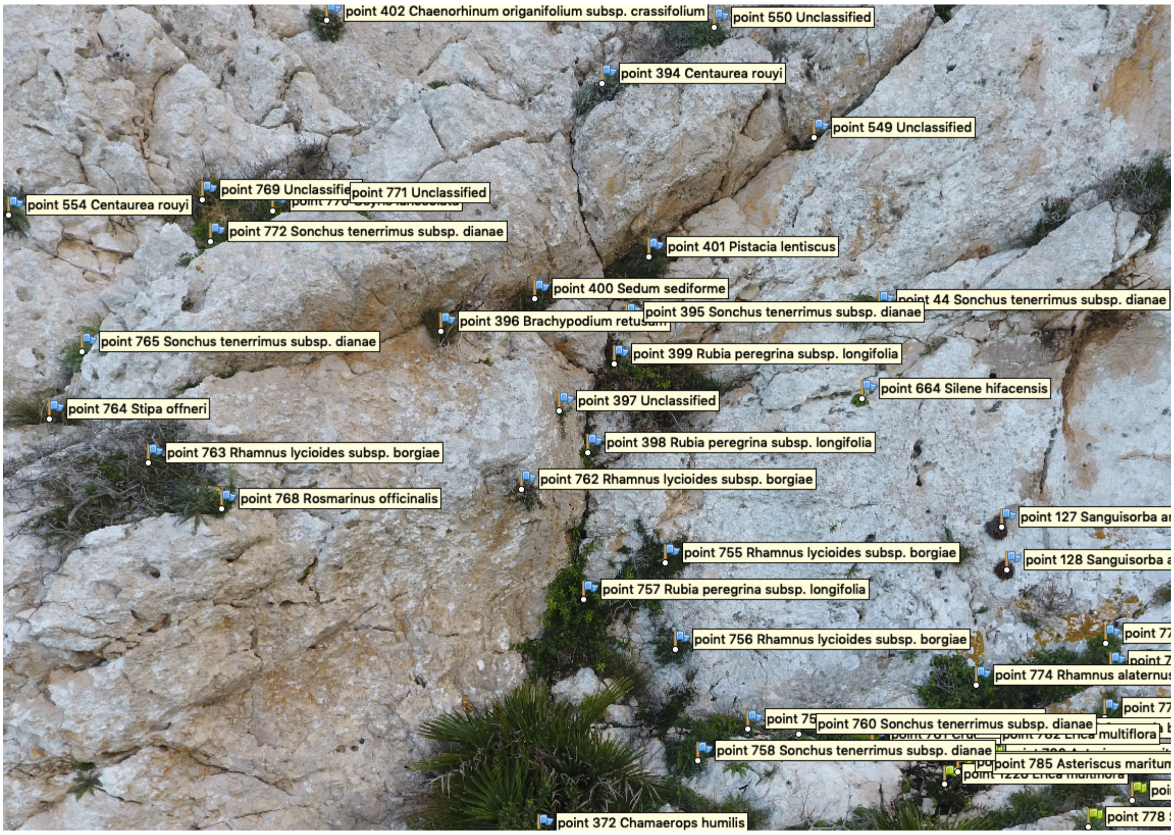

Fig. 3.7. An example of photo-tagging with the use of markers. Each marker represents a specimen. Markers stored three data of spatial information in the selected reference system (X, Y, Z) and the information on the plant identity. Cabo de San Antonio (Spain), 03/2019.

Plot size, placement and environmental variables

In any scenario, grain size should not exceed 9-16 m^2 due to the high heterogeneity of cliff surface and the detailed nature of this type of analysis. A larger grain was found to jeopardize the value of geomorphologic variations in slope and local positioning of plants on the wall. Accordingly, in this study plot size was 4 or 9 m^2 for a scenario 1 or 2 research type, respectively. The real plot surface varied according to the specific terrain, but it was represented by the plain extension of the geometric shape used for plotting.

In order to understand how a plant assemblage responds to cliff heterogeneity, a systematic design for plot placement should be preferred. In this way, plot locations on the cliff and surrounding space will be more objective. Sampling design should also include in the experimental area all the boundary zones of the cliff surface. Such design guarantees the inclusion in plot location of all the major environmental elements that contributed to shape a vertical and sub-vertical cliff environment, including the inclination gradient extremes. Species occurrence on non-vertical environments such as crests, ledges and the base of a cliff were included in the study. The plant assemblage of such areas is actually affected by biotic and abiotic influences due to the proximity of the cliff.

On the contrary, a random plot placement in the shortest continuous surface occupied by a species must be preferred for a scenario 2. In such cases, the target species are often sparsely distributed on the cliff. A reduced research zone for placing plots would facilitate the probability of species encountering (see appendix, Fig. S3.1 – S3.3).

For both scenarios, the absence of fractures was considered as an *a-posteriori* exclusion criterion for plot placement. If the cliff does not show any sign of fracturation, plant colonisation results impossible due to the absence of a physical medium for seed dispersal and young seedlings establishment. Thus, all sampled areas with 0 fractures were removed after the placement of circular plots in the 3D model. Conversely, plots with 0 species abundances were maintained, but they were not inserted into statistical ordinations.

Systematic plot placement using Cloud Compare was automatized, but in order to ensure within-plot homogeneity respect to inclination, the initial placement was subsequently adjusted manually. Plots that included different inclination environments (e.g. partially including a vertical cliff section and a ledge) were slightly reallocated (Fig. 3.8).

After plot placement on the 3D model, a set of environmental variables were extracted from each plot fraction of the cliff. All environmental variables were then obtained by remote sensed data in the 3D space and not in the field (Fig. 3.9-3.11, 3.13)

Inclination. In order to calculate a plot inclination, the Gaussian mean inclination of the non-vegetated plot surface was calculated. The calculation is performed in Cloud Compare using the point cloud normal. It returns a continuous quantitative value ranging from 0°

(perfectly horizontal) to 180° (overhang perfectly specular to the horizontal). Subsequently, inclination values were categorised into 10° span ordered classes and used in the continuous or categorised form according to the best result of the ecological analysis (Fig. 3.9).

Fracturation. Connected to inclination, the factor that limits the establishment of plants on rocky environments is the suitable growth medium. In this work fracturation is considered as the sum of the amount of fractures, holes, small cavities and any other structure that can retain soil and allow the seed germination and plant establishment. Fracturation was calculated as a semiquantitative ordered descriptor. It was a 0-4 index, with 0 = absence of fracturation; 1 = very low fracturation; 2 = medium fracturation; 3 = highly fracturated surface; and 4 = pure rocky soil substrate. Fracturation values per plot were manually added in the dataset based on the digital plot surface. The evaluation was assessed from aerial photos and the 3D photo-textured mesh.

Distance from base, distance from brink (or crest), distance from (both) edges. The minimum metric distance from the cliff boundary perimeter to the centroid of each plot was calculated using the software CloudCompare (Fig. 3.10). A boundary area refers to the spatial limit of the vertical extension of a cliff. It may be the base (e.g. the lower boundary) or the brink (or crest, the higher boundary). The term "distance from edges" refer to the least distance between the centroid of a plot and the base or the crest.

Plant cover. A greenness index (ExGI) was calculated from the obtained RGB values of the dense point cloud (Woebbecke et al., 1995). Index calculation (eq. 1) was carried out in Cloud Compare for the whole point cloud. Points were classified as vegetation when their ExGI values were greater than 0.015. Plant cover per plot was classified as the percentage of points classified as vegetation (Fig. 3.11).

$$ExGI = 2g - r - b \quad (1)$$

$$r = \frac{R^*}{(R^* + G^* + B^*)} \qquad g = \frac{G^*}{(R^* + G^* + B^*)} \qquad b = \frac{B^*}{(R^* + G^* + B^*)} \quad (2)$$

$$R^* = \frac{R}{R_{max}} \qquad G^* = \frac{G}{G_{max}} \qquad B^* = \frac{B}{B_{max}} \quad (3)$$

Local and regional aspect (used synonym "orientation"). It is a topographic feature that refers to the main direction toward which the plot is faced. The term "local" refers to the micro-topographic orientation changes in the analysed cliff area. On the other hand, a regional orientation refers to the main aspect of the cliff system at a regional scale (e.g. N-faced mountain sector).

Local aspect for each plot is calculated in the program Cloud Compare with the plug-in Facets (Dewez et al, 2016). First, a raster-type layer of information on orientation is assigned to the dense cloud by CloudCompare. In this phase, orientation is a quantitative variable given by an angle (1 – 360 °) and includes the vegetation surface (DSM point cloud of the area). Subsequently, the plugin reclassifies the point cloud and distributes the variation of orientation in *n* planar facets with a user-defined maximum reciprocal distance. Finally, facets are categorised in families of orientation of x ° span. For this study, the distance among facets was set to 1 m and the span to 15°. A final aggregation of families was produces to further categorise local orientation as a single qualitative descriptor of 4 classes: N, E, S, W (Fig. 3.12, 3.13).

Regional orientation was assumed by the position of the entire experimental area respect to the referring mountain orientation. As for local aspect, regional plot aspect was categorised as a single qualitative descriptor of 4 classes: N, E, S, W.

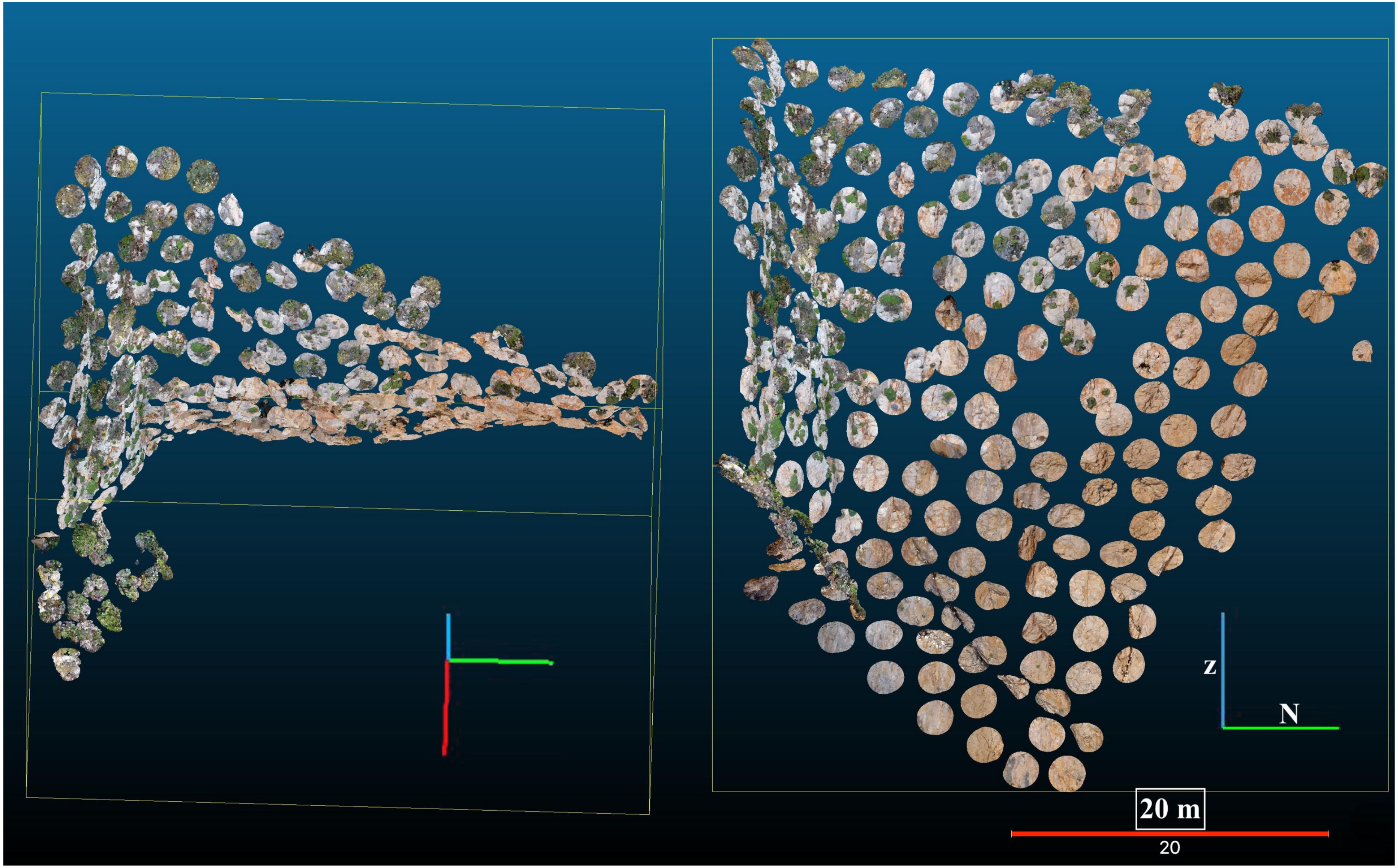

Fig. 3.8. Systematic plot placement within the 3D space represented in Fig. 3.5 and 3.6. Each circular plot was the statistical unit used in a scenario 1 research. In this model plot measured 4 m^2. Plot labels were omitted from visualization. See case study 1 for more information on plot characteristics.

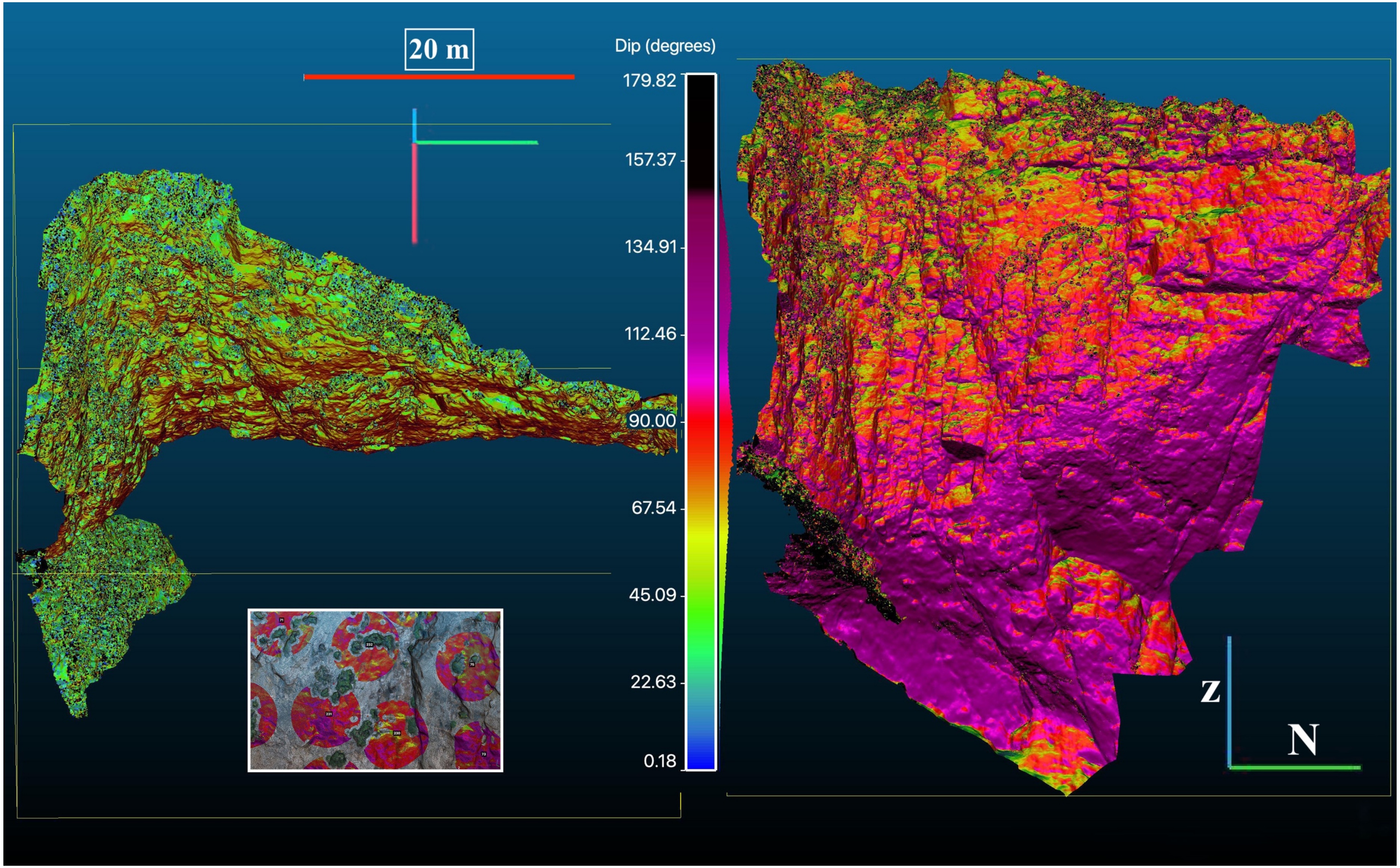

Fig. 3.9. Same area of Fig. 3.5-3.6. Inclination layer extracted from the dense point cloud. The first extrapolation is biased, including vegetation (DSM). The small box on the left shows how inclination values for each plot were cut in order to not consider the vegetation covered areas. Dip = inclination. Values are expressed in degrees of an angle (°).

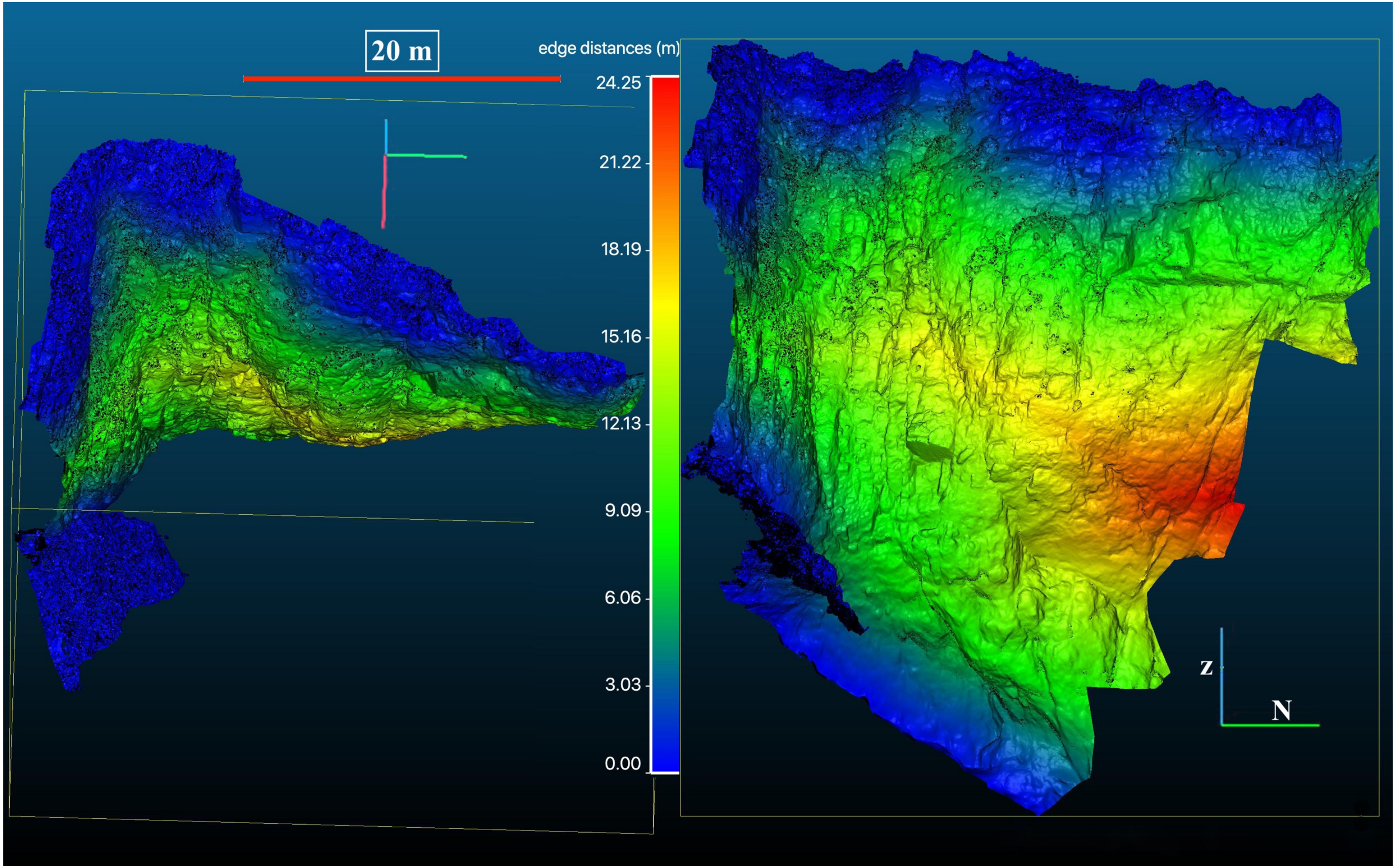

Fig, 3.10. Distance from cliff boundaries (edge distance) as a quantitative layer of environmental information. Same area of Fig. 3.5-3.6. Each plot centroid (not visualized) retained the information.

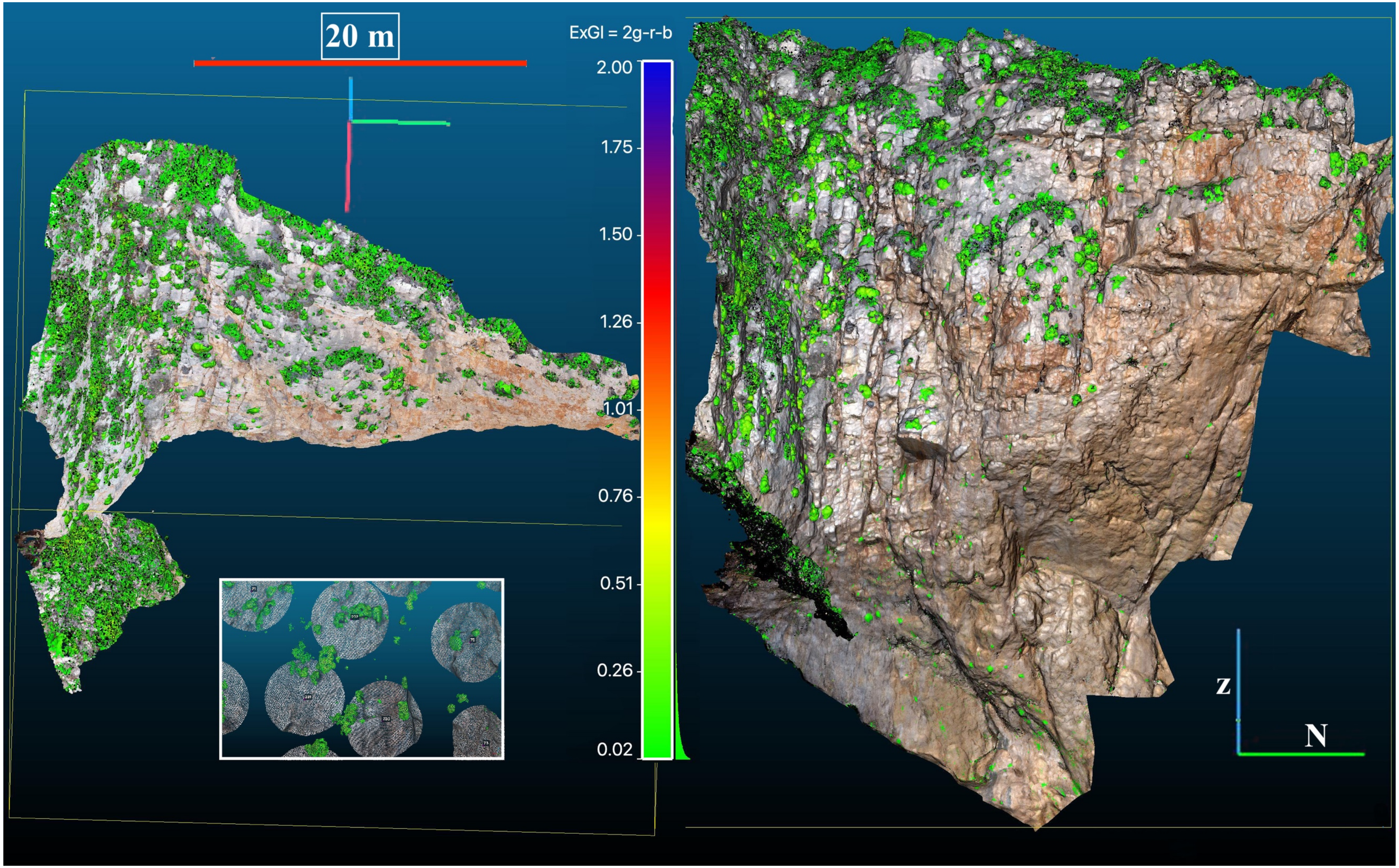

Fig. 3.11. Plant cover plotted on top of the RGB point cloud of Cap d'Or Pessebret (Fig. 3.15-3.16). For each plot (represented in the small box), plant cover was extracted as a %.

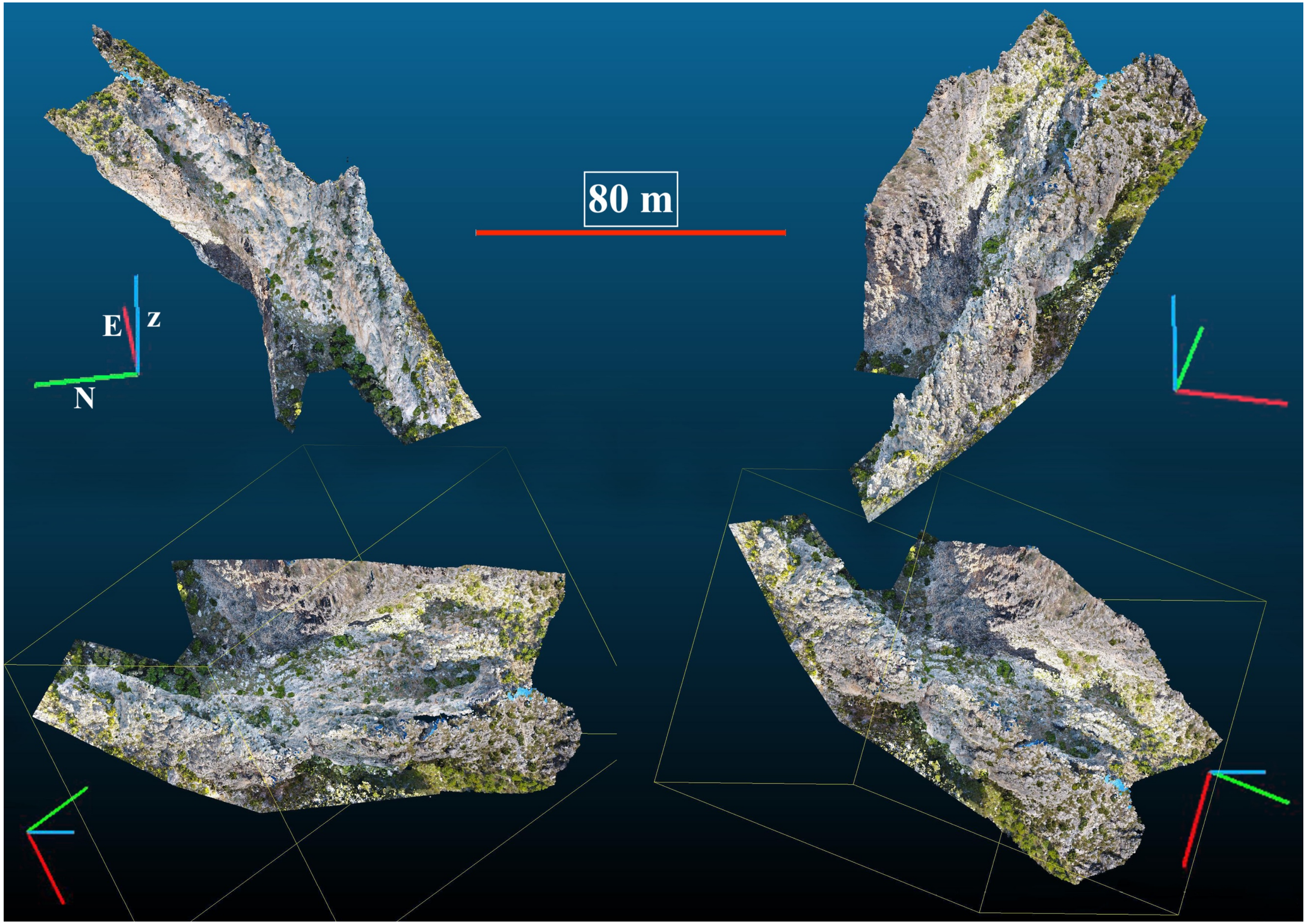

Fig. 3.12. Four different perspective representations of the same point cloud. The area is labelled Cofano East (Italy). Each representation of the dense cloud has the same scale and is produced by the location and RGB values of 47.381.000 points. Z refers to the vertical positive direction. N is North. E is East. For further details on the area see results: case study 3.

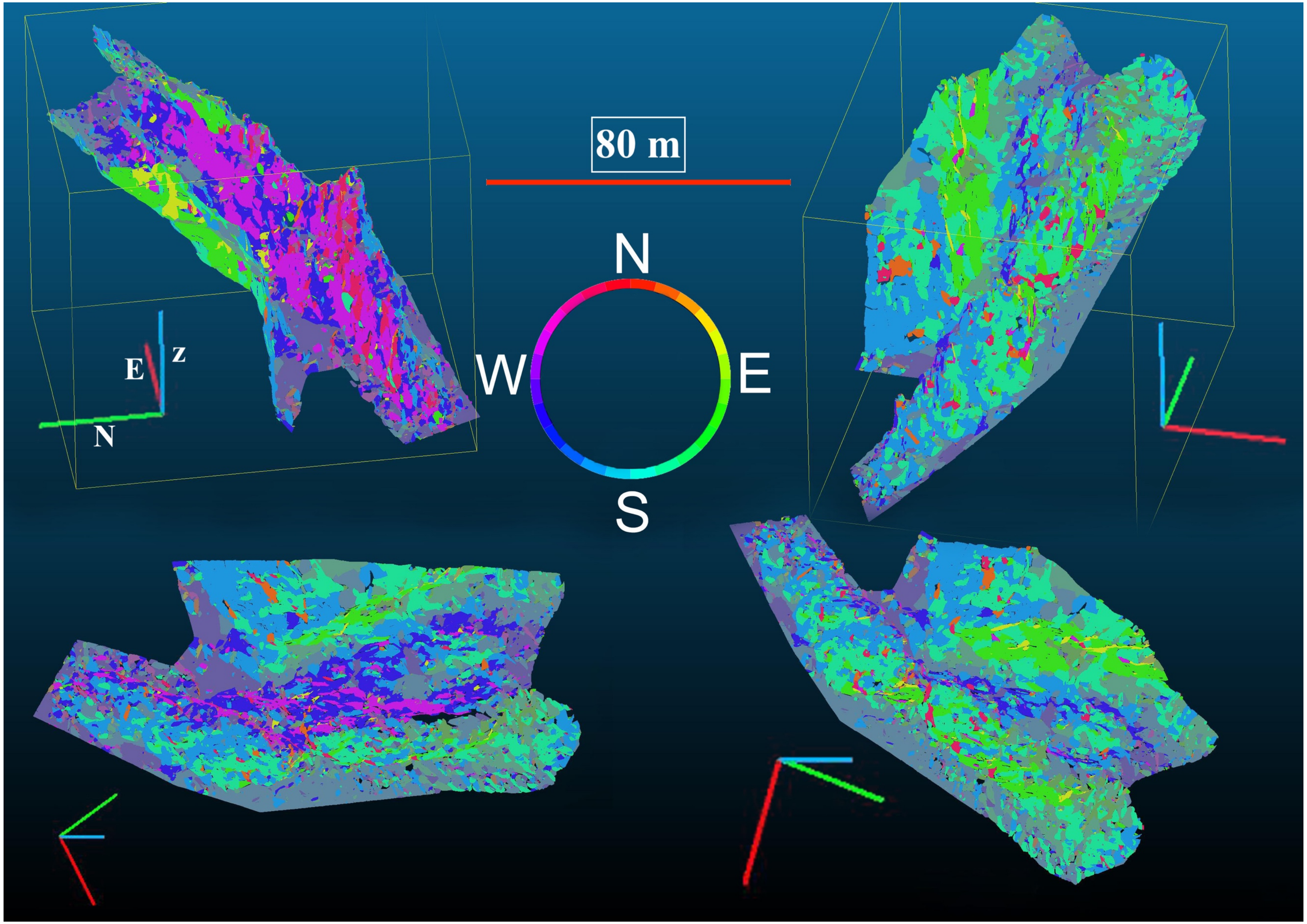

Fig. 3.13. The resulting recategorization in orientation families of the dense cloud in Fig. 3.12. Colour gradient refers to the facets local orientations. Each colour of the gradient scale represents a family of orientations of 15° span.

Statistical analysis

For scenario 1, species abundances and family composition for the whole surveyed area and the total plot area were summarised and represented using the software Excel and R 3.6.1 (R Core Team 2019). Endemism rates (number of endemic species for the Valencian Community region and its confining regions/total number of species) were calculated per each plot. Moreover, a median value was calculated for each class of inclination and plotted using boxplots using the software Tableau. The mean value ± 1 s.d. was also calculated for each class.

Simple linear regressions were performed in order to study the effect of microtopography on plant cover.

In order to determine the species niche selection, the Y data matrix of *n x p* (plot x species absolute abundances) was regressed upon an X data matrix *n x q* (plot x scaled environmental variables) using Constrained Additive Ordination (CAO; Yee, 2006a).This is a multivariate alternative technique to Generalised Additive Model (GAM) for the analysis of the relationship between plant species and environmental variables. CAO is performed by the class of Reduced-Rank Vector Generalized Additive Models (RR-VGAMs), which are a nonparametric extension of Quadratic Reduced-Rank Vector Generalised Linear Models (QRR-VGLMs). In brief, according to Yee (2015) they can be interpreted as a GAM fitted to each species against a *q* number of predictors forming a latent variable; the main advantage of CAO is that, as GAMs, it is model-driven and allows the data to speak for themselves. Species data are regressed upon the condensed final latent variable axis using a smoothed curve. Each response curve in the ordination diagram thus represents the niche preference of each species respect to the environmental gradient formed by all the selected environmental variables.

The model was implemented in R 3.6.1 (R Core Team 2019) using the R studio interface (RStudio Team, 2018) and the library VGAM 1.1-2 (Yee, 2006b; 2015; 2019).

The unconstrained principal component analysis (PCA) was used to summarise the species abundances distributional properties. Redundancy analysis (RDA), a form of constrained analysis, was used to assess the influence of microtopography explanatory variables on the species data. Results were visualised as correlation triplots. In both ordination methods, the species data matrix was Hellinger transformed prior to each analysis. In all RDA analyses both the adjusted and unadjusted R^2 values were extrapolated (Peres-nieto et al., 2006). ANOVA like permutation tests were performed to test the global significance of the RDA analyses and each of their axes. A significance test for each term (constraining variable) in the presence of all the other variables in the model was also performed [permutation by = 'margin'] (Legendre et al., 2011).

Statistical ordinations were implemented in R 3.6.1 (R Core Team 2019) using the package vegan 2.5-6 (available at https://CRAN.R-project.org/package=vegan).

Results

Five study cases are here presented to show how the earlier described methodology can be applied to the whole plant assemblage (scenario 1) or to target species (scenario 2) on a fine scale (sensu Wiens, 1989).

Scenario 1: Community plant ecology

Case study 1: Cap D'or. Alicante, Spain

Methods

Location. This scenario 1 survey was represented by two areas located a few hundred meters from each other along the coastal cliffs of Cap D'Or in the Eastern Spanish province of Alicante. Cap D'Or (38° 41' 16" N; 0° 9' 11" E) is a small carbonate coastal massif pertaining to the Prebetic mountain belt which once connected continental Spain to Balearic Islands. All the coastal cliffs in this area were formed between 15 and 10 million years ago due to a distension movement of the Mediterranean Basin (Sanz de Galdeano & Ruiz Cruz, 2016).

The main investigation area, Cap D'Or Pessebret is located at the southwestern end of the cape (Fig 3.14); the other area, Cap D'Or Cueva de les Cendres, is located 300 m to the northeast of Pessebret. With its 2974 m^2 in surface (Fig 3.5-3.6), Pessebret was a surveyed area almost 4.5 times larger than that of Cueva de les Cendres (687 m^2) and showed a quite high environmental heterogeneity, with frequent variations in its inclination (Fig 3.9), and an abrupt change in local aspect. Conversely, Cueva de les Cendres is a continuous cliff surface with an almost homogeneous inclination and a slight E-SE aspect gradient (Fig. 3.43 C). Both cliff areas are phytogeographically homogeneous, share the same chasmophytic flora and were sampled using the same sampling design.

Community ordination analysis of Cueva de les Cendres will not be commented further here. This area resulted in fact spatially limited and environmentally homogeneous and did not show enough variability with respect to the selected explanatory variables. However, Cueva de les Cendres and Pessebret were considered as a single sampling unit as regard the analysis of plant cover-inclination and endemism rate relationships.

Fig. 3.14. The peninsula of Cap D'Or. The study area labelled Pessebret is located in the centre of the frame.

Details on flight mission, analysed surface, camera-to-cliff distance and resulting dense point cloud for the study areas of Cap D'Or Pessebret and Cap D'Or Cueva de les Cendres are shown in Table 3.1. Pessebret is part of an NNW-SSW oriented peninsula. The cliff area is located on the East sector; thus, its regional orientation is homogeneously East facing. Conversely, at local level the wall results deeply folded roughly in the middle of its horizontal extension. This feature (particularly visible in Fig 3.6) produced a double local orientation: half of the local cliff aspect is North-oriented, whereas the rest faces East. Moreover, half of the cliff area is overhanging, with an inclination up to 170° (Fig. 3.9).

The area is a sea cliff; the surveyed zone included its upper edge but did not cover the entire vertical extension of the cliff.

The 3D model covered a partial vertical distance of the cliff wall (50 m) and the transect had a horizontal length of 60 m. The maximum altitude of the sampled area is 105 m.

Image analysis and 3D model building. Two separate flights were carried out in April 2019 for the survey. Flights were performed in separate days according to optimal weather conditions (cloudy days with low wind speed).

Photo positions were firstly converted from WGS84 to WGS84 UTM 31 ellipsoid. The first, unrefined 3D model covered an area of 5000 m^2. This model was imported in CloudCompare and divided into 2 subsets: a) Pessebret partial; the most heterogeneous area was selected as a scenario 1 type; and b) Pessebret total; a wider research area was studied for tracking the extant individuals of the target species *Silene hifacensis*.

Sampling design and statistical analyses. In order to understand how plant species responded to cliff heterogeneity, a systematic design was selected for plot placement. Sampling design also included in the experimental area all the boundary zones of the cliff surface, including the upper edge and a large ledge. Such design ensured the inclusion in plot location of all the major environmental elements that contributed to shape a vertical and sub-vertical cliff environment, including the inclination gradient extremes. Species occurrence on sub-vertical environments such as the big ledge at the base of the area, were influenced by the proximity of the cliff and thus were added to the analysis.

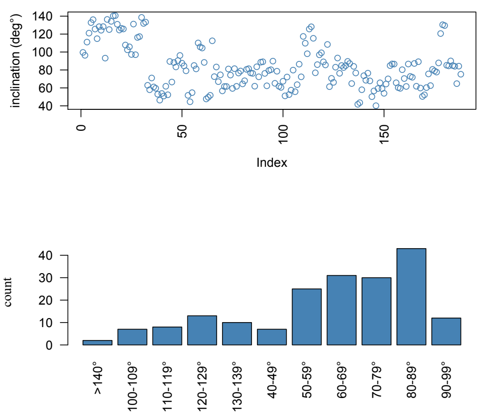

Fig. 3.15. Up: Scatterplot of the continuous inclinations encountered in the statistical units. Down: Histogram of categorised inclination data.

Circular plots (Fig 3.8) had a size of 4 m^2. The radius of a plot to cover such area measured 1.128 m. The distance among plots was set at a ½ radius (0.564 m). Such sampling scheme resulted in 228 plots, 188 of which resulted non-empty. This dataset was used for the analysis of community composition. In addition, a second dataset was prepared by adding 40 non-empty plots from the area of Cap D'Or Cueva de les Cendres. This merged data matrix (188 + 40 plots) was used to investigate the relationship among plant cover, inclination, endemism rates and fracturation through the use of linear regressions.

The plot quantitative inclination values were also transformed in 11 ordered classes of 10° amplitude each (Fig 3.15).

Statistical analysis. Two simple linear regression analyses were performed in order to study a) the relationship between plant cover and inclination; and b) the relationship between plant cover and fracturation. In order to perform the first linear regression, both plant cover (%) and inclination (slope degrees) were transformed using their natural logarithm + 1. For the second linear regression only plant cover was transformed in its natural logarithm + 1.

The niche selection of the 21 most abundant species in Pessebret was determined using a Constrained Additive Ordination (CAO; Yee, 2006 a). CAO was fitted under a Poisson model of rank 1 with three non-linear degrees of freedom for all species, choosing the best 100 models (Yee 2006a; 2006b). Quantitative inclination (Inclin), distance from the edges (dist_edges) and fracturation index (fracturation) were the three variables defining the microhabitat latent variable. Environmental variables were scaled to zero mean and unit variance prior to analysis.

Statistical ordination methods were performed to model the unconstrained (PCA) and constrained (RDA) species distributional properties. For the redundancy analysis (RDA), the used explanatory variables were categorical inclination, local orientation, fracturation and distance from the edges. Species data matrix were Hellinger transformed prior the analysis. PCA results were graphically displayed using a correlation biplot (scaling 2). The RDA ordination used a distance triplot (scaling 1). Sites were plotted using their fitted site scores (lc scores, linear combinations of explanatory variables).

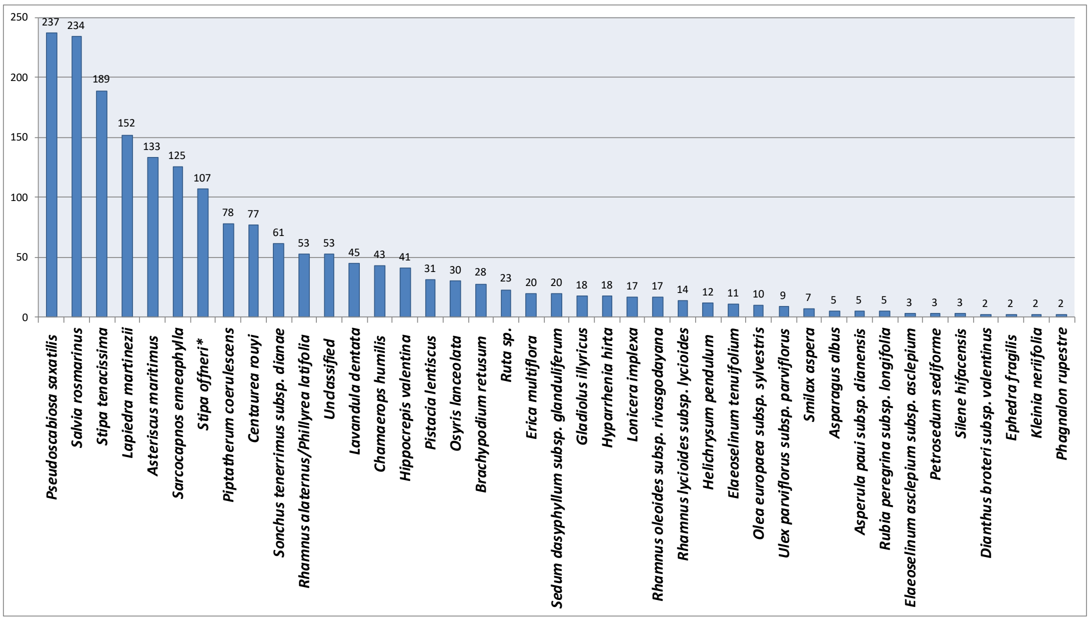

Fig 3.16. Barplot of species abundances in the entire surveyed area of Pessebret.

A total amount of 1945 individual plants belonging to 43 species were recorded on the surveyed area of Pessebret (Fig. 3.16). The majority of specimens were identified by a photographic evaluation with only 53 (2.7 %) unidentified specimens. By including cliff boundaries in the survey, some of the most abundant species were exclusively chasmophytic (e.g. *Pseudoscabiosa saxatilis*) and also typical of Mediterranean dry grasslands (e.g. *Stipa tenacissima)*. The most abundant species encountered were *P. saxatilis* (237 plants), *Salvia rosmarinus* (234), *S. tenacissima* (189), *Lapiedra martinezii* (152), *Asteriscus maritimus* (133), *Sarcocapnos enneaphylla* (125) and the complex of species grouped as *Stipa offneri** (107). The least abundant species were *Ephedra fragilis*, *Phagnalon rupestre* and *Dianthus broteri* subsp. *valentinus*. *Stipa offneri** represents a group of species formed by *Helictrotrichon filifolium*, *Melica minuta* and *Stipa offneri* because of their shared ecological niche and hard-to-distinguish morphological habit.

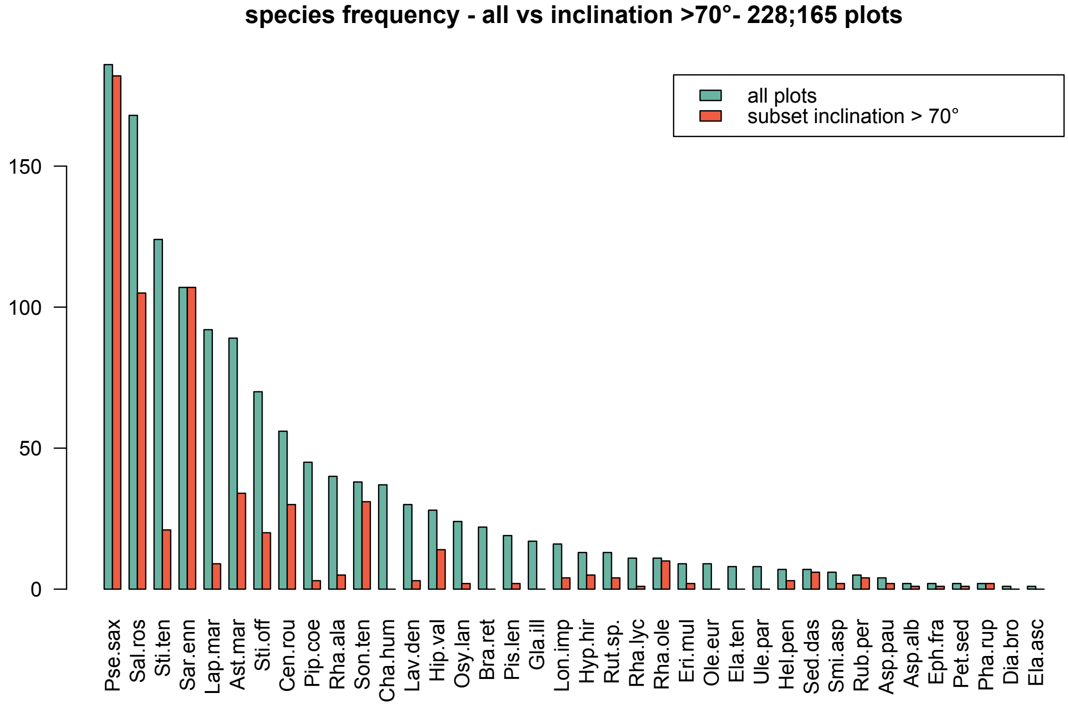

Fig. 3.17. Barplot of species abundances in the plot surface. Abbreviations refer to the species names in Fig 3.16.

A total of 1360 specimens were found in the 228 surveyed plots (188 + 40 empty plots), comprising 38 of the 43 encountered species for the entire area (Fig. 3.17). 72.3% (165) of the plots exceeded an inclination of 70°. The minimum plot inclinations were in the 40-49° range, whereas the most inclined plots reached up to 170° (Fig 3.15).

Fig. 3.17shows the species density difference between all and the >70° plot subset (exclusively on cliff). Similarly to what observed when considering the entire studied area, *P. saxatilis*, *S. rosmarinus*, *S. tenacissima*, *S. enneaphylla* and *L. martinezii* were the most abundant species in the entire set of plots. When only the > 70° plot subset was selected, *P. saxatilis*, *S. enneaphylla*, *Sonchus tenerrimus* subsp. *dianae*, *Rhamnus oleoides* subsp. *rivasgodayana* and *Sedum dasyphyllum* subsp. *glanduliferum* maintained their absolute abundances, whereas all the other species were encountered in minor numbers. Some species (e.g. *S. tenacissima*, *L. martinezii*, *Piptatherum coerulescens* and *Rhamnus alaternus*) were significantly less frequent in > 70° plots, whereas species as *Chamaerops humulis*, *Brachypodium retusum* and *Gladiolus illyricum* resulted completely absent.

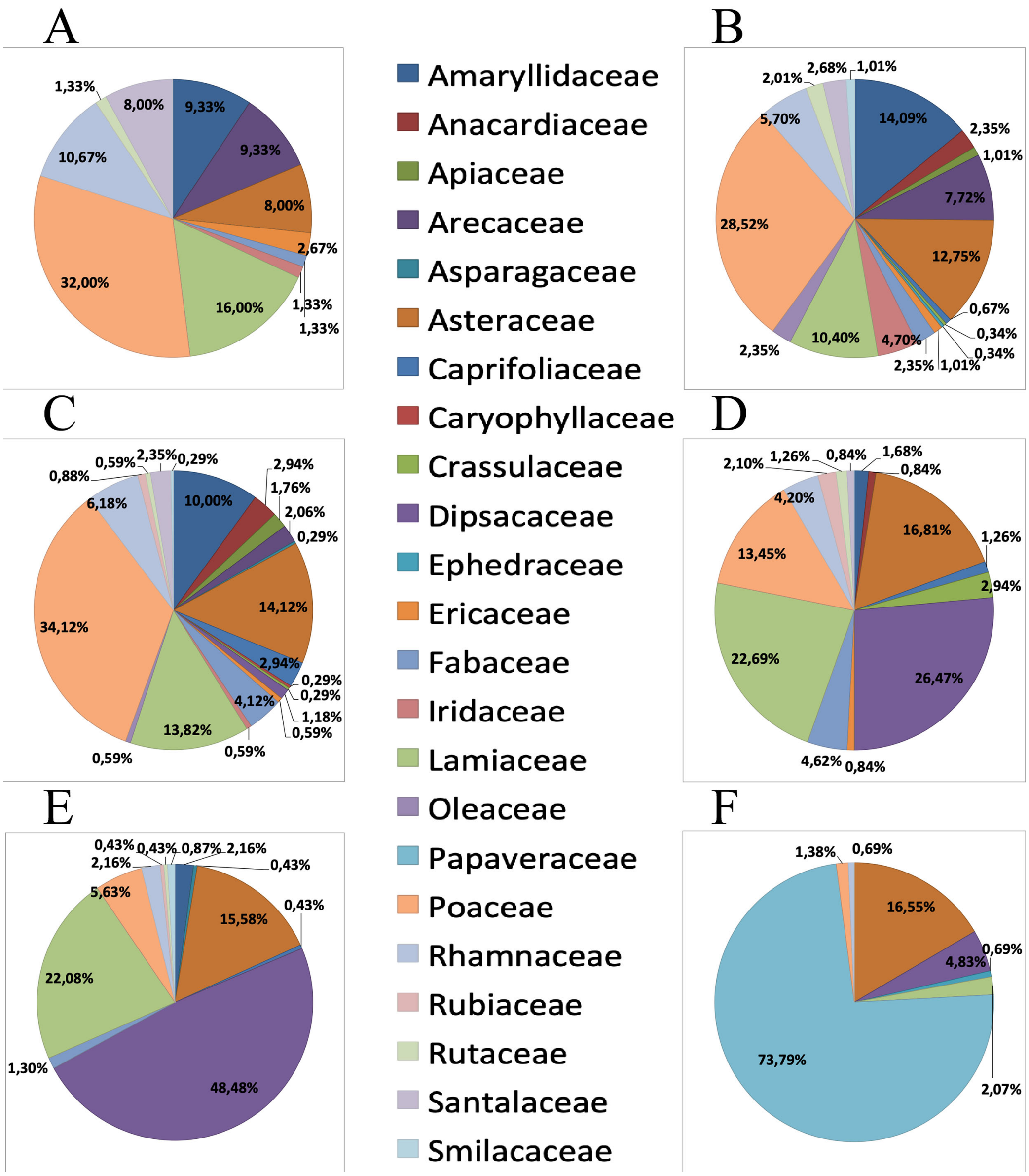

Fig. 3.18. Pie chart of family compositional data per category of inclination. A: inclination 40° - 49°; B: inclination 50° - 59°; C: inclination 60° - 69°; D: inclination 70° - 79°; E: inclination 80° - 89°; F: inclination > 90°

Fig 3.18 illustrates the distribution of plant families in the inclination strata. Poaceae were the most abundant family (32 - 34%) between 40° and 70° but decreased on subvertical and overhanging plots. Rhamnaceae, Amaryllidaceae, Arecaceae and Santalaceae followed a similar pattern of relative abundances. Asteraceae and Lamiaceae maintained a constant presence (around 8 to 16%) along the entire gradient. By contrast, Dipsacaceae (with one species, *Pseudoscabiosa saxatilis*) started growing only above 70°, and represented 50% of all individuals above 80°. Overhanging areas showed the 74% of abundance represented by

Papaveraceae (one species, *Sarcocapnos enneaphylla*), which in turns were not found in areas with lower inclinations.

Plant cover/inclination				
	Value	StD error	T value	p-value
(intercept)	15.51	0.934	-14.16	< 0.0001
Inclination	-3.012	0.213	16.6	
				$R^2 = 0.470$

Plant cover/fracturation				
(intercept)	0.693	0.05	5.05	< 0.0001
Fracturation	0.707	0.14	13.5	
				$R^2 = 0.477$

Table 3.2. Results of Linear Model on plant cover and environmental variables.

The results of linear model for the 228 plots for the areas of Cueva de les Cendres and Pessebret are shown in Table 3.2. The correlations of plant cover, plot inclination and fracturation are expressed by the equations:

$$Plant\ cover\ [Ln + 1] = -3{,}01183 * Inclination\ [Ln + 1] + 15{,}5115$$

$$Plant\ cover\ [Ln + 1] = 0{,}693279 * Fracturation + 0{,}706506$$

In cover/inclination there was a significant negative correlation between variables. The model revealed that 47% of plant cover variability is expressed by plot inclination (Table 3.2). Fig 3.19 shows that the average endemism % per plot increased with inclination values up to a certain value (between 4.5 and 4.6).

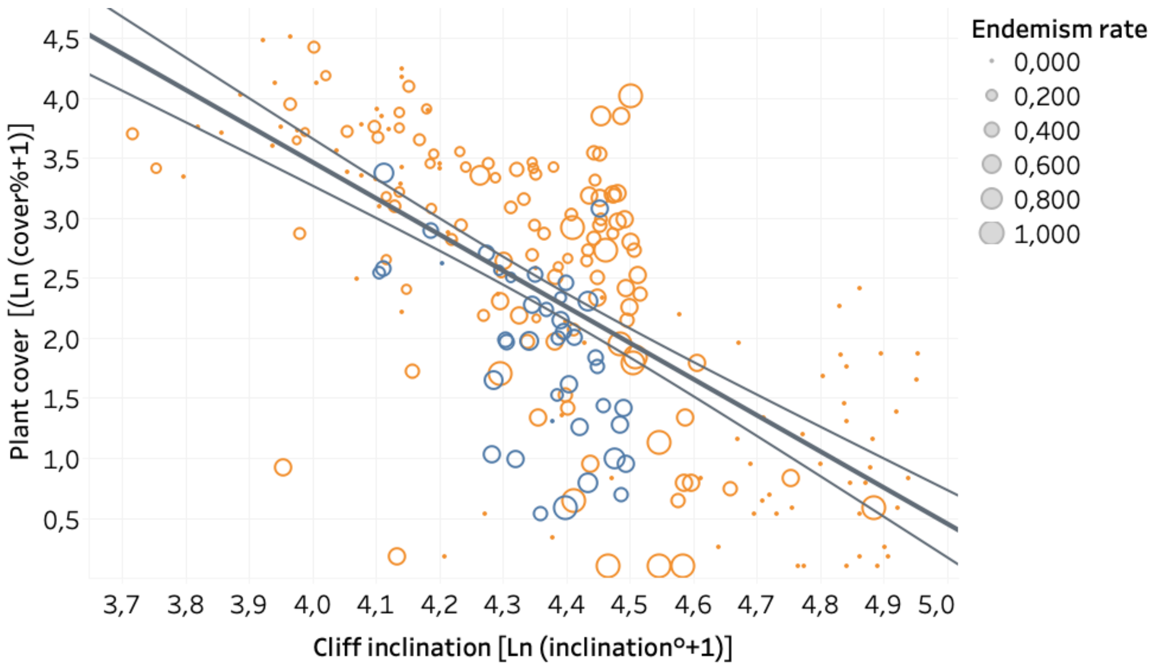

Fig. 3.19. Scatterplot of plant cover on plot inclination. Blue circles are plots from Cueva de les Cendres; orange circles are plots from Pessebret.

Regression line in Fig. 3.20 shows that plant cover and fracturation were significantly and positively correlated.

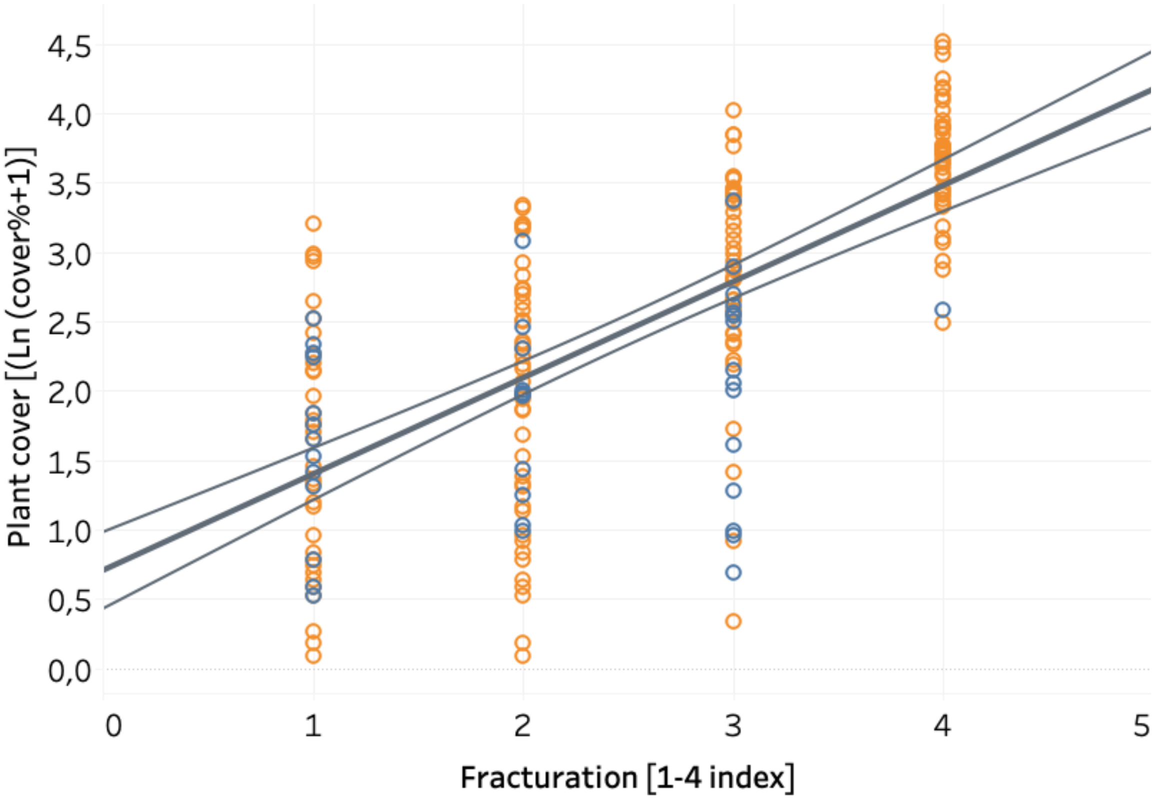

Fig. 3.20. Scatterplot of plant cover on plot fracturation index. Blue circles are plots from Cueva de les Cendres; orange circles are plots from Pessebret.

Endemic species were on average 30.3 ± 21.2 % in plots with an inclination of 70° - 79° and 47 ± 26.7 % in 80° - 89° (Fig. 3.21). At higher inclinations, plots hosted a limited number of species (up to 3, but mostly one) (Fig. 3.22). For this reason, the 90° - 99° inclination class represented a buffer category. At lower inclinations, endemism % increased with inclination, meanwhile after the threshold both the average endemism rate and number of species decreased. Inside the buffer category (12 plots) endemism levels were particularly high (an average of 51.4 ± 34.4 %). Standard deviations 2-3 times higher than the average of endemism % were encountered for plots exceeding 99°.

Another characteristic of the endemism % was its non-linear incremental increase before the overhang. The increasing rate between 40° - 49° and 50° - 59° was 65%, meanwhile the increasing rate between 60° - 69° and 70° - 79° was 109.6 %.

By excluding the extreme inclination values (> 99°), the species richness per plot followed a unimodal distribution, with the maximum values (13 species) at 60°-69° (Fig. 3.22)

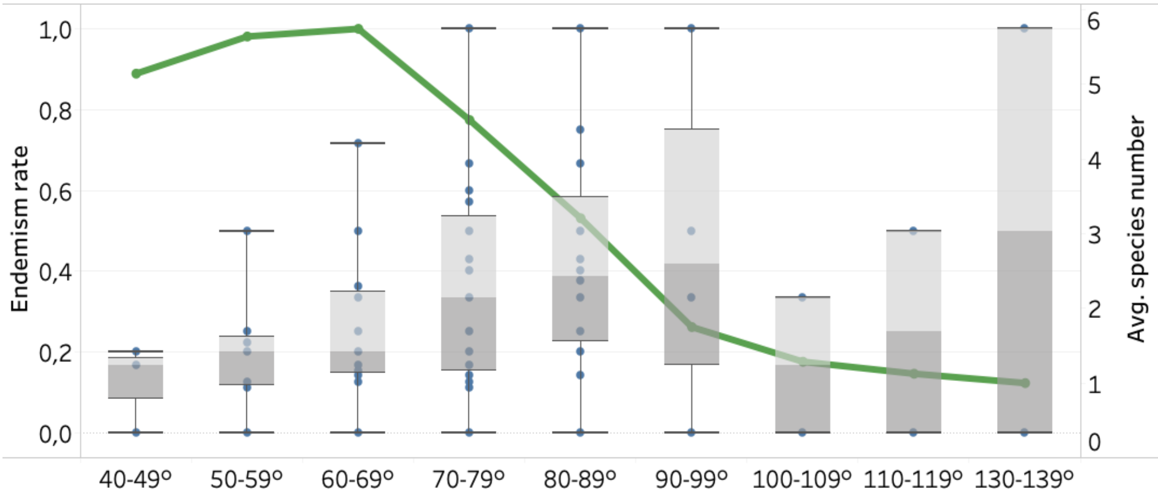

Fig.3.21. Boxplot of endemism % in each inclination category. The green line shows average species number. Data refer to Pessebret and Cueva de les Cendres (228 non-empty plots). Whiskers indicate the maximum extent of the data.

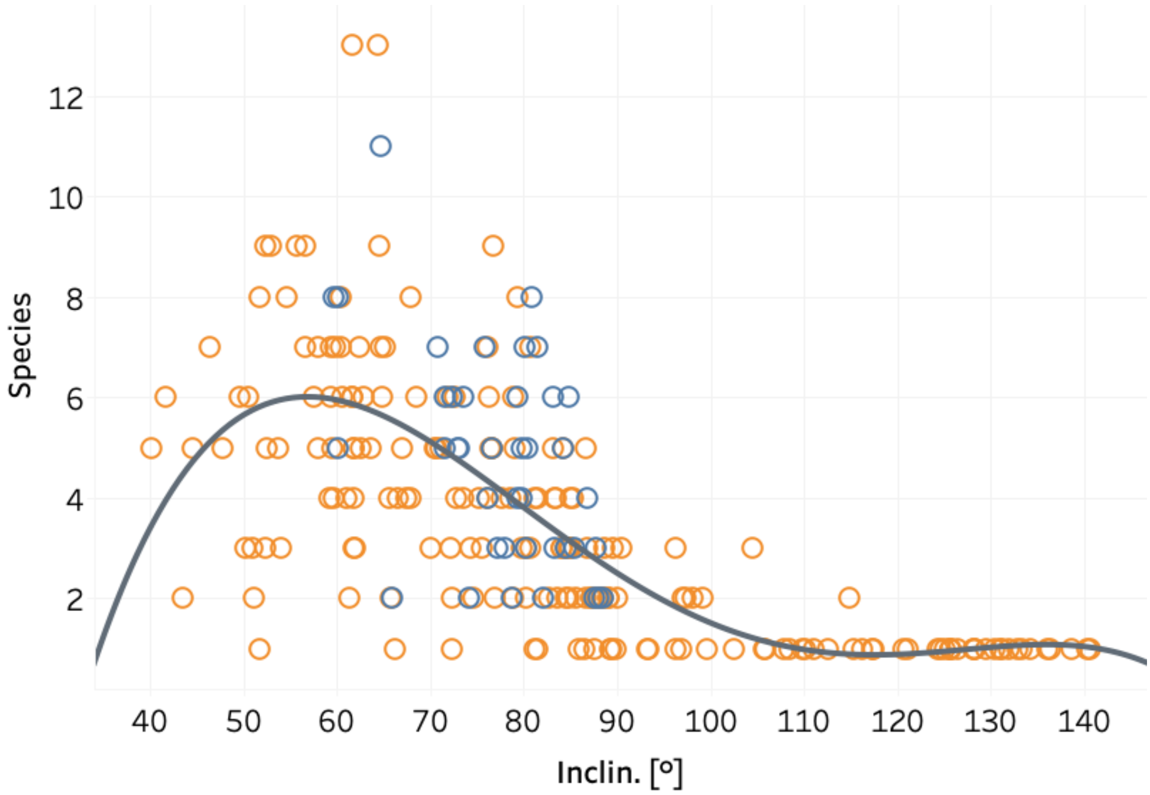

Fig. 3.22. Scatterplot of species richness in the 228 analysed plots. Blue circles are plots from Cueva de les Cendres; orange circles are plots from Pessebret.

Fig 3.23 shows the results of CAO. The majority of species had a clear unimodal response curve. Considering the negative sign of fracturation which shows an increase toward the left direction of latent axis, and the value of inclination which increases toward the right side), the resulting latent variable can be explained as a gradient of cliff habitat preference for the selected species.

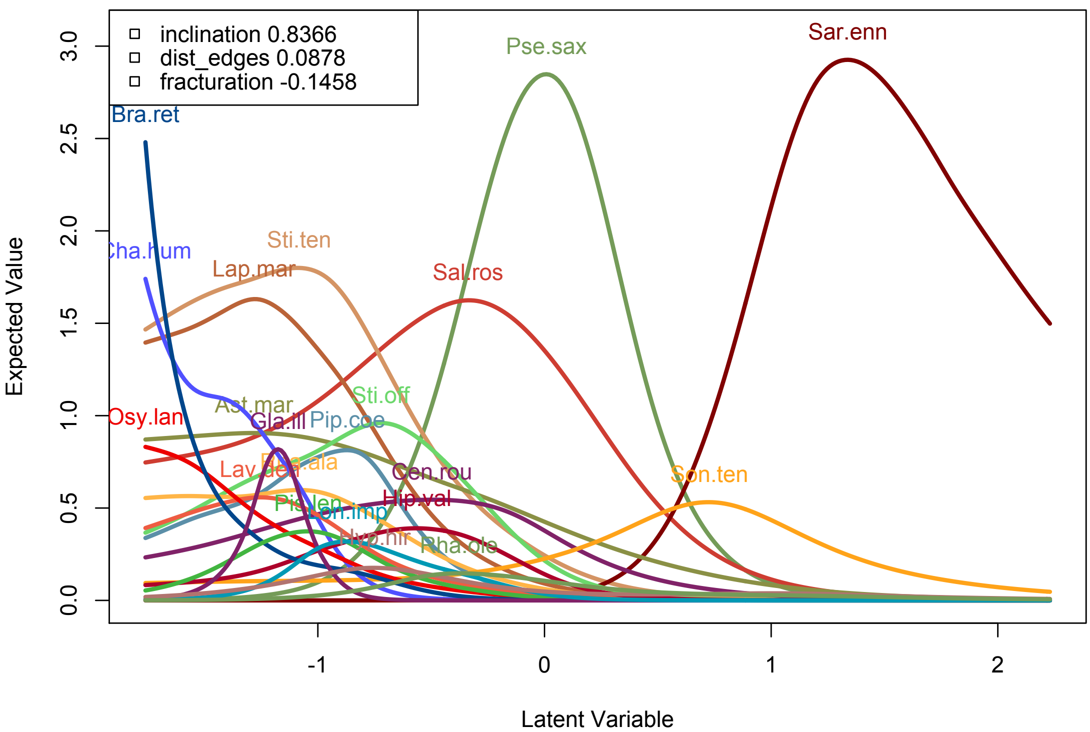

Fig. 3.23. Perspective plot of 21 Cap D'Or Pessebret species (abundance data). Rank-1 Poisson Constrained Additive Ordination (CAO) model. Legend in upper left corner shows the scaled constrained coefficients composing the first ordination axis. **Sar.enn** = *Sarcocapnos enneaphilla*; **Pse.sax** = *Pseudoscabiosa saxatilis*; **Sal.ros** = *Salvia rosmarinus*; **Sti.ten** = *Stipa tenacissima*; **Lap.mar** = *Lapiedra martinezii*; **Ast.mar** = *Asteriscus maritimus*; **Sti.off** = *Stipa offneri*; **Cen.rou** = *Centaurea rouyi*; **Pip.coe** = *Piptatherum coerulescens*; **Rha.ala** = *Rhamnus alaternus*; **Son.ten** = *Sonchus tenerrimus* subsp. *dianae*; **Cha.hum** = *Chamaerops humilis*; **Lav.den** = *Lavandula dentata*; **Hip.val** = *Hippocrepis valentina*; **Osy.lan** = *Osyris lanceolata*; **Bra.ret** = *Brachypodium retusum*; **Pis.len** = *Pistacia lentiscus*; **Gla.ill** = *Gladiolus illyricus*; **Lon.imp** = *Lonicera implexa*; **Hyp.hir** = *Hyparrhenia hirta*; **Rha.ole** = *Rhamnus oleoides* subsp. *rivasgodayana*.

Fig.3.23 highlighted the existence in Pessebret of only two cliff-exclusive species: *Pseudoscabiosa saxatilis* and *Sarcocapnos enneaphylla*, whose habitat segregation clearly appears. The lack of overlap in the species curves indicates their separated ecological niche on cliffs. The response curve of *S. enneaphylla* at the right end of graph, indicates a niche preference characterised by high values of inclination. Conversely, *P. saxatilis* was in the interior of the observed latent variable space (i.e., away from the boundary) and had a more restricted tolerance gradient. *Sonchus tenerrimus* subsp. *dianae* was another chasmophytic species but had very low abundance values. Also, its flat curve indicates a large tolerance relative to niche preference. *Salvia Rosmarinus*, *Asteriscus maritimus*, *Stipa offneri** and *Centaurea rouyi* were more abundant and shared the ability to colonise both cliffs and lesser steep surfaces with *S. tenerrimus*, with a preference toward cliffs. The response curves of most of the other species were roughly quadratic but truncated on the left area. It is plausible that these species have a niche preference shifted toward rocky soils with no to moderate inclinations. Not surprisingly, the ''worst'' species in terms of cliff colonisation resulted *Chamaerops humilis*, *Osyris lanceolata*, *Brachypodium retusum* and *Gladiolus illyricus*. These species were located on the far left of the graph and only occasionally were encountered on the right of -1 value, indicating a negative correlation with cliff habitats.

The total variance expressed by PCA was 0.788. The first two axes combined expressed 34.9% of the variance (PC1: 0.224; PC2:0.125). The biplot graph in Fig.3.24 shows the density distribution of 15 species with a fit higher than 0.06. said the graph shows that species are organised in 3 main groups. The vast majority of species were scattered along the same direction in the first quadrant, showing high negative correlation with *S. enneaphilla* and *P. saxatilis*. As an example, the angle between *S. enneaphilla* and *S. tenacissima* was 117,63°.

S. rosmarinus and *P. saxatilis* were weakly and positively correlated. The first species was also negatively correlated to *S. enneaphilla* (angle 154.79°) and neutrally to group 1. When plots were grouped according to the overhanging factor (Fig 3.24, different colour of objects) a separation between plots projected on the negative and positive PC1 semi-axis appeared.

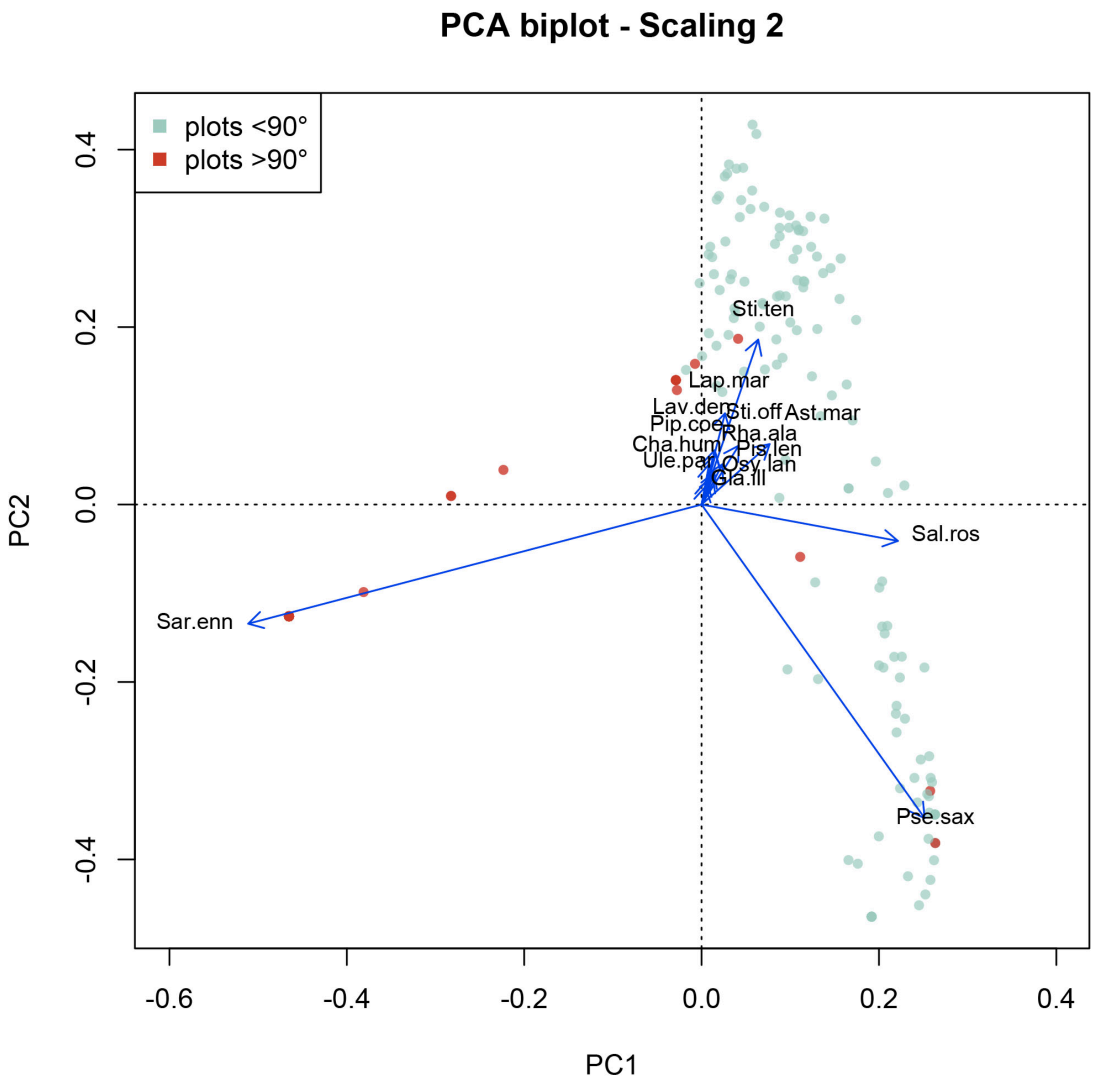

Fig. 3.24. PCA biplot of Pessebret Hellinger transformed species data. Objects used wa scores.

Sar.enn = *Sarcocapnos enneaphilla*; **Pse.sax** = *Pseudoscabiosa saxatilis*; **Sal.ros** = *Salvia rosmarinus*; **Sti.ten** = *Stipa tenacissima*; **Lap.mar** = *Lapiedra martinezii*; **Ast.mar** = *Asteriscus maritimus*; **Sti.off** =

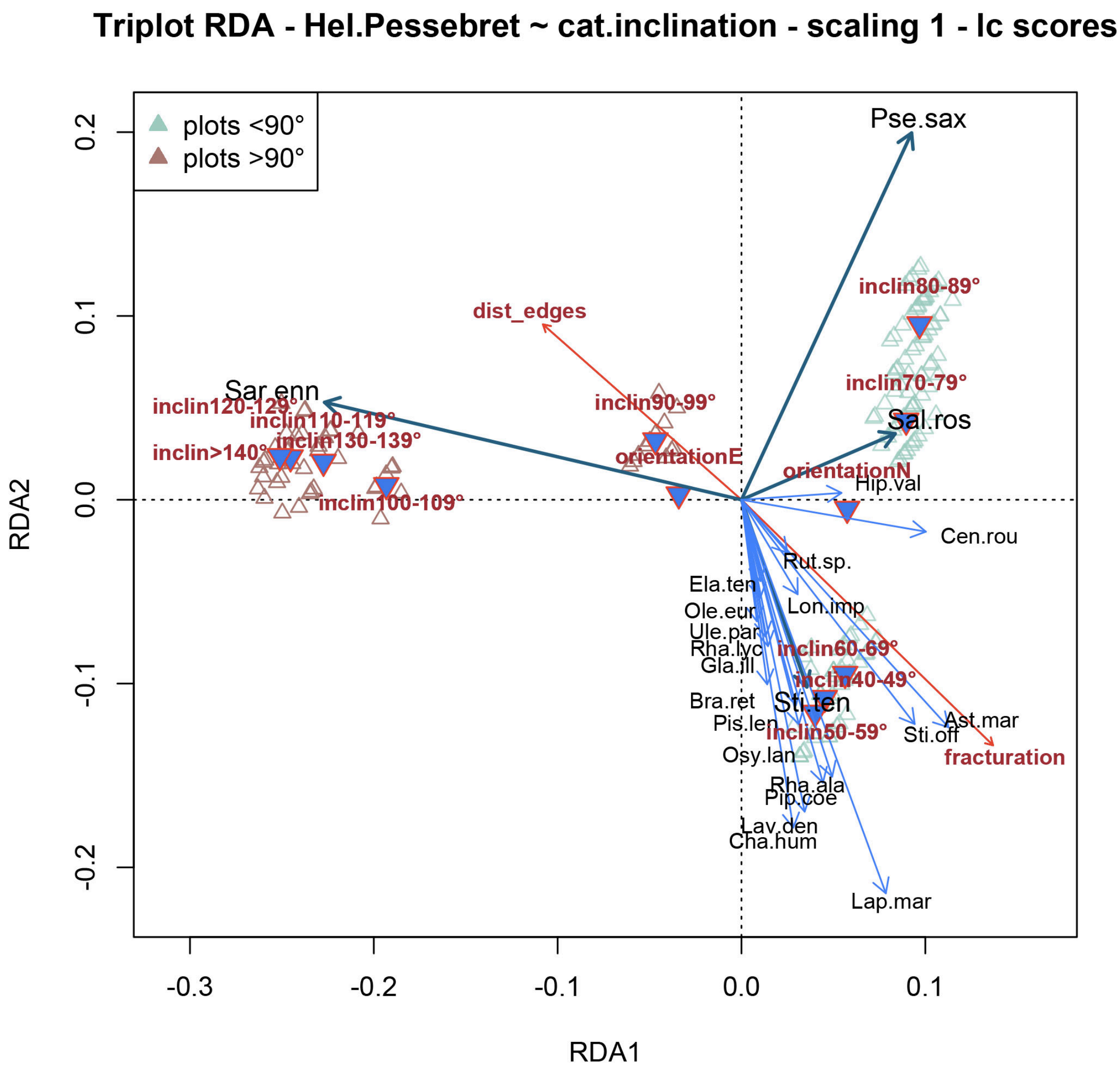

Fig 3.25. RDA of species abundances in Pessebret constrained by fine scale microtopographic features of the cliff. Two groups of response variables are plotted in the same multivariate space. Group 1: dark blue arrows represents species with a goodness of fit ≥ 0.21; group 2: pale blue arrows are species with a goodness of fit between 0.02 and 0.21. Group 1 is plotted using a multiplying factor of 0.3447 over its species scores; group 2 uses a multiplying factor of 2.349.

Sar.enn = *Sarcocapnos enneaphilla*; **Pse.sax** = *Pseudoscabiosa saxatilis*; **Sal.ros** = *Salvia rosmarinus*; **Sti.ten** = *Stipa tenacissima*; **Ast.mar** = *Asteriscus maritimus*; **Sti.off** = *Stipa offneri*; **Cen.rou** = *Centaurea rouyi*; **Pip.coe** = *Piptatherum coerulescens*; **Rha.ala** = *Rhamnus alaternus*; **Son.ten** = *Sonchus tenerrimus* subsp. *dianae*; **Cha.hum** = *Chamaerops humilis*; **Lav.den** = *Lavandula dentata*; **Hip.val** = *Hippocrepis valentina*; **Osy.lan** = *Osyris lanceolata*; **Bra.ret** = *Brachypodium retusum*; **Pis.len** = *Pistacia lentiscus*; **Gla.ill** = *Gladiolus illyricus*; **Lon.imp** = *Lonicera implexa;* **Hyp.hir** = *Hyparrhenia hirta*; **Rha.ole** = *Rhamnus oleoides* subsp. *rivasgodayana*; **Rut.sp.** = *Ruta angustifolia*; **Ela.ten** = *Elaeoselinum tenuifolium*; **Ole.eur** = *Olea europaea* var. *sylvestris*; **Ule.par** = *Ulex parviflorus* subsp. *parviflorus*; **Rha.lyc** = *Rhamnus lycioides* subsp. *lycioides*; **Lap.mar** = *Lapiedra martinezii*

RDA analysis (Fig. 3.25) had a constrained fraction of the total variance of 42% (R^2 = 0.42). The adjusted R^2 value was instead 0.377. The analysis yielded 12 canonical axes and 8 unconstrained axes for the residuals. The cumulative proportion of variance explained by the first two axes was 0.35 of the total variance and 83.5 % of the constrained variance. The first axis held 0.25 and the second 0.1 of the total variance. The permutation test of the RDA analysis was significant for the overall results and for the first 4 axes of variation ($P < 0.001$). A significance test for each term revealed that inclination and orientation were highly significant ($P < 0.001$), meanwhile distance from the edges was weakly significant ($P < 0.05$). Conversely, fracturation was found to not be significant. The significance test showed a greater variance of plant abundances explained by inclination (0.219) respect to other terms (orientation 0.014, distance from edges 0.006).

Species assemblages were clearly recognisable and configured into 3 groups according to two main sets of inclination values. The negative RDA1 axis (second and third quadrant) hold one single species positively correlated with inclinations higher than 90° (*Sarcocapnos enneaphilla*). At the study site the overhang was situated on the eastern side of the cliff, thus this species and all the plots on the left side of the RDA space were found to be positively correlated uniquely with the East orientation. *Pseudoscabiosa saxatilis* was found to be highly and positively correlated only with inclinations between 70° to 90°. Moreover, the species was almost neutrally associated to orientation (with a very weak preference over North). *Salvia rosmarinus* had similar characteristics, but with a higher correlation with North-oriented plots and a tolerance toward a set of lower slope conditions. Following a gradual shift toward lower inclinations, *Hippocrepis valentina*, *Centaurea rouyi* and *Asteriscus maritimus* were indifferently associated to all inclination classes except overhang, with a preference of the latest taxon toward low inclinations. Accordingly, the block of species on the lower end of the graph were found to be positively correlated with only low inclination values. This block was characterized by some components of the thermo-xerophilous Mediterranean grasslands such as *Brachypodium retusum*, *Gladiolus illyricus*, *Elaeoselinum tenuifolium*, *Ulex parviflorus* together with small shrub and trees of the Mediterranean maquis. Their negative association with the variable distance from edges can be interpreted as their tendency to form assemblages at the base and crest, but not on the cliff.

Case study 2: Cabo de San Antonio cliffs. Alicante, Spain

Methods

Locations. The second case study on a scenario 1 survey was illustrated by two Spanish areas located 400 m from each other. They were situated on opposite cliffs of the coastal peninsula of Cabo de San Antonio (38° 48' 9" N; 0°11'40" E) in the Eastern Spanish province of Valencia, Spain (Fig.3.26).

Fig. 3.26. The two opposite oriented areas of Cabo de San Antonio. Left: North oriented cliffs; right: South-oriented cliffs.

Not far from Cap D'Or, Cabo de San Antonio is located in the area of the province of Alicante denominated Marina Alta. This important endemism-rich area (Medail & Quezel, 1997) is also part of the Prebetic mountain belt in the easternmost continental area of Spain. The abundant cliffs which characterise this zone share a common phytogeographic and geologic history with the adjacent Cap D'Or (Rivas-Martínez et al. 2004; Sanz de Galdeano & Ruiz Cruz, 2016). Conversely to Cap D'Or (N-S) though, the peninsula of Cabo de San Antonio extends along a W-E axis. This characteristic gives a North to East to South orientation to its cliff system.

The two research areas, denominated Cabo de San Antonio North (CSAN) and Cabo de San Antonio South (CSAS) according to their opposite North-South orientation, were located on the uppermost limit of the coastal cliff and at the easternmost part of the cape (Fig. 3.26). The CSAN area extends over 600 m^2 in a vast vertical cliff (Table 3.1). It coincides with the highest altitude reached by the vertical cliffs of the peninsula (150 m from the upper edge). Cliffs at the South-oriented face of the peninsula were generally less steep, and with a lower extension and altitude. Thus, the area surveyed in order to produce the CSAS 2D model was less extended (240 m^2) and its maximum altitude was 140 m.

Both areas were selected for their high environmental heterogeneity. In fact, frequent variations in inclination were encountered along the entire surface. The study areas were by design homogeneous in local, but opposite in regional orientation.

The 3D models covered a vertical distance of 18 m (CSAN) and 15 m (CSAS). As for Cap D'Or, the surveyed zones were inaccessible from the sea. Then, the models comprised the cliff ridge but not its base.

Image analysis and 3D model building. Each zone was surveyed separately in mid-April 2019 with the purpose to cover each area in high detail. For this reason, camera-to-cliff distance was set to minimum values. Camera settings, number used batteries and dense cloud specifics are shown in Table 3.1. Photo positions were converted from WGS84 to WGS84 UTM 31 ellipsoid prior to the analysis.

Sampling design. Similarly to what done at Cap D'Or, a systematic study design was implemented for plot placement. In both areas, the cliff sub-vertical surface presented small semi-horizontal pockets of soil mixed to a limestone pavement. Their inclusion in the analysis permitted to further expand the surveyed inclination gradient.

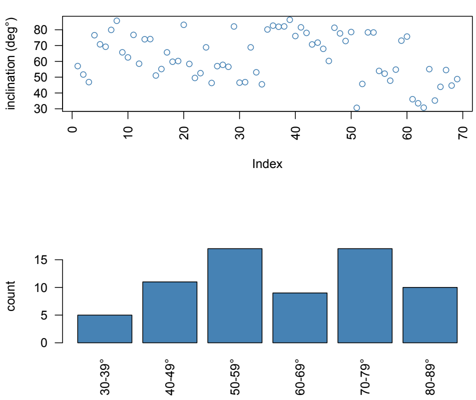

Fig. 3.27. Up: plot continuous inclinations. Down: histogram of categorised inclination data.

Like for case study 1, circular plots had a grain size of 4 m^2 and were spaced at a ½ radius distance (0,56 m). A total of 69 non-empty plots were places, of which 33 were allocated in CSAS and 36 in CSAN.

Quantitative inclination values per plot were transformed in 6 ordered classes spanning 10° each (Fig 3.27).

Statistical analysis. An unconstrained (PCA) and a constrained (RDA) analysis of species distributional properties was performed. For the redundancy analysis (RDA), the used explanatory variables were categorical inclination, global orientation, fracturation and distance from the edges. Species data matrix were Hellinger transformed prior of each analysis. PCA results were graphically displayed using a correlation biplot (scaling 2). RDA ordination results used a distance triplot (scaling 1). Following the suggestions of Oksanen (2019), sites were plotted using their weighted sums of species (wa scores).

Results

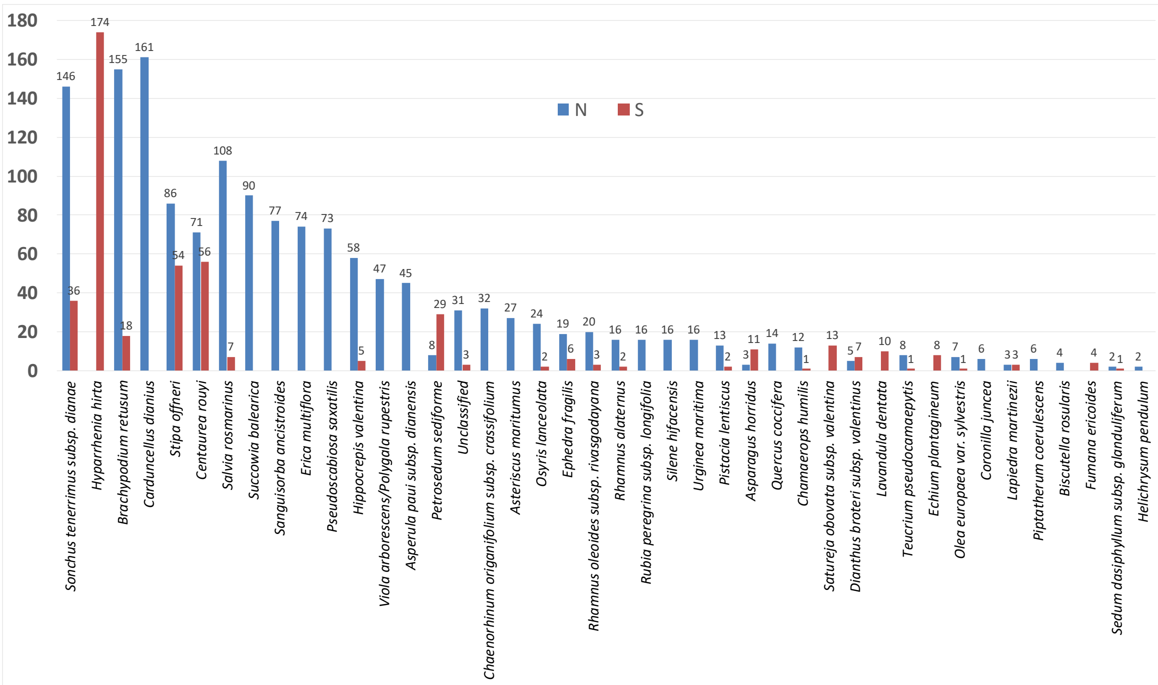

Fig. 3.28. Barplot of species abundances in the entire surveyed area. Red bars represent species abundances in CSAS; blue bars in CSAN. Species with only one individual were not added in the graph. *Urginea maritima* is now a synonym of *Charybdis maritima* (L.) SPETA

A total amount of 1963 individual plants belonging to 46 species were marked in the two 3D models of the areas. (Fig 3.28) In CSAN the total amount of species (38) and their abundances (1472 specimens) were considerably higher than in CSAS (27, 457 plants). The graph also shows that species abundances in CSAS were skewed. Only one single species, *Hyparrhenia hirta*, contributed with almost 40% to the total amount of individuals. Other abundant species in this area were less than one third in number: *Sonchus tenerrimus* subsp. *dianae* (36), *Stipa offneri* (54) and *Centaurea rouyi* (56). Conversely, CSAN showed an even distribution of individuals among the dominant species. *Sonchus tenerrimus* subsp. *dianae* was the most abundant species, with almost 10% of all specimens, followed by *Carduncellus dianius*, *Brachypodium retusum* and *Salvia rosmarinus*.

Unclassified plants were 2.06% for CSAN and only 0.06% for CSAS. Overall there were 34 (1.7%) unclassified markers.

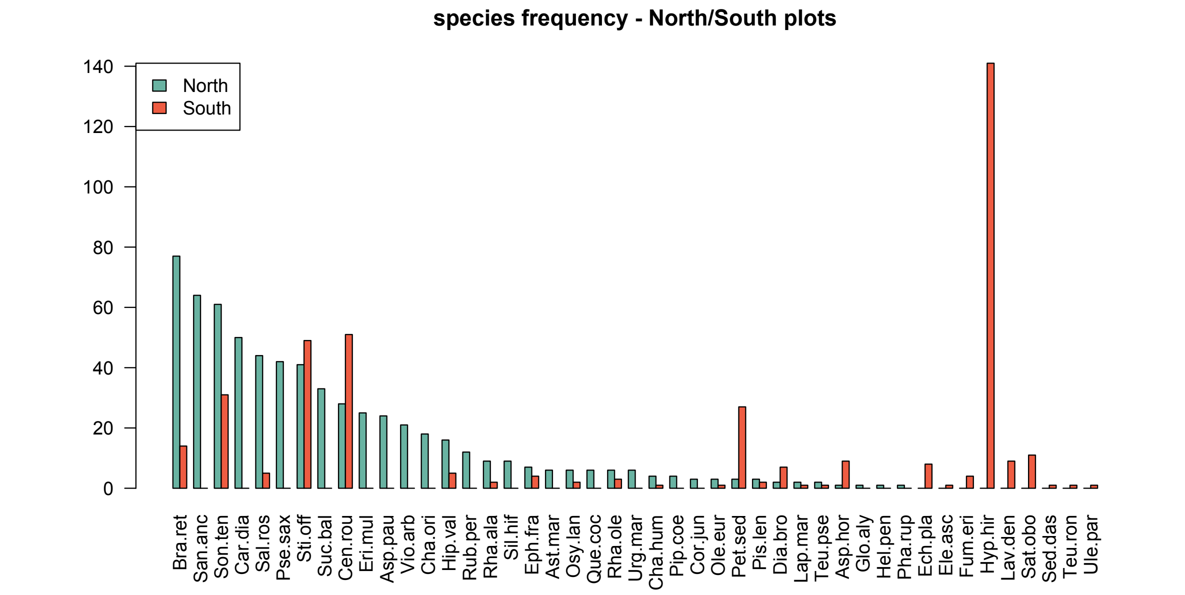

Fig 3.29. Barplot of species absolute abundances in the 69 surveyed plots. The North/South partition refers to the CSAN and CSAS, respectively. Acronyms refer to the species names in 3.28.

The plots covered the variation of species densities from an inclination of 30° to a maximum of 86°. Plot samples preserved the main characteristics of species abundance and richness encountered in the entire area (Fig 3.28). They contained 1060 specimens (almost 50% of the overall species in the two areas) pertaining to 45 taxa (Fig 3.29).

Inside the plots, thirty-six species (2 less than in the entire area) were encountered for CSAN, and 27 (same number of species than the entire area) for CSAS. Different taxa such as *S. offneri*, *C. rouyi* and *S. tenerrimus* subsp. *dianae* were encountered in consistent numbers for each area. However, by comparing their densities, it can be seen that their abundances were often very different for each zone. In general, barplots in Fig 3.29 (plots) and Fig 3.28 (entire 3D model) provides also information about an overall species segregation respect to cliff orientation. It can be seen that the total amount of shared taxa between CSAN and CSAS reached 40% of the total (18 species). On the other hand, another 40 % of species were exclusively encountered on CSAN and 20% only on CSAS.

Plots in CSAN were characterised by a proportional repartition of species among several taxa. *B. retusum* was the most abundant species (77), followed by *Sanguisorba ancistroides* (64), *S. tenerrimus* subsp. *dianae* (61), and *C. dianius* (50). Accordingly, plots in CSAS were characterised by the overall dominance of one species (141 individuals of *H.*

hirta), which contributed for 36% to the overall species abundance. Other abundant species were *C. rouyi* (51), *S. offneri* (49), *S. tenerrimus* subsp. *dianae* (31) and *Petrosedum sediforme* subsp. *dianum* (27).

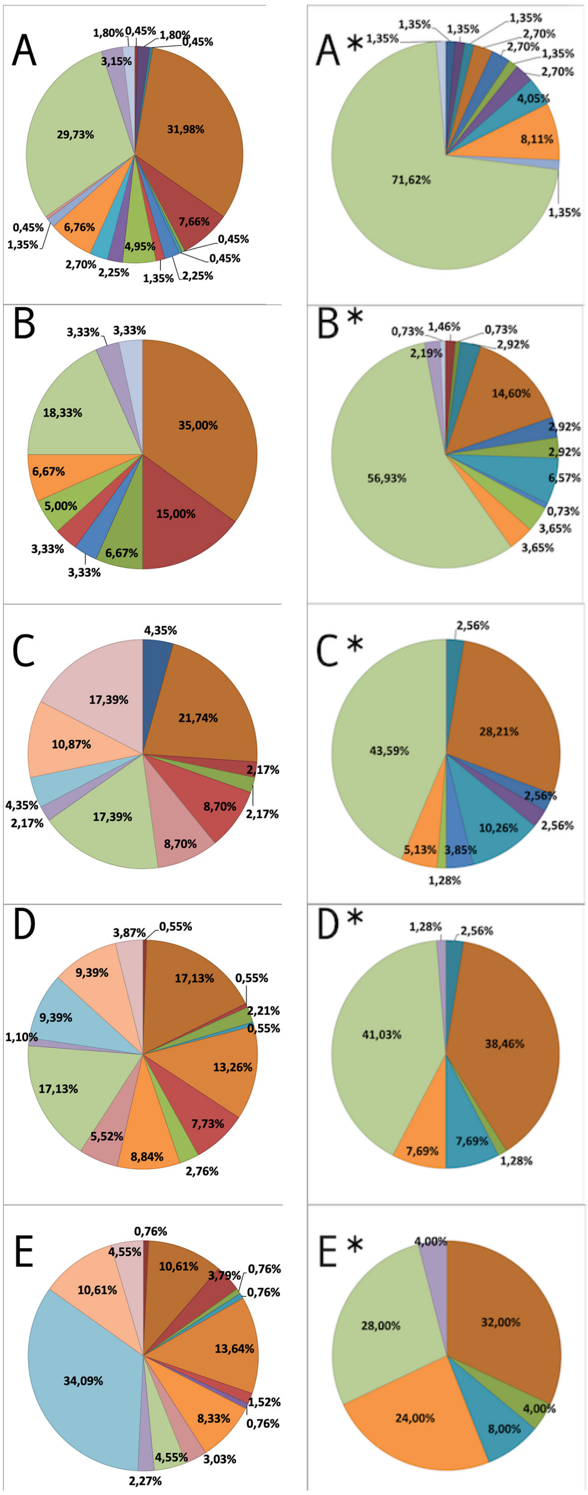

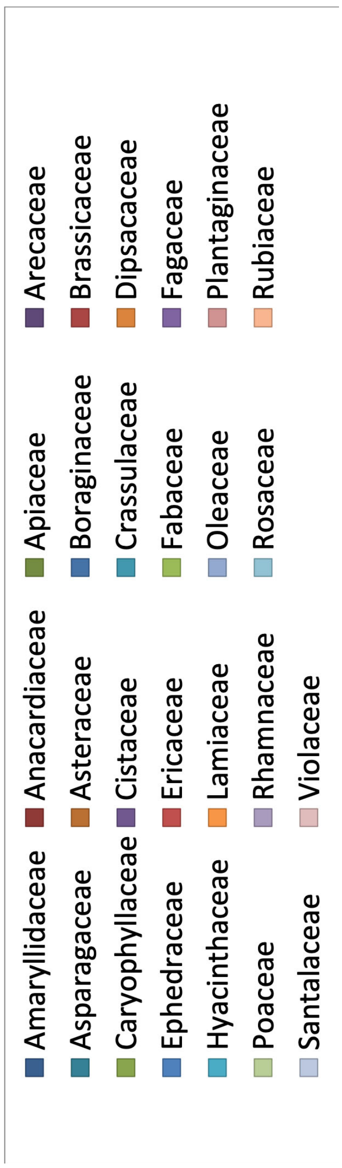

Fig 3.30. Pie chart of family compositional data per category of inclination and area. Asterisks refer to the CSAS area. Each letter refers to a class of inclination:

A: <50°; B: 50-59; C: 60-69°; D: 70-79°; E: 80-89°

The pie charts in 3.30 showed the distribution of plant families on different inclination strata in CSAN (left) and CSAS (right, letters with *).

Poaceae and Asteraceae were overall the two most abundant families on both areas. Poaceae in CSAS exceeded other families between 30° and 80° (72 – 41 %; Fig 3.30 A* to D*). The relative abundance of this family decreased gradually with slope. Asteraceae on CSAS were poorly represented at inclinations < 50° (3%; Fig 3.30 A*) and increased steadily in each inclination class up to 80° (15 – 39 %; Fig 3.30 B* to D*). In CSAN instead, both Poaceae and Asteraceae decreased with inclination, but at different rates (Fig 3.30 A-D) In fact, the families were more abundant on lower inclinations (30 - 32 % at < 50°) and maintained a lower but comparable presence between 50° and 80° (18 % to 17 % - Poaceae; 35 to 17 % - Asteraceae).

With the exception of plots at 60° – 69°, 5 to 13 % of taxa encountered in each area to up to 79° were Lamiaceae. Crassulaceae and Asparagaceae were mainly encountered on CSAS, along the entire inclination gradient to up to 80°

Conversely, Brassicaceae, Dipsacaceae, Ericaceae, Fagaceae, Rosaceae and Violaceae were found exclusively on CSAN. The inclination classes 70° - 79° and 80° - 89° of CSAN (Fig. 3.30 D-E) were characterised by the appearance of Dipsacaceae (13 %) and Rosaceae (9 to 34 %). In the study area, both families are represented by a single species: *Pseudoscabiosa saxatilis* and *Sanguisorba ancistroides*, respectively. Furthermore, Poaceae and Asteraceae reduced consistently their presence in the last inclination category of CSAN. As for what concerns CSAS, the steepest areas were characterised by an almost equally distributed family pool of Poaceae (28 %), Asteraceae (32 %) and Lamiaceae (24%) (Fig 3.30 E).

Endemism levels increased with plot inclination for both CSAN and CSAS at comparable values (Fig 3.31). The overall minimum % was 29.1 ± 16.1 % for plots with < 50° slope. The number increased to 44 ± 21 % in 50° – 59° and 48.1 ± 15.4 % in the next category. The highest endemism % was reached in the most vertical plots (80° – 89°), with an average of 54.3 ± 12.3 % of endemic species. It is worth to note that the increment in overall endemism levels per category of slope did not follow a linear growth. In fact, the increment was very close to logarithmic. In percentage, the levels of endemism increased of 14.9 % from the < 50° category to 50° – 59°. The subsequent increase from the 50° – 59° to 60° - 69°was less steep (4.1 %) and that from 70° - 79° to 80° - 89° was only 0.41 %.

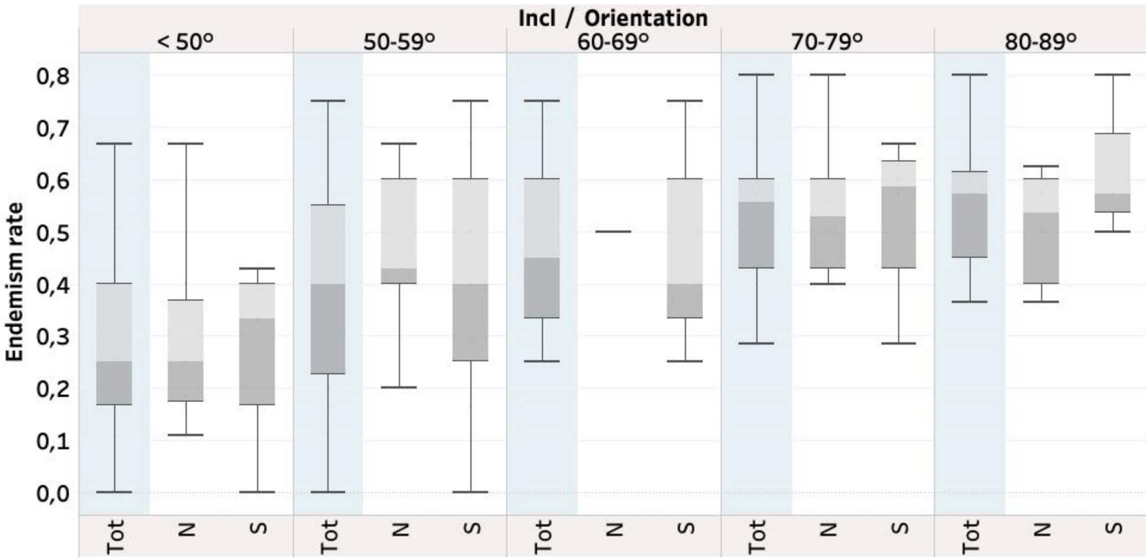

Fig. 3.31. Boxplot of endemism % for the overall analysis and for each orientation, broken down by inclination classes. Whiskers indicate the maximum extent of the data.

The total variance expressed by PCA was 0.719. The first two axes together explained 33.1% of the variance (PC1: 0.206; PC2:0.125). The resulting PCA biplot shown in Fig. 3.32 shows only the 19 species with a goodness of fit higher than 0.1. Furthermore, objects in the analysis were grouped according to their zone, which corresponded in this case to their regional orientation. By looking at the biplot, it is clear that the first axis of variation holds almost completely the variance associated to zone/orientation. A group of three species (*Carduncellus dianius* + *Salvia rosmarinus* + *Brachypodium retusum*) most contributed to the negative side of the first axis. By contrast, *Hyparrhenia hirta* was found to be the major contributor of the positive PC1 semi-axis. Based upon their contribution, direction and the grouping of the objects, these species can be interpreted as the most frequent and exclusive in the N/S assemblages.

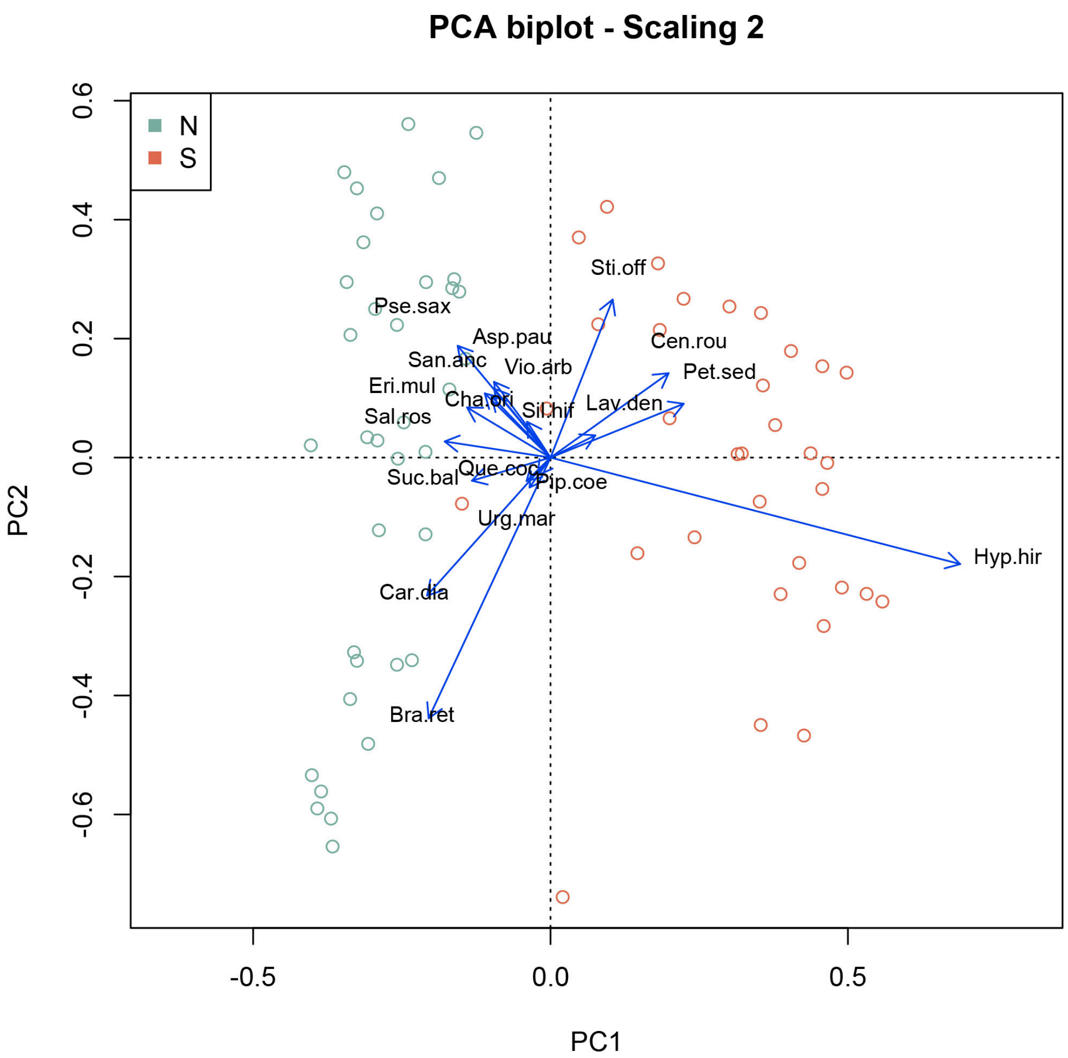

Fig. 3.32. PCA biplot of CSAS and CSAN combined Hellinger transformed species data. Objects used wa scores.

Furthermore, species seem to be scattered in 4 main groups respect to PC1 + PC2. The first group is located in the first quadrant and is formed by *Centaurea rouyi*, *Lavandula dentata*, *Petrosedum sediforme* subsp. *dianum* and *Stipa offneri*. The second group has the same contribution of group 1 to the positive direction of PC2. It is formed by many species in the second quadrant: *Asperula paui* subsp. *dianensis*, *Chaenorhinum origanifolium* subsp. *crassifolium*, *Erica multiflora*, *Pseudoscabiosa saxatilis* and *Sanguisorba ancistroides*. The third group appears to be neutral or slightly negatively correlated to group 2 and is pointing toward the negative direction of PC2. It is formed by *B. retusum C. dianius*, *Piptatherum coerulescens* and *Charybdis maritima*. Finally, *H. hirta* is marginally positively correlated with group 1. This species located on the fourth sector contributes greatly to the positive part of PC1 and poorly to the negative part of PC2.

The constrained fraction of the total variance in the RDA analysis (Fig. 3.33) was 34.9 % ($R^2 = 0.3485$). The adjusted R^2 was 0.2616. The analysis resulted in 8 canonical axes and 45 unconstrained axes for the residuals. The cumulative proportion of variance explained by the first two axes was 0.2644 of the total variance or 75.9 % of the constrained variance. The first axis held 0.18 and the second 0.09 of the total variance. Furthermore, the proportion of variance explained by the first residual structure (PC1) was less than half (0.079) of the first constrained axis. That meant that there was not any residual structure in the response data.

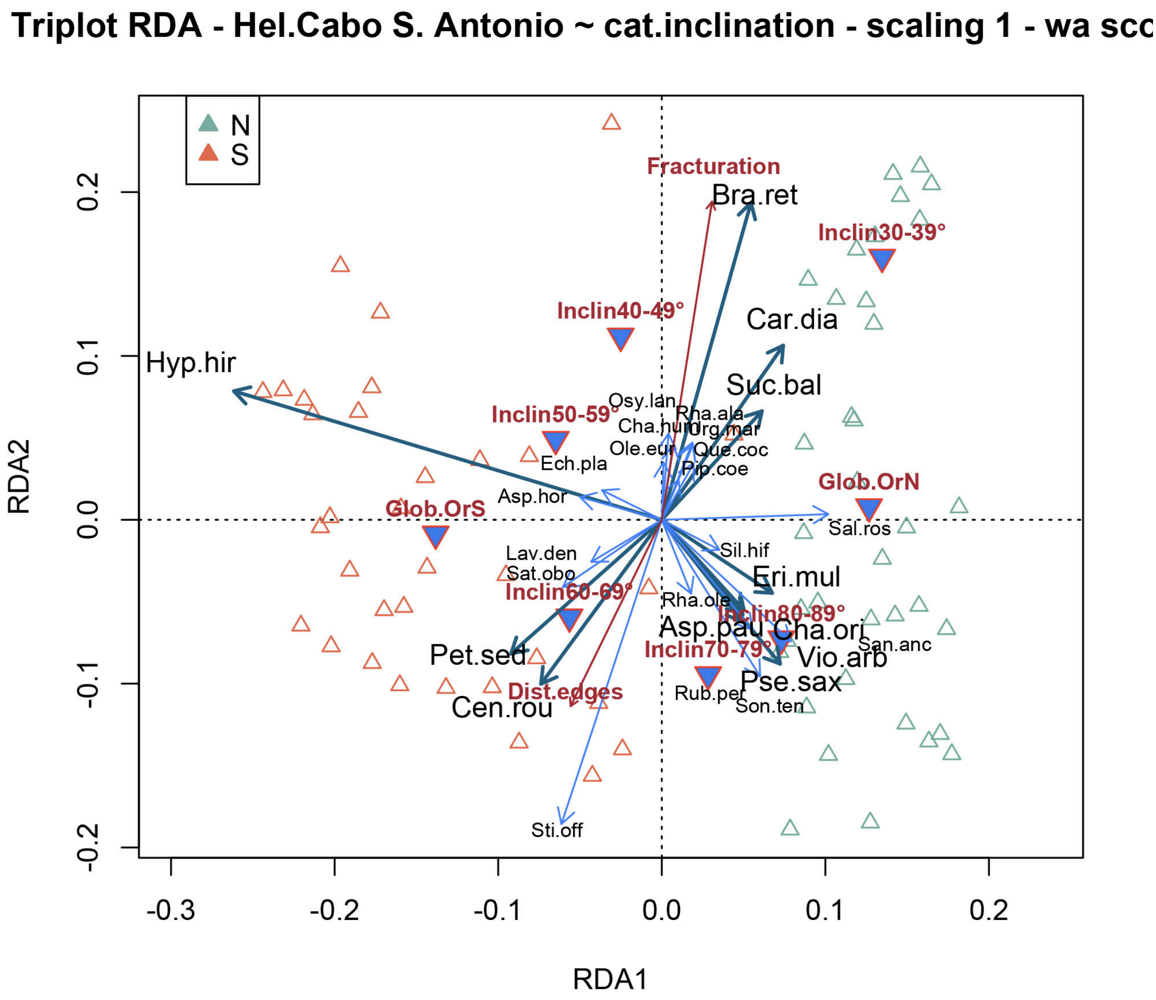

Fig. 3.33. RDA triplot of species abundances in CSAS and CSAN combined datasets, constrained by fine scale microtopographic features of the cliff. Two groups of response variables are plotted in the same multivariate space. Group 1: dark blue arrows represents species with a goodness of fit ≥ 0.21; group 2: pale blue arrows are species with a goodness of fit between 0.02 and 0.21. Group 1 is plotted using a multiplying factor of 0.0941 over its species scores; group 2 uses a multiplying factor of 0.519. Constraints are indicated as red arrows and red/blue triangles. Sites are grouped according to their regional orientation, which corresponds with their location.

Asp.pau = *Asperula paui* subsp. *dianensis*; **Bra.ret** = *Brachypodium retusum*; **Car.dia** = *Carduncellus dianius*; **Cen.rou** = *Centaurea rouyi*; **Cha.ori** = *Chaenorhinum origanifolium* subsp. *crassifolium*; **Eri.mul** = *Erica multiflora*; **Hyp.hir** = *Hyparrhenia hirta*; **Lav.den** = *Lavandula dentata*; **Pet.sed** = *Petrosedum sediforme* subsp. *dianum*; **Pip.coe** = *Piptatherum coerulescens*; **Pse.sax** = *Pseudoscabiosa saxatilis*; **Que.coc** = *Quercus coccifera*; **Sal.ros** = *Salvia rosmarinus*; **San.anc** = *Sanguisorba ancistroides*; **Sil.hif** = *Silene hifacensis*; **Sti.off** = *Stipa offneri*; **Suc.bal** = *Succowia balearica*; **Urg.mar** = *Charybdis maritima*; **Vio.arb** = *Viola arborescens/Polygala rupestris*; **Asp.hor** = *Asparagus horridus*; **Cha.hum** = *Chamaerops humilis*; **Ech.pla** = *Echium plantagineum*; **Ole.eur** = *Olea europaea* var. *sylvestris*; **Osy.lan** = *Osyris lanceolata*; **Rha.ala** = *Rhamnus alaternus*; **Rha.ole** = *Rhamnus oleoides* subsp. *rivasgodayana*; **Rub.per** = *Rubia peregrina* subsp. *longifolia*; **Sat.obo** = *Satureja obovata* subsp. *valentina*; **Son.ten** = *Sonchus tenerrimus* subsp. *dianae*.

The permutation tests for the whole RDA analysis and the first two constrained axes was significant with $P < 0.001$. Also, RDA3 was significant but with $P < 0.01$; other axes resulted to be not significant. Orientation and distance from the edges were highly significant ($P < 0.001$), and inclination was significant with a lesser confidence level ($P < 0.05$). As for the first case study, fracturation was found to be not significant. Furthermore, the contribution of orientation to the total constrained variance in the permutation test was the highest (39 %), followed by inclination (23 %) and distance from edges (10 %).

Variabile	Asp.pau	Bra.ret	Car.dia	Cen.rou	Cha.ori	Eri.mul	Hyp.hir	Pet.sed	Pse.sax	Suc.bal	Vio.arb
Glob.OrN	0,903	0,293	0,630	-0,652	0,940	1,176	-1,230	-0,822	0,922	0,728	0,970
Glob.OrS	-0,907	-0,623	-1,001	1,026	-0,961	-1,265	1,478	1,203	-0,934	-1,147	-1,006
Inclin30-39°	-0,462	1,842	1,906	-1,904	-0,378	-0,266	-0,837	-1,857	-0,421	1,874	-0,306
Inclin40-49°	-1,197	0,908	0,615	-0,591	-1,179	-0,947	0,677	-0,392	-1,189	0,469	-1,162
Inclin50-59°	-0,903	0,163	-0,120	0,140	-0,916	-0,928	0,894	0,301	-0,910	-0,091	-0,926
Inclin60-69°	0,174	-0,900	-0,949	0,949	0,131	0,173	0,467	0,936	0,153	-0,968	0,095
Inclin70-79°	1,132	-1,014	-0,755	0,733	1,107	0,883	-0,526	0,548	1,120	-0,659	1,084
Inclin80-89°	1,260	-0,668	-0,326	0,299	1,256	1,174	-0,923	0,084	1,258	-0,206	1,250
Dist_edges	64,5	169,6	171,2	10,3	66,6	82,6	80,6	22,3	65,6	163,4	68,4

Table 3.3. Table of correlations among constraints and group 1 of species for the RDA ordination. Values refer to the planar representation of the RDA according to the first 2 axes of constrained variance (RDA1 and RDA2). Categorical explanatory variables were projected at right angle on each species response variable. To better compare correlations among species, the resulting values were scaled for each species to zero mean and unit variance. Correlation between response variables and distance from edges (a continuous constraining variable) was calculated as the angle between response and explanatory variables. Colour grade indicates a positive (blue), neutral (white) and negative (red) correlation.

Species assemblages were configured in 4 main groups according to two main blocks of variables (Table 3.3): orientation and inclination. From the canonical coefficients and the position of the centroids in the triplot, it can be seen that orientation was the main contributor of RDA1 axis and (inclination + distance from edges) of RDA2 axis. The grouping colour of the objects gave a further evidence of a division of RDA1 in 2 semi-axes. Thus, the angle between species and the first axis can be interpreted as species preferentiality toward a North (positive RDA1) or South (negative RDA1) regional orientation. The intensity of such preferentiality can be deducted by the proximity of response variables with RDA1 or the small projected distance with orientation centroids: the closer they were the higher was the preference. Conversely, the proximity with RDA2 indicates the sharing level of species between CSAN and CSAS.

The triplot also shows that inclination and distance from the edges played a fundamental role in the dispersion of species along RDA2 axis. It can be seen that the positive RDA2 semi-axis was associated with low inclinations (30° to 60°) and a small distance from edges. The negative RDA2 semi-axis was characterised by high inclinations (60° - 90° and edges distances. Overall, inclination categories were inversely scattered respect to the increasing direction of RDA2. According to this interpretation, the angles between species and RDA2 indicate their preferentiality toward a cliff habitat. Thus, a closer proximity of response variables and positive RDA2 indicates species found on less steep surfaces closer to the cliff base and ledges. Conversely, those species which appeared close to negative RDA2 were found preferentially on sub-vertical/vertical surfaces and far from the cliff boundaries.

The first plant assemblage could be observed in the first quadrant. This group was characterised by species found close to the cliff edges, at low inclinations and preferentially on the North-oriented area. The main species were grasses and small shrubs such as *B. retusum*, *C. dianius, P. coerulescens* and *S. balearica*, but also nano-phanerogams and trees such as *O. europaea var. sylvestris*, *O. lanceolata*, *C. humilis* and *R. alaternus*.

The second assemblage was also encountered preferentially (if not exclusively) on CSAN. It is represented in the triplot by species in the fourth quadrant. The vast majority of species in this group were small shrubs positively correlated with a growing gradient of inclinations from 60° to 90°. Main species pertaining to this group were *A. paui* subsp. *dianensis*, *C. origanifolium* subsp. *crassifolium*, *P. saxatilis*, *S. hifacensis* and *S. tenerrimus* subsp. *dianae*. *S. rosmarinus* was found to be in between these 2 groups, being encountered both at low and high slopes along the entire gradient of distance from cliff borders.

The third assemblage (third quadrant) was the South-oriented equivalent of the second group. Species of this group were small shrubs, succulents or grasses correlated positively with high slope and distance from edges. Main elements of this group were *C. rouyi*, *L. dentata*, *P. sediforme* subsp. *dianum*; and *S. offneri*.

Finally, the fourth group can be observed in the second quadrant. Small angles of response variables with RDA1 negative semi-axis suggested that species of this group were found exclusively on the South-oriented area (CSAS). It is formed by *H. hirta*, *A. horridus* and *Echium plantagineum*. As group 1, this assemblage was encountered mainly on low inclinations, but appeared to be less influenced by slope values. Moreover, contrarily to group 3 these three species were not influenced by the position on the cliff.

Case study 1+2: a combination of datasets and life form distribution

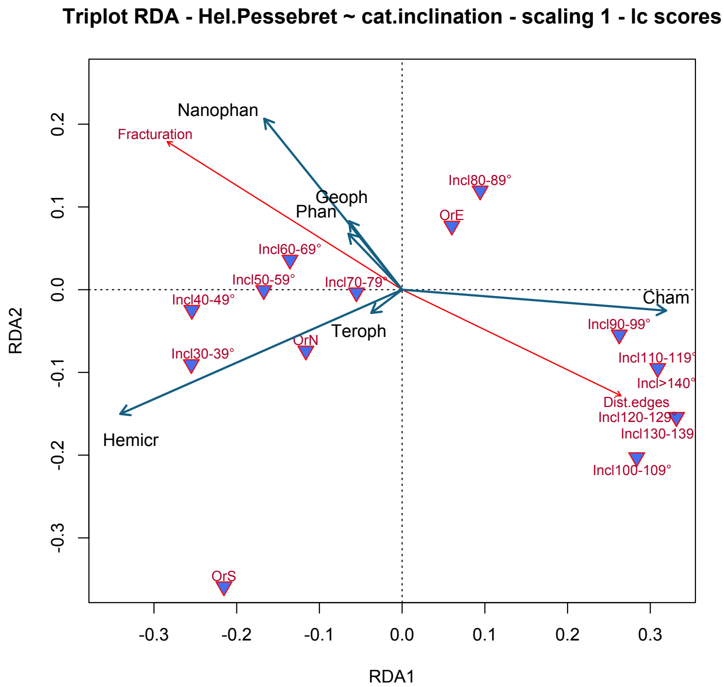

Fig 3.34. RDA biplot of life form abundances in Pessebret, CSAS and CSAN combined datasets, constrained by fine scale microtopographic features of the cliff. Blue arrows represent response variables. Red arrows and red/blue triangles represent constraints. Scaling 1.

The datasets of Pessebret (188 non-empty plots, case study 1) and CSAS+CSAN (69 non-empty plots, case study 2) were merged in order to study the relationship among microtopography and ecological life forms (Raunkiær classification system). The final dataset was composed by 937 specimens belonging to chamaephytes, 118 to geophytes, 699 to hemicriptophytes, 473 to nanophanerophytes, 92 to phanerophytes and 41 to terophytes. A redundancy analysis was performed on the resulting 257 plots. Inclination was categorised in 11 classes, covering a slope gradient from 30° to > 140°. Other constraints were distance from edges, regional orientation (N;S;E) and fracturation. Results of the canonical analysis were summarised in fig 3.34 biplot.

The RDA expressed a low total variance (0.340), whose constrained fraction was 43.3 % (R^2 = 0.433). The adjusted R^2 was 0.397. The cumulative proportion of variance explained by the first two axes was 0.4 of the total variance and 93 % of the constrained variance. The first axis held most of the constrained variance (0.71), meanwhile RDA2 was 0.218. It was noticeable that the proportion of total variance explained by the first residual structure (PC1) was 0.2, a value smaller than the first canonical axis (0.31) but considerably higher than RDA2 (0.09), hinting a for a secondary residual structure in the response data.

According to the permutation test the overall RDA was significant ($P < 0.001$), meanwhile only the first 2 axes resulted significant at $P < 0.001$. Orientation and inclination were the unique significant constraints ($P < 0.001$) with a contribution to the constrained variance of 26.7 % (orientation) and 15.2 % (regional orientation).

From the RDA biplot (Fig. 3.34) it can be seen that chamaephytes were by far the group better and positively correlated with subvertical-vertical slopes (70° to 90°) and overhanging areas. Also, this life form was more often encountered on East and North-oriented areas than on South-oriented. However, results in relation with cliff regional orientation should be taken with caution. In fact, there was a disproportion between E and (N+S) plots in the merged dataset.

The RDA biplot also showed that phanerophytes and geophytes had shorter projections, indicating that they were either present over most portions of the dataset or related to intermediate ecological conditions (all inclination categories except overhang). However, these life forms together with nanophanerophytes were negatively correlated with distance from edges, meaning that they were preferentially found on the cliff boundaries (base and crest) rather than in the middle of the cliff. Finally, hemicriptophytes and therophytes were positively correlated with both a South and a North regional orientation. However, the projection onto these life forms of the South centroid of regional orientation is more pronounced, indicating a closer relationship. Another observation regards the inverse relationship that these life forms have with an increasing gradient of inclinations. Moreover, they also were negatively correlated with distance from the edges as the previous group (nanophanerophytes, phanerophytes and geophytes).

Scenario 2: Target species

Case study 3: comparison of 2 narrow endemic chasmophytes at Monte Cofano, Trapani, Italy

Methods

Location and object of research. Monte Cofano (38.1 °N; 12.66 °E) is a coastal carbonate massif (659 m a.s.l.) situated on the north-west limits of the Tyrrhenian Sicilian coasts (Fig. 3.35). Geologically, this endemism-rich area is the westernmost part of the carbonate platform denominated Panormide. This grey/white dolomitic platform includes several other isolated coastal mountains in North-West Sicily.

Fig 3.35. North oriented coastal cliffs of Monte Cofano (Italy).

Monte Cofano is characterised by an extensive cliff system facing all cardinal points. The northern and southern areas were also selected as study site for cliff microclimate analysis shown in Chapter 1. From a bioclimatic point of view, the whole territory falls into the thermomediterranean bioclimatic belt. According to the last floristic checklist (Gianguzzi et al., 2005), Monte Cofano and its surround natural reserve are populated by 647 taxa. The overall endemic component exceeded 7 %, but this percentage did not take into account nor exclusively the cliff habitats nor recent taxonomic adjustments. However, cliffs in this area are populated by a large number of narrow endemic species. Among them, two model species were selected for this work: *Pseudoscabiosa limonifolia* (VAHL) DEVESA and *Erica sicula*

GUSS. subsp. *sicula* (Fig.3.3). Both species have a strictly chasmophytic ecology and share the same life form (small chamaephyte). *E. sicula* is stricly endemic to this area, meanwhile *P. limonifolia* is scattered along few relictual populations on other coastal cliffs lying in the Panormide Carbonate Platform. Further results on the distribution and phylogeography of *P. limonifolia* will be shown in Chapter 4.

These 2 species were selected for this study by taking in account the feasibility of photo-identification. Species dimensions (20 cm to 1-2 m) and both vegetative and phenological aspects discriminated well single individuals from a camera-to-cliff distance of up to 8 m. All surveys were carried out between April and May 2019, following the phenological peak of *Erica sicula* (Fig 3.3 D).

The scope of research was to investigate their niche selection in relation to the exclusive presence on cliffs. Both quantitative compositional and environmental data were used in this case to characterise the ecological preferences of each species.

Sampling design, image analysis and 3D model building. The whole area of Monte Cofano was divided in 4 sectors according to the principal orientations of the mountain. For each sector, one cliff surface was selected for the aerial survey (Fig 3.36). Moreover, areas were selected based upon the high environmental heterogeneity for the sector. As a consequence, frequent variations in local orientation and inclination were encountered on each zone (see Fig. 3.12 and 3.13 for Cofano West)

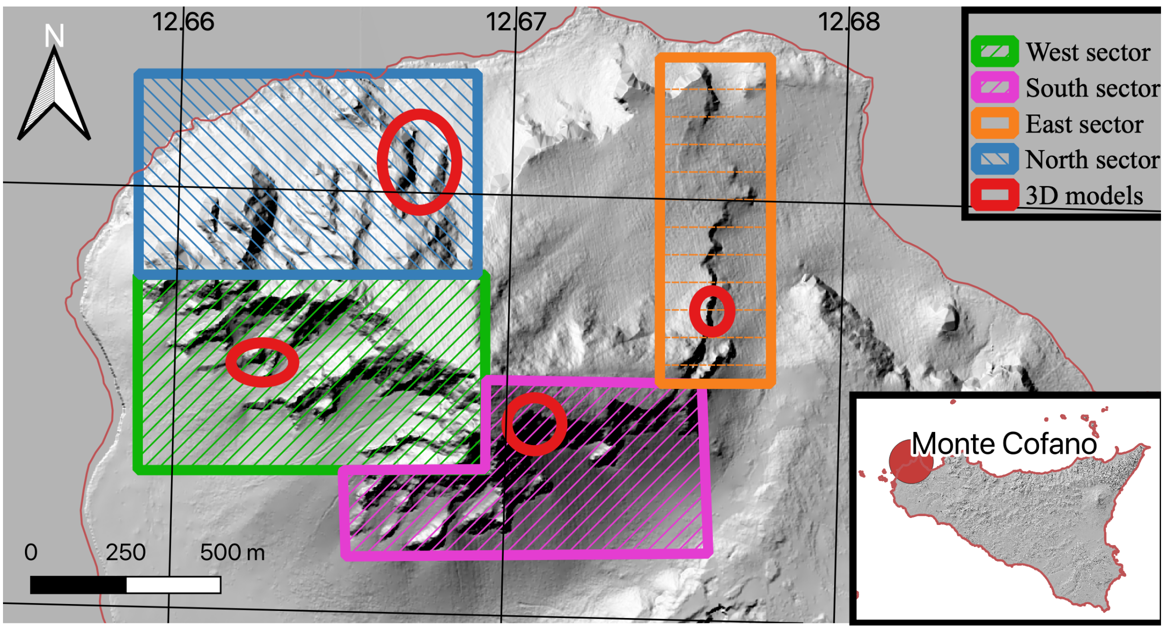

Fig. 3.36. The topographic unit of Monte Cofano divided in 4 sectors of different regional orientation.

The four study areas were Cofano North (N), Cofano East (E), Cofano West (W) and Cofano South (S). Altitude was calculated from the base of the cliff and were comparable among the four zones: Cofano N 150 m; Cofano W 179 m; Cofano S 400 m and Cofano E 245 m.

All details concerning the number of photos, pixel dimension on the ground (GSD), batteries used, and flight details are given in Table 3.1. Camera-to-cliff distance ranged from 3 to 8 metres. The largest cliff system surveyed was Cofano N (25462 m^2). Other areas were less extended: Cofano S, the second area by extension, was in comparison 60 % of Cofano N (14782 m^2). The West and East areas were the least extended, respectively covering 11456 m^2 and 6600 m^2.

Photo positions were firstly converted from WGS84 to WGS84 UTM 33 ellipsoid. From the photoaligned dataset it was observed a complete absence of both model species from Cofano South. As a consequence of that, this area was excluded from further analyses and marked as negatively correlated with both species. Further detailed field surveys in the south sector of Monte Cofano confirmed this absence on the entire cliff system.

For this case study, plot shape was squared and measured 9 m^2. It was the result of a 27 m^3 cube orthogonal projection on the 3D model of cliff surface. Species were sparsely distributed on cliffs. Due to this reason, sampling units were larger in order to reduce the probability of empty plots.

A total of 278 plots were equally distributed among North, East and West areas (Fig 3.37 left) Contrarily to a scenario 1 operation, systematic design was substituted by a random plot placement. The placement in each area was carried out only inside the minimum surface that contained all individuals. Such type of design was implemented in order to maximise the probability of encountering individuals in the plot.

Moreover, plot surfaces were selected with comparable fracturation values. As a consequence of the lack of significance in previous analyses, this variable was equalised in the plot placement.

Quantitative inclination values per plot were transformed in 6 ordered classes of 10° span each (Fig 3.37 right)

Statistical analysis. Datasets from where both species co-existed were merged (Cofano E and Cofano N). Niche selection was determined using two separate Constrained Additive

Ordinations (CAO; Yee, 2006 a). Both ordinations were fitted under a Poisson model of rank 1 with 2.5 non-linear degrees of freedom for both species, choosing the best 100 models (Yee 2006a; 2006b). Quantitative inclination (Inclin), and distance from the base (dist_base) were chosen for defining the microhabitat latent variable in the first analysis. By contrast, inclination (inclin) and distance from the ridge (dist_ridge) were used for the second analysis. Environmental variables were scaled to zero mean and unit variance prior to analysis.

A redundancy analysis (RDA) was implemented to study species distributional properties. For this purpose, the entire datasets of N, E and W areas of Cofano were merged. Explanatory variables were categorical inclination, local orientation, global orientation (or zone), distance from the base and distance from the ridge. Species data matrix were Hellinger transformed prior the analysis. RDA ordination results used a distance triplot (scaling 1) with lc scores.

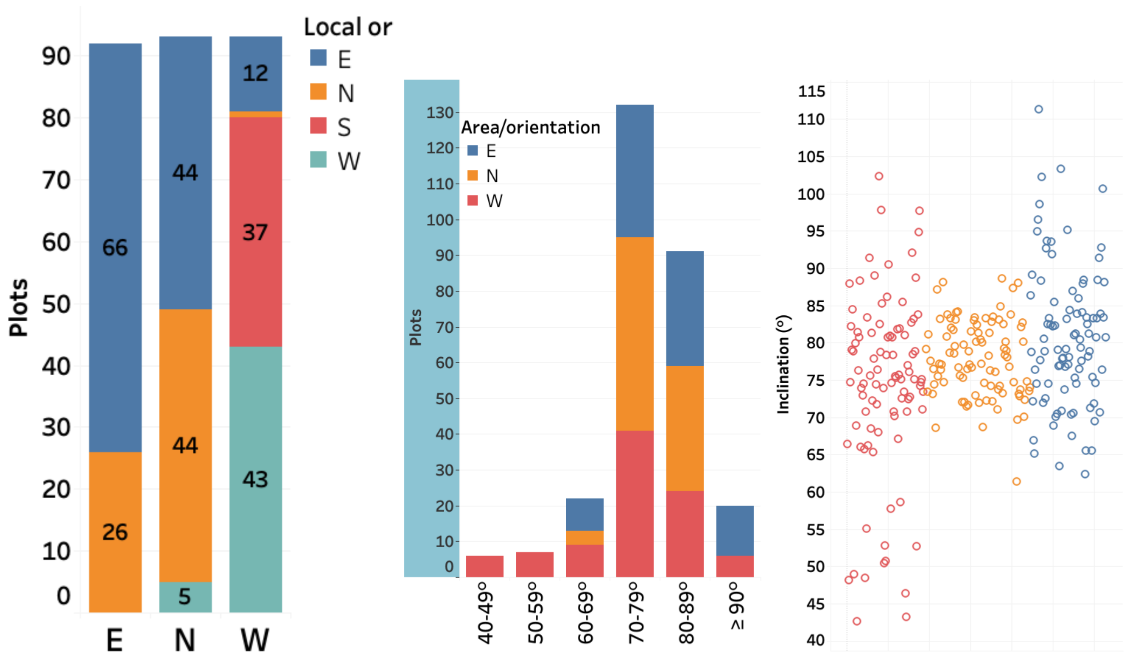

Fig. 3.37 left. Barplot of local orientations in the surveyed plots. Each bar represents a research area.

Fig. 3.37 right. Scatterplot of plot continuous inclinations and the resulting barplot categorisation into 6 inclination classes.

		Inclination1											
		Grand Total		50-59°		60-69°		70-79°		80-89°		Overhang. > 90°	
Global or	Local or	Eri sic	Pseu limo	Eri sic	Pseu limo	Eri sic	Pseu limo	Eri sic	Pseu limo	Eri sic	Pseu limo	Eri sic	Pseu limo
E	E	145	5			26	0	77	3	42	2	0	0
	N	56	35			3	1	27	23	26	11	0	0
	Total	201	40			29	1	104	26	68	13	0	0
N	E	127	33			6	0	76	17	45	16		
	N	74	151					45	78	29	73		
	W	9	7			3	0	6	4	0	3		
	Total	210	191			9	0	127	99	74	92		
W	E	23	0	1	0			10	0	12	0	0	0
	N	2	0					2	0				
	S	50	0	0	0	10	0	22	0	16	0	2	0
	W	76	0	0	0	5	0	51	0	20	0	0	0
	Total	151	0	1	0	15	0	85	0	48	0	2	0
Grand Total		562	231	1	0	53	1	316	125	190	105	2	0

Table 3.4. Individuals of *P. limonifolia* and *E. sicula* encountered in the studied plots, categorised per class of inclination, local and global orientation. Red and blue gradients indicate each species relative abundance.

A total amount of 562 individuals of *E. sicula* and 231 of *P. limonifolia* were marked inside plots (Table 3.4). *E. sicula* was encountered on all global orientations, whereas *P. limonifolia* was not recorded from Cofano West. Contrarily to *P. limonifolia*, few individuals of *E. sicula* were found on plots with 50° - 59° inclinations and overhanging. Moreover, this species was substantially more present on the 60° - 69° class (53 individuals against 1 individual of *P. limonifolia*). Both species were found preferentially between 70° and 89°, but with different abundances. Overall, *P. limonifolia* was less frequent than *E. sicula*. By contrast, it was more frequent on locally and globally North-oriented plots.

CAO results are shown in Fig 3.38. It can be seen that only *P. limonifolia* had a unimodal response curve in both analyses. The bell-shaped curve indicates that the species was well represented in the dataset. By contrast, in both analyses *E. sicula* had expected values which were highest at low site scores. Its response curve was linear, suggesting a negative geometric relationship with the latent variable. The analyses revealed that the scaled constrained coefficient relative to the plot position increased in opposite directions of the latent variable. This characteristic can be observed by the sign of dist_base (negative) and dist_ridge (positive). Both analyses were ultimately describing a similar niche selection process, but by using different constraints. In fact, the negative sign of distance from the base in the first analysis indicates an increase distance from the base toward the left direction of latent axis (Fig. 3.38 A). Conversely, the positive sign of distance from the ridge in the second analysis (Fig. 3.38 B) shows an increase distance from the ridge toward the right direction of latent axis. The almost identycal linear response of *E. sicula* in both analyses indicates a positive correlation with the ridge and a negative correlation with the base of the cliff. According to this interpretation, both the peaks shown by *E. sicula* at low site scores could be interpreted as a complete and unique preference for ridges as regard its position on the cliff.

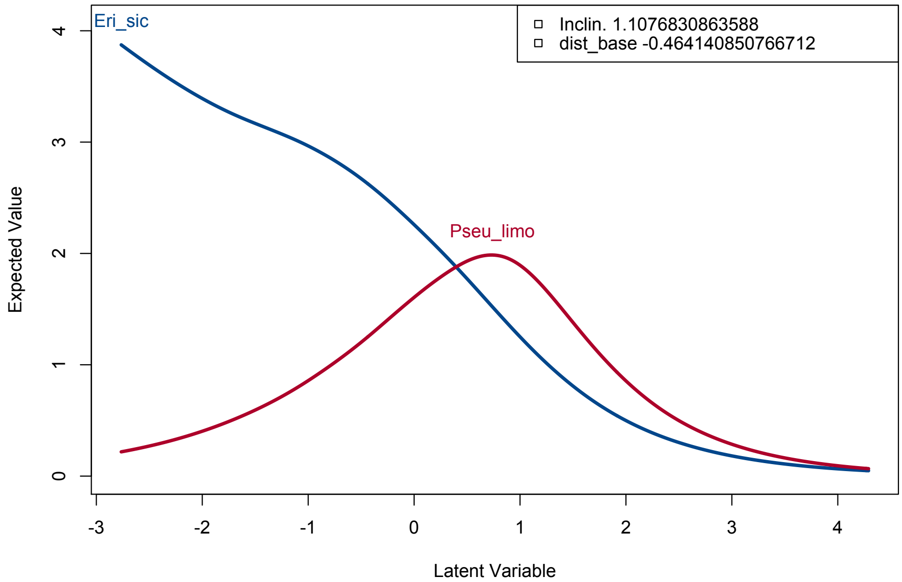

A

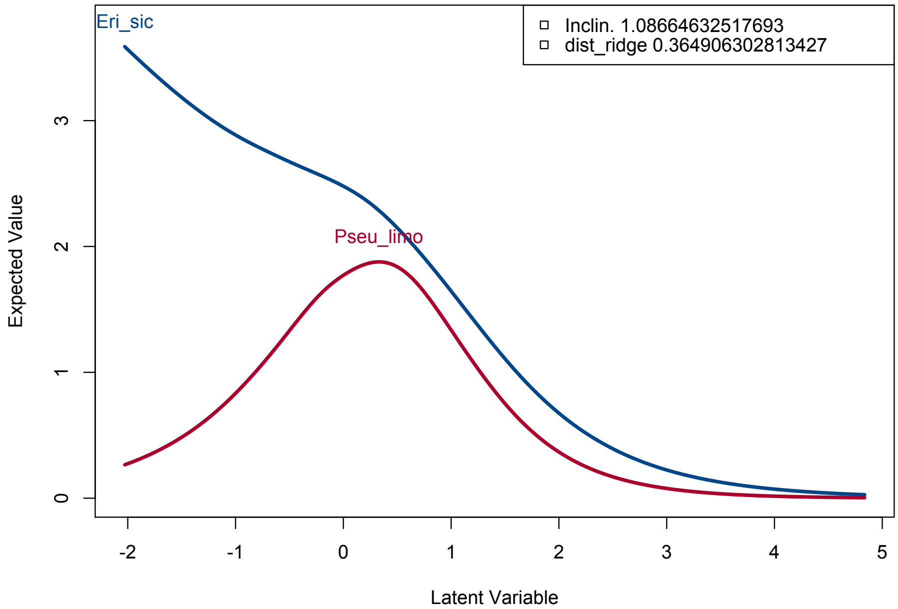

B

Fig. 3.38. CAO perspective plots. Legend in upper right corner shows the scaled constrained coefficients. composing the first ordination axis. Fig 3.38 A: latent variable includes inclination and distance from the cliff base. Fig 3.38 B: Latent variable is formed by inclination and distance from the cliff ridge.

At the same time, inclination plays the major role in the latent variable of both ordinations, with a gradient of increasing slopes toward the right direction. The unimodal response of *P. limonifolia* in both analyses indicates a cliff habitat preference, but with overall minor abundances with respect to *E. sicula* (curve height). Also, its decreasing curve at the extremes indicates a small ecological tolerance. Specifically, it represents a negative correlation with both the proximity of the base (Fig. 3.38 A) and the crest of the cliffs (Fig. 3.38 B). Furthermore, the response curve of this species in the second analysis was slightly shifted toward the left end of latent variable, indicating a slight preference toward the proximity of cliff ridges. Moreover, the gradual decrease of the curves toward the right direction and the superposition with *P. limonifolia* provide information on the species tolerance toward the inclination gradient and the colonisation of the same slopes of *P. limonifolia*.

The redundancy analysis (Fig. 3.39) had a total variance of 0.286. The constrained fraction of the total variance was 47.2 % ($R^2 = 0.4721$), whereas the adjusted R^2 was 0.4482. The analysis produced only 2 canonical axes and 2 residual axes. The proportion of variance explained by the first canonical axis RDA1 was 57 % of the constrained variance, whereas RDA2 held 43% of it. The first residual axis was larger (PC1, 0.399 of total variance) than both canonical axes. This means that the first residual structure of the data had more variance than the structures explained by the chosen explanatory variables.

The permutation tests for the whole RDA analysis was significant for $P < 0.001$. When the test was applied to canonical axes, both resulted equally significant at $P < 0.001$. On the other hand, the permutation test on constraints was not significant for the variables distance from base and distance from ridge. Other variables resulted significant for $P > 0.001$. In the test, inclination held the highest portion of constrained variance (0.044; 32.7 %), followed by local orientation (0.031; 23.1 %) and global orientation (0.01; 7.4 %).

The 2 species are positioned on different quadrants of the ordination triplot (Fig. 3.39). From the graph it is possible to observe that most of the characteristics explained by the subset of data used in CAO remained valid. *E. sicula* is positively associated with a vast gradient of inclinations (60° to 89°) but finds the highest association with the 70° - 79° class. Moreover, this species does not have a preferential global orientation, but Cofano North appears to be marginally predominant in its distribution. As for what concerns local orientation, the species resulted slightly more correlated with East-facing surfaces then with other aspects. Conversely, a slight negative correlation was found with locally South-oriented plots.

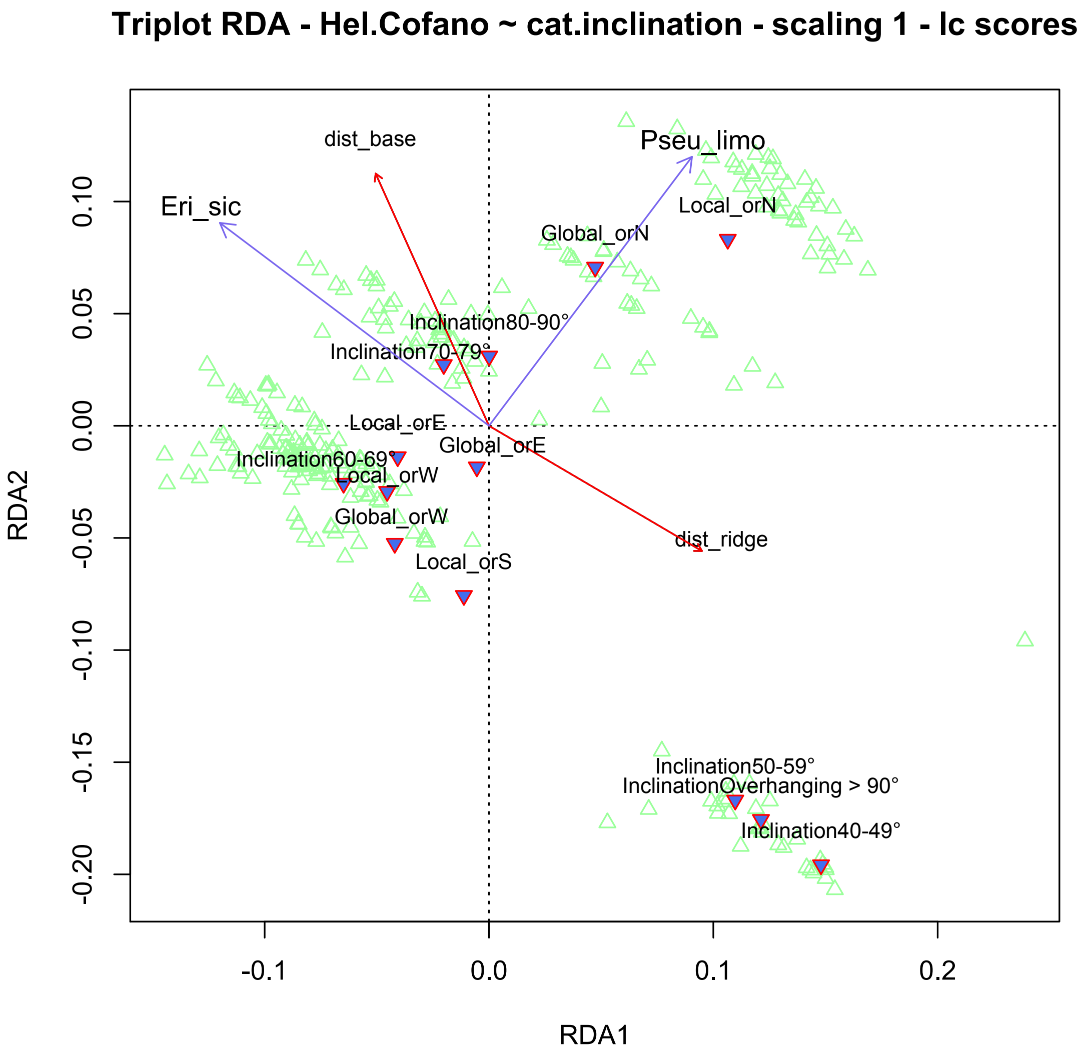

Fig. 3.39. RDA triplot of the combined datasets Cofano North, Cofano East and Cofano West. Species abundances were constrained by fine scale microtopographic features of the cliff. Blue arrows represent the species scores. A multiplying factor of 0.015 was applied over their scores. Constraints are indicated as red arrows and red/blue triangles. Sites are indicated with green triangles.

P. limonifolia resulted positively associated with the North site, and marginally correlated with the East area. As expected, this species was absent (negatively correlated) with Cofano West. Locally, *P. limonifolia* was highly and only associated with North-oriented patches of cliffs. Contrarily to *E. sicula*, this species was only positively correlated with high inclination values (70° to 89°). The highest association was encountered with the 80° - 89° class.

Case study 4: comparison of two chasmophytes, a narrow endemic species with a closely related widespread taxon. Capo Gallo, Palermo, Italy

Methods

Location and object of research. Following case study 3, a second survey was carried out using *P. limonifolia* as model species. The research area was located on the summit section of the cliffs of Capo Gallo (38°12' 57"N; 13° 18' 10" E). This mountain, as well as Monte Cofano, is a coastal carbonate massif situated on the north-west limits of Tyrrhenian Sicilian coasts. The two mountains share most of their geomorphologic, geologic and phytogeographic characteristics. In fact, Capo Gallo and its adjacent mountain represent the easternmost areas of the carbonate platform denominated Panormide.

The cliff system of Capo Gallo extends continuously along its North, West and East sides. The north-exposed cliffs were also characterised by their vertical continuous extension of up until 300 m. Together with Monte Cofano, Capo Gallo is an area rich in endemic species, whose chasmophytes are a considerable component (Raimondo et al., 2001). Moreover, in this area can be found the easternmost population of the model species *P. limonifolia* (see also Chapter 4).

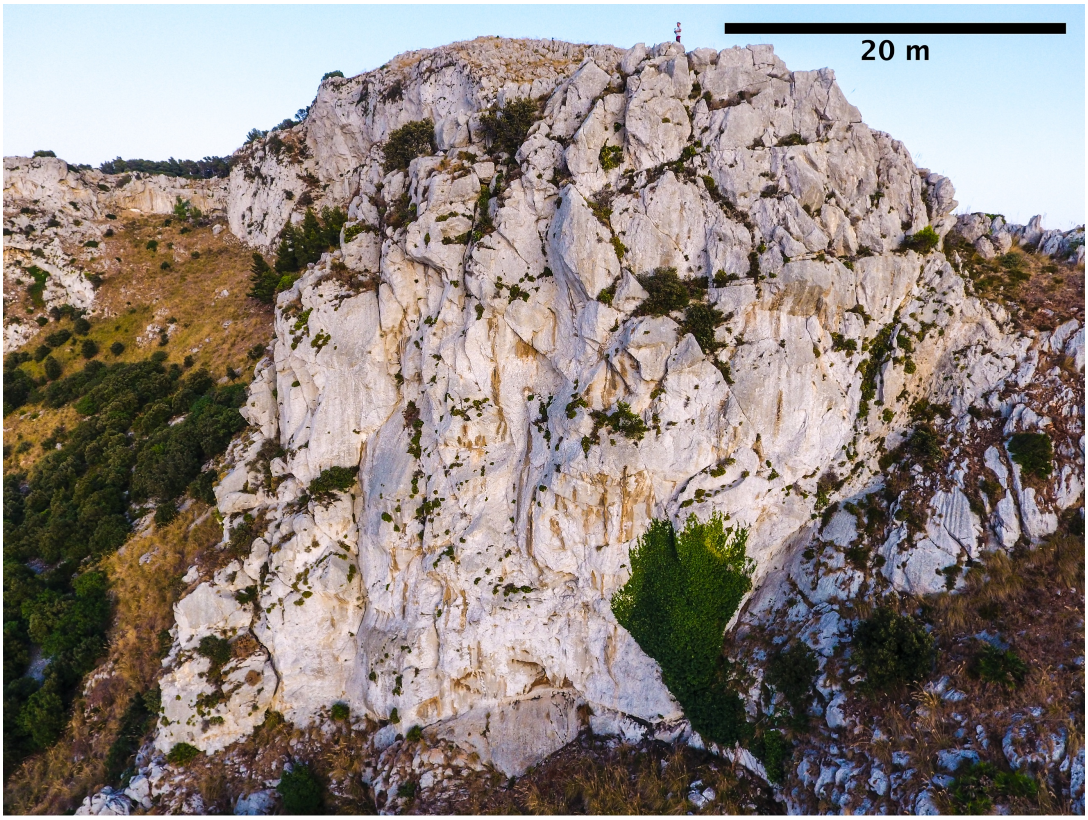

Fig. 3.40. The surveyed area of Capo Gallo.

The object of this case study was to confront the narrow local orientation preferences of *P. limonifolia* with a widespread chasmophyte species. The second target species selected for this purpose was *Lomelosia cretica* (L.) GREUTER & BURDET, a close relative taxon. Both species belong to the family Caryophyllaceae s.l. (APG IV, 2016) or to Dipsacaceae s.s. Conversely to *P. limonifolia*, *L. cretica* has a wider distribution, being endemic of the coastal areas of South Italy and the Balearic Islands. This species can be found colonising a wide range of cliff environments, both according to orientation and slope values, adapting sometimes even to a non-rupicolous ecology (Balearic Islands). Moreover, *L. cretica* is a chamaephyte that forms large cushions of 40 cm - 3 m. Thus, the species is easily identified from a photographic survey thanks to its dimensions and the green/silver vegetative aspect.

The survey was carried out in July 2019, following the phenological peak of *P. limonifolia* (Fig. 3.3 A)

Sampling design, image analysis and 3D model building. A small area on the North-exposed cliffs of Capo Gallo was selected (Fig. 3.40). The surveyed cliff, denominated simply Gallo, is situated at an altitude of 400 m (calculated from its base). This area represents the uppermost limit of a 300 m long vertical cliff. The wall results shaped in a semi-cylindrical form, gradually folding along a South to East to North curve. A detailed information about the number of photos, Ground Sample Distance, batteries used, etc. are given in Table 3.1. Camera-to-cliff distance ranged from 3 to 5 metres. The final surveyed surface measured 6118 m^2

For this case study, the cliff was simplistically modelled as a continuous homogeneous surface, whose unique environmental variability was its local orientation.

Photo positions were firstly converted from WGS84 to WGS84 UTM 33 ellipsoid.

Plot placement followed substantial modifications respect to previous case studies. The entire vertical component of the surveyed area was fractioned in 11-5 m wide-contiguous sectors. The fractioning was performed following a South to East to West transect. Each sector corresponded to the intersection between the original point cloud and a 5 x 5 x 35 m digital box. The flat approximation of a single sector surface was 5x35m = 175 m^2. Species abundances were standardised for visual representation. Scaling of abundances was relative to each species maximum abundance.

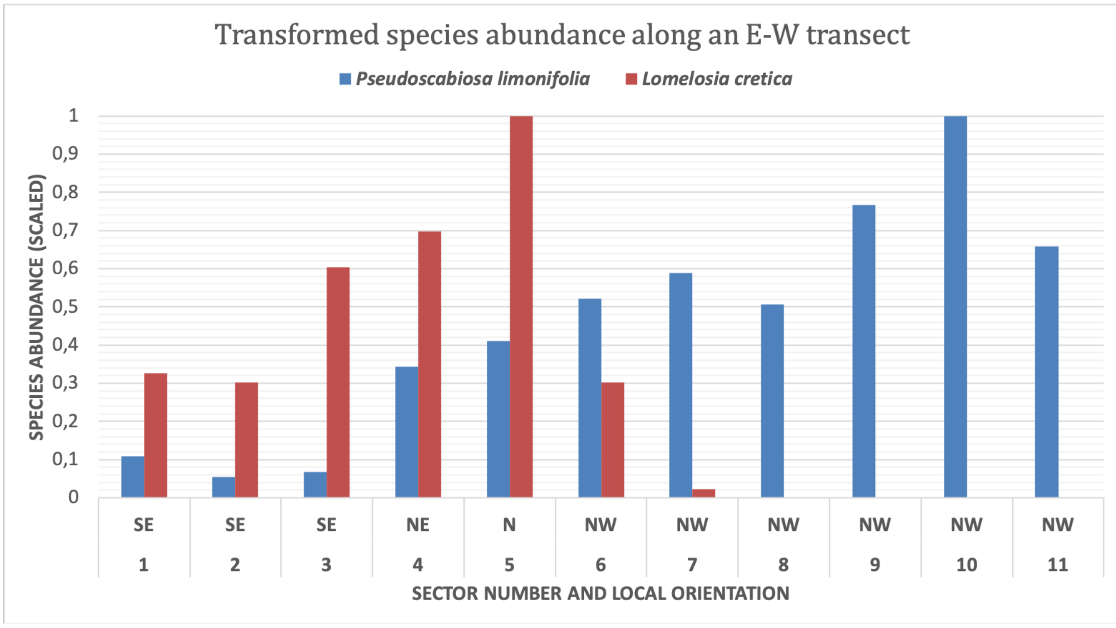

Fig. 3.41 up. Barplot of scaled species densities along a local orientation gradient. Fig. 3.41 down. 3D model of Gallo. Red points are individuals of *L. cretica*. Blue points are individuals of *P. limonifolia*.

	L. cretica	P. limonifolia
N	43,0	30,0
NE	30,0	25,0
NW	14,0	295,0
SE	53,0	17,0
Grand Total	140,0	367,0

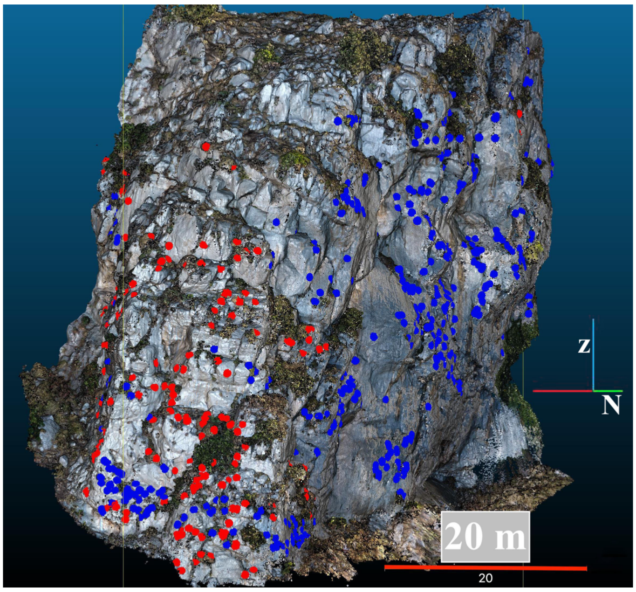

A total of 367 individuals of *P. limonifolia* were found for the area. *L. cretica* was found to be less frequent (140 individuals) (Table 3.5; Fig. 3.41 down). This latter species was encountered preferentially on the South-East to North locally oriented plots. Moreover, no individuals were found on the North-West plots. Conversely, *P. limonifolia* was present on all the surveyed plots, but with different densities (Fig. 3.41). The barplot in Fig. 3.41 also shows that a substantial incremental in its frequency was observed in the North-West plots 9 to 11.

Case study 5: Visual census for plant conservation and population monitoring. Toix and Cap d'Or (Alicante), Spain

Methods

Scope of research. Another approach to the application of drone-based surveys on chasmophyte species is to study the total distribution/conservation of target species. In order to test the discriminatory power of aerial photos and 3D modelling, the Iberian *Silene hifacensis* ROUY EX WILLK. was selected as target species. This taxon is an Iberian-balearic endemism, with a reduced number of remaining individuals. It is a strict chasmophyte, whose distribution of natural populations is reduced to 2 continental areas and the island of Ibiza. In the period 2009 – 2019 the continental populations reduced from 3 to 2 and the number of individuals from 74 to 16 (CIEF, 2018).

Starting from 2008 the species was included in a conservation project directed by the Centre for Forestry Research and Experimentation (CIEF) of the Valencian Community. Thanks to the conservation efforts, the species was replanted on extinct areas and the remaining populations were recovered by in-situ replanting.

The scope of this case study was to investigate the remaining natural populations of *S. hifacensis* with the use of aerial surveys and 3D models. The main research goal was to build 3D models of the cliffs where the species survived and localise the remaining adult individuals and replanted seedlings.

Location. Two geographic areas and 3 populations were investigated: Toix (38°37'56" N; 0° 1'6" E; 1 population) and Cap D'Or (38°41'16" N; 0° 9'11" E; 2 populations). Within Cap D'or, two separate zones were surveyed: Cap D'Or Pessebret and Cap D'Or Cueva de les Cendres. The fieldwork involved in the survey of *S. hifacensis* was then partially overlaid to case study 1.

Sampling design, image analysis and 3D model building. Each population was surveyed separately in mid-April 2019. Although the position of adult individuals on cliffs was known to the personnel involved in the conservation project, by experimental design this information was undisclosed at the moment of the survey. The unique *a-priori* condition was a knowledge of the population boundaries. Within each zone, the scope of survey was to cover a large portion of the cliff in order to spot (if any) new individuals outside the boundaries of the known population. For this purpose, a nested design was implemented:

- A general survey taken with a high camera-to-cliff distance (not useful for species photo-identification), was performed. The survey covered a large portion of the cliff surface in the near proximity of the know populations of the target species. The scope of the survey was to allocate afterward the sub-level 3D model surveys.
- Within each general survey, the area within the known population of the species was surveyed.
- A series of randomly selected zones, nested within the general survey of each topographic unit, were inspected by producing small 3D models (50 – 300 m^2).

Camera settings, number of batteries used, and dense cloud specifics of the final 3D models are shown in Table 3.1. However, data in Table 3.1 do not account for the general survey or for any empty sub-level survey. In this context, the details on the survey of Toix in Table 3.1 correspond to the 3D model of the fraction where the species was encountered. The area Cap d'Or Pessebret surveyed for this case study is labelled "Cap d'Or Pessebret complete" and corresponds to a larger portion of the area used in case study 1.

Prior to any analysis, photo positions were converted from WGS84 to WGS84 UTM 31.

For each sub-level survey, two sets of aerial photos taken at different distances from the cliff were acquired. The goal was to individuate the threshold sampling distance necessary for a photographic identification of the species.

Encountered specimens passed a 2-step validation process in order to enhance the photointerpretation accuracy and avoid false positives. Once plants were identified and markers were added, their position in the 3D space along with the photographic crop of the specimen from different camera angles were photo-interpreted independently by a second botanist. Only markers with a unanimous consensus on their identity were added to the final list.

Results

The initial identification of all individuals was confirmed by a 2-step validation. A total of 35 individuals of *Silene hifacensis* were identified. Six of them were native mature plants, meanwhile 32 were plantules derived from the conservation campaigns of assisted seed dispersal. No individuals were encountered outside of the boundaries of the known populations. One native individual was encountered in Toix (Fig. 3.42), 2 in Cap d'Or Pessebret complete (Fig. 3.43 A-B) and 4 in Cap d'Or Cueva de les Cendres (Fig 3.43 C-D). Plantules were encountered only in the 3D model of Cap d'Or Cueva de les Cendres.

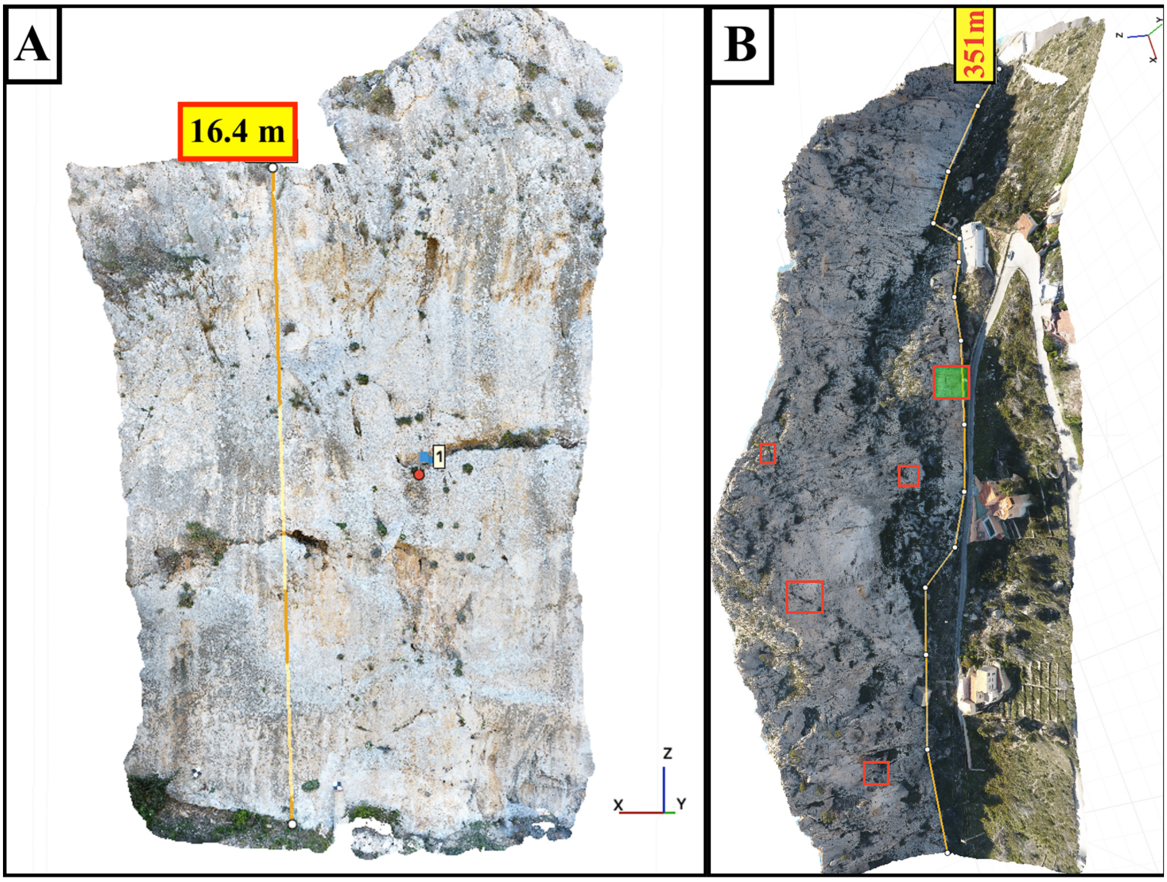

Fig. 3.42. 3D model of Toix. A: zone where an individual was encountered. B: the general survey of Toix. Red boxes are the surveyed zones within the general survey. Green box is the unique zone where one individual was encountered (Fig. 3.42 A). X = East; Y=North; Z=vertical positive direction.

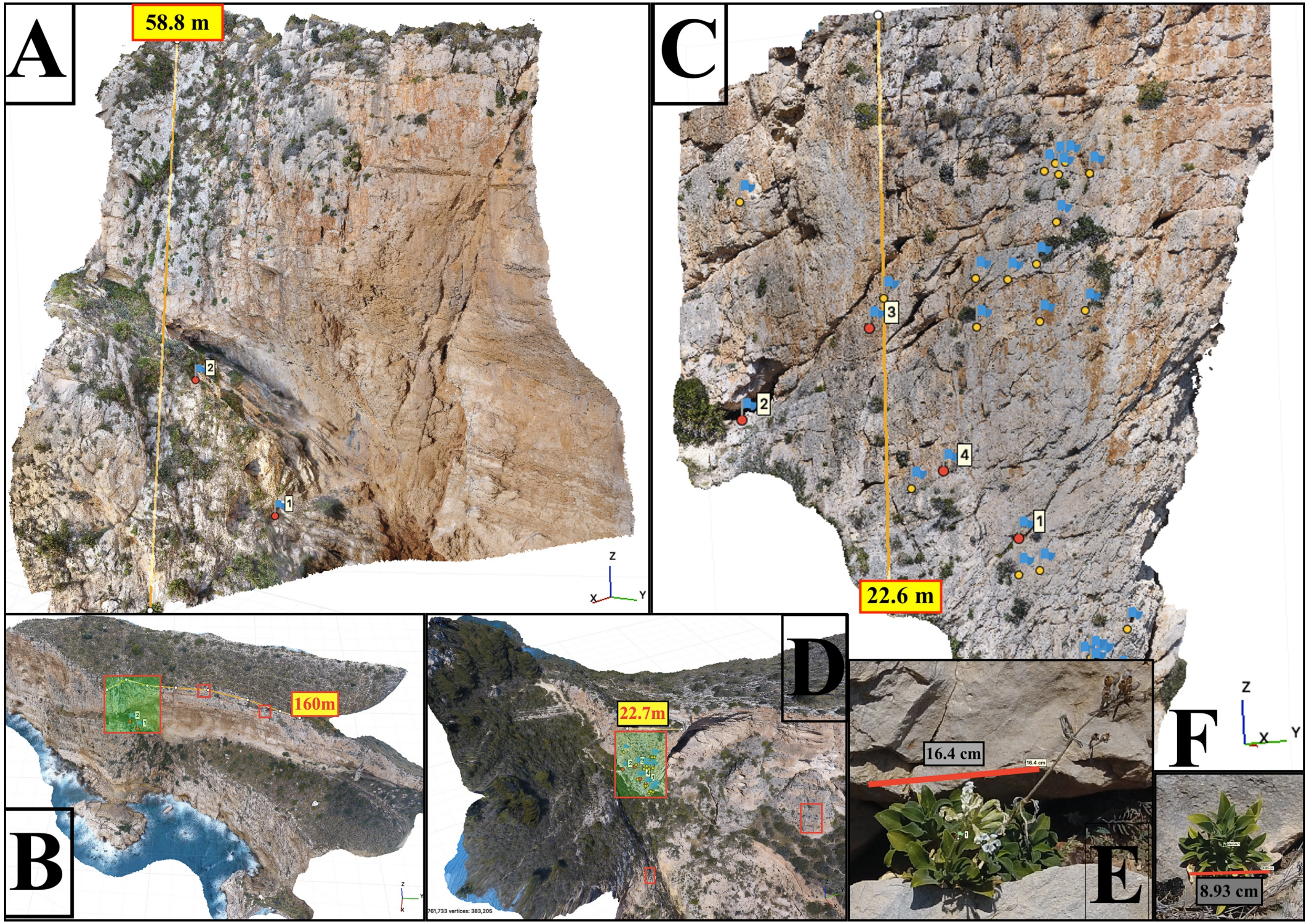

Fig. 3.43. 3D models of Cap d'Or Pessebret complete and Cap d'Or Cueva de les Cendres. A: Cap d'Or Pessebret complete. The area corresponds with the known location of the population of *S. hifacensis*. B: 3D model of the general survey of Cap d'Or Pessebret complete. C. Cap d'Or Cueva de les Cendres. The area corresponds with the known location of the population of *S. hifacensis*. D: 3D model of the general survey of Cap d'Or Cueva de les Cendres. Red boxes are the surveyed zones within the general survey. Green box is the known location of the population (Fig. 3.42 A). E: the dimension of a flowering native individual. F: young plantule, resulted from assisted seed dispersal on the cliff surface. X = East; Y=North; Z=vertical positive direction. Red markers are native individuals. Yellow markers are young plantules.

Discussion

In his historic work, Davis (1951) stated: "The differences in the minor habitats of the rock face (unfortunately extremely difficult to investigate) are highly important in determining the differentiation of chasmophyte communities". Seventy years after his detailed observations, a few studies still exist analysing the assembly rules of cliff plant communities (Larson et al., 2000 and citations therein). Even fewer authors used a numerical approach to investigate the species-microtopography relationships (Escudero, 1996; Graham & Knight, 2004; Kuntz & Larson, 2005).

Assembly rules governing fine-scale niche selection on cliffs have therefore remained understudied. This is in contrast with a wide scientific consensus on the remarkable ecological, conservation-related and phytogeographic value of these areas in the Mediterranean basin (Bragazza, 2009; Domínguez et al., 2003; García et al., 2002; Lavergne et al., 2004; Médail & Verlaque, 1997; Pérez-García et al., 2012; Thompson 2005; Villar & García, 1989). Indeed, the inaccessibility of cliffs, as well as the technical requirements necessary for an extended sampling, have limited the work of many ecologists to long distance observations and empirical deductions on plant/cliff relationships (e.g. Davis, 1951; Francini & Messeri, 1956).

Traditionally, botanists analysed extensively and successfully the structure and diversity of these communities at regional scale by using a phytosociological approach (Escudero & Pajarón, 1994; Terzi et al., 2018; a review on Eastern Mediterranean: Wagensommer, 2017). Despite the production of consistent classifications at a broad scale, this method was found to underestimate the high spatial and ecological heterogeneity at a fine-scale of vertical habitats. This underestimation is probably caused by the exclusive selection of the most significant ("ideal") plant assemblage for a given environment (Escudero, 1996). Furthermore, the traditional sampling design was often constrained by the accessible portion of a cliff. Moreover, sampling design and effort might not be fine enough to identify fine scale microtopographic changes and vegetation patches. Again, this is possibly caused by the obligated long-distance between the researcher and the plant assemblage. The number of relevès used in works on chasmophytic communities were often reduced (e.g. Romo diez, 2008), and/or the quadrat unit sampled large surfaces (e.g. Sciandrello & D'Agostino, 2014).

By contrast, some authors and local authorities focused only on the total distribution/conservation of target species by the use of visual and photographic techniques (CIEF, 2018; Mifsud, 2013; Milliken & Pendry, 2002). In particular, Goñi & Guzman (2006) proposed a list of inspection methodologies in order to overcome the difficulties of a visual census on cliffs. These authors suggested to estimate the area of occupancy and population size of chasmophytes by taking a series of perpendicular photos of the cliff from a certain distance. Afterward, they inferred the number of specimens with a ground measurement taken at the base of the cliff paired with a correction factor. However, the described technique (although useful in absence of any other data) did not have any validation measurement in support of such estimates. Furthermore, the fine scale spatial distribution of a chasmophyte on cliffs is often highly heterogeneous (as seen in case study 3).

The finest level of inspection involved quadrat sampling while on rappel (which is risky and requires specific skills). This technique used photographic or visual estimation of plant cover and/or species densities. Slope or (if any) other microtopographic variables (Kuntz & Larson, 2005) were likely estimated by sight. The latter technique represents the standard for conservation projects involving seedling and population surveys at fine scale (e.g. *Silene hifacensis*, CIEF, 2018). The technique was also used to analyse the anthropic pressure on climbing routes (Lorite et al. and citations therein, 2017; Nuzzo, 1995; 1996). By the way, this sampling methodology appears to be spatially limited: it precludes the accessibility of the cliff from the top due to the difficulty to fix a rope. Moreover, the surveying space is limited to the nearest areas of the descending line. It has also to be underlined the costs, times and technical difficulties of such method. It has been estimated that such sampling/seedling technique for a conservation project had to involve at least 6 teams of 2 specialised climbers for 10 days per year. The estimated costs in such case would exceed 6000 € for a total surveyed surface of 7200 m^2 (P. Ferrer, personal communication).

My proposed methodology applied the aerial photogrammetric techniques on inaccessible cliffs. Compared to other sampling/monitoring methods, it has the enormous advantage of producing massive amounts of data. Such amount of quantitative compositional and environmental data was extracted with a relatively inexpensive technique. Moreover, the spatial statistics were produced via a remote sensed 3D point cloud. Such data were continuously extended over an entire vertical façade, giving to the operator the possibility of afterward selecting an adequate quadrat size and sample number. It has also to be underlined that plot sampling obtained by transects along the cliff boundary (Chapter 2) were considerably less precise concerning microtopography. The 3D model approach represents then an advantage over the qualitative data gathered in the field from visual estimations (Chapter 2).

Moreover, any other survey methodology on cliffs was spatially limited to the visible portion of the cliff, notwithstanding the longer fieldwork required for data obtention.

Regarding the compositional data of entire cliff communities, the combined datasets analysed in case study 1 and case study 2 encountered almost 4000 individual specimens of 56 taxa in 3840 m^2. Even by overcoming the economic and technical unfeasibility of a comparable sample collection by rappel, the inaccessible terrain would have made such sampling more approximate and overall improbable to be carried out for all species.

Moreover, in the combined case study 3 and 4 were spotted almost 600 specimens of the narrow endemic species *P. limonifolia* and 562 of *E. sicula*. The total plotted space for the first species was 4430 m^2 and 2500 m^2 for *E. sicula*. Thus, it can be possible to estimate a species/flat surface density of 1.3 individuals/10 m^2 for *P. limonifolia* and 2.2 individuals/10 m^2 for *E. sicula*. It must also be underlined that the number of plots (and counted specimens) for the areas of case study 3 (Monte Cofano) was limited by the necessity to provide a comparable number of plots between zones. In fact, the extension of just one of the 4 surveyed areas (Cofano North) was 10 times (25500 m^2) the entire plot space where *E. sicula* abundance was measured.

Apart from the nature and amount of obtained data, another important advantage of the proposed methodology concerns the economic and logistic aspect. All the provided working examples with the exception of Cap D’Or Pessebret (case study 1) were the results of a single aerial survey operated by a single researcher. Flight times were possible to be estimated by multiplying the number of used batteries for an average of 20 min flight/battery. Thus, the maximum flight time was ≅ 80 minutes/area (mission), for an overall of ≅ 3 hours and 40 m of aerial surveying in case study 3. Theoretically, in order to just survey the same surface by using a sample collection by rappel, it would have been necessary 12 specialised operators, 80 working days and almost 50.000 €.

The environmental data retrieved from the 3D models confirmed also the importance of local micro-topography to discriminate among environments. The only previous application of such technique on plant ecology, to my knowledge, was provided by Niederheiser et al. (2018). In that case, the authors created a parallel photogrammetric protocol on alpine terrains characterised by screes and high roughness. Both our studies used a different series of 3D modelling tools in order to investigate a (mostly hidden) spatial variability. In the case of cliffs, the application of this new aerial + 3D methodology was especially useful in disclosing the importance of inclination gradients. Such gradients were neglected when a 2D approach was used for cliff surveys (e.g. Buonanno et al., 2017). The extreme values of the vertical gradient encountered in Pessebret were a good example of this. Only through the use of 3D it has been possible to sample severely prohibitive areas at 140° or more. Paired with an extended sampling effort, the ordination analyses discriminated smoothly the close relationship between *Sarcocapnos enneaphylla* and overhanging areas.

By definition, inclination shapes the difference between a cliff and the surrounding elements. As previously observed by Davis (1951), this variable is fundamental for differentiating various chasmophyte communities. Inclination is in fact directly correlated to the amount of soil that can be accumulated on a sloped surface. Other important factors influenced by inclinations are the incident solar radiation and the amount of rainfall that can reach the cliff surface. Inclination also influences local wind microclimatic conditions (Larson, 2000). From the biological point of view, inclination has a major influence on the seed dispersal and the reproductive traits of species. My results are in line with the hypothesis proposed by Davis and some of the results of Escudero (1996). Actually, inclination was always the major contributor governing the local assembly on cliffs in my analyses. The assemblages were clearly discriminated according to this variable in all the surveyed areas. As an example, the analysis of Pessebret revealed that inclination explained 11 times more variance than the combination of all the other significant microtopographic variables. In Cabo de San Antonio inclination explained 22% of the tested variance. Also, single exclusive chasmophytes (*E. sicula* and *P. limonifolia*) were found to have mainly a different sensitivity to inclination (32.7% of the variation).

Moreover, these results make oneself ask what truly differentiate a chasmophyte species. From the CAO analysis of Pessebret, inclination had an evident filtering role for cliff colonisation. Just 2 species were specialised to live exclusively on vertical/subvertical/overhanging surfaces: *Sarcocapnos enneaphylla* and *Pseudoscabiosa saxalis*. For these two true chasmophytes, vertical areas embody their unique suitable environment. A decreasing gradient of inclinations represent for them a barrier for colonisation, an environmental filter they could not cross. The opposite is valid for several other species. They showed a certain tolerance toward a growing degree of slope. For *Rhamnus oleoides* subsp. *rivasgodayana*, *Sonchus. tenerrimus* subsp. *dianae*, *Salvia Rosmarinus* and *Asteriscus maritimus* vertical zones constitute a permeable filter in their spatial distribution. The third category of species was the typical taxa of the Mediterranean dry grasslands such as *Gladiolus. Illyricus, Lapiedra martinezii*, *Stipa tenacissima* and *Brachypodium retusum* or shrubs and nanophanergams like *Chamaerops humilis* and *Osyris lanceolata*. For this group, the only suitable surfaces for colonisation were horizontal or sub-horizontal patches. A growing gradient of verticality for these species is correlated with a growing intensity of abiotic filtering. Encountering such species inside the boundaries of a cliff was demonstrated not to be associated with slope, but instead it is due to the patchiness of a cliff surface. In fact, a cliff face has inside several non-vertical patches made by small ledges and tasks of soil. These species are found only on areas with low inclinations, around on inside the perimeter of the cliff surface.

The evidence that gentle slopes retain soils was revealed by the linear relationship between inclination and plant cover. The increase of cover values with less steep areas can be correlated to the amount of soil. In this sense, the vegetation cover was the biotic response to a colonisable zone. The extraction of these data represented another innovation of this research. In fact, "cleaning" (or in this case detecting) vegetation on a digital surface model (DSM) was normally conducted by applying a filtering algorithm based on the heights. In the case of a 3D surface of a vertical space, the mean elevation was the prevalent spatial dimension, producing the algorithm failure. In order to overcome this problem, we used the excess green index (ExGI). This index, based on the RGB pixel colours was previously applied in other UAV based vegetation monitoring works (Larrinaga et al., 2019; Sonnentag et al., 2012). However, previous works used such index only on the orthorectified photomosaic and not on a 3D model.

It is known that patterns of species compositional data are determined by the simultaneous effect of biotic and abiotic constraints (Cadotte & Tucker, 2017; Paine, 1966; Patterson, 1980; Thompson et al., 1996).In the case of cliffs habitat, the effect of the biotic component is not only produced by the inclination filter. The proximity of cliff boundaries is in fact directly correlated with an increasing disturbance of the cliff assemblage. A close distance with a reachable area would increase the probability of encountering external destabilizing factors such grazing or fires (Davis, 1951; Lavergne et al., 2004; Thompson, 2005). Moreover, boundary areas are by definition ecotonal zones, characterised in the case of cliffs by a gradient of decreasing slope and soil accumulation. The consequence of the reduction of slope would produce a proportional increase in soil retention, which in turns permit the establishment of a higher number of non-specialised plants with large canopy (regression model of case study 1). This factor plays an important role in increasing a localized interspecific competition for light resources. Chasmophytes are known to have a slow growth (Davis, 1951); models of endemic/widespread congeners demonstrated the scarce interspecific competition of chasmophytes (Lavergne et al., 2004). Thus, a decrease in inclination and increase in disturbance and competition caused by the proximity of boundaries in the end reduce or exclude strict chasmophytes from the assemblage. In the analyses of variance of case study 1 and 2, however, the boundary proximity was significant but did not explain a great amount of the assemblage variation. By contrast, the boundary proximity factor was relevant when specific chasmophyte species were analysed singularly (case study 3). The low variance explained by the first two analyses can be ascribed to the number and position of the tasks of soil on the cliff surface. The intrinsic heterogeneity of micro-topography on cliffs made the factor low inclination-high amount of soil dispersed azonally along ledges and holes in the entire cliff surface. The consequence of that is reflected on a scarce significance of the value “position” of the plot in the cliff with respect to the boundaries. An example is provided by case study 2. The “cliff” space in the entire Cabo de San Antonio survey measured 18 m in height for CSAN and 17 m for CSAS. Both areas were characterized by a high number of intermediate areas with a minor slope inside the cliff space. The North side was surrounded by a Mediterranean shrubland (*Rosmarinion officinalis*), meanwhile the South was immerged in a continuum of rocky soil communities (*Rhamno borgiae-Teucrietum rivasii*) and xerophilous grasslands (*Teucrio pseudochamaepitys-Brachypodietum ramose/Hyparrhenion hirtae*). According to their relatively small heights, the increased proximity to boundaries was expected to show the ecotone between cliffs and the surrounding vegetations. And yet, the results of the ordination demonstrated that the distance from the edges did not constitute the most important variable for segregating entire plant assemblages.

A different picture is observed when only rare chasmophytes are studied (case study 3 and 4). The results of CAO ordinations showed that the proximity of cliff boundaries have an important effect on species densities. It is possible that both species were equally absent from the base because of a major probability of fire disturbance in the area. On the other hand, the analysis underlined a preferentiality of *E. sicula* for the crest of the cliff. This behaviour could be explained by a superior tolerance toward interspecific competition of the latter species.

All the analyses revealed also an absence of significance for the value fracturation on species composition. According to my initial hypothesis, fracturation could have contributed to the structure of cliff communities in relation with the soil amount, difficulty in affixing roots and ability to seed dispersal. The proposed semiquantitative ordered descriptor gave the maximum value (4) to plots with only rocky soils, which corresponded with minor inclinations. However, large portions of vertical cliffs appear as well severely fractured (value 3) but with scarce or absent vegetation. A negative result in this case hints for the fact that species richness and densities are not mainly connected to the amount of fractures on the cliff.

Regional orientation was confirmed to be together with inclination the most relevant factor in the assemblage structure (case study 2). By contrast, local orientation did not explain a great amount of variation. While we can deduct that changes in local orientation are weakly important for the entire assemblage, the result for single chasmophytes reveal the opposite. In case study 3, the “widespread” endemic *Pseudoscabiosa limonifolia* was almost limited to a single combination of inclination values and local/regional orientations. Conversely, the narrow endemic *Erica sicula*, whose distribution was limited to the area of Cofano, resulted “widespread” along almost all combination of subvertical/vertical inclinations and local/regional orientations. In the test of variance inclination expressed the highest portion of variation (32.7 %). It was local (and not regional) orientation that explained the second highest portion of variance in the dataset. Here, one species was characterised by a limited tolerance toward cliff microtopography. The ecological niche occupied by *P. limonifolia* seems to be completely overlaid by *E. sicula*. Thus, the latter species’ stenochory might be the result of biogeographic factors, rather than topo-climatic constraints.

Another example of the influence of local orientations on chasmophytes’ niche segregation was found in case study 4. Here a true widespread chasmophyte (*Lomelosia cretica*) struggled to colonise the portion of cliff with a North-Western local orientation, where instead *P. limonifolia* was prosperous. By contrast, *P. limonifolia* was always present in the studied surface but reduced its relative abundance in sectors with an East to Southeast local orientation. Knowing that *L. cretica* does not normally have a set of orientation preferences, I advocate a phenomenon of interspecific competition for the same niche. According to this hypothesis the widespread species was, against the initial expectations, less competitive than the narrow endemic relative.

In order to explain the results of case study 3 and 4, it is possible to advocate the effect of specialization in strict chasmophytes. In general, this evolutionary model sees in the adaptation and specialization to marginal habitats the reason, at a cost, of the loss of competitive ability in other ecological situations (Imbert et al, 2012). Microclimatic stability produced by a North to North-west local and regional orientations (see chapt. 1), entwined with geographical isolation favoured in *P. limonifolia* an adaptation and specialization to a topoclimatic habitat. For this reason, this species was locally more competitive than *L. cretica*, but lost as a consequence of its specialisation any ability to colonise cliffs with other local and regional orientations.

A final note regards the effectiveness of the choice of target species. *Lomelosia cretica* and *Pseudoscabiosa limonifolia* were easily spotted from photos taken at up to 8 metres from the surface. Overall, they performed surprisingly well thanks to their peculiar vegetative characteristics. *Erica sicula* was as well easily identifiable for the cushion dimension. However, the vegetative aspect of this species is photographically indistinguishable from the widespread congener *E. multiflora*. The latter species was as well commonly found in the area of Cofano, on cliffs and in the surrounding landscape. In this case, the survey took in consideration the disjunct flowering period of the two species. In fact, *Erica sicula* has a winter-spring blooming stage, whereas *E. multiflora* preferentially flowers in late summer-Autumn. Photo identification was then smoothly performed thanks to the phenological aspect of the species, which is covered in a dense layer of pink-white flowers. The last target species, *Silene hifacensis*, resulted very challenging. First, the species resulted indistinguishable from *Pseudoscabiosa saxatilis* or *Pallenis maritima* in the photographic set with a distance of 3-5 metres. It was only by using the closest sensor-to-cliff distance that it was possible to identify. Even with flights proximal to the cliff surface, in many cases it was only the flowering stage of *P. maritima* that permitted to identify plantules. Thus, in comparison with other model species *S. hifacensis* did not perform well as target species for a scenario 2 research. The reason is related to its morphological similarity to other species growing in the same areas where the plant lives.

Conclusions and future developments

The focus of this chapter was to show the pros and cons of analysing vegetation composition and its location properties by using a 3D modelling approach. The main goal was to set a methodology to collect from remote a large number of quantitative and accurate ecological data on cliffs in the context of the Mediterranean basin.

The division of the scope of research into a scenario 1 or 2 came to meet the necessities of different research applications on cliffs. The photographic detection of every individual plant confirmed the effectiveness of small drones to provide high level of image details from inaccessible areas. The quality and quantity of extracted data expanded the field of use of such instruments advocated by Cruzan et al. (2016) for fine scale ecological analyses. Moreover, through the use of digital plotting and 3D modelling it has been possible to link different hidden environmental variables with the spatial patterns exhibited by the assemblage. The heterogeneity of studied cliffs and the tools for remote sensed plot placement provided examples of the adaptability of such technique on many different field situations. Moreover, examples of scenario 2 surveys proved the usefulness of UAVs monitoring for target species and conservation issues. Overall, the provided flight and sampling protocols represent an improvement on the extant cliff surveying methods based on optic tools or rappelling (Graham & Knight, 2004; Goñi & Guzman, 2006) or the use of UAVs (Buonanno et al., 2017). In conclusion, the joint use of aerial photography with UAVs and 3D modelling was demonstrated to be a new, fundamental, tool to study the plant-microtopography relationship on cliffs.

Future developments in 3D modelling techniques and UAV technology will expand further the use and affordability of this protocol for a wider audience. My next improvements will include the effect of solar radiation and wind speed on cliff micro-zonation.

Bibliography

Baena, S., Moat, J., Whaley, O., & Boyd, D.S. (2017). Identifying species from the air: UAVs and the very high resolution challenge for plant conservation. PloS one, 12(11), e0188714. https://doi.org/10.1371/journal.pone.0188714

Bennie, J., Huntley, B., Wiltshire, A., Hill, M.O., Baxter, R. (2008). Slope, aspect and climate: spatially explicit and implicit models of topographic microclimate in chalk grassland. Ecol. Model. 216 (1), 47–59.

Bragazza, L. (2009). Conservation priority of Italian Alpine habitats: a floristic approach based on potential distribution of vascular plant species. Biodivers & Conservation 11:2823–2835

Bramer, I, Anderson, B.J., Bennie, J., Bladon, A.J., De Frenne, P., Hemming, D., Hill, R.A., Kearney, M.R., Körner, C, Korstjens, A.H., Lenoir, J., Maclean, I.M.D., Marsh, C.D., Morecroft, M.D., Ohlemüller R., Slater, H.D., Suggitt, A.J., Zellweger, F. & Gillingham, P.K. (2018). Advances in monitoring and modelling climate at ecologically relevant scales. In D. A. Bohan, A. J. Dumbrell, G. Woodward, & M. Jackson (Eds.). Advances in ecological research: Vol. 58. Next generation biomonitoring: part 1 (pp. 101-161).

Buonanno, M., Aronne, G., Strumia, S., Danzi, M., Santo, A., Santangelo, A. (2017). Cliff vegetation monitoring using close range photogrammetry and UAS: Technical issues and practical hints. In Proceedings of the Small Unmanned Aerial Systems for Environmental Research, 5th International Conference, Vila Real, Portugal, 28–30 June 2017.

Cadotte, M.W. & Tucker, C.M. (2017). Should Environmental Filtering be Abandoned? Trends in Ecology & Evolution, Volume 32, Issue 6

CIEF. (2018) INFORME TÉCNICO 03/2018 Plan de Recuperación de Silene hifacensis en la Comunitat Valenciana. Resultados de las Actuaciones de Conservación

Castroviejo, S. (coord. gen.) (1986-2012). Flora iberica 1-8, 10-15, 17-18, 21. Real Jardín Botánico, CSIC, Madrid.

Cruzan, M.B., Weinstein, B.G., Grasty, M.R., Kohrn, B.F., Hendrickson, E.C., Arredondo, T.M., & Thompson, P.G. (2016). Small unmanned aerial vehicles (micro-UAVs, drones) in plant ecology. Applications in plant sciences, 4(9), apps.1600041. https://doi.org/10.3732/apps.1600041

Davis, P. (1951). Cliff Vegetation in the Eastern Mediterranean. Journal of Ecology, 39(1), 63-93.

Dewez, T.J.B., Girardeau-Montaut, D., Allanic, C., Rohmer, J. (2016). FACETS : a Cloudcompare plugin to extract geological planes from unstructured 3d point clouds, Int. Arch. Photogramm. Remote Sens. Spatial Inf. Sci., XLI-B5, 799-804

Domínguez, F., Moreno, J.C. & Sáinz, H. (2003). Rarity and threat relationships in the conservation planning of Iberian flora. Biodiversity and Conservation, 12: 1861-1882.

Escudero, A. (1996). Community patterns on exposed cliffs in a Mediterranean calcareous mountain. Vegetatio 125, 99–110 https://doi.org/10.1007/BF00045208

Escudero, A., & Pajarón, S. (1994). Numerical Syntaxonomy of the Asplenietalia petrarchae in the Iberian Peninsula. Journal of Vegetation Science, 5(2), 205–214. Retrieved from www.jstor.org/stable/3236153

Forsmoo, J., Anderson, K., Macleod, C.J.A., Wilkinson, M.E., DeBell, L., Brazier, R.E. (2019). Structure from motion photogrammetry in ecology: Does the choice of software matter? Ecol. Evol. 9: 12964– 12979. https://doi.org/10.1002/ece3.5443

Francini, E. & Messeri, A. (1956). L'isola di Marettimo nell'arcipelago delle Egadi e la sua vegetazione. Webbia, 11:1, 607-846, doi: 10.1080/00837792.1956.10669652

García, M.B., Guzmán, D., Goñi, D. (2002). An evaluation of the status of five threatened plant species in the Pyrenees. Biol. Conservation 103:151–161

García, M.B., Domingo, D., Pizarro, M., Font, X., Gómez, D., Ehrlén, J. (2020). Rocky habitats as microclimatic refuges for biodiversity. A close-up thermal approach. Environmental and Experimental Botany, Volume 170

Gianguzzi, L., La Mantia, A., Ottonello, D., Romano, S. (2005). La flora vascolare della Riserva naturale di Monte Cofano (Sicilia occidentale). Naturalista Sicil. 29 (3-4): 107-152.

Goñi, D., Garcia, M.B., Guzman, D. (2006). Métodos para el censo y seguimiento de plantas rupicolas amenazadas. Pirineos, 161:33-58.

Graham, L., Knight, R.L. (2004). Multi-scale comparisons of cliff vegetation in Colorado. Plant Ecology 170, 223–234. https://doi.org/10.1023/B:VEGE.0000021675.32902.7f

Imbert, E., Youssef, S., Carbonell, D., Baumel, A. (2012). Do endemic species always have a low competitive ability? A test for two Mediterranean plant species under controlled conditions. Journal of Plant Ecology, 5: 305-312.

Kuntz, K.L. & Larson, D.W. (2005). The relative influence of microhabitat constraints and rock climbing disturbance to vegetation on Ontario’s Niagara Escarpment. Cliff Ecology Research Group, Dept of Integrative Biology, University of Guelph, Ontario, Canada.

Larrinaga, A.R., Brotons, L. (2019). Greenness Indices from a low-cost UAV imagery as tools for monitoring post-fire forest recovery. Drones 3, 6.

Larson, D.W., Matthes, U., & Kelly, P.E. (2000). Cliff Ecology: Pattern and Process in Cliff Ecosystems.

Lavergne, S., Thompson, J.D., Garnier, E. and Debussche, M. (2004). The biology and ecology of narrow endemic and widespread plants: a comparative study of trait variation in 20 congeneric pairs. Oikos, 107: 505-518. doi:10.1111/j.0030-1299.2004.13423.x

Legendre, P., Oksanen, J. & ter Braak, C.J.F. (2011). Testing the significance of canonical axes in redundancy analysis. Methods in Ecology and Evolution 2, 269–277.

Lorite, J., Serrano, F., Lorenzo, A., Cañadas, E.M., Ballesteros, M., Peñas, J. (2017). Rock climbing alters plant species composition, cover, and richness in Mediterranean limestone cliffs. PLoS ONE 12(8): e0182414. https://doi.org/10.1371/journal.pone.0182414

Médail, F. & Quézel, P. (1997). Hot-Spots Analysis for conservation of Plant Biodiversity in the Mediterranean Basin. Annals of the Missouri Botanical Garden, 84, 112-127. http://dx.doi.org/10.2307/2399957

Médail, F. & Verlaque, R. (1997). Ecological characteristics and rarity of endemic plants from Southeast France and Corsica: implications for biodiversity conservation. Biol. Conserv., 80: 269-281.

Mifsud, S. (2013). Distribution of some rare or endemic chasmophytic and rupestral species growing along the coastal cliffs of the Maltese Islands. Webbia: Journal of Plant Taxonomy and Geography, 68:1, 35-50, DOI: 10.1080/00837792.2013.807451

Milliken, W., & Pendry, C. (2002). Maritime cliff vegetation of Flamborough Head.

Niederheiser, R., Rutzinger, M., Bremer, M., Wichmann, V. (2018). Dense image matching of terrestrial imagery for deriving high-resolution topographic properties of vegetation locations in alpine terrain. International Journal of Applied Earth Observation and Geoinformation. 66. 146 - 158. 10.1016/j.jag.2017.11.011.

Nuzzo, V. A. (1995). Effects of Rock Climbing on Cliff Goldenrod (Solidago sciaphila Steele) in Northwest Illinois. American Midland Naturalist. 133:229-241.

Nuzzo, V. A. (1996). Structure of cliff vegetation on exposed cliffs and the effect of rock climbing. Canadian Journal of Botany. 74:607-617.

Oksanen, J.A. (2019). Design decisions and implementation details in vegan.

Paine, R.T. (1966). Food web complexity and species diversity. American Naturalist 100, 65–75

Papadopoulou, A., & Knowles, L.L. (2016). Toward a paradigm shift in comparative phylogeography driven by trait-based hypotheses. Proceedings of the National Academy of Sciences of the United States of America, 113 29, 8018-24 .

Patterson, B.D. (1980). Montane mammalian biogeography in New Mexico. The Southwestern Naturalist 25, 33–40

Peres-Neto, P., Legendre, P., Dray, S. & Borcard, D. (2006). Variation partitioning of species data matrices: estimation and comparison of fractions. Ecology 87, 2614–2625.

Pérez-García, F.J., Medina-Cazorla, J.M., Martínez-Hernández, F., Garrido-Becerra, J.A., Mendoza-Fernández, A.J., Salmerón-Sánchez, E., Mota, J.F. (2012). Iberian Baetic endemic flora and the implications for a conservation policy. Ann Bot Fenn 49:43–54

Pignatti, S. (1982). Flora d'Italia. Edagricole, Bologna.

R Core Team (2019). R: A language and environment for statistical computing. R Foundation for Statistical Computing, Vienna, Austria. URL http://www.R-project.org/.

R Studio Team (2018). RStudio: Integrated Development for R. RStudio, Inc., Boston, MA URL http://www.rstudio.com/

Raimondo, F.M., Mazzola, P., Schicchi, R. (2001). Rapporti fitogeografico fra i promontori carbonatici della costa tirrenica della Sicilia. - Biogeographia 22: 65-77

Rivas-Martínez, S., Penas, A., Díaz, T. (2004). Biogeographic Map of Europe.

Romo Diez, A.M. (2008). Contribution to the knowledge of rupicolous plant communities in the limestone areas of North Africa. Collectanea Botanica.. 27. 10.3989/collectbot.2008.v27.6.

Sanz de Galdeano, C. & Ruiz Cruz, M.D. (2016). Late Palaeozoic to Triassic formations unconformably deposited over the Ronda peridotites (Betic Cordilleras): Evidence for their Variscan time of crustal emplacement. Estudios Geológicos 72(1): e043. http://dx.doi.org/10.3989/egeol.42046.368.

Sciandrello, S. & D'Agostino, S. (2014). Distribution patterns and floristic analysis of the Colymbada Tauromenitana (Guss.) Holub populations in Sicily (Italy). Acta Botanica Croatica. 73. 385–400. 10.2478/botcro-2014-0006.

Sonnentag, O., Hufkens, K., Teshera-Sterne, C., Young, A.M., Friedl, M., Braswell, B.H., Milliman, T., O'Keefe, J., Richardson, A.D. (2012). Digital repeat photography for phenological research in forest ecosystems. Agric. For. Meteorol. 152, 159–177.

Terzi, M., Jasprica, N., Caković, D., Di Pietro, R. (2018). Revision of the central Mediterranean xerothermic cliff vegetation. Applied Vegetation Science. 21. 10.1111/avsc.12386.

Thompson, J.D. (2005). Plant evolution in the Mediterranean. Oxford University Press, Oxford

Thomson, J.D., Weiblen, G., Thomson, B.A., Alfaro, S. and Legendre, P. (1996). Untangling multiple factors in spatial distributions: lilies, gophers, and rocks. Ecology 77, 1698–1715

Villar, L. & García, M.B. (1989). Vers une banque de données des plantes vasculaires endémiques des Pyrenées. Acta Biol. Mont., IX: 261-274.

Wagensommer, R.P. (2017). Phytosociological investigation on the thermo-chasmophilous vegetation of the Eastern Mediterranean territories. PhD thesis of Università degli Studi di Catania.

Wiens, J.A. (1989). Spatial scaling in ecology. Funct. Ecol. 3, 385–397

Woebbecke, D.M., Meyer, G.E., Von Bargen, K., Mortensen, D.A. Color indices for weed identification under various soil, residue, and lighting conditions. Trans. Am. Soc. Agric. Eng. 1995, 38, 259–269.

Yee, T.W. (2006) a. Constrained additive ordination. – Ecology 87: 203–213.

Yee, T.W. (2006) b. VGAM Family Functions for Reduced-Rank Regression and Constrained Ordination. Beta version 0.6-5. http://www.stat.auckland.ac.nz/~yee/VGAM/doc/rrvglm. pdf.

Yee, T.W. (2015). Vector Generalized Linear and Additive Models. Springer Series in Statistics, DOI 10.1007/978-1-4939-2818-7 7

Yee, T.W. (2019). VGAM: Vector Generalized Linear and Additive Models. R package version 1.1-2. URL https://CRAN.R-project.org/package=VGAM

Chapter 4: Distribution, ecology, conservation status and phylogeography of *Pseudoscabiosa limonifolia*, a paleo-endemic chasmophytic species from Sicily (It).

Introduction

The species *Pseudoscabiosa limonifolia* (VAHL) DEVESA (Fig 4.1) is a North-western Sicilian endemic occurring, according to literature (Gianguzzi & La Mantia, 2008; Lojacono, 1909; Raimondo, 2011; Romano et al., 1994), exclusively on cliffs of four isolated zones.

Fig 4.1. *Pseudoscabiosa limonifolia*. Up left: topography of species habitat. Capo Gallo (Palermo), Italy. Down left: inflorescence with a pollinator of the Apoidea superfamily. Marettimo (Trapani), Italy; July 2017. Right: a flowering plant in Marettimo at the end of June 2018. Scale bar unit: 1 cm.

It is a member of a Mediterranean central-western genus of narrow endemic plants firstly described by Devesa (1984) and corresponds to *Scabiosa* sect. *Asterothrix* FONT QUER as treated by Verlaque (1986). The genus pertains to the family Caprifoliaceae (APG IV, 2016) and subfamily Dipsacaceae. Besides *P. limonifolia*, the genus includes two more species: *Pseudoscabiosa saxatilis* (CAV.) DEVESA, endemic to the Valencian Community (Spain) and *Pseudoscabiosa grosii* (VAHL) DEVESA, growing in Andalusia (Spain) and northern Morocco (Fig 4.3). The populations of *P. grosii* in Morocco were previously classified as *Pseudoscabiosa africana* (FONT QUER) ROMO, CIRJANO, PERIS & STÜBING (Romo et al., 1997). However, this classification was found to be not valid.

Fig 4.2. Fruits of *P. limonifolia.*

The three chasmophytic endemic species, members of a well cladistically-supported genus (Avino & al., 2009; Caputo et al., 2004; Carlson et al., 2009), show the same chromosome number (2n = 10; Mayer and Ehrendorfer, 1999) and a similar ecology. Moreover, all the species share a similar morphology of the dispersion units (cypsela; Fig 4.2), with some characters helping the diaspore to be carried by the wind (pterochorous or pogonochorous dispersal syndromes) (Caputo et al 2004; Mayer and Ehrendorfer 1999).

All the species live in similar microclimatic conditions on dolomitic cliffs influenced by the sea proximity. Moreover, the portion of cliffs above the altitude of 400 m are frequently covered by adiabatic mists. Overall, the genus is found inside the Thermo- and Meso-mediterranean bioclimatic belts (see also chapter 1, meteorological stations CSAN and COFN) (Fig 4.3).

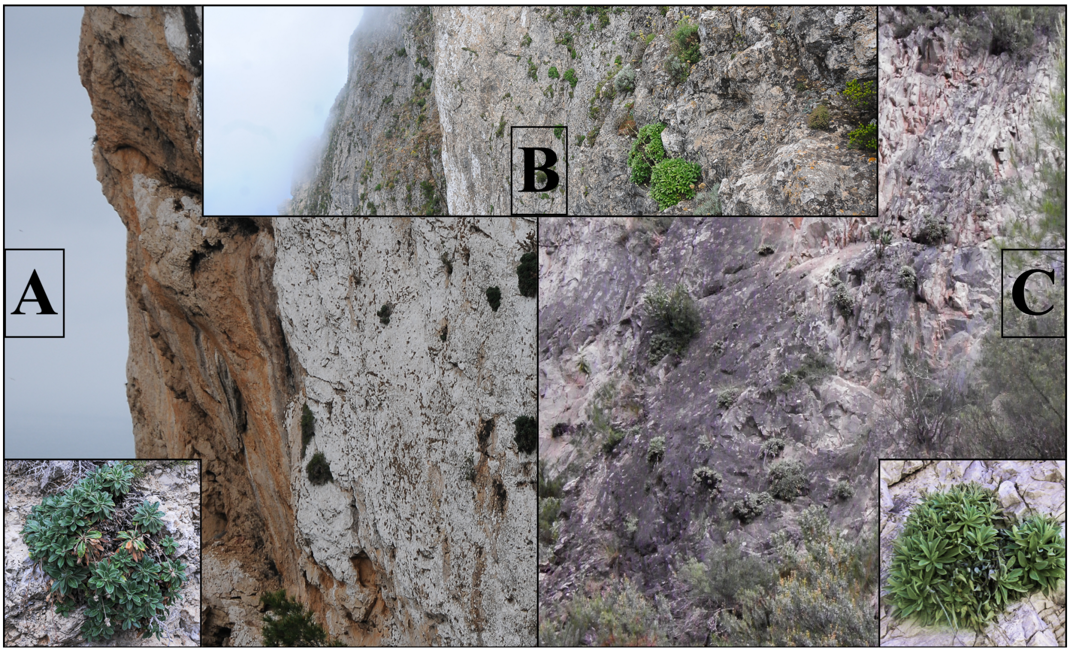

Fig. 4.3. Similar topography of cliff habitat in the genus *Pseudoscabiosa*. Fig 4.3 A: a population of *P. saxatilis* in Cap D'Or (Alicante), Spain. Fig 4.3 B: *P. limonifolia* on the cliffs of Marettimo (Trapani), Italy. Fig 4.3 C: Photo of P. Ferrer. *P. grosii* in its habitat in Otivar (Granada), Spain.

While the narrow, exclusively chasmophytic ecology is shared among the three species, both *Pseudoscabiosa saxatilis* and *Pseudoscabiosa grosii* appear to have a more pronounced hair presence on both leaf surfaces and a wider distribution (data retrieved from the Anthos database, available at www.anthos.es). The denser amount of leaf trichomes, probably, allowed the spanish/moroccan species to be more resistant to evapotranspiration losses and thus permitted their colonisation of cliffs 20-30 km far from the sea.

Field observations of the populations of *P. saxalitis* on cliffs in Eastern Spain, revealed that the species is abundant between 50 and 800 m (the altitudinal limit selected for this research). This species is distributed on cliffs with any regional orientation besides South. Only occasionally, few individuals were observed growing on South-oriented cliffs, but in the close proximity of an East or West topographic discontinuity [e.g. Montgò (Alicante), Spain]. Moreover, the observations carried out in chapter 2 and 3 demonstrated that, contrarily to *P. limonifolia*, changes in local orientation did not cause the exclusion of *P. saxatilis* from a cliff assemblage. A common ecological characteristic of *P. saxatilis* and *P. limonifolia* is their abundancy on cliff discontinuities and edges, where winds tend to accelerate due to a change in the direction of cliff curvature.

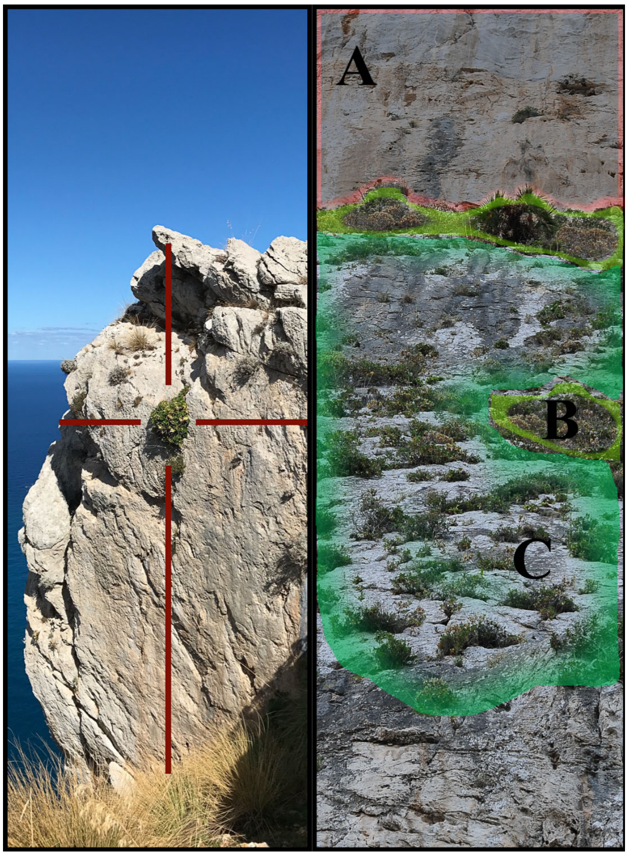

Fig. 4.4. Left: individuals of *P. limonifolia* are commonly found at a certain distance from the cliff boundaries. Right: patches of the cliff surface with overhanging (A) or low inclinations (B) are not suitable for colonisation. Only areas between 70° and 90° (C) are populated by this species. Capo Gallo (Palermo), Italy.

Despite these similarities, as demonstrated in chapt. 3, *P. limonifolia* is more sensitive to microtopography. The species was in fact encountered only in the portion of cliffs with inclination between 70° to 90° (Fig 4.4, right). Moreover, individuals of this species were found preferentially far from the cliff ridge and always at a certain distance from the cliff base (Fig. 4.4, left). These ecological requirements make this species the most stenochorous of the genus, reducing its populations to grow on isolated groups in the Northwestern sea cliffs of Sicily.

Various authors noticed the phytogeographic and ecologic peculiarities of *Pseudoscabiosa limonifolia* (Brullo et al., 1995; Francini & Messeri, 1956; Gianguzzi & La Mantia, 2008; Guarino & Pasta, 2018). Despite the rarity of this species, no previous work studied in detail its fine scale distribution and ecology.

At the present day there is not an official IUCN assessment for *P. limonifolia*. The species was historically categorised as Rare in the 1997 IUCN Red List of threatened plants (Gillet & Walter, 1997) and was inserted in the regional red list of endangered vascular plants in Sicily as Endangered (Raimondo et al., 2011). However, both studies had an important shortcoming, not mentioning the IUCN criteria for categorization.

The disjunct distribution of this vicariant genus of strict chasmophytes, its systematic isolation and specialization to the cliff habitat made it a perfect case study for investigating the genetic structure of chasmophytes in the Mediterranean.

In detail, the goals of the present investigation were: 1) to assess the genetic variability among all the extant populations of *P. limonifolia* through comparing the degree of cpDNA variation; 2) to compare this variability to that of its 2 closely related species; 3) to evaluate its colonisation patterns in Sicily, also considering its diaspore anemochorous dispersal syndrome. Furthermore, a new IUCN conservation assessment for *P. limonifolia* has been produced. Through an extensive fine scale mapping, it was possible 1) to estimate the actual species distribution; 2) to characterize the narrow ecological requirements of this endemic obligated chasmophyte; and 3) to identify the threats that could endanger its survival.

Materials and methods

Sample design and species collection

Sample collection for the acquisition of genetic material and species distribution assessment were carried out between 2016 and 2019.

A regional survey was first performed. Topographic units with potentially suitable habitat for the species were selected by using fine scale maps, geomorphological elaborations, and with a distance from the sea not higher than 10 km. Field surveys were carried out in the

North-western Sicilian coast. All the topographic units with N to W-facing cliffs were explored in the range 200-800 m a.s.l. The survey extended in the main island from the Capo Zafferano massif (PA; 38° 6' 40" N, 13° 32' 8" E) to the mountain of Erice (TP; 38° 2' 19" N, 12° 35' 12" E), an area spanning approximately 84 km. The investigated area corresponds to the zone denominated "coastal cliff belt" in Fig II The known distribution of *P. limonifolia* was also verified in the localities for which herbarium specimens (in the herbaria of PAL, Università degli Studi di Palermo; CAT, Università di Catania; MPU, Universitè de Montpelier; MA, CSIC-Real Jardin Botanico de Madrid) and published literature (Gianguzzi & La Mantia, 2008; Lojacono, 1909; Raimondo, 2011; Romano et al., 1994) were available.

A more specifically targeted field survey was conducted in all the areas where the species was encountered during the regional survey and in the island of Marettimo (Trapani). During the specific survey all the cliff systems were accurately inspected using transects and observation points. As a consequence of the narrow ecological niche of the species, systematic surveys were performed only on cliffs showing East, North and West orientation. Nevertheless, also South-facing cliffs were inspected, but not systematically.

Field surveys were carried out along two independent continuous transects following the cliff profile at its upper and lower edges along the entire topographic unit. If the cliff system appeared to be completely inaccessible from its top or its bottom, observation points were set in the closest suitable area opposite to the cliff wall (Goñi et al., 2006). In fact, for some areas (Fig 4.5) local conditions prevented the possibility of continuous transects due to security reasons.

All transects were recorded using a GPS device and the WGS84 ellipsoid. Every 50 to 100 m, a waypoint marker with species presence/absence was recorded. Moreover, each marker contained a photographic note to allow future tracking of the species presence on contiguous grid units in the landscape. All visual observations were carried out observing the vertical cliff surface using a 10 x 50 binocular (Celestron). GPS points were quality-checked using the software QGIS version 3.6 (2019). Each observation point was subsequently classified in one or more markers of species presence/absence. This operation was performed using field notes, sketches and photos.

Additional GPS points of species presence were positioned in QGIS at a subsequent time using close-range aerial photographs taken with a small UAV (for details see chapt. 3). The total number of GPS points that marked species presence were plotted on a 20 x 20 m grid. The plain surface occupied by the grid tiles marked with presence was calculated. Subsequently, the vertical extent which characterised the species habitat was considered. For this purpose, the tiles were projected on terrain with a Digital Elevation Model (DEM) 2 x 2 m of the areas. This operation permitted to calculate the real terrain surface occupied by the species.

Fig 4.5. Vertical sea cliffs in the West sector of the island of Marettimo (Trapani), Italy. Continuous transects were substituted with observation points by boat and from the ridges.

Plant sampling and DNA extraction

Samples of *Pseudoscabiosa limonifolia* were collected from all known populations, to cover the entire species distribution range. For each sample, a GPS point (WGS84) was recorded along with its ellipsoidal altitude (e.g. Fig 4.6, right). Six to thirty individuals were collected per each population according to the population extent and to the variability of landscape conditions.

Each sample was collected with the aid of a tree pruner (Fig 4.6, left). Sampled specimens were separated by a minimum spatial distance of 100 m in order to enhance the likelihood of gathering genetically unrelated individuals. Distance from individuals was considered for both the horizontal and vertical dimension. Sampling for the collection of plant material followed the same principles used for mapping the species distribution: it was stratified along two horizontal transects on two different altitudinal layers, the base and crest of the cliff systems. Labels of populations, their geographic location, and extent and number of individuals sampled per population are given in Table 4.1 and 4.2. Geographic position of each sample is shown in the fine scale distribution maps (Fig 4.9-11).

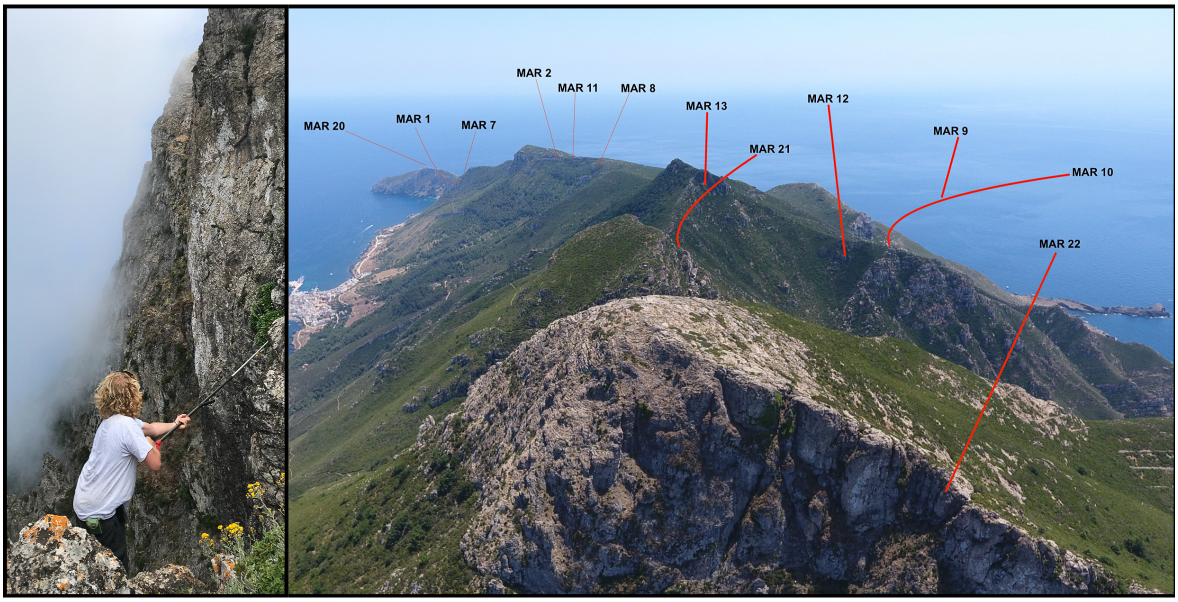

Fig. 4.6. Left: the collection of a ramet with the aid of a tree pruner. Right: georeferenced samples in the fragmented cliff landscape. Island of Marettimo (Trapani), Italy.

Fresh adult leaves from mature individuals were collected, dried in silica gel on site and stored at room temperature until being processed. Total genomic DNA was isolated and purified following the protocol given by Doyle et al. (1987) with minor modifications. The extraction buffer consisted of 4% CTAB (hexadecyltrimethylammonium bromide), 1.4 M NaCl, 20mM EDTA, 100mM Tris-HCl pH 8, 2% PVP (polyvinylpyrrolidone), and 0.2% 2-mercaptoethanol. After the first centrifugation to separate the aqueous phase, 700 µl of 100% isopropanol were added to the samples which were then stored at -80°C for 3-12 hours. After a second centrifugation to help precipitating the nucleic acid pellet, isopropanol was poured off and substituted with 200 µl of wash buffer (70% ethanol and 10mM sodium acetate). After a third centrifugation, wash buffer was poured off and pellets were allowed to air dry at 37°C to be then resuspended in 30 µl ultrapure water. DNA quality was checked by electrophoresis in 1% agarose gels before amplification.

DNA amplification, sequencing and alignment

The universal primers a and b designed by Taberlet et al. (1991) were used to amplify the *trnT-trnL* intergenic spacer of the chloroplast DNA. PCR reactions were performed in 50µl, containing approximately 50-100 ng of genomic DNA, 3 units of Taq polymerase (NETZYME™ DNA Polymerase, EPICA S.L., Valencia, Spain), 0.6 µM of each primer (10 µM), 0.2 mM dNTPs, and 28 µl of ultrapure water. Thermal cycling started with a denaturation step at 94°C lasting 2 min, followed by 30-35 cycles each comprising 50 s denaturation at 94°C, 50 s annealing at 53°C, 1.5 min elongation at 72°C, and ended with a final elongation cycle of 3 min at 72°C. PCR products were separated by electrophoresis on horizontal 2% agarose gels in 1× TAE buffer and stained with ethidium bromide. PCR products were purified using the High Pure PCR Product Purification Kit (Roche Diagnostics, Barcelona, Spain) according to the manufacturer's instructions, and sequenced with an ABI 3100 Genetic Analyser using the ABI BigDye Terminator Cycle Sequencing Ready Reaction Kit (Applied Biosystems, Foster City, California, U.S.A.). The intergenic spacer proved difficult to sequence at the 5′ end, due to a long poly-A region. Thus, samples were mostly sequenced in forward direction. Sequences were checked and edited in 4PEAKS software (available at https://nucleobytes.com/4peaks/index.html), and aligned using the software MEGA (Kumar et al., 2018).

Phylogenetic and genetic diversity analysis

The method of statistical parsimony (Templeton & al., 1992) was used to construct a haplotype network from the *trnT-trnL* haplotypes using the TCS software (Clement et al., 2000). Insertions and deletions were treated as a fifth character state and coded as a single mutational event (Simmons & al., 2001). Root probabilities under neutral coalescent theory was also calculated. (Castelloe and Templeton, 1994; Crandall et al., 1994).

Parameters of genetic diversity and differentiation were estimated for all the 3 *Pseudoscabiosa* species following the statistical methods described by Pons & Petit (1995, 1996), using the programs Haplodiv and Permut (https://www6.bordeauxaquitaine.inra.fr/biogeco/Production-scientifique/Logiciels/Contrib-Permut/Permut).

Population genetic parameters were computed both by taking into account the distance between haplotypes (ordered alleles; v_S, v_T, N_{ST}) and by ignoring them (unordered alleles; h_S, h_T,G_{ST}).

To test for the presence of a phylogeographic structure in the cpDNA data set, N_{ST} and G_{ST} values were compared with those obtained after 1,000 random permutations using the U-statistics (Burban et al. 1999; Pons and Petit 1996). According to Pons and Petit (1996), $N_{ST} > G_{ST}$ indicates that similar haplotypes are found together in the same population more often than are randomly chosen haplotypes, suggesting that the populations are phylogeographically structured. The geographical structure of genetic variation was assessed by the analysis of molecular variance (AMOVA, Excoffier & al., 1992) using Arlequin (Excoffier & al., 2005) under different a priori grouping conditions shown in Table 4.6 using 10,000 permutations.

Environmental and spatial data, conservation assessments

The threats to *P. limonifolia* were determined from field observations and categorized following the IUCN threats classification scheme (IUCN, 2012b). The species habitat was classified according to the European Red List of Habitats (2016) and the vegetation type according to the European Habitat Directive (DIR 92/43/EEC). Following the IUCN criteria (2012a), a grid of 2 x 2 km was used for assessing the Area Of Occupancy (AOO), defined as the area within the extent of occurrence of the species. According to the same document guidelines, the Extent Of Occurrence (EOO) for the species was calculated and species locations annoted. The sea surface was excluded from the total assessed EOO territory under the IUCN Red List Categories and Criteria statement that EOO may exclude "discontinuities or disjunctions within the overall distribution of the taxa". However, a second EOO assessment, labelled EOO_{SEA} considered as well the sea surface.

Wind direction and speed were calculated for 15 offshore 12.5 x 12.5 km areas along the Sicilian coasts. Wind data were elaborated from monthly averaged means of satellite datasets QuikSCAT Level 2B for a period of 10 years (Fore et al., 2013).

Results

Species distribution and IUCN status

Toponym (Italy)	Label	Code	Coordinates EPSG 4326	N	H	Geographic range (m)	Altitude min max range (m)	Nearest population (Km)
Capo Gallo (Palermo)	Gallo	CGE	38,2134 N 13,2977 E	24	A(24)	2666,73	76,63 554,74 478,11	MANO – 3,92
Pizzo Manolfo (Palermo)✶	Manolfo	MANO	38,1871 N 13,2679 E	10	A(10)	531,6	280,92 460,04 179,12	CGE – 3,92
Monte Pecoraro (Palermo)	Pecoraro	PEC	38,1629 N 13,1279 E	13	B(13)	1684,47	318,31 833,77 515,46	MANO – 12,56
Monte Monaco (Trapani)✶	Monaco	MON	38,1662 N 12,7576 E	6	C(6)	128,65	300,62 433,49 132,87	COF – 10,26
Monte Cofano (Trapani)	Cofano	COF	38,1056 N 12,6692 E	8	C(8)	719,57	94,15 452,92 358,77	MON – 10,26
Isola di Marettimo (Trapani)	Marettimo	MAR	37,9717 N 12,0563 E	30	B(30)	6391,52	74,8 605,9 531,1	COF – 55,81
TOT				91	3	112,15 Km	759 m	

Table 4.1. Collection details for the 6 populations of *Pseudoscabiosa limonifolia* sampled for this study in North-West Sicily. ✶ = newly discovered localities during this study. N = Sample size. H = haplotypes. Geographic range and altitude refer to the sampled individuals. Nearest population refers to the plain distance between population centroids.

The presence of *P. limonifolia* was confirmed in all the four already known sites (Marettimo, Pecoraro, Cofano and Gallo). During this work, two new populations were found (Monaco, Manolfo). Samples of flowering plants from the new populations were collected and stored at the herbarium of Botanic Garden of Valencia (Spain) under the accession numbers VAL242611 and VAL242612.

The overall real surface occupied by the species was 6.87 km^2 (Fig 4.7). This measurement took in consideration the vertical nature of the species habitat in a 20 x 20 m grid. Considering only the plain surface, the species was encountered on an overall 3.1 km^2. The largest population was found in Marettimo (4.16 km^2, vertical surface. 60% of the total), followed by Pecoraro (1.41 km^2) and Gallo (1.06 km^2). The new populations of Monaco and Manolfo are the least extended populations in vertical surface (0.03 km^2 and 0.05 km^2 respectively).

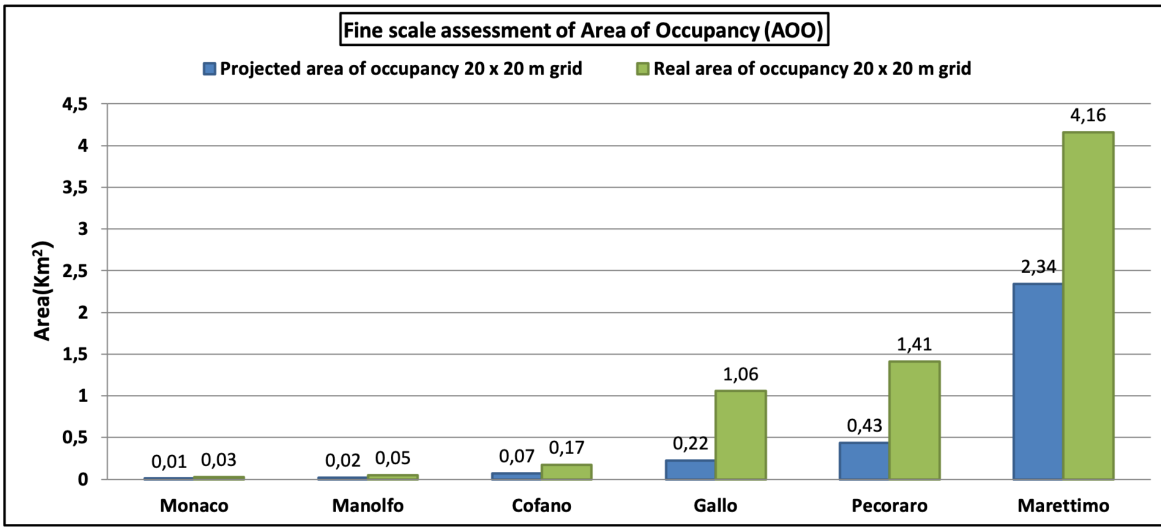

Fig. 4.7. Barplot of the geographic extent of *Pseudoscabiosa limonifolia* obtained from a 20 x 20 m grid. Projected area of occupancy (blue) refers to the plain tiles occupied by the species. Real area of occupancy instead takes in consideration the vertical component of the tiles, calculating also the vertical extent of terrain occupied by each tile.

All populations were considered geographically isolated units, with large interruptions of kilometres of unsuitable habitat dividing them. Hence, in the IUCN terminology, the population resulted naturally fragmented and each subpopulation was geographically isolated from the others. The minimum distance between populations was recorded between Gallo and Manolfo (3.92 km), whereas individuals on the island of Marettimo were the most distant from the closest population (Cofano, 55.8 km) (Table 4.1). The geographic extent of the species distribution, slope characteristics and plant sampling for the phylogeographic analysis are shown in Fig 4.9-11.

All populations grew on coastal cliffs, with a maximum distance of 2-3 km from the sea shoreline. Not all coastal mountainous areas with a suitable habitat were colonised by the species. In fact, *P. limonifolia* was encountered only on the topographic units that exceeded the maximum altitude of 400 m a.s.l. The species grew in the range 75 m to 834 m a.s.l., although population density was maximum at 450-500 m (Table 4.1).

Table 4.3. Optimal environmental conditions for *P. limonifolia*.

Inclination	≥ 70° and ≤ 90°
Regional orientation	N; W
Local orientation	NNE to N to NW
Position on cliff	Central, far from boundaries
Altitude	400 to 500 m a.s.l.

Locally, *P. limonifolia* was observed to grow only in discrete populations on the shaded portions of the cliffs (Fig. 4.1). Concerning plant-microtopography relationships, visual

Table 4.2. Date and details of used DNA from *Pseudoscabiosa grosii* and *Pseudoscabiosa saxatilis*.

N = Sample size. H = haplotypes.

Toponym (Spain)	**Label**	**Code**	**Coordinates EPSG 4326**	**N**	**H**
Pseudoscabiosa grosii (Font Quer) Devesa					
Granada, Cerro de la Cruz, 05.2014	Otivar	OTI	36°52'20"N 3°44'24.53" W	5	D(5)
Granada, Peña Escrita. 05.2014	Almuñecar	ALM	36°49'N 3°45'27.37" W	10	D(10)
Pseudoscabiosa saxatilis (Cav.) Devesa					
Alicante, Penyal de Ifac. 04.2014	Ifac	IFA	38°38'10"N 0° 4'26.51"E	5	E(5)
Alicante, Morro de Toix. 04.2014	Toix	TOI	38°37'57"N 0° 1'16.14"E	8	H(8)
Valencia, Tavernes de la Valldigna. 04.2014	Valldigna	TVA	39° 4'56.10"N 0°16'16.98" W	8	L(3) I(5)
Alicante, Cabo de San Antonio. 04.2014	Cap de San Antoni	CSA	38°48'15"N 0°11'41.17" E	7	G(7)
Alicante, Cap d'Or. 04.2014	Cap d'Or	CAD	38°40'55"N 0° 9'0.15"E	10	F(9) H(1)
Alicante, Aitana. 05.2014	Aitana	AIT	38°38'59"N 0°15'18.72" W	6	E(6)

surveys confirmed the narrow ecological niche of the species, that was restricted to a set of environmental conditions both locally and at regional scale (Table 4.3. See also chap. 3). The optimal average slope conditions for *P. limonifolia* were 80° ± 10°. Visual observations on multiple populations confirmed the results presented in chapt 3 about the unimodal species response curve with respect to inclination, with the lowest threshold for species occurrence observed at 65° slope. Like every other species in Sicily which gets to colonising cliffs, *P. limonifolia* was absent above the upper limit of 90-95° slope.

All observations confirmed the absence from South-facing cliffs. By far, the preferred set of orientation conditions that supported the species was found on a fraction of the total cliff surface, with a local and regional North to North-west exposure. The species was also encountered on other regional orientations such as East and West (Cofano, Marettimo), but always on locally North-oriented cliff walls.

Individuals were often isolated and sparsely located on the cliff surface, with a distance ranging between 4 m and 8 m from each other. At Gallo, Pecoraro and Marettimo (the largest populations) the species showed a patched distribution on continuous vertical environments due to microtopographic changes in the local cliff aspect (Fig. 4.6, 4.8).

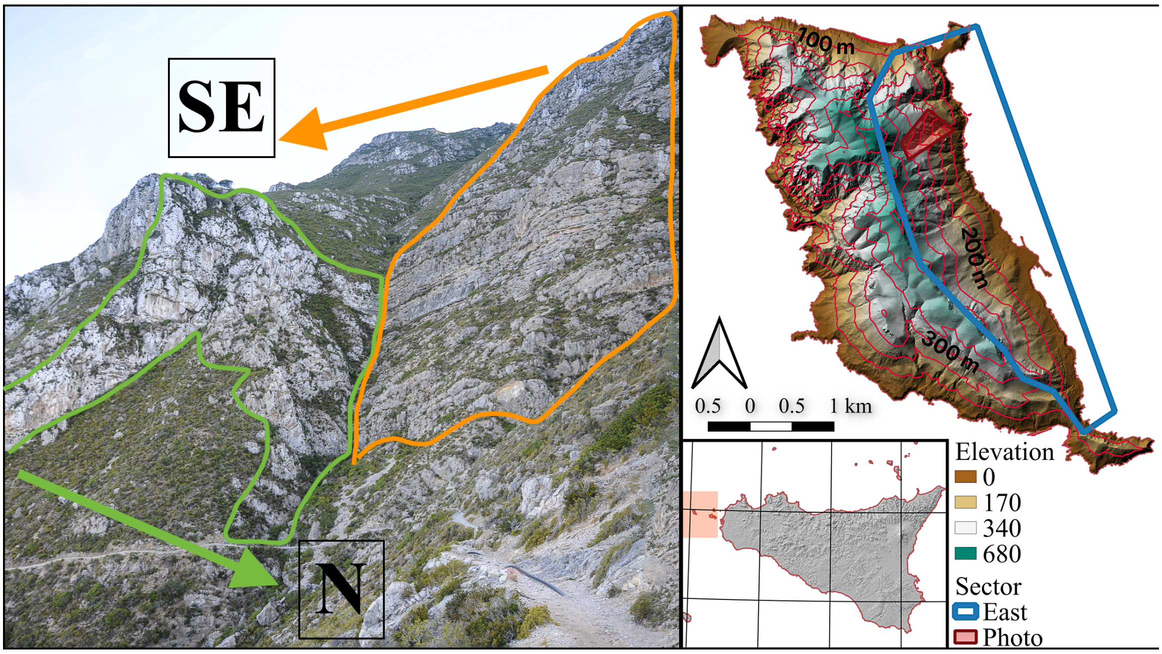

Fig. 4.8 An example of microtopography heterogeneity in the cliffs of Marettimo, Italy. The photo shows a zone inside the East sector of the island. *P. limonifolia* was found on the cliff with a North local orientation (green line), but not on the contiguous SE-facing area (orange line).

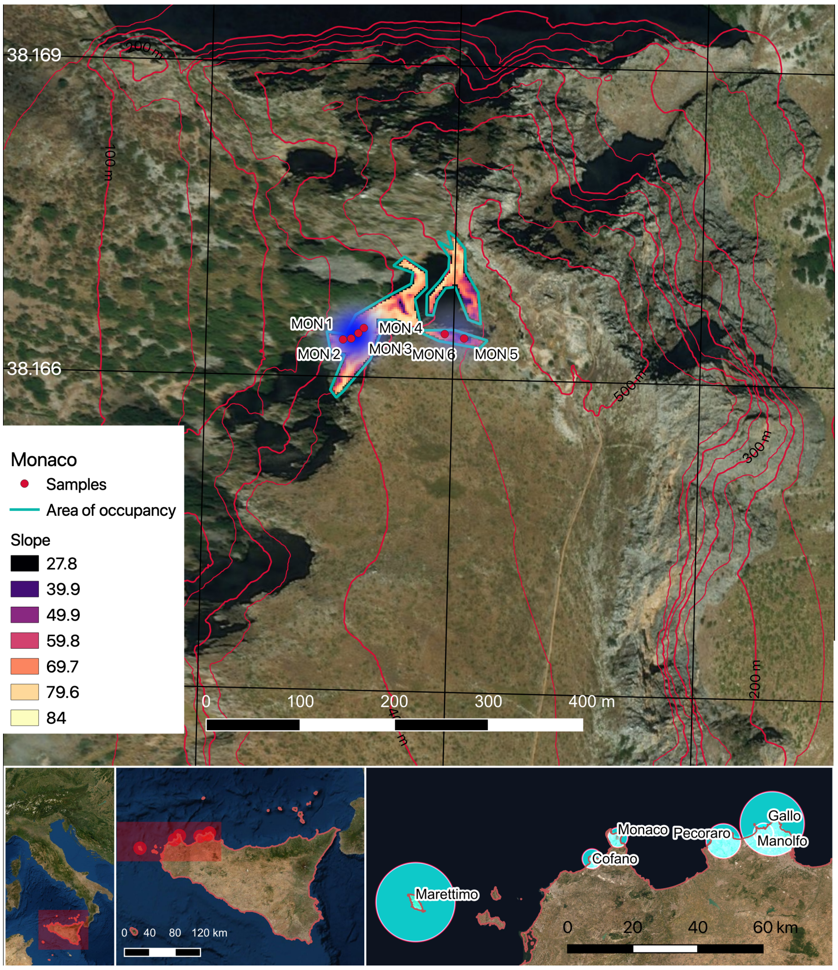

Fig. 4.9

Geographic distribution and sampling of *Pseudoscabiosa limonifolia* I.

Newly discovered population of Monaco. Dimension of circles are proportional to the number of plant samples

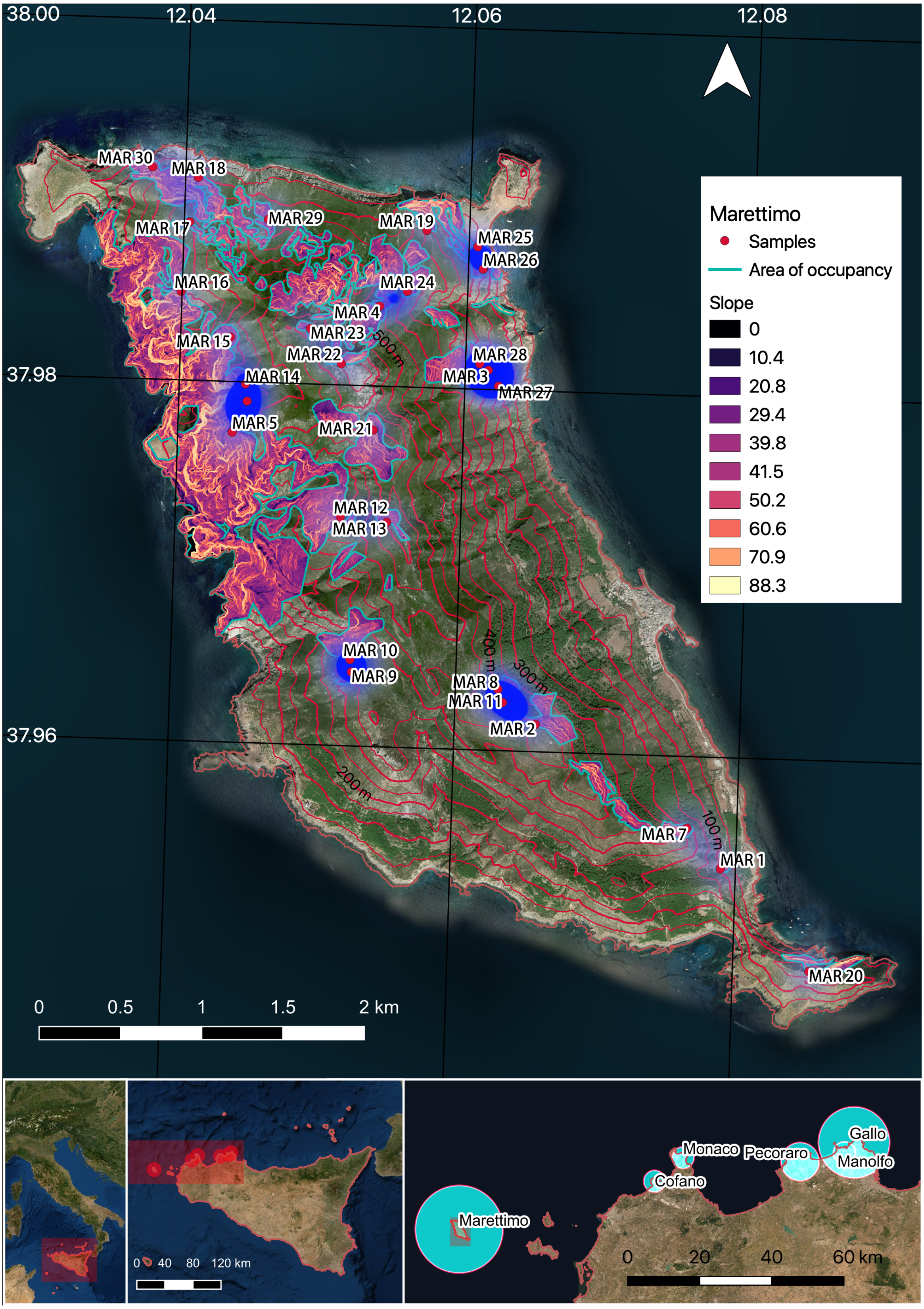

Fig. 4.10 A. Geographic distribution and sampling of *Pseudoscabiosa limonifolia* II. Population of Marettimo.

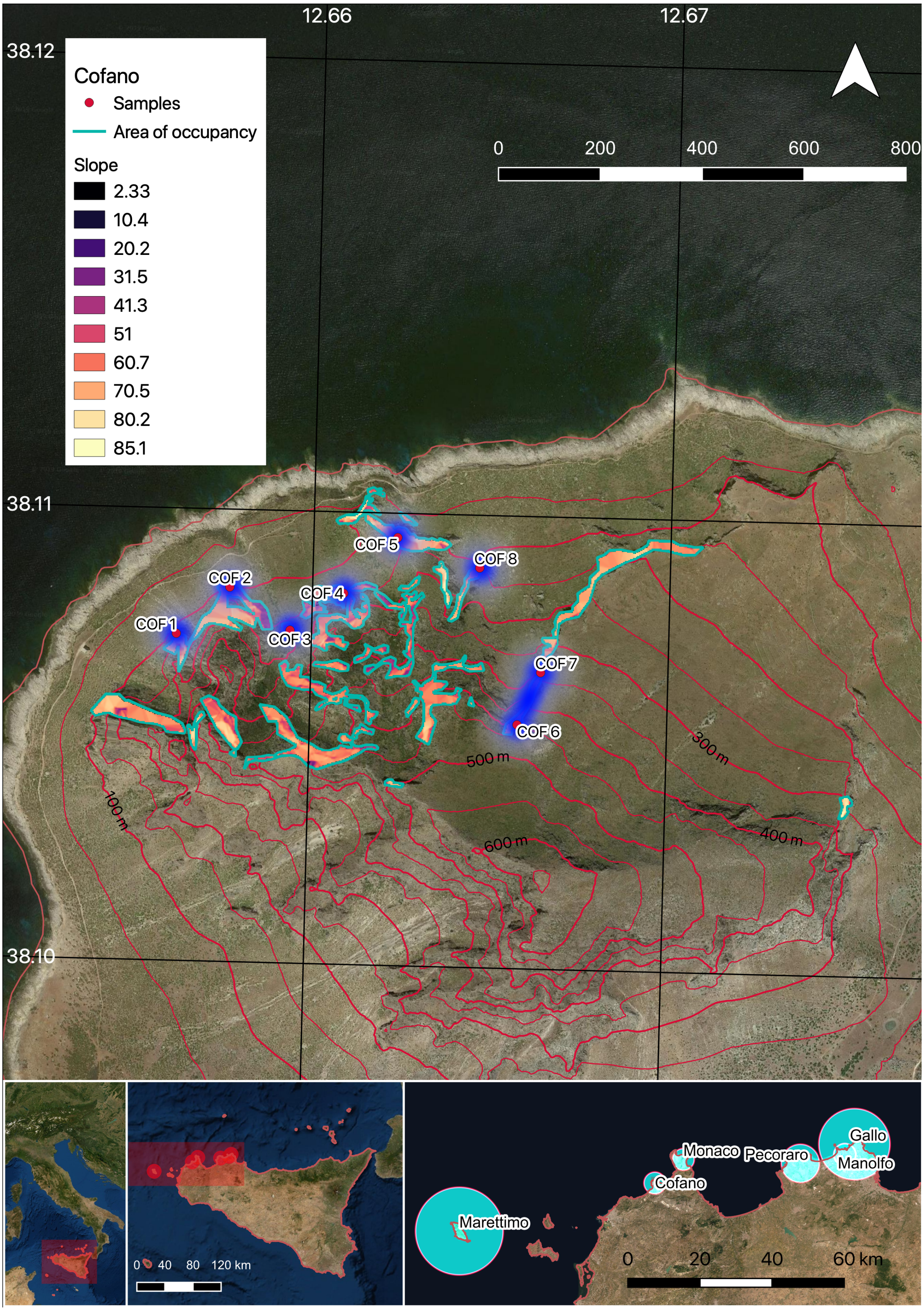

Fig 4.10 B. Geographic distribution and sampling of *Pseudoscabiosa limonifolia* III. Population of Cofano. Dimension of circles are proportional to the number of plant samples.

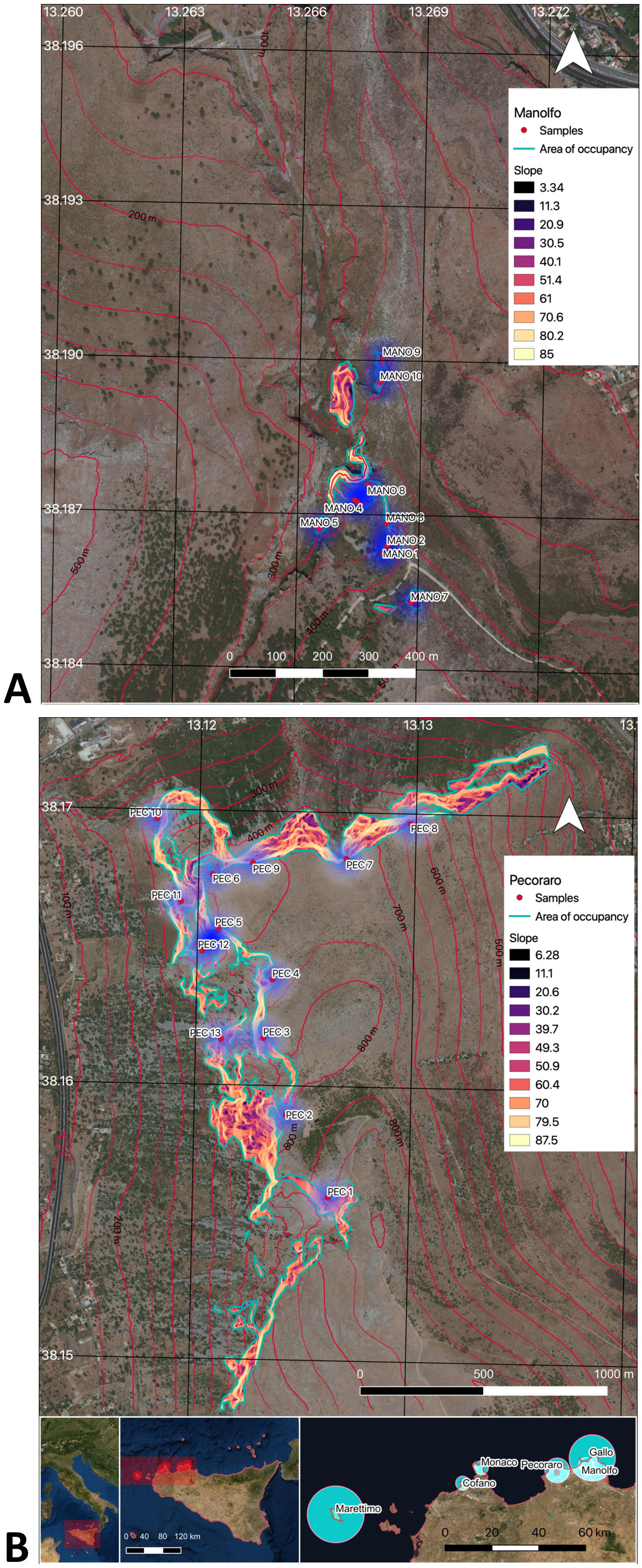

Fig 4.11. Geographic distribution and sampling of *Pseudoscabiosa limonifolia* IV. A: newly discovered population of Manolfo. B: Population of Pecoraro. Dimension of circles in Fig. 4.11 B are proportional to the number of plant samples.

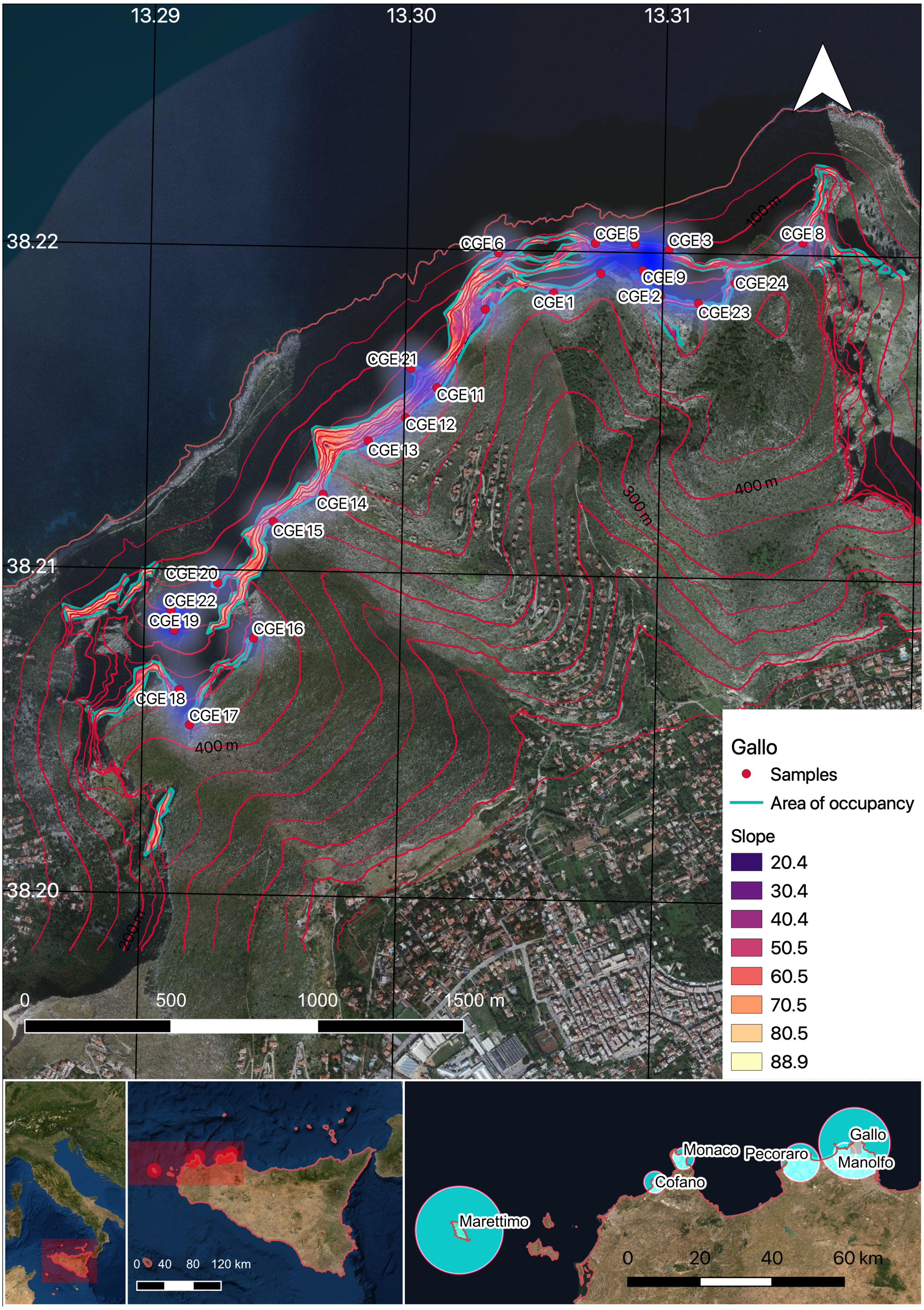

Fig. 4.11 C. Geographic distribution and sampling of *Pseudoscabiosa limonifolia* V. Population of Gallo. Dimension of circles are proportional to the number of samples.

The observed seed recruitment at the base of a cliff was scarce or non-existent. The species was observed to scarcely tolerate interspecific competition.

Threats were detected in all localities but were especially intense in the newly discovered populations of Manolfo and Monaco due to their low altitude. Climate change, severe droughts and temperature extremes (threat 11.2-3) were the main threats, followed by increase in fire frequency/intensity (threat 7.1.1) and expansion of domestic or semi-domesticated sheep and goats, which were often allowed to roam in the wild in Sicily (threat 2.3). In the largest population of Marettimo, a growing population of the introduced mouflon (*Ovis aries musimon*) represents a newly detected menace, being observed eating the plant caulinar leaves and floral scapes. Other minor threats included natural events like landslides (threat 10.3) and plants attacked by leaf and flower-mining lepidopters (threat 8.4) (Fig. 4.12).

Fig. 4.12. A number of individuals show evidence of insect-related damage. Up-left: leaf mining larva, unknown lepidopter. Right: foliar damage of the leaf mining lepidopter in Marettimo. Centre-left: empty epicalyx after that the seed was eaten. Down-left: a caterpillar (unknown lepidopter species) feasting on the ovaries of the capitulum (mm scale bar).

The calculated EOO of *Pseudoscabiosa limonifolia* was 148,58 km^2. EOO_{SEA} was instead 780.78 km^2. According to the 2x2 km survey, the total AOO of the species was 68 km^2, being found on 17 grid units. The AOO and EOO of *P. limonifolia* are shown in Fig. 4.13 and 4.14.

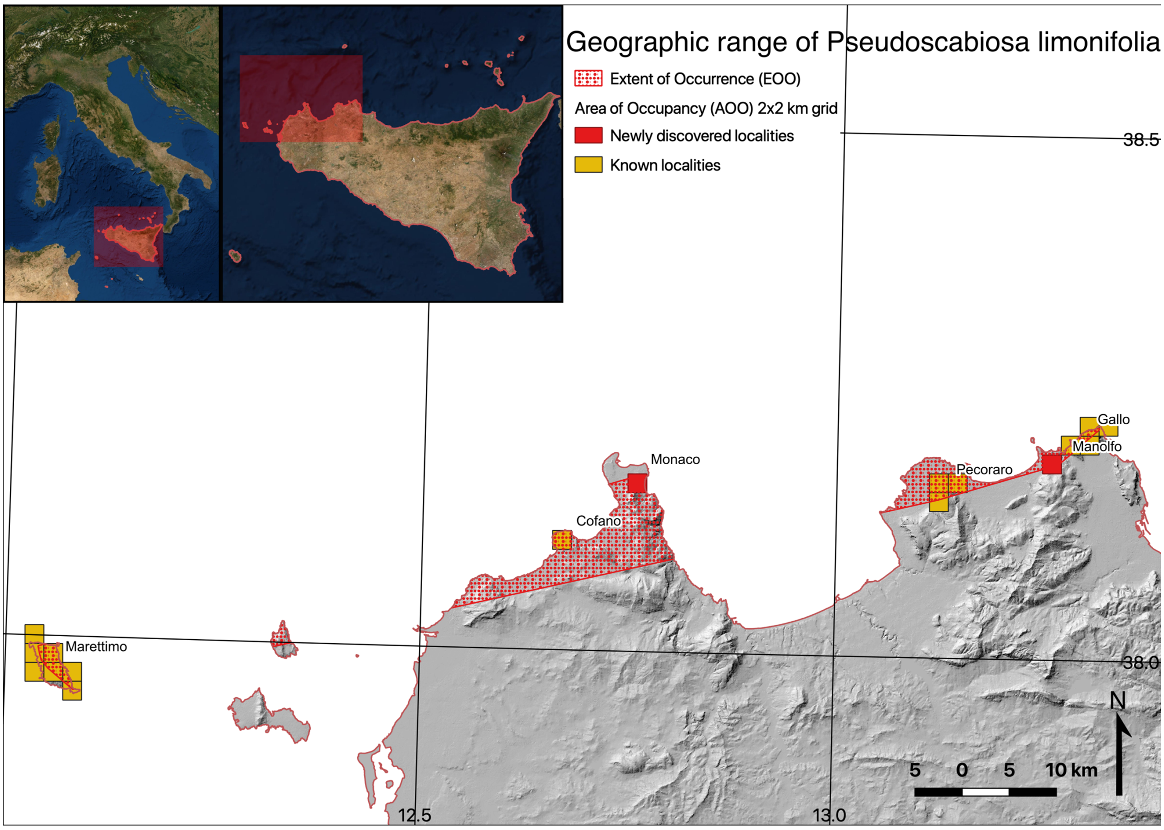

Fig. 4.13. Geographic range of Pseudoscabiosa limonifolia according to a 2 x 2 km grid sampling. The map shows also the Extent of Occurrence without sea (EOO) of the species. The 2 newly discovered populations are coloured in red. Both their positions resulted intermediate between known populations.

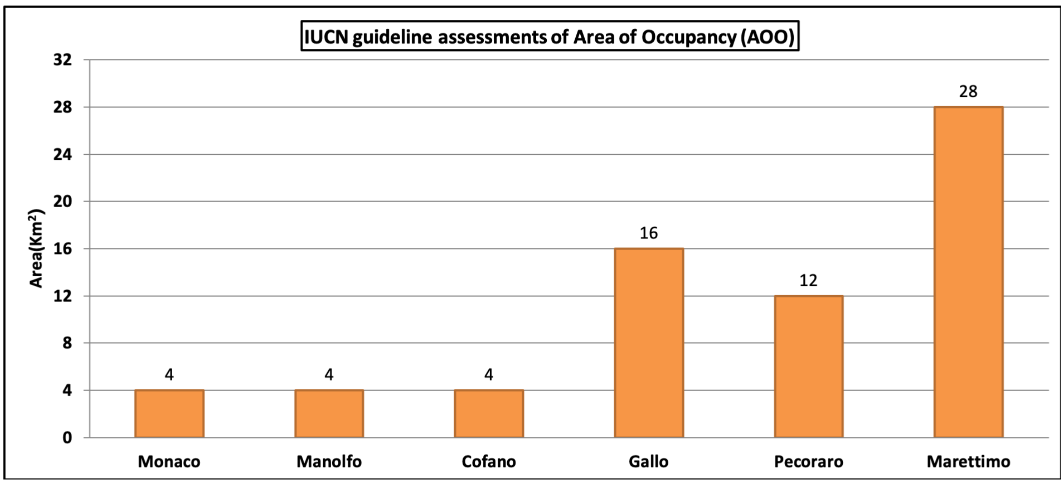

Fig. 4.14. Barplot of the geographic extent of *Pseudoscabiosa limonifolia* obtained from a 2 x 2 km grid according to the IUCN standards).

Sequence variation and phylogenetic relationships among haplotypes

A total of 91 samples were collected from the 6 studied populations of *Pseudoscabiosa limonifolia* (Table 4.1). In addition (Table 4.2), 59 stored samples were extracted and analysed for the species *Pseudoscabiosa saxatilis* and *P. grosii*, for an overall of 150 aligned sequences for the whole genus. The length of the *trnT–trnL* spacer ranged between 498 and 506 bp with a total aligned length of 517 base pairs. Ten polymorphic sites were detected in this study (Table 4.4) of which five were single nucleotide substitutions, three nucleotide insertions-deletions events of 5-6 bp in length, and two mononucleotide indels of poly-T and poly-A stretches composed, respectively, of 11-16 and 9-12 bp. Overall, ten haplotypes (A-L) were identified (Table 4.4). No haplotype was shared between species. *P. limonifolia* showed three haplotypes, denominated A-B-C, that only differed in the number of microsatellite repeats. Each Sicilian population was monomorphic for its haplotype, being fixed for a single sequence. Three haplotypes were shared between two populations. In the case of sequence A and C, the shared monomorphic haplotype appeared on adjacent populations, whereas haplotype B was encountered on 2 distant and non-proximal populations (MAR and PEC). *P. grosii* showed no haplotype variability and only haplotype D was recovered. *P. saxatilis*, had the highest haplotype variability, with six identified haplotypes. In this species, all but two populations were fixed for a single haplotype, only two haplotypes (E, H) were shared between two populations, meanwhile one population possessed 2 exclusive haplotypes. The geographic distribution of haplotypes is shown in Fig 4.16.

Haplotype	39	129	239-254 $[T]_n$	321 $[GTATA]_{1/2}$	343 $[ACTATT]_{1/2}$	362	364 $[ATATA]_{1/0}$	369	462-473 $[A]_n$	517	F	f
P. limonifolia												
A	C	A	$[T]_{11}$	$[GTATA]_2$	$[ACTATT]_1$	G	$[ATATA]_1$	T	$[A]_{10}$	C	14	0.093
B	C	A	$[T]_{12}$	$[GTATA]_2$	$[ACTATT]_1$	G	$[ATATA]_1$	T	$[A]_{10}$	C	43	0.287
C	C	A	$[T]_{12}$	$[GTATA]_2$	$[ACTATT]_1$	G	$[ATATA]_1$	T	$[A]_{11}$	C	34	0.093
P. grosii												
D	C	C	$[T]_{15}$	$[GTATA]_1$	$[ACTATT]_1$	T	$[ATATA]_1$	T	$[A]_{11}$	C	15	0.1
P. saxatilis												
E	C	A	$[T]_{15}$	$[GTATA]_1$	$[ACTATT]_1$	T	$[ATATA]_1$	T	$[A]_{12}$	T	11	0.073
F	C	A	$[T]_{13}$	$[GTATA]_1$	$[ACTATT]_2$	T	$[ATATA]_1$	T	$[A]_9$	C	9	0.06
G	C	A	$[T]_{14}$	$[GTATA]_1$	$[ACTATT]_1$	T	-----	A	$[A]_{11}$	T	7	0.047
H	T	A	$[T]_{15}$	$[GTATA]_1$	$[ACTATT]_1$	T	$[ATATA]_1$	T	$[A]_{10}$	C	9	0.06
I	C	A	$[T]_{16}$	$[GTATA]_1$	$[ACTATT]_1$	T	$[ATATA]_1$	T	$[A]_{12}$	C	5	0.033
L	C	A	$[T]_{15}$	$[GTATA]_1$	$[ACTATT]_1$	T	$[ATATA]_1$	T	$[A]_{12}$	C	3	0.02

Table 4.4. Haplotypes of genus *Pseudoscabiosa* based on the polymorphic sites of trnT-trnL intergenic spacer.

Haplotype network construction under statistical parsimony resulted in a single and resolved network in which all connections fall within a 95% plausible set of relationships (Fig. 4.15). A total of ten unsampled or extinct haplotypes were inferred. *P. limonifolia* haplotypes (A - C) are connected to the other species by the highest number of mutational steps, and a minimum of four missing intermediate haplotypes. The highest root probability was assigned by TCS to the internal haplotype B (P = 0.39), present in *P. limonifolia* and which showed the highest frequency (0.287).

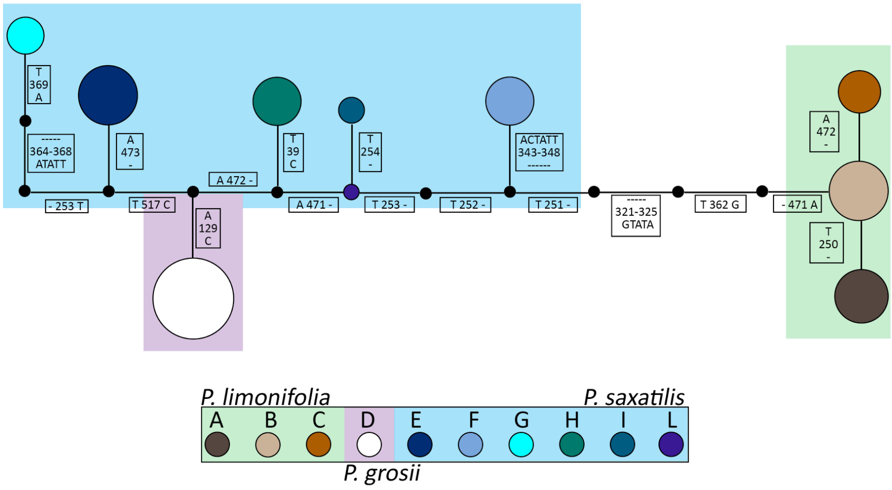

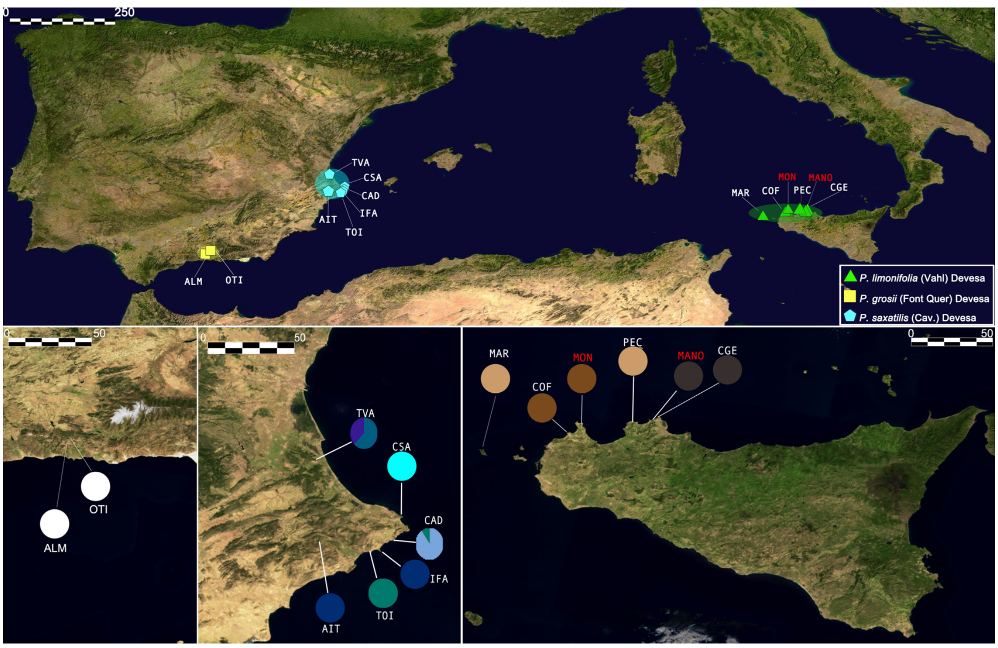

Fig. 4.15 up. Haplotype network of the genus Pseudoscabiosa. Blue, purple and green boxes group the respective species.

Fig 4.16 down. Geographic distribution of haplotypes. Above: the known geographic distribution of each species. Sampling sites are indicated within each species' range. Codes for population names refer to Table 4.1 and 4.2. Down: from West to East, geographic distribution of haplotypes for each species. Pie charts on each locality represent the proportion of different haplotypes. Colour scheme refers to Fig 4.15.

Genetic diversity and population structure

Parameters of genetic diversity and structure are given in Table 4.5. The results obtained in this study indicate high levels of genetic diversity, both at the genus and the species levels.

Parameter	Species			
Populations	P. limonifolia	P. saxatilis	P. grosii	Total value
No. of individuals	91	44	15	150
No. of haplotypes	3	6	1	10
No. of polymorphic sites	2	5	0	9
h_S	0.114 (0.1143)	0.123 (0.0888)	-	0.09 (0.052)
h_T	0.756 (0.055)	0.927 (0.0824)	-	0.945 (0.0186)
G_{ST}	0.849 (0.1603)	0.868 (0.0897)	-	0.904 (0.0545)
v_S	0.143 (0.1432)	0.084 (0.0545)	-	0.072 (0.0492)
v_T	0.750(0.3433)	0.933 (0.2054)	-	0.923 (0.0469)
N_{ST}	0.809 (0.21)	0.910 (0.0541)	-	0.923 (0.0518)

Table 4.5. Estimates of genetic diversity and differentiation measures for ordered (v_s, v_t, N_{st}) and unordered (h_s, h_t, G_{st}) haplotypes in genus *Pseudoscabiosa*, and their standard deviations. h_s and v_s, intrapopulation diversity, h_t and v_t, total diversity, G_{st} and N_{st}, global genetic differentiation among populations.

Overall, total genetic diversity was high across all populations of *Pseudoscabiosa* for ordered and unordered haplotypes (v_t = 0.923 ± 0.0469 and h_t = 0.945 ± 0.0186*,* respectively). Interpopulation differences contributed the most to the overall coefficients of differentiation (G_{ST} = 0.904 ± 0.0545 < N_{ST} = 0.923 ± 0.0518), while overall within-population variation, by contrast, was low, with average haplotypic diversity values of h_s = 0.09 ± 0.052 and v_s = 0.072 ± 0.0492. Considering each species separately, within-population variation was absent in *P. limonifolia* as for in *P. grosii,* which should be considered a single entity without any genetic difference in the individuals. *P. saxatilis* on the other hand shows a limited amount of within-population variation.

The highest h_t was observed in *P. saxatilis* (0.927) with its 6 separated haplotypes, followed by *P. limonifolia* (0.756). With each of the three haplotypes present in 2 different populations, the differentiation between populations of *P. limonifolia* was lower (i.e. G_{ST} = 0.849; N_{ST} = 0.809) then for *P. Saxatilis*. The latter species exhibited a very high and significant population genetic structure, with N_{ST} = 0.910 based on ordered haplotypes, and G_{ST} = 0.868 based on unordered haplotypes, indicating that most of the variation, both in terms of genetic distance and number of haplotypes was found among populations. Putting this in other words, 80% of the total genetic variation is distributed among *P. limonifolia* populations and between 91% and 95 % among *P. saxatilis* populations. The global test of phylogeographical structure was significant ($G_{ST} < N_{ST}$ with $P > 0.05$) and revealed the presence of a phylogeographical pattern in *Pseudoscabiosa*. These results were in accordance with the evaluation of differentiation using hierarchical analysis of molecular variance.

Groups	*Source of variation*	*d.f.*	*Sum of squares*	*Variance components*	*Percentage of variation*
None specified $F_{ST} = 0.97980$	Among populations	13	306.612	2.27319	97.98
	Between populations	136	6.375	0.04688	2.02
Species $F_{CT} = 0.68918$ $F_{SC} = 0.95304$ $F_{ST} = 0.98540$	Among species	2	197.912	2.21344	68.92
	Among populations withing species	11	108.7	0.95140	29.62
	Within populations	136	6.375	0.04688	1.46
P. saxatilis $F_{ST} = 0.92460$	Among populations	5	75.557	2.05732	92.46
	Within populations	38	6.375	0.16776	7.54
P. limonifolia $F_{ST} = 1$	Among populations	5	33.143	0.46861	100
	Within populations	85	0	0	0

Table 4.6. Analysis of molecular variance for 91 individuals of *P. limonifolia*, 44 of *P. saxatilis* and 15 of *P. grosii* based on chloroplast DNA trnT–trnL sequence data

When variation between species was taken into account (Table 4.6), the AMOVA revealed populations to be significantly differentiated at species level, with 68.92 % of the variation detected among species ($F_{CT} = 0.68918$, $P = 0.00$), 29.62 % among populations within species ($F_{SC} = 0.95304$, $P = 0.00$), only 1.46 % of variation within populations and a genetic differentiation coefficient ($F_{ST} = 0.9854$), very close to fixation for alternate haplotypes in different species. Overall, from the analysis resulted that more than 2/3 of the variation found in *Pseudoscabiosa* was due to differences between species and about 1/3 to populations within species. When species were analysed separately, differentiation for *P. saxatilis* was even stronger, with 92.46% of genetic variation detected among populations and only 7.54% within populations ($F_{ST} = 0.92460$), meanwhile for *P. limonifolia* 100% of the total genetic variation is between its populations, with zero variation within populations ($F_{ST} = 1$).

A phylogeographic hypothesis based on the species actual genetic structure is shown in Fig 4.17. A widespread ancestor (Fig 4.17 up) colonised the coastal cliffs of Sicily. A subsequent climate-induced reduction of suitable cliff habitats shaped the actual area of distribution (Fig. 4.17 down). Main wind directions in the Sicilian channel and along the actual coastlines of NW Sicily is shown in Fig. 4.18. The colonisation pattern of *P. limonifolia* with respect to its anemochorous dispersal syndrome likely followed a West-East direction, pushed by the frequent North-western/Western winds (Fig. 4.18).

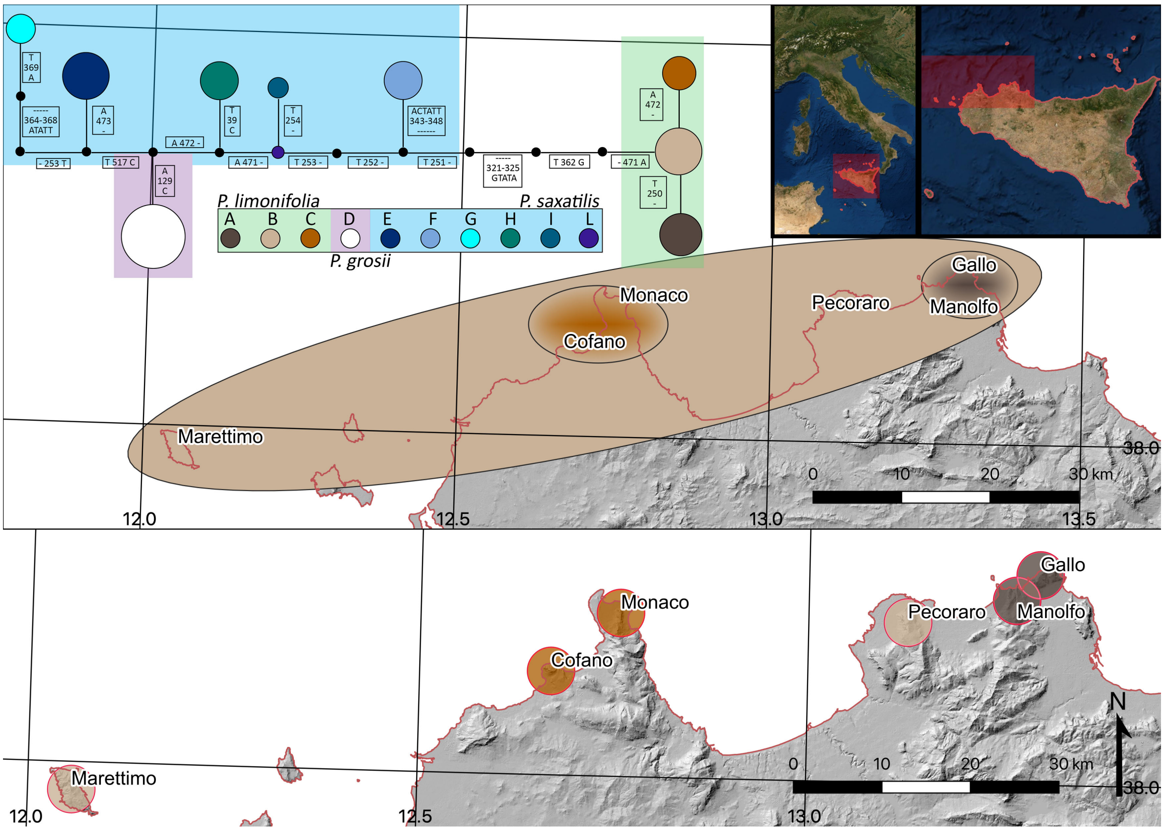

Fig. 4.17. Phylogeographic hypothesis to explain the current distribution of the genetic diversity of *P. limonifolia*. Up: a hypothetical historic ancestor of *P. limonifolia*. Down: extant geographic distribution of haplotypes.

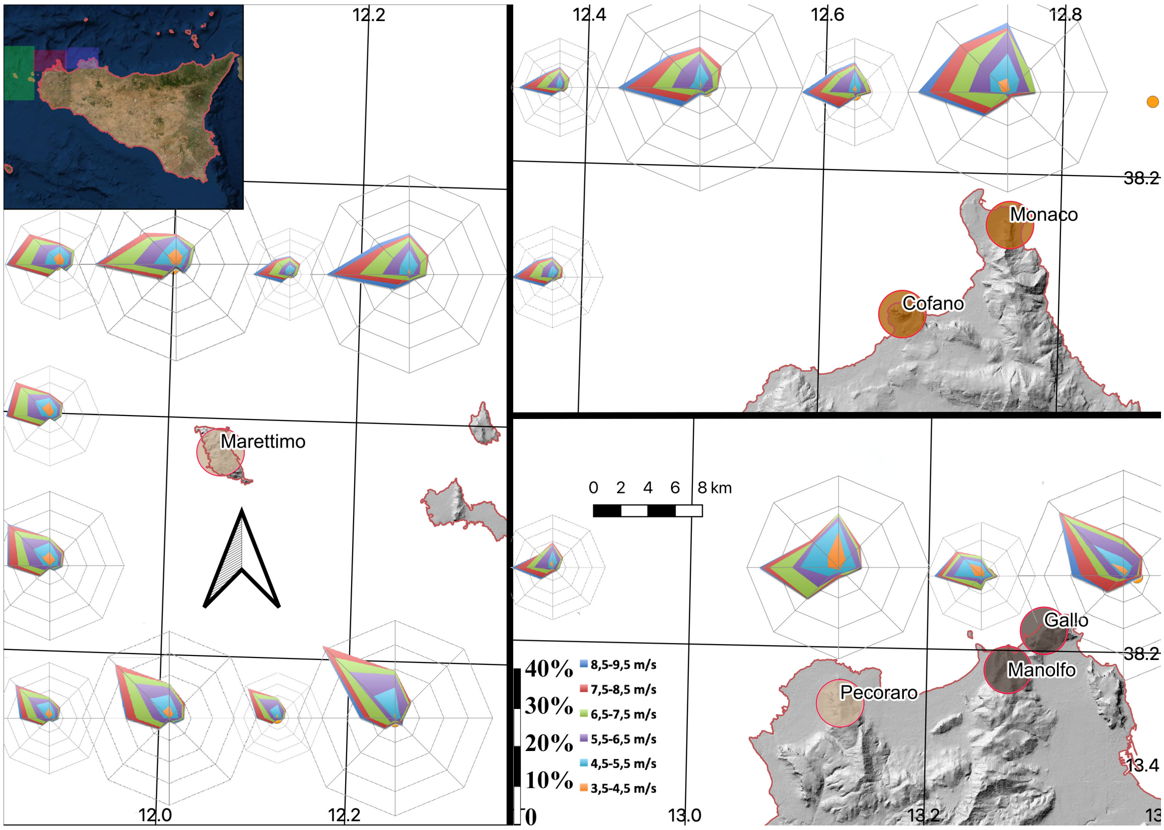

Fig. 4.18. Dominant wind directions and intensities in the Sicilian strait. Populations of *P. limonifolia* are represented by circles. Each circle is coloured with respect to the population monomorphic haplotype. Colour scheme follows Fig. 4.15. Wind data are elaborated from QuikSCAT level 2B (10-year monthly average: 1999-2009).

Discussion

Plant distribution, conservation status and ecological characteristics

P. limonifolia pertains to the SW Italian alliance *Dianthion rupicolae* BRULLO & MARCENÒ 1979, which is characterised by perennial chasmophytes living on limestone coastal cliffs. This endemic vegetation community is dominated by chamaephytes forming small cushions on near vertical surfaces. The most common species found with *P. limonifolia* were other cliff-exclusive chasmophytes such as *Erica sicula* GUSS., *Helichrysum pendulum (C.PRESL)* C.PRESL. *Bupleurum dianthifolium* GUSS., *Asperula rupestris* TINEO, *Dianthus rupicola* BIV., *Iberis semperflorens* L., *Lomelosia cretica* (L.) GREUTER & BURDET, etc.

In the European Habitat Directive (DIR 92/43/EEC) this vegetation type is categorized as Rocky slopes with chasmophytic vegetation (code 8210). Following the European Red List Of Habitats, the species lives in a rare and fragmented fraction of the H3.2d Mediterranean base-rich inland cliff. In fact, after the regional survey and the numerical ordination analysis carried out in chapt 3, it resulted clear that *Pseudoscabiosa limonifolia* was an extreme specialist. The preferentiality of a single set of environmental conditions (Table 4.3) made the species distribution on the cliff zones coded 8210 resembling more a system of metapopulations rather than a single continuous population.

According to the results, the inclusion of *Pseudoscabiosa limonifolia* in the IUCN Red List results challenging and should account for several factors. The proposed categorization should follow the criteria *B1* and *B2*. The species suffers severe fragmentation within and among subpopulations due to an extreme specialization, but such fragmentation is natural within the definition of chasmophytic species, hence should not be taken in account for the assessment. Moreover, the suitable patches of rupicolous habitat not occupied by the species are unlikely produced by an historic and/or anthropogenic reduction of its AOO. Although a decline in number of individuals and locations is observable, the species habitat is generally naturally protected, with most individuals located in inaccessible places with little climatic instability and without much economic interest. Demographic and environmental stochasticity are used as important factors in predicting the viability of species with limited distributions and/or small populations. However, the number of individuals of *P. limonifolia* (estimated to be approximately less than 884,000 individuals, see density estimated in chapt. 3 case study 3 multiplied by the area occupied by the species using 20 x 20 m tiles and vertical terrain) and the long life span of the species is a buffer against random fluctuations in births and deaths that might trigger the total extinction of the species. On the other hand, the high habitat specificity might compromise recovery after possible anthropogenic disturbances, especially on some localities within the subpopulations.

Globally, nine locations can be described for the species. Marettimo has 2 locations. Cofano, Monaco, Manolfo have 1 location. As Marettimo, Gallo and Pecoraro subpopulations are each formed by 2 locations. Individuals encountered on the western sector of the island of Marettimo form 1 location. This area is unlikely menaced by fires because of the presence of barren slopes and high cliffs. For this location, the main threat is the presence of mouflons. The introduced population of mouflons results understudied by zoologists. Six individuals coming from a Tuscan breeding farm were introduced in Marettimo in 1976 (Sacchi et al., 1994). In 1994, the population was formed by about 50 individuals (Sacchi et al., 1994). During my field observations I did not count nor estimate the total population of mouflons. However, on the western sector of the island was not uncommon to observe herds of 20 to 40 individuals each. The intensity of damage caused by this species is unknown. In general, no single plant was observed to be completely grazed. The damage was limited to the floral scape in the early stage and the inner part of the rosette (appendix Fig. S.4.1). The remaining part of this subpopulation might be menaced by fires, especially due to the fact that the island has an enormous fuel load produced by a thriving Mediterranean shrubland.

Globally, herbivory should be considered the most threatening factor for the species. All locations are affected in some percentage by goats and, as mentioned above, by mouflons.

Fire is a variable to consider as a potential local extinction factor for certain locations. In summer 2020 (29-30/07/2020) the subpopulation of Cofano, whose North cliffs host its principal location, was affected by an extended fire. The extent of damage of the subpopulation is yet to be determined, but many of the individuals encountered during the study carried out in chapt. 3 in COFN were destroyed or severely damaged by fires. Some individuals of Monaco and Gallo West, especially those living at the base of the cliffs, were found dead after wildfires in 2017 and 2018. For this reason, the major threats of the locations in Monaco and Gallo West, Pecoraro West and Manolfo are wildfires. The locations at Gallo North and Pecoraro North are naturally shielded by continuous vertical cliffs and the unique potential threats, beside grazing, are severe droughts and temperature extremes. For topographic constraints, the locations (coinciding with their subpopulations) of Manolfo and Monaco are the smallest and most threatened by such consequences of climate change.

Flower and fruit predation was detected throughout the population, but data recorded were not quantitative and hence future trends could not be predicted.

Even though 2 new subpopulations were discovered, the overall Extent Of Occurrence (148,58 km^2, without sea; 780.78 km^2, with sea) and Area Of Occupancy (68 km^2) remained within the boundaries of the Endangered category of criteria *B1* and *B2*.

The measured microclimate at the subpopulation living in Cofano (meteorological station of COFN, chapt. 1) and the species mesic preferential altitude are a concerning indicator of the potential impact of an anthropogenic climate change on the species fitness. Climate change is nowadays one of the primary factors of variations in the patterns of distribution of species and habitats (Bellard et al., 2012). Severe droughts and heatwaves are already affecting the species distribution in the newly discovered subpopulations of Monaco and Manolfo. A multi-year observation of the individuals in these subpopulations showed that many specimens are reducing their vegetative parts. Some did not survive the 2018 Summer season.

For all the aforementioned reasons, I then propose the categorisation of *Pseudoscabiosa limonifolia* (VAHL) DEVESA in the IUCN Vulnerable category according to *B1ab(iv,v) + 2ab(iv,v)*.

The discovery of two previously unknown locations of *P. limonifolia*, together with their haplotypic identity equal to their contiguous populations, supports the categorization into a paleoendemic species whose range has been reduced in ancient times. In general, a very great genetic differentiation was found on the genus, which was probably caused by a reduced or non-existent gene flow between populations at any level.

Palaeoendemics are defined as paleogeographic relics which have survived in a limited portion of their past territory (Favarger and Contandriopoulos, 1961; Wulff, 1943). Although the seeds of *P. limofolia* are potentially suitable for long distance dispersal, the high ecological specificity and the low capacity for recruitment of this taxon makes those events improbable. The suitable habitat for species colonisation constitutes a fraction of an already naturally fragmented cliff distribution on the territory. Thus, colonization events on suitable cliffs are not expected to be frequent for this species, because the ecological niche is distributed on sparse, distant "ecological islands" (Stebbins, 1980). Moreover, the species was observed to suffer interspecific competition. Few adult individuals were spotted living in co-existence with other species. Plantules were never individuated at the base of the cliff or on areas with a dense vegetation cover. This was probably due to a slow growing rate. Competition with fast growing species which colonise less steep surfaces resulted always in disfavour of *P. limonifolia*.

Local extinctions are not expected to be frequent for the species, because of the microclimatic stability created by the North-oriented coastal cliffs where it lives (see chapt. 1). This pattern of scarce colonisation and persistence on suitable sites is typical of many other rare species growing preferentially on cliffs (Fernández-Mazuecos et al., 2014; López-Pujol et al., 2013; Silva et al., 2015). Minor amplitude of extreme temperatures, a shady habitat with few daily and seasonal temperature fluctuations, together with high, constant humidity represent the strict ecological requirements for the species (chapt. 1, meteorological station COFN). That suggests that *P. limonifolia* may be a relict species from the more humid climate that prevailed in the Central-Western Mediterranean in the late Tertiary (Combourieu-Nebout et al., 2015; Jiménez-Moreno et al., 2010; Postigo Mijarra et al., 2009).

Another remarkable aspect of the relict distribution of *P. limonifolia* was its absence from intermediate areas between populations. North-facing cliffs were in fact present on several coastal mountains within the regional survey. It was observed that the species was not present on topographic units that had an altitude minor than 400 m a.s.l. In the 150 m – 200 m a.s.l. range this absence could be caused by the Quaternary sea level fluctuations. Conversely, those uninhabited coastal mountains with North-facing cliffs in the range 200 m - 400 m a.s.l. might be a hint of the species failure to adapt to an increasing aridification, to the establishment of summer drought, and to subsequent Quaternary glacial cycles (Suc, 1984). In adverse, arid periods the species found probably shelter in the upper part of the actually colonised sea cliffs, followed by a recolonization of the lower areas during more humid periods. The clear tendency toward decline detected in the populations at lower overall altitudes (Manolfo and Monaco) would support the hypothesis of an historic restriction in their range due to paleoclimate changes.

For all these historic and ecologic reasons, the impoverished intrapopulation genetic diversity and the current narrow distribution range (with only 6 populations in Sicily) might be the result of a distribution range reduction process. The potential sites with suitable conditions for the species reduced drastically during the quaternary glacial/interglacial cycles and jeopardized the distribution of small populations/metapopulations. In general, the microclimatic conditions of the sites where the species is found in the present days are not only extremely rare in the central-western Mediterranean territories, but also quite distant from each other. Conservation efforts should especially focus on the protection of this calcareous cliff habitat, which *P. limonifolia* shares in the Mediterranean area with other endemics such as *Naufraga balearica* CONSTANCE & CANNON (Fernández-Mazuecos et al., 2014; Rosselló, 2010), *Bupleurum dianthifolium* Guss., *Hirtellina fruticosa* (L.) DITTRICH and *Hieracium lucidum* GUSS. (Krak et al., 2012).

Future climatic variability and the tendency toward aridification (MAGRAMA, 2014) might further reduce the populations of *P. limonifolia*. A local extinction of Manolfo and Monaco populations will likely happen in the near future due to habitat transformation. The island of Marettimo (686 m a.s.l), as well as Pecoraro (850 m a.s.l.), could represent reservoirs for the species survival in a future with less rainfall and air humidity and are worth of protection. There, the species shows its largest geographic extent and reservoir of reproductive individuals. More importantly, along the cliff system of these two areas will likely persist the suitable microclimatic conditions for the species existence.

High genetic structure and phylogeographic hypothesis

My results are in line with Carlson et al. (2009), who demonstrated that *P. saxatilis* is the closest taxon of *P. limonifolia*. In contrast with its sister species, *Pseudoscabiosa limonifolia* has a very reduced overall genetic diversity and a complete genetically structured population network. A total of only two polymorphic loci were detected on a poly(A) and poly(T) mononucleotide repeats, which produced 3 different haplotypes. The most geographically distributed and abundant haplotype B differs from haplotype A by a single T nucleotide deletion, while the difference with haplotype C is a single A nucleotide insertion. Then, the genetic distance between A and C is higher and relying on 2 polymorphisms respect to that of B from both A and C (1). This fact, in addition with a lesser genetic distance to the sister clade of *P. saxatilis* is a compelling proof that the populations of Pecoraro (PEC) and Marettimo (MAR) have the ancestral haplotype (B) for the species. With respect to the whole genus, the coalescent theory (Crandall & Templeton, 1993) predicts that interior nodes of a gene network represent ancestral haplotypes, whereas those located at tip nodes evolved subsequently. Statistical parsimony identified also haplotype B as the ancestral genotype of

Pseudoscabiosa, but with a moderate probability. As a confirmation, outgroup comparison with the closest available sequence in GeneBank (*Dipsacus japonicum*, accession number MH074865.1, data not shown) supported this hypothesis. Thus, *P. limonifolia,* or its closest extinct ancestor in between the two species, was likely plesiomorphic with respect to the extant species in the genus.

By contrast, the only presence in *P. limonifolia* of 2 polymorphic loci characterised by a single base difference in highly variable regions does not indicate neither a high overall genetic diversity for the Sicilian species nor an ancient diversification of the extant haplotypes. This could instead suggest that the species recently colonised the Sicilian island, and that the colonization event was followed by a fast expansion and subsequent local differentiation. However, the latter hypothesis shows several weaknesses: 1) the absence of *P. limonifolia* in the African Mediterranean coastal territories; 2) the low competition ability and narrow ecological characteristics of the species; and 3) the phylogeographic pattern of its sister clade, *P. saxatilis.*

A strong phylogeographic structure and a lack of genetic intrapopulation diversity in chasmophytes is more the rule than an exception. Other works for rare cliff species achieved similar results (Fernández-Mazuecos et al., 2014; Mejías et al., 2018). In general, this is related to the fragmented nature of cliff habitats. Anywhere in the Mediterranean region high levels of endemic species are often encountered on cliffs (Bragazza, 2009; Domínguez et al., 2003; Lavergne et al., 2004; Médail & Verlaque, 1997; Pérez-García et al., 2012; Villar & García, 1989), probably due to the association of endemic taxa with low dispersal ability, the high habitat specificity of these taxa, and their naturally fragmented distribution patterns (García et al., 2002; Lavergne et al., 2004; Thompson 2005).

The high genetic distance of adjacent population in *P. saxatilis* demonstrated a long-time persistence and genetic isolation of such populations, excluding seed dispersal between close topographic units at least from the Pleistocene. This lack of maternal genetic exchange among populations is also found in *P. limonifolia* and is particularly surprising in a wind-dispersed species (e.g. comparing to the genus Helichrysum in the Mediterranean; Herrando-Moraira et al., 2017). The only encountered exception to this assumption was a "long-distance" dispersal between the populations of Toix (TOIX) and Cap D'Or (CAD). In fact, haplotypes F (CAD) and H (TOIX and CAD) are remarkably different and their simultaneous presence in CAD could be only explained by a seed dispersal colonisation. However, it must be underlined that the geographic distance among these two populations is of 12 km.

This plesiomorphic condition of haplotype B respect to A and C contrasts with the disjunct geographic distribution of this haplotype in *P. limonifolia*, because between MAR and PEC (B) the populations Cofano (COF) and Monaco (MON) (C) lie not far from each other. Conversely, haplotype A appeared in the Easternmost range of the species distribution with the populations of Gallo (CGE) and Manolfo (MANO). An event of long distance dispersal should be therefore excluded and a different hypothesis (summarised in Fig 4.17) has to be sought to explain the current distribution of the genetic diversity of *P. limonifolia*.

The narrow microclimatic requirements and biological traits of *P. limonifolia* show a high ecological specificity, which in turns drastically reduced the species capacity for colonisation and establishment because of the lack of current suitable sites. The optimal living conditions of the species require a reduction in both thermal oscillations and incoming solar radiation, and a constantly high air humidity. This microclimate is predominantly hyper-oceanic and very similar to the climatic conditions occurring during the Early Pliocene, with year-round moisture and warm temperatures (e.g. Fauquette and Bertini, 2003), and mean annual temperatures exceeding 22 °C (Combourieu-Nebout et al., 2015; Fauquette et al., 1999, 2007). Under these conditions it is likely that the ancestors of the actual Sicilian species were also distributed on the paleo-coastal cliffs of the nearby African shores.

Also, the high degree of disjunction between *P. saxatilis* and *P. limonifolia* invokes an old vicariance process originated most probably in the Iberian or African plates. The direction of gene flow and gradual disjunction should have followed a W-E direction from the modern territories of Algeria and Tunisia towards Sicily, as suggested from actual dominant wind directions in the Sicilian strait, and as observed in other plant groups (e.g., Hilpold & al., 2011; Lo Presti & Oberprieler, 2011).

A possible series of dispersal events might have occurred in this period of optimal climatic conditions, both occasional long-distance dispersal (Cowie & Holland, 2006; Fernández-Mazuecos & Vargas, 2011) or stepping-stone dispersal via emerged islands during low sea level periods (Stöck & al., 2008). Later on, the colonisation pattern of Sicily could have followed, likely as for the African shores, a West-East direction according to the main wind directions. The presence of the ancestral haplotype on the westernmost population of

Marettimo supports this hypothesis. However, according to the present paleogeographic and geologic reconstructions (Di Maggio et al., 2014; 2017), the vast part of Sicily was submerged at the end of the Messinian salinity crisis. According to this perspective, the successful colonisation of the paleo-Sicilian archipelago unlikely occurred before 3.6 Ma.

The development of the Mediterranean climate regime, punctuated by a dry summer season, occurred in the late Pliocene (Suc, 1984). The beginning of the Glacial/Interglacial (G/I) cycles in the Pleistocene, contributed to the intensification of Mediterranean climate conditions during the mesic interglacials and dry glacials (Pons et al., 1995). During these periods, the species likely underwent a series of multiple bottlenecks and expansions which contributed to reduce its genetic diversity and geographic distribution to the present one. According to this hypothesis, the scattered present populations are relicts of a formerly widespread cliff species that underwent extinction in most of its past areal.

The general low maternal genetic flow between populations in the genus and the absence of individuals with haplotype B in COF+MON and MANO+CGE populations implies a previous existence of A/B and B/C on site followed by a local B haplotypic extinction. The presence of haplotypes A and C on contiguous isolated populations indicates their earlier origin on a larger area that included the actual adjacent populations. This hypothesis would also explain the absence of (A, C) individuals in the central population of Pecoraro.

In contrast to the reduced genetic diversity of *P. limonifolia*, a remarkable amount of evidences makes the three species paleoendemic (Thompson, 2005). In fact, it has been demonstrated that the phylogenetic position of the genus *Pseudoscabiosa* in the Dipsacaceae s.s. (Caprifoliaceae s.l., APG IV; 2016) is basal (Caputo & Cozzolino, 1994; Caputo et al., 2004; Carlson et al., 2009). The closest taxon of the genus *Pseudoscabiosa* is a distant widespread herbaceous relative, *Succisa* or *Succisella* (Carlson et al., 2009). This, together with the similar conservative environment where the three *Pseudoscabiosa* species live and many ancestral characters as the presence of bark on trunks, suggests a relict condition for the genus. The sister groups *P. saxatilis* and *P. grosii* share the same vegetative characters but differ in the fruit morphology. *P. grosii* lacks a corona, has enhanced plumosity in calyx bristles, and a different epicalyx shape (Mayer & Ehrendorfer; 1999). Moreover, both these species have a differentiated morphology from *P. limonifolia*, both in the vegetative and fruit morphology: a) the star shaped trichomes have a central elongated hair in *P. saxatilis* and *P.*

grosii, but not in *P. limonifolia* (Romo et al., 1997); b) the foliar hair is positioned on the lower page in *P. limonifolia* and on both pages in *P.saxatilis* and *P. grosii*; and c) hair of the calyx bristles are only vestigial in *P. limonifolia*, but well developed in *P.saxatilis* and *P. grosii*. According to Mayer & Ehrendorfer (1999), the presence of an epicalyx corona in both *P. limonifolia* and *P. saxatilis* but not in *P. grosii* makes the former more related to each other than to the latter. Furthermore, these authors stated that *P. saxatilis* and *P. limonifolia* would form a more apomorphic sister group. My morphological interpretations, however, which were corroborated by the phylogeographic results, suggest a different conclusion. In fact, the present study provides a new insight in a remarkable overall haplotypic diversity for a cliff-exclusive genus. It was found that a deep molecular divergence of several indels and substitutions separated *P. limonifolia* from the western clade of *P.saxatilis+P.grosii* indicating an old vicariance of the two clades. Conversely, only 2 mutations separated the unique *P. grosii* haplotype from *P. saxatilis*. In addition to the slight haplotypic distance, the 2 species are very similar in their vegetative characters. The absence of a corona in the diaspore of *P. grosii* is paired with an enhanced plumosity of the calyx bristles. However, these two characters have a similar evolutionary meaning correlated with an anemochoric dispersal syndrome. The position of *P. grosii* on the haplotype network makes *P. saxatilis* paraphyletic for the studied marker, which in turn suggests a dichotomy of the Spanish/African species. Probably *P. grosii*, similarly to *P. limonifolia*, differentiated due to an increased geographic distance between the two species which promoted allopatric speciation in more recent times. My results are then in contrast with the phylogenetic tree of the Dipsacaceae drawn by Carlson et al. (2009). My hypothesis is that the ancestral relative of *Pseudoscabiosa* colonised the cliff areas of the Prebetic-Baetic-Rifan fragmented microplates and the Maghrebid belt during the Tertiary. The genus underwent an ancient and gradual vicariant disjunction between the western Iberian-Alboran clade and the eastern Maghrebid-Sicilian clade. As previously stated, the western clade underwent a later geographic isolation which led to the present species distribution.

Morphological footnotes

The calyx of *P. limonifolia* has 5 bristles according to the species original description by Devesa (1984) who used herbarium individuals from populations of Gallo and Marettimo. This number was defined fixed to 4 by Mayer & Ehrendorfer (1999) analysing herbaria specimens from populations of Gallo and Cofano. During the observations performed for this thesis from all the extant populations it can be said that the calyx bristles vary in number within and among individuals indistinctively. The most common number is 5 but 4 to up to 7 bristles were counted.

The oldest living individuals of the species were found in the population of Marettimo. The more stable climatic conditions of the island with high, constant humidity and continuous sea winds blowing through all year favoured the longevity of single plants. Many individuals formed here the largest cushions known for the species (up to 3 m wide). The amount of bark on branches and the width of the main trunk suggested that some individuals had at least 100 years or more.

Vegetative leaves are very variable in their length and shape according to plant age and climatic characteristics of the area. The highest values of leaf length and width were observed in Marettimo. The main leaf shape in this population was lanceolate. Plants inspected at Cofano and on the new population of Monaco had shorter leaves and a defined obovate shape. In these populations some individuals showed a unique broadly crenate margin not found in any other location (Fig. S4.2). This character, to my knowledge, was not previously described for the species or the genus. The other populations varied in leaf shape from obovate to oblanceolate.

Conclusions

The discovery of two new populations of *P. limonifolia* contributed to enlarge the species Area of Occupancy by 8 km^2 (IUCN-based approach, 2 x 2 km tiles). In the terminology adopted by IUCN, 2 new subpopulations and a same number of locations were added to the population. However, this did not alter the given categorization of Vulnerable for the species.

A fine-scale systematic survey at regional level highlighted the importance of physical prospecting cliff habitats for population ecology and plant conservation. The results regarding the distribution of *P. limonifolia* with a finer unit size (20 x 20 m) suggested that a) the vertical component of distribution in narrow endemic chasmophytes makes a great difference in the range estimation (doubling the total distribution); and b) that the IUCN-based kilometric grid is not totally suitable for the study of chasmophytes. In fact, the surface occupied by the species using a 20 x 20 m terrain-based grid was an order of magnitude lesser of the 2 x 2 km plain distribution (6.87 km^2 and 68 km^2, respectively).

The narrow ecology and local adaptation of *P. limonifolia* were refined through a fine-scale research on the environmental drivers that lead to its extant distribution. The encountered patterns of genetic structure confirmed the species relictual state, highlighting a paleogeographic history of habitat reduction. Changes in habitat availability were linked to bioclimatic changes during the Plio-Pleistocene period. Random genetic drift and multiple bottlenecks structured the genetic variation in *P. limonifolia*. This result was suggested by a diffused population monomorphism, a pattern of genetic similarity of contiguous populations and a disjunct distribution of the ancestral haplotype (Ellstrand & Elam, 1993; Hutchison & Templeton, 1999;).

Bibliography

Anthos. 2011[2020]. Information System of the plants of Spain. Real Jardín Botánico, CSIC - Fundación Biodiversidad. Electronic resource at www.anthos.es. Consultation carried out in March 2011[2020].

Avino, M., Tortoriello, G. & Caputo, P. (2009). A phylogenetic analysis of Dipsacaceae based on four DNA regions. Pl. Syst. Evol. 279: 69–86.

Bellard, C., Bertelsmeier, C., Leadley, P., Thuiller, W. and Courchamp, F. (2012). Impacts of climate change on the future of biodiversity. Ecology Letters, 15: 365–377. doi: 10.1111/ j.1461-0248.2011.01736.x

Bragazza, L. (2009). Conservation priority of Italian Alpine habitats: a floristic approach based on potential distribution of vascular plant species. Biodivers & Conservation 11:2823–2835

Brullo, S. & Minissale, P. & Spampinato, G. (1995). Considerazioni fitogeografiche sulla flora della Sicilia. Ecologia Mediterranea. 21. 99-117.

Burban, C., Petit, R.J., Carcreff, E., Jactel, H. (1999). Rangewide variation of the maritime pine bast scale Matsucoccus feytaudi Duc. (Homoptera: Matsucoccidae) in relation to the genetic structure of its host. Molecular Ecology, 8: 1593-1602.

Caputo, P. & Cozzolino, S. (1994). A cladistic analysis of Dipsacaceae (Dipsacales). Pl. Syst. Evol. 189: 41–61.

Caputo, P., Cozzolino, S. & Moretti, A. (2004). Molecular phylogenetics of Dipsacaceae reveals parallel trends in seed dispersal syndromes. Pl. Syst. Evol. 246: 163–175.

Carlson, S.E., Mayer, V. and Donoghue, M.J. (2009). Phylogenetic relationships, taxonomy, and morphological evolution in Dipsacaceae (Dipsacales) inferred by DNA sequence data. Taxon, 58: 1075-1091. doi:10.1002/tax.584003

Castelloe, J., Templeton, A.R. (1994). Root probabilities for intraspecific gene trees under neutral coalescent theory. Molecular Phylogenetics and Evolution, 3: 102-113.

Clement, M., Posada, D., Crandall, K.A. (2000). TCS: A computer program to estimate gene genealogies. Molecular Ecology, 9 (10) pp. 1657-1659.

Combourieu-Nebout, N., Bertini, A., Russo-Ermolli, E., Peyron, O., Klotz, S., Montade, V., Fauquette, S., Allen, J., Fusco, F., Goring, S., Huntley, B., Joannin, S., Lebreton, V., Magri, D., Martinetto, E., Orain, R., Sadori, L. (2015). Climate changes in the central Mediterranean and Italian vegetation dynamics since the Pliocene. Review of Palaeobotany and Palynology. 218. 10.1016/j.revpalbo.2015.03.001.

Cowie, R.H. & Holland, B.S. (2006). Dispersal is fundamental to biogeography and the evolution of biodiversity on oceanic islands. J. Biogeogr. 33: 193–198. https://doi.org/10.1111/j.1365-2699.2005.01383.x

Crandall, K.A., Templeton, A.R. (1993). Empirical tests of some predictions from coalescent theory with applications to intraspecific phylogeny reconstruction. Genetics. 134. 959-69.

Crandall, K.A., Templeton, A.R., Sing, C.F. (1994). Intraspecic phylogenetics: problems and solutions. In Scotland R.W., Siebert D.F., Williams D.M., Models in Phylogeny Reconstruction. Clarendon Press, Oxford, 273-297.

Devesa, J.A. (1984). Pseudoscabiosa, género nuevo de Dipsacaceae. Lagascalia 12: 213–221.

Di Maggio, C., Madonia, G., Vattano, M., Agnesi, V & Monteleone, S. (2014). Evoluzione geomorfologica della Sicilia occidentale
AIGEO - Incontro di studio "Evoluzione geomorfologica di lungo termine del paesaggio nell'Italia meridionale".

Di Maggio, C., Madonia, G., Vattano, M., Agnesi, V., & Monteleone, S. (2017). Geomorphological evolution of western Sicily, Italy. Geologica Carpathica, 68, 80 - 93.

Domínguez, F., Moreno, J.C. & Sáinz, H. (2003). Rarity and threat relationships in the conservation planning of Iberian flora. Biodiversity and Conservation, 12: 1861-1882.

Doyle, J.J., Doyle, J.L. (1987). A rapid DNA isolation procedure for small quantities of fresh leaf tissue. Phytochemical Bulletin, 19: 11-15.

Ellstrand, N.C. & Elam, D.R. (1993). Population Genetic Consequences of Small Population Size: Implications for Plant Conservation. Annual Review of Ecology and Systematics 1993 24:1, 217-242

European Red List Of Habitats (2016). ISBN 978-92-79-61588-7 https://ec.europa.eu/environment/nature/knowledge/pdf/terrestrial_EU_red_list_report.pdf

Excoffier, L., Smouse, P.E., Quattro, J.M. (1992). Analysis of molecular variance inferred from metric distances among DNA haplotypes: application to human mitochondrial DNA. Genetics, 131: 79-491.

Excoffier, L., Laval, G., Schneider, S. (2005). Arlequin ver. 3.0: An integrated software package for population genetics data analysis. Evolutionary Bioinformatics Online, 1: 47-50.

Fauquette, S., Bertini, A. (2003). Quantification of northern Italy Pliocene climate from pollen data: evidences for a very peculiar climate pattern. Boreas 32, 361–369.

Fauquette, S., Suc, J.-P., Guiot, J., Diniz, F., Feddi, N., Zheng, Z., Bessais, E., Drivaliari, A. (1999). Climate and biomes in the west Mediterranean area during the Pliocene. Palaeogeogr. Palaeoclimatol. Palaeoecol. 152, 15–36.

Fauquette, S., Suc, J.-P., Jiménez-Moreno, G., Favre, E., Jost, A., Micheels, A., Bachiri-Taoufiq, N., Bertini, A., Clet-Pellerin, M., Diniz, F., Farjanel, G., Feddi, N., Zheng, Z. (2007). Latitudinal climatic gradients in Western European and Mediterranean regions from the Mid-Miocene (~15 Ma) to the Mid-Pliocene (~3.6 Ma) as quantified from pollen data. In: Williams, M., Haywood, A.M., Gregory, F.J., Schmidt, D.N. (Eds.), Deep-time perspectives on climate change: marrying the signal from computer models and biological proxies. The Micropalaeontological Society Special Publications. The Geological Society, London, pp. 481–502.

Favarger, C., Contrandriopoulos, J. (1961). Essai sur l'endémisme. Bulletin de la Société botanique Suisse, 71: 383-408.

Fernández-Mazuecos, M. & Vargas, P. (2011). Historical isolation versus recent long-distance connections between Europe and Africa in bifid toadflaxes (Linaria sect. Versicolores). PLoS ONE 6: e22234. https://doi.org/10.1371/journal.pone.0022234

Fernández-Mazuecos, M., Jiménez-Mejías, P., Rotllan-Puig, X., Vargas, P. (2014). Narrow endemics to Mediterranean islands: Moderate genetic diversity but narrow climatic niche of the ancient, critically endangered Naufraga (Apiaceae). Perspectives in Plant Ecology Evolution and Systematics. 16. 190-202. 10.1016/j.ppees.2014.05.003.

Fore, A.G., Stiles, B.W., Chau, A.H., Williams, B.A., Dunbar, R.S., Rodríguez E. (2013). Point-wise Wind Retrieval and Ambiguity Removal Improvements for the QuikSCAT Climatological Data Set. Accepted for publication in IEEE Trans. Geoscience and Remote Sensing, doi:10.1109/TGRS.2012.2235843, 2013.

Francini, E. & Messeri, A. (1956). L'isola di Marettimo nell'arcipelago delle Egadi e la sua vegetazione. Webbia, 11:1, 607-846, doi: 10.1080/00837792.1956.10669652

García, M.B., Guzmán, D., Goñi, D. (2002). An evaluation of the status of five threatened plant species in the Pyrenees. Biol. Conservation 103:151–161

Gianguzzi, L., La Mantia, A. (2008). Contributo alla conoscenza della vegetazione e del paesaggio vegetale della Riserva Naturale “Monte Cofano” (Sicilia occidentale) (con allegata Carta sinfitosociologica della vegetazione, scala 1:20.000). Fitosociologia, 45 (1), Suppl. 1: 1-55.

Gillet, H.J., Walter, K.S. (1997). IUCN red list of threatened plants.

Goñi, D., Garcia, M.B., Guzman, D. (2006). Métodos para el censo y seguimiento de plantas rupicolas amenazadas. Pirineos, 161:33-58.

Guarino, R. & Pasta, S. (2018). Sicily: the island that didn’t know to be an archipelago. Berichte der Reinhold-Tüxen-Gesellschaft – 30: 133 - 148.

Herrando-Moraira, S., Carnicero, P., Blanco-Moreno, J.M., Sáez, L., Véla, E., Vilatersana, R. and Galbany-Casals, M. (2017). Systematics and phylogeography of the Mediterranean

Helichrysum pendulum complex (Compositae) inferred from nuclear and chloroplast DNA and morphometric analyses. Taxon, 66: 909-933. doi:10.12705/664.7

Hilpold, A., Schönswetter, P., Susanna, A., Garcia-Jacas, N. & Vilatersana, R. (2011). Evolution of the central Mediterranean Centaurea cineraria group (Asteraceae): Evidence for relatively recent, allopatric diversification following transoceanic seed dis- persal. Taxon 60: 528–538.

Hutchison, D.W., Templeton, A.R. (1999). Correlation of pairwise genetic and geographic distance measures: inferring the relative influences of gene flow and drift on the distribution of genetic variability. Evolution 53: 1898 – 1914.

IUCN (2012a). Red List categories and criteria, version 3.1, second edition. https://portals.iucn.org/library/node/10315

IUCN (2012b). Threats Classification Scheme v. 3.0. https://www.iucnredlist.org/resources/threat-classification-scheme

Jiménez-Moreno, G., Fauquette, S., Suc, J.P. (2010). Miocene to Pliocene vegetation reconstruction and climate estimates in the Iberian Peninsula from pollen data. Rev. Palaeobot. Palyno. 162, 403-415.

Krak, K., Caklová, P., Chrtek, J., Fehrer, J. (2012). Reconstruction of phylogenetic relationships in a highly reticulate group with deep coalescence and recent speciation (Hieracium, Asteraceae). Heredity. 110. 10.1038/hdy.2012.100.

Kumar, S., Stecher, G., Li, M., Knyaz, C., Tamura, K. (2018). MEGA X: Molecular Evolutionary Genetics Analysis across computing platforms. Molecular Biology and Evolution 35:1547-1549

Lavergne, S., Thompson, J.D., Garnier, E. and Debussche, M. (2004). The biology and ecology of narrow endemic and widespread plants: a comparative study of trait variation in 20 congeneric pairs. Oikos, 107: 505-518. doi:10.1111/j.0030-1299.2004.13423.x

Lo Presti, R.M. & Oberprieler, C. (2011). The central Mediterranean as a phytodiversity hotchpotch: Phylogeographical patterns of the Anthemis secundiramea group (Compositae, Anthemideae) across the Sicilian Channel. J. Biogeogr. 38: 1109–1124. https://doi.org/10.1111/j.1365-2699.2010.02464.x

Lojacono Poiero, M. (1888-1909). Flora Sicula, o Descrizione delle Piante vascolari spontanee o indigenate in Sicilia. 3 voll. – Tip. Virzì, Palermo.

López-Pujol, J., Martinell, M.C., Massó, S. et al. (2013). The ‘paradigm of extremes’: extremely low genetic diversity in an extremely narrow endemic species, Coristospermum huteri (Umbelliferae). Plant Syst Evol 299, 439–446. https://doi.org/10.1007/s00606-012-0732-3

MAGRAMA. (2014). Cambio Climático: bases físicas. Guía resumida del Quinto Informe de Evaluación del IPCC. Edita Fundación Biodiversidad, Oficina Española de Cambio Climático, Agencia Estatal de Meteorología, Centro Nacional de Educación Ambiental.

Mayer, V. & Ehrendorfer, F. (1999). Fruit differentiation, palynology, and systematics in the Scabiosa group of genera and Pseudoscabiosa (Dipsacaceae). Plant Systematics and Evolution. 216. 135-166. 10.1007/BF00985103.

Médail, F. & Verlaque, R. (1997). Ecological characteristics and rarity of endemic plants from Southeast France and Corsica: implications for biodiversity conservation. Biol. Conserv., 80: 269-281.

Mejías, J.A., Chambouleyron, M., Kim, S. et al. (2018). Phylogenetic and morphological analysis of a new cliff-dwelling species reveals a remnant ancestral diversity and evolutionary parallelism in Sonchus (Asteraceae). Plant Syst Evol 304, 1023–1040. https://doi.org/10.1007/s00606-018-1523-2

Pérez-García, F.J., Medina-Cazorla, J.M., Martínez-Hernández, F., Garrido-Becerra, J.A., Mendoza-Fernández, A.J., Salmerón-Sánchez, E., Mota, J.F. (2012). Iberian Baetic endemic flora and the implications for a conservation policy. Ann Bot Fenn 49:43–54

Pons, O., Petit, R.J. (1995). Estimation, variance and optimal sampling of gene diversity. I: haploid locus. Theoretical and Applied Genetics, 90: 462-470.

Pons, O., Petit, R.J. (1996). Measuring and testing genetic differentiation with ordered versus unordered alleles. Genetics, 144: 1237-1245.

Pons, A., Suc, J.P., Reille, M., Combourieu Nebout, N. (1995). The history of dryness in regions with a Mediterranean climate. In: Roy, J., Aronson, J., di Castri, F. (Eds.), Time Scales of Biological Responses to Water Constraints.Acad. Publishing bv, Amsterdam, pp. 169–188

Postigo Mijarra, J.M., Barrón, E., Gómez Manzaneque, F., Morla, C. (2009). Floristic changes in the Iberian Peninsula and Balearic Islands (South-West Europe) during the Cenozoic. J. Biogeogr. 36, 2025-2043.

QGIS Development Team (2019). QGIS Geographic Information System. Open Source Geospatial Foundation Project. http://qgis.osgeo.org

Raimondo F.M. (2011). Emergenze floristiche nella provincia di Trapani. in Naturalista sicil., S. IV, XXXV (1), pp. 9-19.

Raimondo, F.M., Bazan, G. & Troìa, A. (2011). Taxa a rischio nella flora vascolare della Sicilia. In Biogeographia: Lavori della Società italiana di Biogeografia, vol. XXX, pp.229-239

Romano, S., Ottonello, D. & Marcenò, C. (1994). Contributo alla floristica siciliana: nuovi rinvenimenti e ulteriori dati distributivi di alcune entità indigene ed esotiche. Naturalista Sicil. s. 4, 23 (1-2):3-14.

Romo, A., Cirujano, S., Peris, J.B. & Stübing, G. (1997). Beiträge zur Kenntnis der Gattung Pseudoscabiosa (Dipsacaceae). Feddes Repert. 108: 31–38.

Rosselló, J.A. (2010). Naufraga balearica Constance & Cannon. In: Bañares, A., Blanca, G., Güemes, J., Moreno, J.C., Ortiz, S. (Eds.) Atlas y libro rojo de la flora vascular amenazada de España. Adenda 2010. Dirección General de Medio Natural y Política Forestal (Ministerio de Medio Ambiente, y Medio Rural y Marino) y Sociedad Española de Biología de la Conservación de Plantas; Madrid, pp. 46-47.

Sacchi, O., Zava, B., Ziliani, U., Baratelli D. (1994). Osservazioni sul muflone (Ovis ammon musimon) nell'isola di Marettimo. I Congresso Italiano di Teriologia. Pisa. Riassunti, 151.

Silva Hernández de Santaolalla, J., Lim, S., Kim, S., Mejías, J. (2015). Phylogeography of cliff-dwelling relicts with a highly narrow and disjunct distribution in the Western Mediterranean. American journal of botany. 102. 10.3732/ajb.1500152.

Simmons, M.P., Ochoterena, H. & Carr, T.G. (2001). Incorporation, relative homoplasy, and effect of gap characters in sequence-based phylogenetic analyses. Syst. Biol. 50: 454–462.

Stebbins, G.L. (1980). Rarity of plant species: a synthetic viewpoint. Rhodora.; 82:77–86.

Stöck, M., Sicilia, A., Belfiore, N.M., Buckley, D., Lo Brutto, S., Lo Valvo, M. & Arculeo, M. (2008). Post Messinian evolutionary relationships across the Sicilian channel: Mitochondrial and nuclear markers link a new green toad from Sicily to African relatives. B. M. C. Evol. Biol. 8: 56. https://doi.org/10.1186/1471-2148-8-56

Suc, J.P. (1984). Origin and evolution of the Mediterranean vegetation and climate in Europe. Nature. 307. 429-432. 10.1038/307429a0.

Templeton, A.R., Crandall, K.A., Sing, C.F. (1992). A cladistic analysis of phenotypic associations with haplotypes inferred from restriction endonuclease mapping. III. Cladogram estimation. Genetics, 132: 619–633.

The Angiosperm Phylogeny Group. (2016). An update of the Angiosperm Phylogeny Group classification for the orders and families of flowering plants: APG IV. Bot J Linn Soc. ;181:1–20. doi: 10.1111/boj.12385.

Thompson, J.D. (2005). Plant evolution in the Mediterranean. Oxford University Press, Oxford

Verlaque, R. (1986). Étude biosystématique et phylogénétique des Dipsacaceae. IV. — Tribus des Scabioseae (phylum #4) et conclusion. Rev. Cytol. Biol. Veg. Botaniste 9: 97–176.

Villar, L. & García, M.B. (1989). Vers une banque de données des plantes vasculaires endémiques des Pyrenées. Acta Biol. Mont., IX: 261-274.

Wulff, E.V. (1943). An introduction to historical Plant Geography. Chronica Botanica Waltham, Massachusetts, 1-223.

Final conclusions

This thesis provided compelling evidence that cliffs are zones characterised by an abrupt environmental variation. Such variation is created by the topographic and geomorphologic nature of the cliff, *i.e.* the ever-changing angle of the vertical component and the geographical orientation of the cliff surface. In return, these characteristics modulate a series of physical factors that enhance the environmental heterogeneity of these habitats and, overall, make them drastically different from their surroundings.

The proposed methodology in chapter 3 applied the aerial photogrammetric techniques on inaccessible cliffs. It produced massive amounts of quantitative compositional and environmental data retrieved via a remote sensed 3D point cloud. Such data were continuously extended over an entire vertical façade, giving to the researcher the possibility of afterward selecting an adequate quadrat size and sample number. By contrast, plot sampling obtained with transects along the cliff boundary (Chapter 2) were considerably less precise concerning microtopography, but well adapted to study the regional diversity of cliff vegetation.

Studies of plant-environment relationships of cliff assemblages were scarce in literature largely due to the physical and logistic challenges that investigators have to face. This thesis provides new and useful insights into how the ecology of plants in cliff habitats can be investigated using UAV (Unmanned Aerial Vehicles) technology when coupled with appropriate analytical tools. In so doing, the work offers new and important ecological information about species occupying significant areas in the western Mediterranean. In addition, the thesis clearly demonstrates how such investigative tools can be used by life scientists in other similarly extreme and physically challenging environments. The described methodology and the results achieved have significant potential for use in the future conservation management and monitoring of vegetation in these and similar regions.

Through the used 3D model approach, it was possible to estimate for the first time the species/flat surface density for two narrow endemic chasmophytes (chapter 3). Moreover, it was possible to show that the inclination gradient of a cliff surface is the major variable governing the local assembly rules. The assemblages were clearly discriminated according to this variable in all the surveyed areas. Moreover, the cliff space was characterised by a continuous change in inclination, which in turn produced a highly heterogeneous mix of different communities. From an ecological standpoint, the results of Chapter 3 demonstrated that cliff environments are ecotonal by nature. These results pose the question of how many of the species inhabiting cliffs can be truly called chasmophytes. From the analyses produced in Chapt. 3, just 2 over 38 species resulted specialised to live exclusively on vertical/subvertical/overhanging surfaces. A decreasing gradient of inclinations represents for them a barrier for colonisation, i.e. an environmental filter they cannot cross. Other species showed a certain tolerance toward a growing degree of slope. Vertical zones constitute for them mostly a permeable filter in their spatial distribution. A third group was not related to "cliffs", but to the areas within the cliffs that have horizontal or sub-horizontal inclinations. A growing gradient of verticality for the species in this group is correlated with a growing intensity of abiotic filtering, possibly due to the scarcity of soil and/or water. Encountering such species inside the boundaries of a cliff was demonstrated not to be associated with slope, but instead it is due to the patchiness of a cliff surface.

Regional orientation was confirmed to be along with inclination the most relevant factor in the assemblage structure (chapt 3, case study 2; Chapt 2). By contrast, local orientation did not explain a great amount of variation. Moreover, case study 3 and 4 of Chapt. 3 showed the effect of specialization in strict chasmophytes. Microclimatic stability produced by a North to North-west local and regional orientations (see Chapt. 1), entwined with geographical and genetic isolation (Chapt.4) favoured in *Pseudoscabiosa limonifolia* an adaptation and specialization to a topoclimatic habitat. For this reason, this species was locally more competitive than widespread chasmophytes such as *Lomelosia cretica*. By contrast, as a consequence of its specialisation, *Pseudoscabiosa limonifolia* lost any ability to colonise cliffs with other local and regional orientations.

The recorded profiles of temperatures through a progressive distance from the cliff surface were especially divergent in South-oriented areas (Chapt. 1). Such thermal effect related to surface proximity showed quantitatively how air, air under canopy and soil temperatures on cliffs resulted positively influenced by southern orientations and negatively by northern orientations.

Throughout my data, one or another cliff orientation produced similar patterns of microhabitat complexity. The resulting trends of temperatures, solar radiation and relative humidity constitute the topography-driven repeating patterns of cliff microclimates. Data shown in Chapt. 1 contributed to understand the importance of terrain complexity in cliffs. The compositional dataset, coupled with the microclimatic characterization suggested that cliffs do not represent at all a homogeneous environment from a conservation standpoint. Overall, these results confirm the necessity of a microclimatic-based approach on cliff areas in order to precisely allocate topoclimatic microrefugia (Patsiou et al., 2014).

As expected, a difference in incoming solar irradiance among North-South zones determined a proportional trend of differences in temperatures. For the North oriented zones, the overall trend of solar irradiance was always lower than the corresponding South-oriented zones. The correlation between the summer sun elevation and the total insolation received by the cliff was shown. Moreover, as suggested by the graphs in appendix 1, sun trajectory (the sun azimuth angle) is determinant in order to understand seasonal trends and when the North-oriented cliffs are directly exposed to the sunlight.

By measuring the North-South differences in solar radiation income, I also showed that, as a consequence, North-oriented cliffs buffer extreme temperatures. Between 0 and 500 m a.s.l. in the Mediterranean context, maximum rather than minimum temperatures and high levels of solar radiation represent a limiting factor for species distribution. They are in fact a direct proxy of high evapotranspiration levels. According to my observations on floristic data in Sicily, such factors do not limit the distribution of the majority of rupicolous species, which can be found on both North and South orientations within an area. Conversely, they exclude narrow endemic species from South-oriented zones. My considerations are in line with the known link between climatic stability and endemism rates at coarse scale, which is normally mediated by rugged topography (Harrison & Noos, 2017). Therefore, my results support the hypothesis that North-oriented cliffs on coastal areas in the Mediterranean might have protected rare chasmophytes from past climatic changes, promoting the accumulation (if not induced speciation) of singular flora (Davis, 1951; Garcia et al., 2020).

The climatic stability of the North-oriented coastal cliffs was particularly evident in the pattern of diurnal temperature fluctuations and relative humidity. Relative humidity was high and constant, both on a daily basis and year-round. This last factor differentiated these zones from a visible summer drop in moisture observed on the inland and South-oriented zones.

The measured microclimatic difference between the North and South zones was demonstrated to have an eco-physiological effect on rupicolous species through the calculation of intraspecific trait variation. The species shift from low-radiation conditions of shaded cliffs corresponded then to a decrease in the leaf area and a consequent reduction of SLA (Specific Leaf Area). Moreover, the high and persistent levels of humidity encountered in North oriented cliffs potentially contributed to a stimulation of leaf expansion and increase of SLA.

The univocal pattern of decrease in LDMC (Leaf Dry Matter Content) encountered on North-oriented coastal zones was explained to be correlated to the amount of water available in the soil. South zones are characterised by a less availability of water and thus a reduced fresh weight and higher LDMC.

The measured microclimate of North-oriented coastal cliffs was predominantly hyperoceanic, with year-round moisture, small thermoperiods and warm, stable temperatures (*cfr*. Larcher, 2003). According to the most recent paleoclimatic reconstructions (Combourieu-Nebout et al., 2015; Fauquette and Bertini, 2003; Fauquette et al., 1999, 2007), similar conditions were predominant in the South Mediterranean during the Early Pliocene.

Bibliography

Combourieu-Nebout, N., Bertini, A., Russo-Ermolli, E., Peyron, O., Klotz, S., Montade, V., Fauquette, S., Allen, J., Fusco, F., Goring, S., Huntley, B., Joannin, S., Lebreton, V., Magri, D., Martinetto, E., Orain, R., Sadori, L. (2015). Climate changes in the central Mediterranean and Italian vegetation dynamics since the Pliocene. Review of Palaeobotany and Palynology. 218. 10.1016/j.revpalbo.2015.03.001.

Davis, P. (1951). Cliff Vegetation in the Eastern Mediterranean. Journal of Ecology, 39(1), 63-93.

Fauquette, S., Bertini, A. (2003). Quantification of northern Italy Pliocene climate from pollen data: evidences for a very peculiar climate pattern. Boreas 32, 361–369.

Fauquette, S., Suc, J.-P., Guiot, J., Diniz, F., Feddi, N., Zheng, Z., Bessais, E., Drivaliari, A. (1999). Climate and biomes in the west Mediterranean area during the Pliocene. Palaeogeogr. Palaeoclimatol. Palaeoecol. 152, 15–36.

Fauquette, S., Suc, J.-P., Jiménez-Moreno, G., Favre, E., Jost, A., Micheels, A., Bachiri-Taoufiq, N., Bertini, A., Clet-Pellerin, M., Diniz, F., Farjanel, G., Feddi, N., Zheng, Z. (2007). Latitudinal climatic gradients in Western European and Mediterranean regions from the Mid-Miocene (~15 Ma) to the Mid-Pliocene (~3.6 Ma) as quantified from pollen data. In: Williams, M., Haywood, A.M., Gregory, F.J., Schmidt, D.N. (Eds.), Deep-time perspectives on climate change: marrying the signal from computer models and biological proxies. The Micropalaeontological Society Special Publications. The Geological Society, London, pp. 481–502.

García, M.B., Domingo, D., Pizarro, M., Font, X., Gómez, D., Ehrlén, J. (2020). Rocky habitats as microclimatic refuges for biodiversity. A close-up thermal approach. Environmental and Experimental Botany, Volume 170

Harrison, S., Noss, R. (2017). Endemism hotspots are linked to stable climatic refugia Ann. Bot., 119, pp. 207-214, 10.1093/aob/mcw248

Larcher, W. (2003). Physiological Plant Ecology. Ecophysiology and Stress Physiology of Functional Groups. ISBN 978-3-540-43516-7 Springer-Verlag Berlin Heidelberg

Patsiou, T.S., Conti, E., Zimmermann, N.E., Theodoridis, S., Randin, C.F. (2014). Topo-climatic microrefugia explain the persistence of a rare endemic plant in the Alps during the last 21 millennia. Glob. Chang. Biol., 20, pp. 2286-2300, 10.1111/gcb.12515

Acknowledgments

First of all, I thank my supervisor Prof. Dr. Luigi Naselli Flores for his patience and excellent support. He provided me guidance, networking and feedback throughout the entire project. Moreover, the scientific and intellectual freedom he offered me were the base from which I developed the topics of this thesis and the subsequent contributions to plant sciences.

I would also like to thank my co-supervisor, Dr. Mercedes María Verdeguer Sancho for the support in the development of the thesis. Without her help, the thesis would have not obtained a full PhD recognition in Spain.

A special thanks to Dr. Angelo Troia. He provided guidance and shared with me successes and failures as a co-supervisor of the thesis for almost all the PhD period.

Thank to my parents, Giusi and Francesco, who set me off on the road of plant ecology a long time ago.

I would like to express my sincere gratitude to Dr. Riccardo Guarino for introducing me to the incredible scientific network of IAVS. Moreover, the meetings and conversations I had with him were vital in encouraging this work and inspiring me to think outside the box.

I would like to thank Dr. Paolo Madonia for helping with the research project of cliff microclimate. Without his technical expertise and field experience, the initial design of the meteorological stations used for this work would have not been this excellent. Moreover, he helped me with fruitful methods of data cleaning. He also provided some of his data loggers and sensors and carried out a consistent work in installing and maintaining two of the meteorological stations in Sicily throughout the entire PhD period.

I thank Prof. Dr. Francesco Parello for his significant help in providing some of the meteorological sensors used in Chapt. 1.

For the same reasons, I would like to thank Prof. Dr. Carlos Mesejo Conejos, Dr. Amparo Martinez Fuentes and Prof. Dr. Manuel Augusti Fonfria. Their help was essential for carrying out such a logistically complicated research.

Thanks to Prof. Dr. Giuseppe Ciraolo, Dr. Mauro Lo Brutto, Dr. Fulvio Capodici and Dr. Antonino Maltese for their important help and suggestions regarding UAVs, 3D models and optimization of flight plans. Moreover, I thank them for allowing me to use their workstations for the production of the 3D models used in Chapt. 3. The work was also optimised afterward thanks to their essential feedback.

Thanks to Prof. Dr. Lorenzo Gianguzzi for the encouraging conversations about the Sicilian flora and its botanical treasures.

I would like to thank Prof. Dr. Josep Antoni Rossello and Dr. Marcela Rosato of the plant diversity and evolution group of Jardin Botanico de Valencia. They were practically my second family, giving me their trust, technical support, materials and the unconditional use of the laboratory. Moreover, their expertise was vital for the development of the work on *Pseudoscabiosa* in Chapt. 4. Within the same group, I really appreciated all support and familiar atmosphere I received from Alexis Maravilla and Carmen Mansanet (who I also thank for the help in plant identification).

I would like to thank Dr. Pablo Ferrer Gallego and the CIEF group of Valencia, especially Dr. Inmaculada Ferrando and Prof. Dr. Emilio Laguna Lumbreras. Pablo's insight and knowledge of the Spanish flora were essential, especially for the work on *Silene hifacensis* in Chapt. 3. Moreover, he provided a substantial help in selecting the Spanish site for the installation of the meteorological stations.

I also thank Juan Carlos of the Jardin Botanico de Valencia. He helped me without hesitation in the logistical needs necessary for monitoring and installing the meteorological station in Spain.

I would also like to thank the director Joseba Andoni Rodríguez and the members of the Parque Natural del Montgò in Denia for providing me permissions and support in carrying out the research in Cabo de San Antonio. A special thanks goes to Toni Pellicer for the visit on boat to the population of *Silene hifacensis* in isla Midjana. Moreover, his support allowed the work carried out in Cabo de San Antonio to be smoother and less stressful.

Thanks to the three reviewers, Prof. Dr. Errol Vela, Dr. Andrew Napier Gillison and Prof. Dr. Josep Rossellò. Their contribution helped to improve considerably the first draft of the thesis.

Thanks to Prof. Virgilio Caleca for the valuable help he provided in identifying the pollinators of Pseudoscabiosa limonifolia in chapt. 4.

Thanks to Prof. Dr. Maria Antonietta Germanà, who provided a major help in the solution of any bureaucratic problem arisen during the development of the PhD.

I would like to thank Valeriya Gromova for the help during field work, patience and encouragement during the development of this work.

I like to thank my PhD colleagues Amira, Antonino, Gabriele, Nicolò, Manuela and Luca. We supported each other, especially abroad, for the past three years of work.

A final thanks goes to all those people who supported me and/or helped me during long and exhausting field works: Maria C., Sandro P., Giulia L., Martina L., Emilio T., Roberto S., Andrea D.A., Thomas W., Thomas B., Dario S., Natalia M., Javier P., Victoria M., Sergio L., Stefano R., Gaia B. thank you very much!

Appendix

Chapter 1

Chapter 2

Chapter 3

Fig. S3.2. Sampling of Cofano West.

Fig. S3.3. Sampling of Cofano East.

Fig. S3.4. Two examples of field surveys using UAVs.

Chapter 4

Fig. S4.1. Damage caused by herbivory.

Fig. S4.2 Unique broadly crenate margin of vegetative leaves from the population of Cofano.

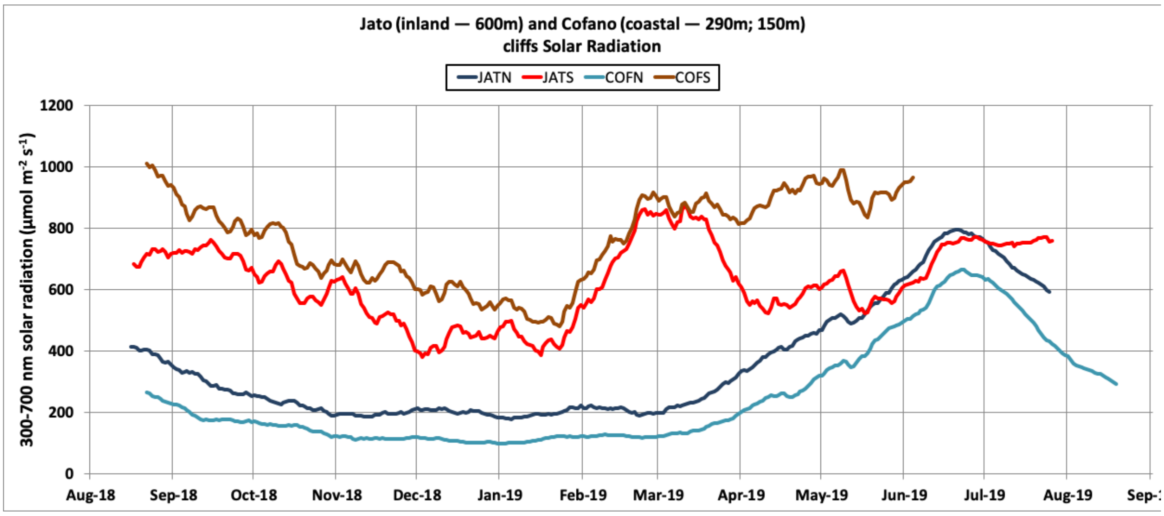

Fig. S1.1. The simultaneous annual trends of solar radiation in JATN (dark blue), JATS (red), COFN (pale blue) and COFS (brown). Each trend line represents a centred moving average of daily values of order 31 days. Each unit of the X axis represents the first day of the corresponding month. The average value of trend lines for a month can be read between two units of the X axis.

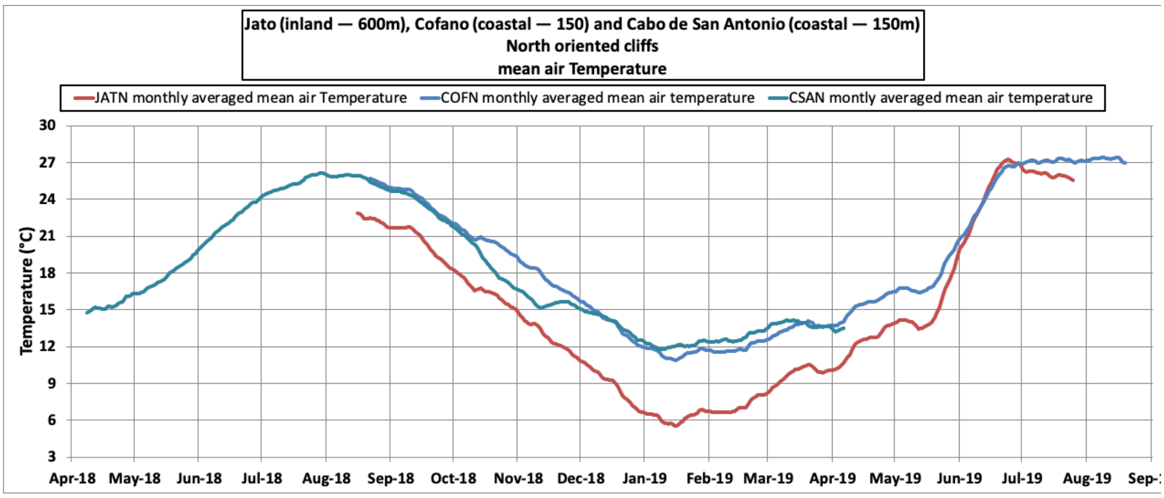

Fig. S1.2. The simultaneous annual trends of air temperatures in JATN (red), COFN (dark blue) and CSAN (turquoise). Each trend line represents a centred moving average of daily values of order 31 days. Each unit of the X axis represents the first day of the corresponding month. The average value of trend lines for a month can be read between two units of the X axis. It is possible to appreciate that despite the geographic distance the coastal North-oriented areas show a similar temperature trend. Overall, air temperatures in the coastal areas were higher than in the inland zone. Also, seasonal fluctuations were limited in these zones with respect to the inland zone.

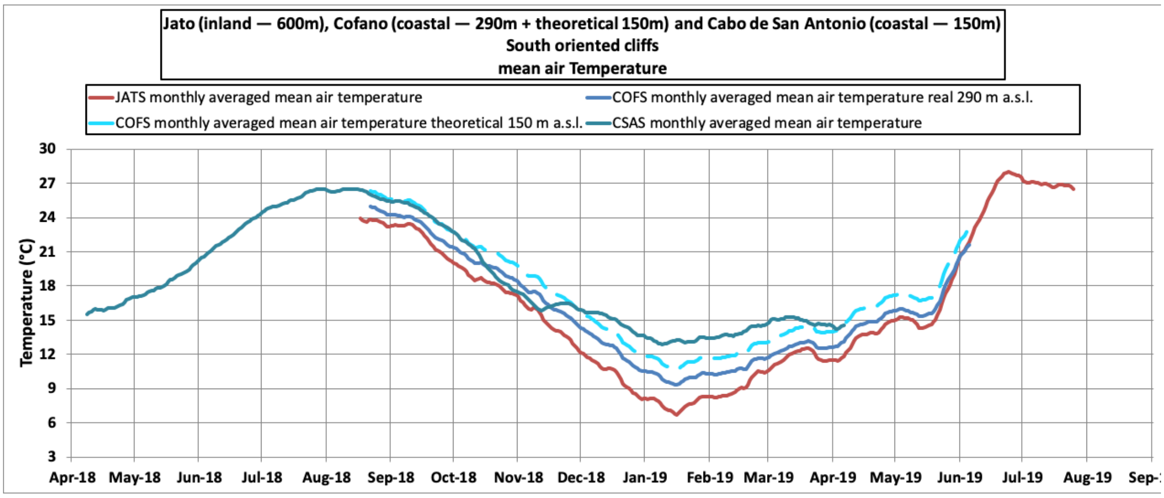

Fig. S1.3. The simultaneous annual trends of air temperatures in JATS (red), COFS (dark blue), CSAS (turquoise) and COFS* (dotted pale blue) if the site of installation would have been positioned at an altitude of 150 m. Each trend line represents a centred moving average of daily values of order 31 days. Each unit of the X axis represents the first day of the corresponding month. The average value of trend lines for a month can be read between two units of the X axis. COFS* was calculated by accounting of a thermal reduction of (-0.98 °C/-100 m (-1,372°C for each hourly measurement of temperature of COFS).

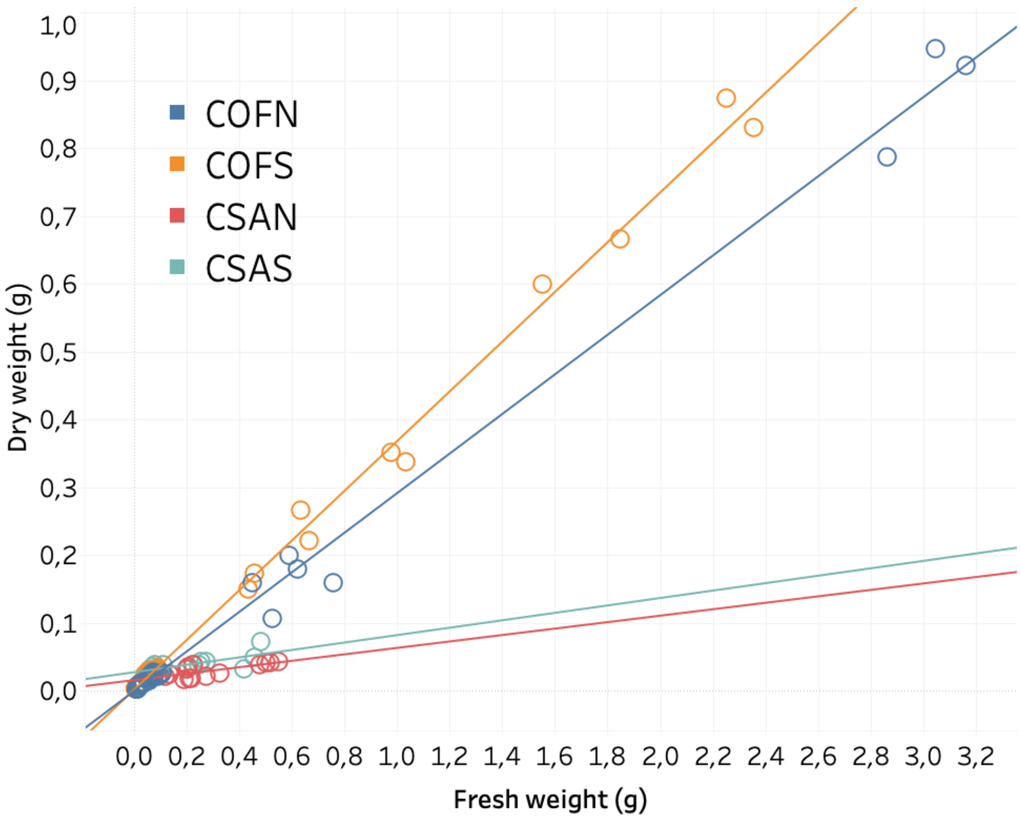

Fig. S1.4. Scatterplot of foliar fresh and corresponding dry weight in the analysed coastal cliffs. Each value is the mean for an individual. Colour scheme refers to the sampling area. Linear regression lines are drawn. R^2 COFN: 0.9936; R^2 COFS: 0.9959; R^2 CSAN: 0.537; R^2 CSAS 0.5127. p COFN < 0.0001; p COFS < 0.0001; p CSAN < 0.001; p CSAS < 0.001.

Fig. S1.5. Left: material used to build some of the installed meteorological stations. Right: installation of a meteorological station.

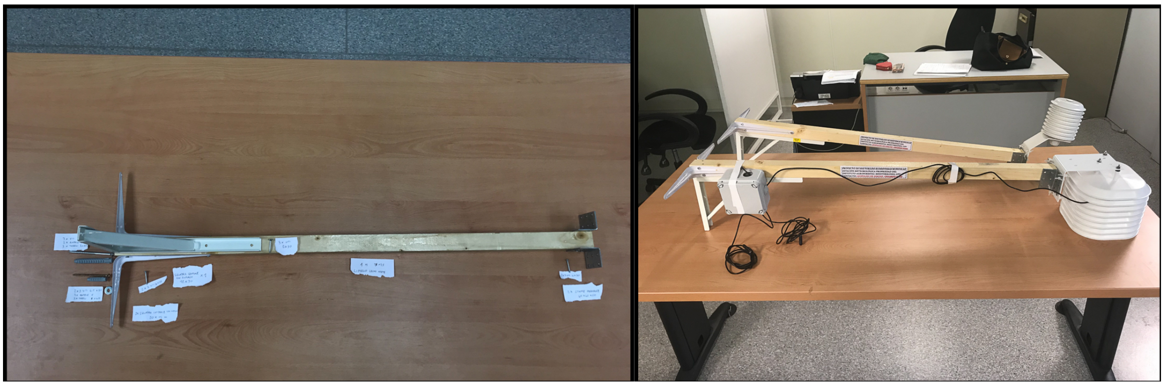

Fig. S1.6. Design of a meteorological station.

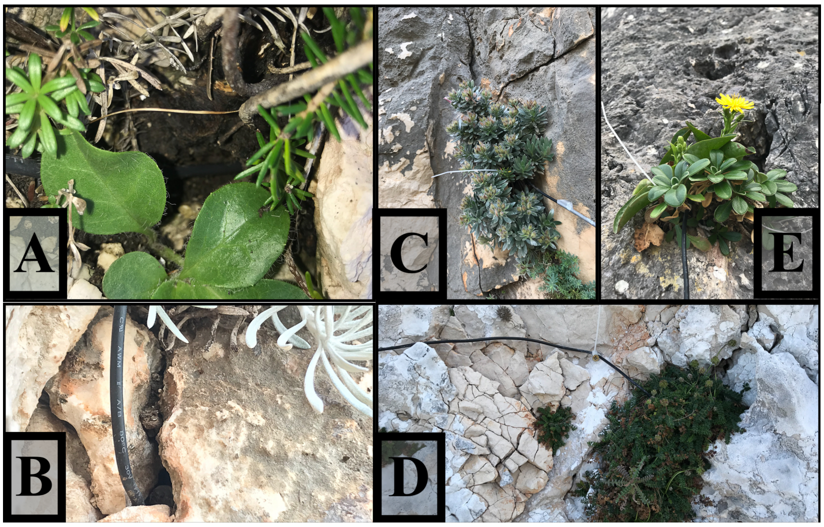

Fig. S1.7. Probes for measuring air under canopy (C-E) and soil (A-B) temperatures. A: COFN soil. B: COFS soil. C: COFS canopy; the species is *Convolvulus cneorum*. D: CSAN canopy; the species is *Sanguisorba ancistroides*. E: COFN canopy; the species are *Pseudoscabiosa limonifolia* and *Hieracium cophanense.*

Fig. S1.8. Technical difficulties arisen from the study. A, B: Corrosion on the North-oriented coastal sites. Corrosion of the metallic support was encountered only in these zones and was caused by salt depositions from marine aerosol. C: A rodent cut a probe of soil temperature, causing the loss of data recording.

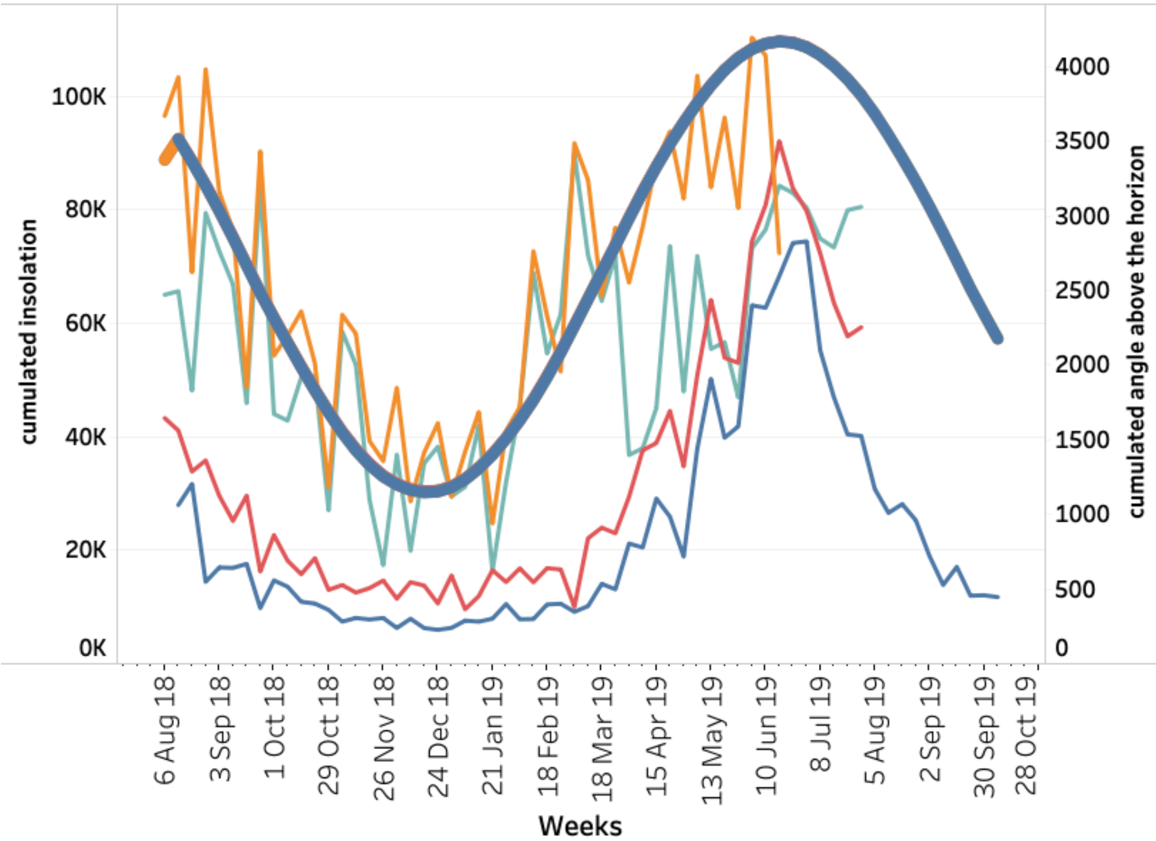

Fig. S1.9. The simultaneous annual trends of cumulated weekly solar radiation (insolation) in JATN (red), COFN (dark blue), COFS (orange) and JATS (turquoise). Unit of cumulated radiation is µmol $m^{-2}s^{-1}$. The sinusoidal line corresponds to the annual trend of cumulated weekly vertical angles produced by the sun position over the horizon (unit: degrees). Each trend line is produced by weekly cumulated values of the corresponding measure. Each unit of the X axis represents the first day of the corresponding week. Overall, the cumulated insolation of a location is proportional to the amount of time the sun is above the horizon. South and North oriented cliff zones have a different cumulated insolation in response to the cumulated angle position of the sun above the horizon, mostly due to the fact that direct solar radiation, no matter the sun angle over the horizon, is shielded by the vertical extent of North-oriented cliffs.

Fig. S1.10. Barplot of cumulated hourly insolation in COFN and COFS (unit: µmol $m^{-2}s^{-1}$). Insolation is categorised according to the sun Azimuth angles, counting from N. Angles have been grouped with a 10° span. Colour shows details about the hour of the day of each insolation value. Each azimuth angle group is formed by solar radiation data gathered preferentially during a discreet hour of the day.

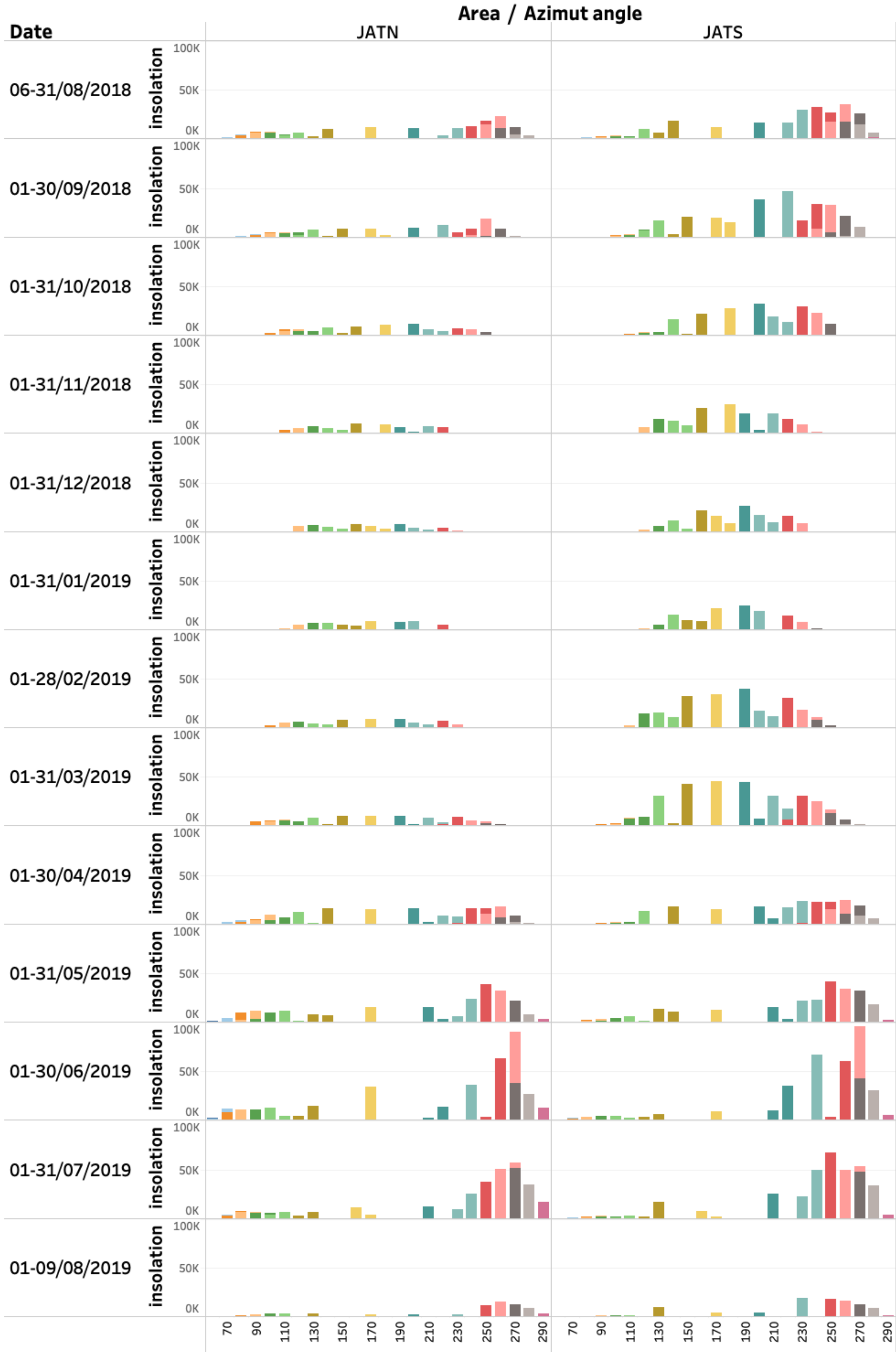

Fig. S1.11. Barplot of cumulated hourly insolation in JATN and JATS (unit: µmol $m^{-2}s^{-1}$). Same colour scheme of Fig. S1.10.

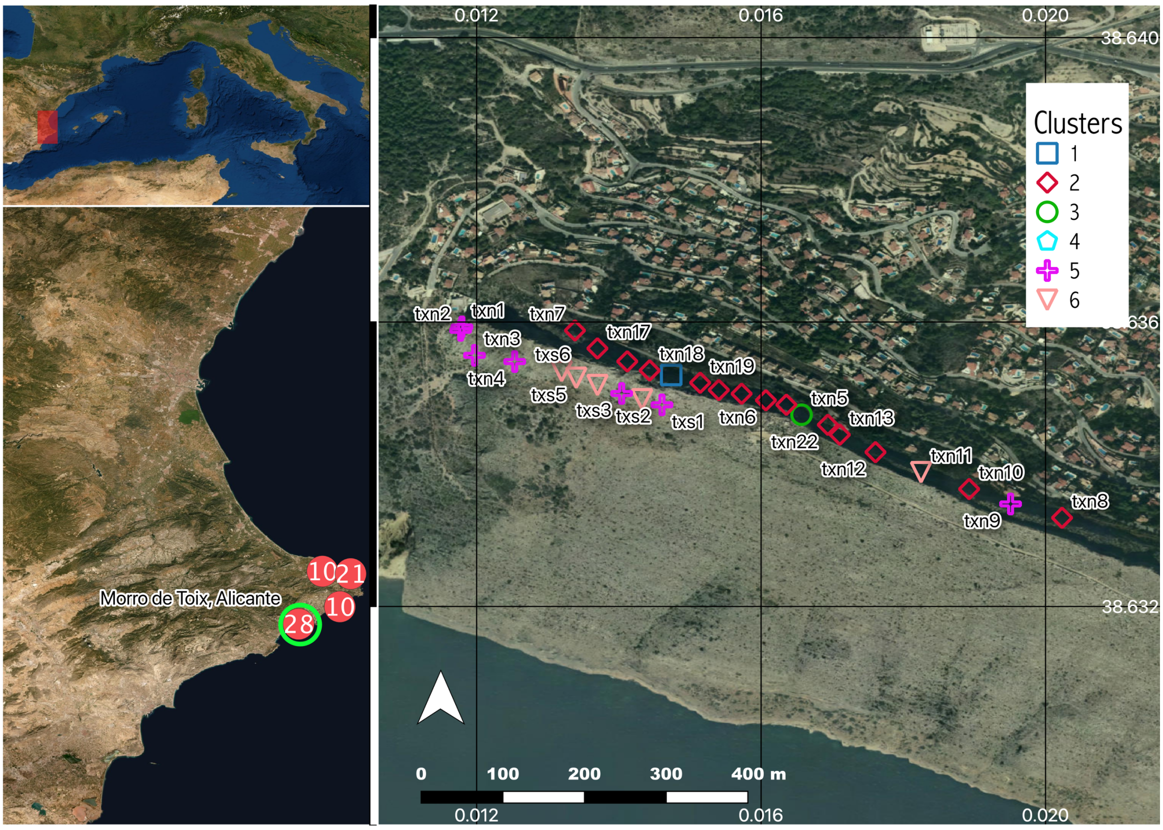

Fig. S2.1 Map of the geographic distribution of the studied sites in Toix, catalogued according to their cluster group.

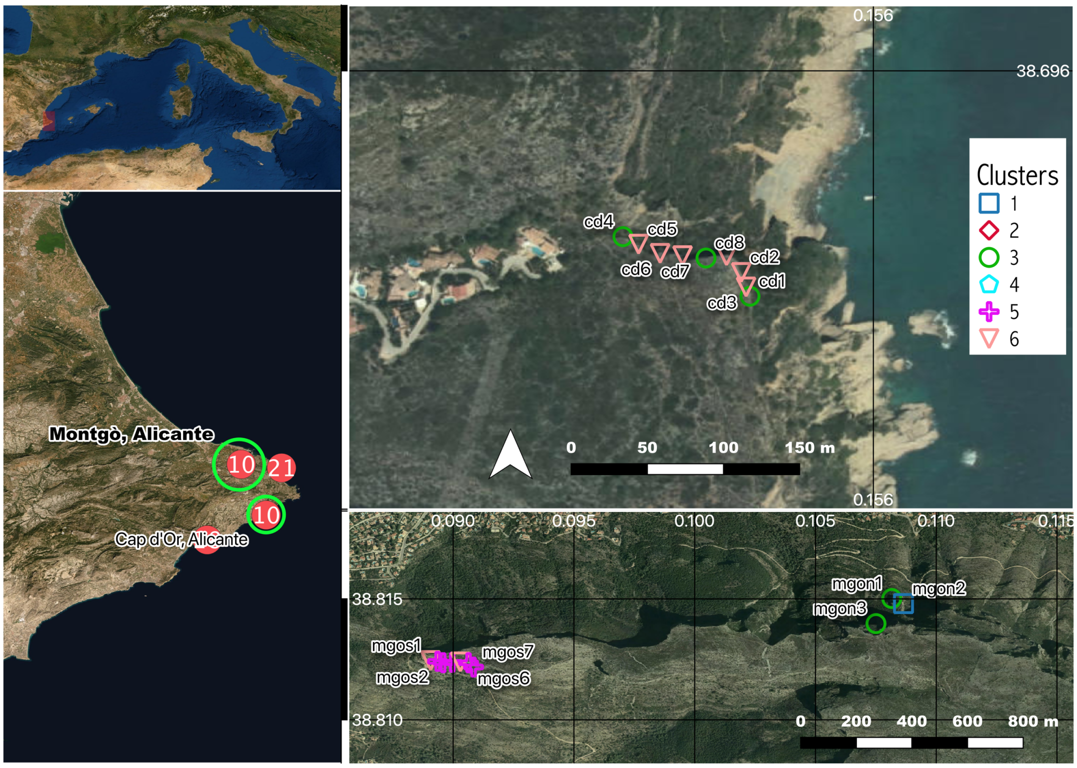

Fig. S2.2 Map of the geographic distribution of the studied sites in Montgò and Cap d'Or, catalogued according to their cluster group. Up: Cap d'Or. Down: Montgò.

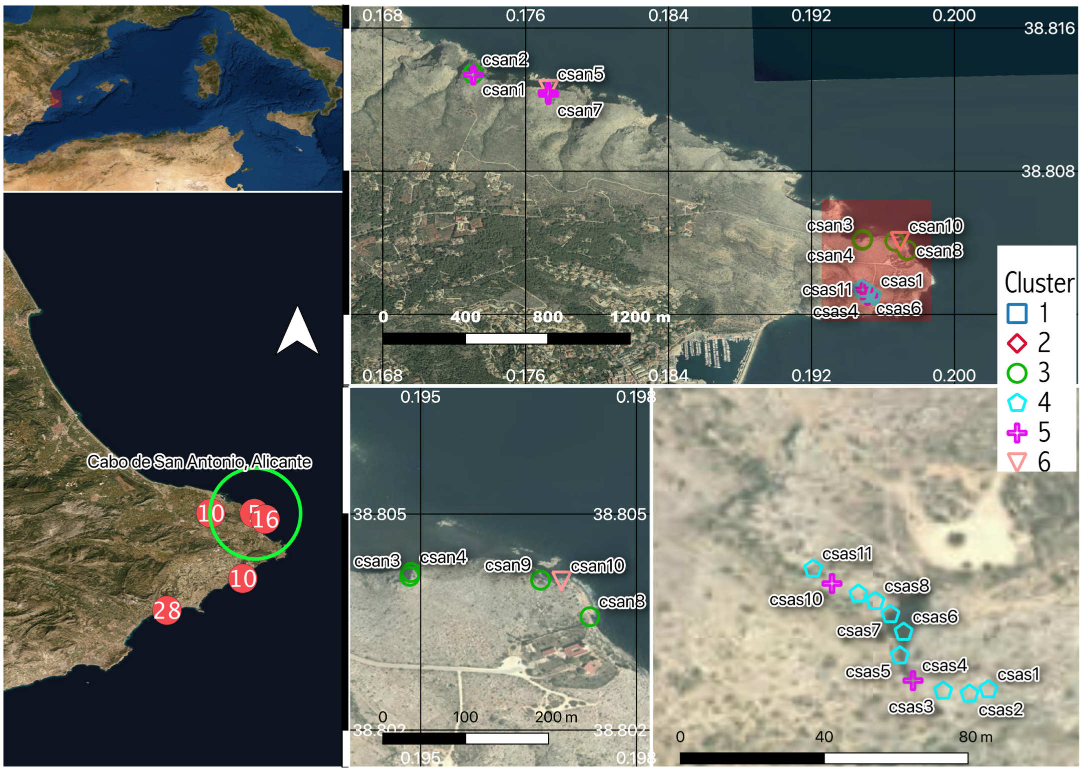

Fig. S2.3 Map of the geographic distribution of the studied sites in Cabo de San Antonio, catalogued according to their cluster group.

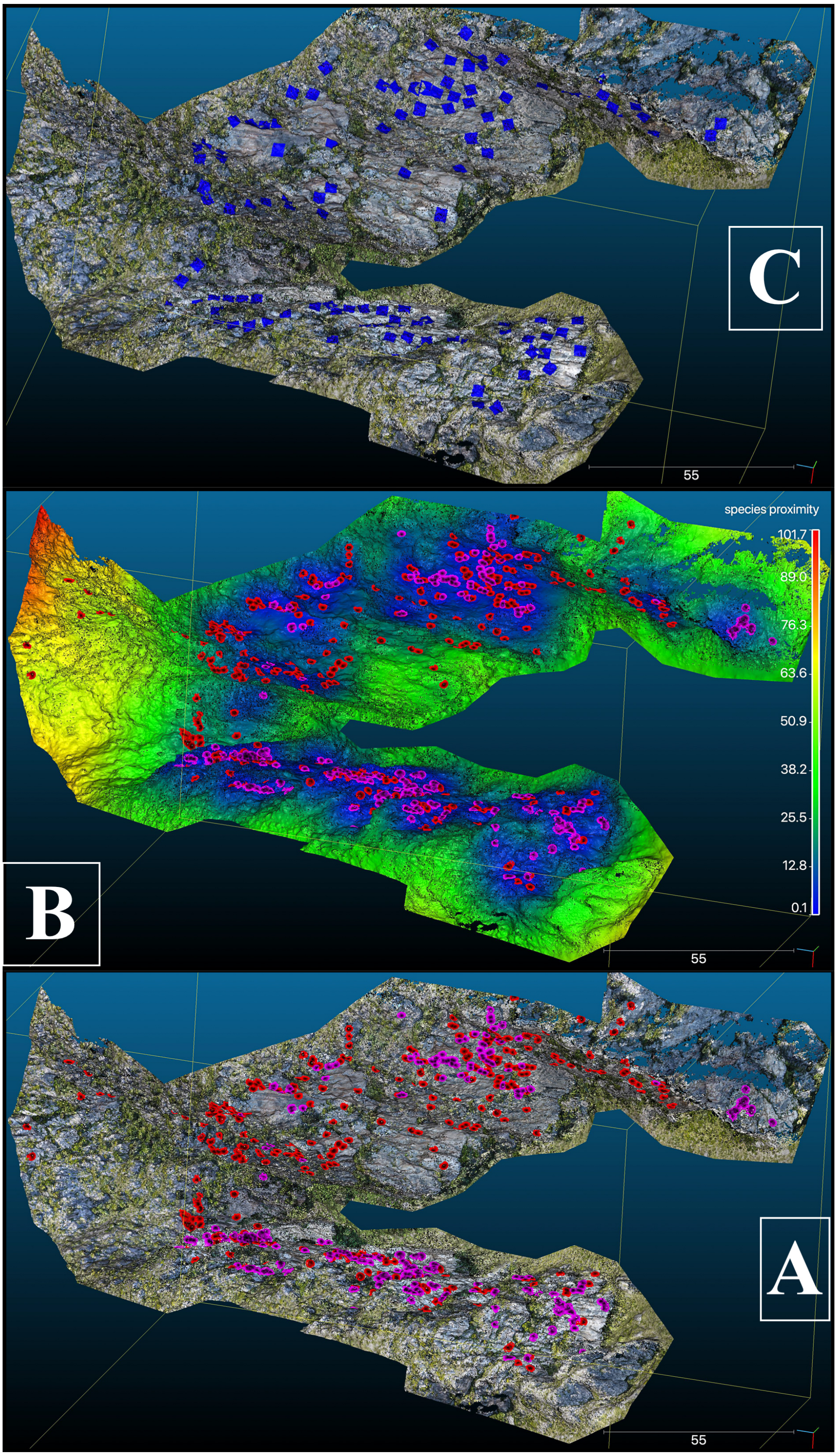

Fig. S3.1. Sampling of Cofano North. Red markers are individuals of *Erica sicula*. Purple markers are individuals of *Pseudoscabiosa limonifolia*. A: RGB view. B: for a scenario 2 selecting the proximity of the species is necessary in order to place plots only in the surface occupied by both species. C: plots. Proximity scale is measured in metres.

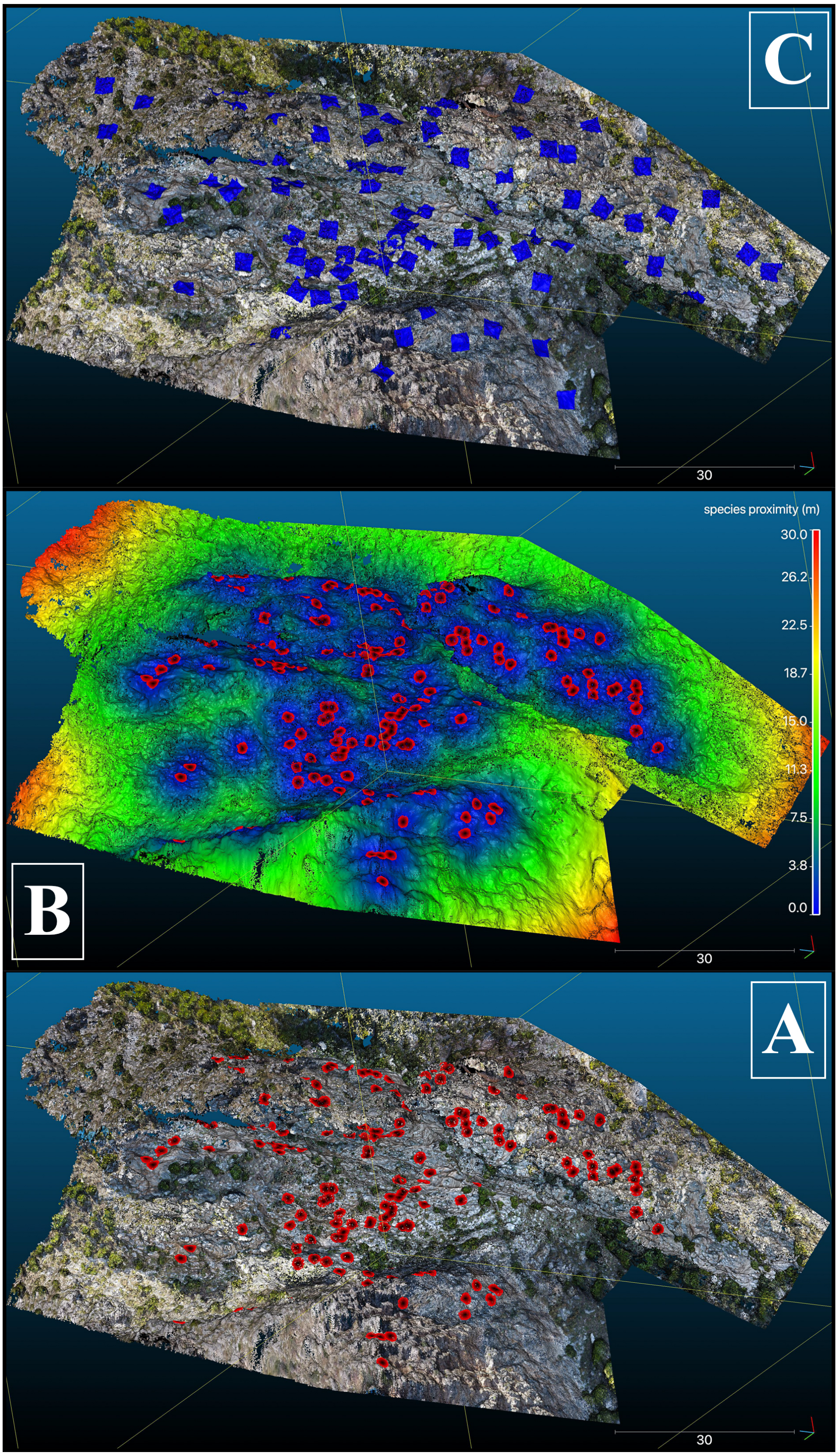

Fig. S3.2. Sampling of Cofano West. Red markers are individuals of *Erica sicula*. A: RGB view. B: for a scenario 2 selecting the proximity of the species is necessary in order to place plots only in the surface occupied by the species. C: plots.

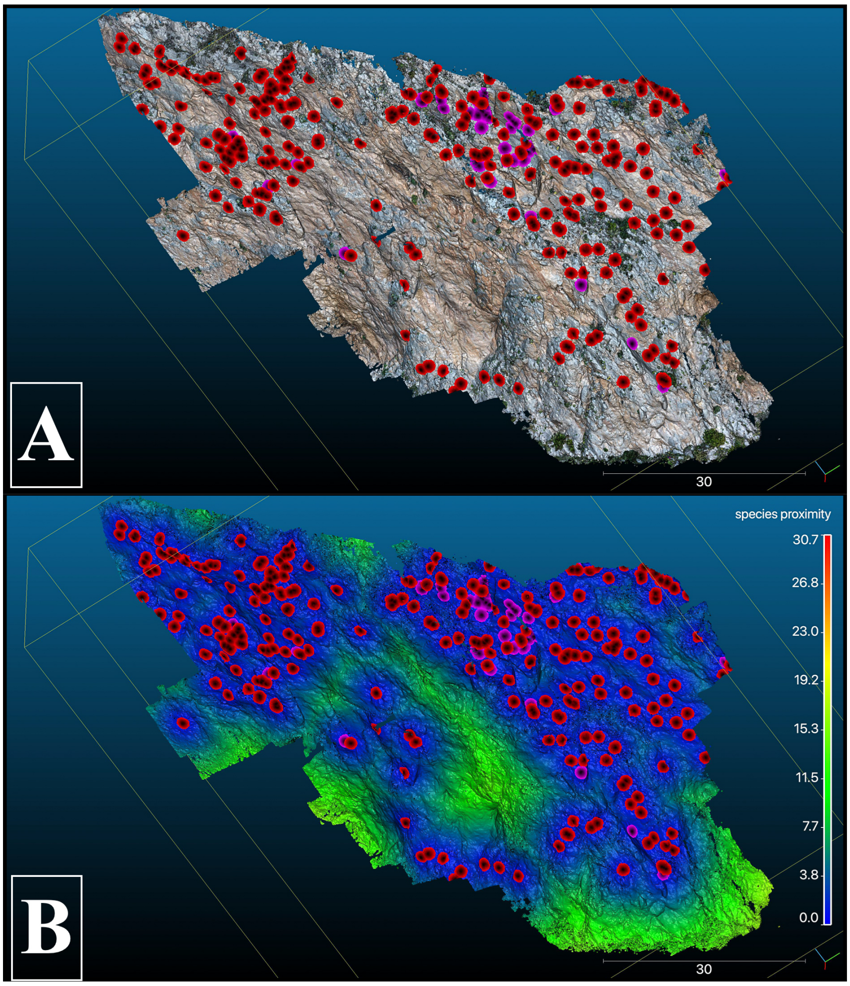

Fig. S3.3. Sampling of Cofano East. Red markers are individuals of *Erica sicula*. Purple markers are individuals of *Pseudoscabiosa limonifolia*. A: RGB view. B: for a scenario 2 selecting the proximity of the species is necessary in order to place plots only in the surface occupied by both species. Proximity scale is measured in metres.

Fig. S3.4. Two examples of field surveys using UAVs. Each marker on the right corresponds to a specimen of *Pseudoscabiosa limonifolia* or *Lomelosia cretica* in Gallo (case study 4).

Fig. S4.1. Damage caused by herbivory (mouflon, *Ovis aries musimon*); 24/06/2018 Marettimo (Trapani), Italy

Fig. S4.2. Vegetative leaves of a specimen of *Pseudoscabiosa limonifolia* from Cofano. Compared to other areas, leaves in this population tend to be shorter and with an obovate shape. Moreover, together with plants from the population of Monaco, they have a unique broadly crenate margin, not found in any other location.

Author's name, affiliation, country

Leopoldo de Simone

Department STEBICEF; Department of Agricultural and Forest Sciences
University of Palermo, Viale delle Scienze Ed. 4
Palermo 90128, Italy

Mediterranean Agroforestry Institute,
Universidad Politecnica de Valencia, Camino de Vera, s/n
46022 Valencia, Spain

Email: leopoldo.desimone@gmail.com
Work 1: leopoldo.desimone@unipa.it
Work 2: dedesi@doctor.upv.es
Mob: +393202619595

This thesis investigates opportunities, challenges and limitations for plant ecological research in the context of Mediterranean cliffs. In detail, chasmophytic species, whose natural habitats are very steep, limestone mountains slopes in the proximity of the sea, in the Central and Western part of the Mediterranean area are considered as study objects. Studies were carried out in the coastal mountain belts of both North-western Sicily and Dianic coasts in the Valencian Community (Spain).

The first chapter investigates the variability of cliff microclimate in three different areas in Sicily and Spain, analysing the environmental conditions created by the cliff at very fine scale. Six independent and comparable datasets including the main meteorological variables were compiled in a total period of 18 months. The resulting spectra of environmental conditions are compared pairwise along two key environmental gradients: North/South cliff orientation and proximity to the sea. Intraspecific leaf traits are used in order to investigate variation in the functional response of plants living on opposite orientations. The resulting variation is then correlated with the influence of microclimatic conditions created by slope and functional aspects of the aforementioned plant traits.

The second chapter presents an ordination of the study sites and of the plant species inhabiting the cliff zones of the mountain belt along the coasts of the Dianic region in Eastern Spain. The study revealed significant correlations between the vegetation units and the sites with reference to the broad North/South geographical orientation. However, it was poorly informative in respect to reveal the major differences observed in the structure of the plant assemblage related to the micro-topographic variations recorded in the dataset.

In the third chapter a proposed survey methodology for investigating hardly accessible vertical environments is described. Challenges and opportunities of plant ecological research in these typically inaccessible areas were also analysed. Through the use of aerial close-range photogrammetry and 3D modelling, it was possible to study the effects of micro-topography on niche segregation, both at community and species level. Ordination methods were used to correlate selected endemic species and entire plant assemblages' to environmental factors such as local and global aspect, slope and distance from cliff edges.

The fourth chapter is addressed at analysing in details the phylogeographic structure of a cliff narrow endemic species, *Pseudoscabiosa limonifolia* (VAHL) DEVESA (Dipsacaceae s.s.), also taking in consideration its closest sister taxa. Furthermore, its total distribution was determined by field surveys, characterizing its habitat, and assessing its conservation status as Vulnerable according to IUCN Red List guidelines.